THE UNIVERSITY
of EDINBURGH

The mechanisms of actions and roles of 5α-reduced glucocorticoids during inflammation and wound repair

Amber Abernethie

Doctor of Philosophy

University of Edinburgh

2018

Abstract

Topical inflammatory diseases are most commonly treated with glucocorticoids, such as hydrocortisone, which have debilitating side effects including a range of systemic metabolic side effects as well as local effects such as to thin the skin and delay wound healing. Safer anti-inflammatory therapies are required and this thesis investigates a novel drug called 5α-tetrahydrocorticosterone (5α-THB) as a safer topical anti-inflammatory treatment. The main foci of this thesis are to assess the effects of 5αTHB on wound repair, as well as to characterise its mechanisms of action.

Defective angiogenesis accounts for impaired wound healing brought about by steroids in many cases. 5αTHB suppressed vessel growth in a mouse e*x vivo* model of angiogenesis, but was less potent in this action than hydrocortisone, suggesting a safer therapeutic profile. To understand the underlying mechanisms, the effect of 5αTHB on gene expression in the mouse aorta during angiogenesis was compared with that of dexamethasone (a selective GR agonist) and hydrocortisone. Whereas dexamethasone and hydrocortisone caused differential expression of genes involved in inflammatory signalling and extracellular matrix remodelling, 5αTHB did not and instead selectively regulated *Pecam1,* involved in vasculature remodelling. This suggested that 5αTHB suppresses angiogenesis through different mechanisms of action in comparison to dexamethasone, and thus may not act through GR. Supporting this, dexamethasone increased the abundance of GR responsive transcripts (*Per1, Hsd11b1, Fkbp51*) whereas 5αTHB only increased the abundance of *Per1*. Furthermore, whereas the GR antagonist RU486 attenuated dexamethasone-regulation of genes, it had no effect on gene regulation by 5αTHB.

To assess GR-mediation of 5αTHB effects, model systems were used to investigate whether 5αTHB is able to bind GR, stimulate its nuclear translocation, and initiate changes in its interaction with co regulator peptides. In a competitive binding assay, dexamethasone and hydrocortisone both decreased the fluorescence polarisation of a GR specific ligand, consistent with GR binding. In contrast, 5αTHB only displaced the specific GR ligand at very high concentrations. In terms of nuclear translocation, 5αTHB also did not have an effect on the ratio of GR in the nucleus and cytoplasm (N/C) of A549 cells, suggesting that GR remained predominantly in the cytoplasm after 5αTHB treatment and did not translocate into the nucleus, whereas dexamethasone increased the N/C ratio at three different time points. Likewise, whereas dexamethasone stimulated changes in the interaction between GR and many co regulator peptides, 5αTHB had no effect. Collectively these results from model systems suggest that 5αTHB does not work through the conventional GR mechanism of action.

Finally, a hypothesis generating approach was taken in order to gain hints into how 5αTHB may be working. A microarray was performed to compare the effects of 5αTHB and dexamethasone on gene expression in human peripheral blood derived macrophages. Both dexamethasone and 5αTHB were able to cause differential expression of genes in these cells. However unexpectedly, out of the 350 genes regulated by dexamethasone, and the 165 genes regulated by 5αTHB, only 35 genes were commonly regulated by both steroids. This suggested that 5αTHB mainly acts through different mechanisms to dexamethasone also in macrophages. In an enrichment analysis of the differentially expressed genes, whereas the NFκB signalling pathway was the top enriched pathway in genes only regulated by dexamethasone,

enriched pathways in genes only regulated by 5αTHB included those related to phagocytosis, the TGF-beta signalling pathway, and Th1-Th2 cell differentiation.

This thesis therefore provides evidence to suggest that 5αTHB may provide a safer topical anti-inflammatory steroid, less harmful to wound repair processes. In addition, the mechanisms underlying the action of 5αTHB differ from those of classical GCs, consistent with its reduced side-effect profile. Other potential mechanisms, such as actions through the mineralocorticoid receptor, must now be explored.

Lay Summary

Inflammatory diseases of the skin, such as eczema, are most commonly treated with a type of drug called a glucocorticoid. But although glucocorticoids are good at reducing inflammation, they have side effects inside the body and on the skin. Glucocorticoids cause colouring and thinning of the skin, and also prevent wounds from healing.

The way in which glucocorticoids prevent wounds from healing is by slowing the growth of new blood vessels, so that oxygen and nutrients cannot enter the wound.

A safer drug is needed which treats inflammation but does not slow the growth of new blood vessels. Our group have found a new drug called 5αTHB, which also treats inflammation but so far seems to have fewer side effects than glucocorticoids inside the body. This thesis explores why this is and also tests whether 5αTHB also has fewer side effects than glucocorticoids on the skin.

The results show that in mice, 5αTHB was less damaging to new blood vessel growth than glucocorticoids, and so is likely to be safer when applied to the skin. In comparison to glucocorticoids, 5αTHB also had different effects on the genes of both mice and humans. These differences could explain why 5αTHB is able to treat inflammation without having side effects.

In summary, this thesis gives evidence that 5αTHB is safer than glucocorticoids for treating skin inflammation. It also provides a starting point for understanding why this is, and future work will look further into this.

Declaration

I declare that this thesis was written by me and is the result of my own work performed at the University of Edinburgh, with the exceptions listed below:

Margaret Binnie (Drug Discovery Core, University of Edinburgh) performed the GR displacement assay.

The MARCoNI GR coregulator peptide recruitment assay was organised by Onno Meijer and performed by René Houtman at PamGene International.

The wet lab work from chapter 5 was performed by Dr Alasdair Jubb, who outsourced the microarray to Edinburgh Genomics.

Undergraduate student Clodagh Mitchell assisted with the GR nuclear translocation assay (chapter 3), and Giorgia Maltese performed the RNA extraction and qPCR from chapter 4.

I declare that this work has not been submitted for any other degree or qualification

Amber Abernethie

Acknowledgements

I would like to say a huge thank you to my supervisors – Ruth Andrew for being an excellent primary supervisor and for her constant support and availability, Paddy Hadoke for his calm guidance and support which always helped me to feel reassured, and Dawn Livingstone for her valuable advice and contribution throughout. I am also extremely grateful to the British Heart Foundation for funding my PhD, and to the BHF/University Centre for Cardiovascular Science for giving me this fantastic learning opportunity.

I really appreciate the training that I have received from many people in the research centre – Annalisa Gastaldello, Mark Macaskill, Mark Nixon, Junxi Wu, Ruth Morgan, Eileen Miller, Tracy Mac, and Rob Ogley, who have all provided instruction or advice on lab work in some way. Special thanks also to Clodagh Mitchell and Giorgia Maltese for their hard work during their lab projects which contributed to this thesis.

Thank you to the collaborators who have provided input to my work – Alasdair Jubb, for allowing me to use his gene expression results and for his guidance during the enrichment analysis; Onno Meijer and René Houtman for organising and conducting the Marconi assay; Margaret Binnie (Drug Discovery Core) who performed the GR binding assay; and Dahlia Doughty Shenton who granted me access of her cell migration equipment as well as contributing her time during its use.

Finally, thank you to my family for their support, patience and encouragement which helped me to get through the PhD.

I would like to dedicate this thesis to my oldest friend Dr Sophie Miller who sadly passed away in 2016, who encouraged me during the PhD and without whose influence during my younger years I may not have began this journey.

Contents

Abstract…..…….1

Lay Summary……4

Declaration…….5

Acknowledgements……...6

List of Figures…….17

List of Tables……...23

Table of Abbreviations……...24

Abstracts from thesis……..……28

Publications from thesis……..….....29

Chapter 1 Introduction …….30

1.1. Glucocorticoids……32

1.2. The Glucocorticoid Receptor……..…….40

1.2.1. Functional domains of GR…….41

1.2.2. 'Classical' genomic signalling by GC……...42

1.2.2.1. GR binding and nuclear translocation…….42

1.2.2.2. Direct gene regulation by GR (Transactivation)…….44

1.2.2.3. Indirect gene regulation by GR (Transrepression)…….45

1.2.3. Additional 'non-classical' genomic GC signalling……...46

1.2.4. Non-genomic signalling of GCs……50

1.3. Achieving cell and tissue specific regulation by GR……...53

1.3.1. Chromatin Accessibility……53

1.3.2. GR isoforms……...54

1.3.3. Post translational modifications……59

1.3.4. Micro RNAs……..60

1.3.5. Ligand selectivity……..61

1.4. Pharmaceutical use of GCs to treat inflammation……..….61

1.4.1. Introduction to inflammation……61

1.4.2. History of anti-inflammatory GC use……62

1.4.3. Dissociating between GR mechanisms……64

1.4.4. The development of a selective glucocorticoid receptor agonist (SEGRA)…….…69

1.4.5. 5α-Reduced glucocorticoids……..73

1.4.6. 5α-Tetrahydrocorticosterone (5αTHB)……75

1.4.7. 5αTHB as a SEGRA with decreased adverse effects on wound healing……..78

1.5. Mechanisms of wound repair in the skin……79

1.6. Mechanism of angiogenesis……..……...83

1.7. Glucocorticoid-mediated effects on wound repair and angiogenesis……..85

1.8. Introduction Summary……88

1.9. Hypotheses and Aims……..89

Chapter 2: Materials and Methods……...90

2.1. Materials and reagents……91

2.1.1. Source and maintenance of animals……91

2.1.2. Outsourced reagents and chemicals……..91

2.1.3. Sources of cultured cells……...91

2.1.3.1. Cell lines……..91

2.1.3.2. Murine bone marrow-derived macrophages (BMDM)……92

2.1.3.2.1. Removal of femur and tibia bones……...92

2.1.3.2.2. BMDM cell isolation, plating and differentiation……...93

2.1.4. Preparation of reagents and solutions…… .94

2.1.4.1. Cell culture medium……...…….94

2.1.4.1.1. Normal serum medium……...…….94

2.1.4.1.2. Serum free medium……...……94

2.1.4.1.3. Stripped serum medium……...……94

2.1.4.2. L929 fibroblast-conditioned medium for BMDMs……95

2.1.4.3. Freezing medium……95

2.1.4.4. Steroid solutions……..95

2.1.5. Cell culture……...95

2.1.5.1. Cell thawing ……95

2.1.5.2. Maintenance and passaging of cells…..……96

2.1.5.3. Cell freezing……96

2.1.5.4. Coating of culture flasks and plates……97

2.2. Laboratory protocols……98

2.2.1. RNA analysis……98

2.2.1.1. Materials……..98

2.2.1.1.1. Tris-Borate-Ethylenediamine tetra acetic acid (TBE) 10x buffer solution……98

2.2.1.1.2. TBE 0.5x buffer solution……98

2.2.1.2. RNA extraction from aorta……..98

2.2.1.3. RNA quantification…… 99

2.2.1.4. Evaluation of RNA quality……100

2.2.1.5. Reverse transcription……101

2.2.1.6. Real-time qPCR……102

2.2.2. Protein analysis……...105

2.2.2.1. Western blotting……105

2.2.2.1.1. Materials and buffers……105

2.2.2.1.2. Whole protein extraction……...105

2.2.2.1.3. Protein extraction of separated nuclear and cytoplasmic components……..……...106

2.2.2.1.4. Protein quantification……...……..…106

2.2.2.1.5. Western blot sample preparation……...107

2.2.2.1.6. Gel electrophoresis and protein transfer to membrane……..107

2.2.2.1.7. Visualisation and quantification of protein on membrane……..…108

2.2.2.1.7.1. Fluorescence……...108

2.2.2.1.7.2. Chemiluminescence……109

2.2.2.2. Quantification of cytokines by ELISA……..110

2.2.2.3. Visualisation of protein by immunofluorescence……..111

2.2.3. *Ex vivo* aorta angiogenesis assay……112

2.2.3.1. Aorta dissection from mouse……112

2.2.3.2. Aortic ring plating and culture……...113

2.2.3.3. Quantification and analysis of angiogenesis……...113

2.2.4. *In vitro* cell migration assay……...115

2.2.5. Measurement of co-regulator peptide recruitment to nuclear receptors……115

2.2.6. Assessment of steroid ability to bind GR ligand binding domain……..116

2.3. Data analysis……..117

Chapter 3: Is 5αTHB less detrimental during wound repair than current glucocorticoid administration?.....118

3.1. Introduction……119

3.2. Hypothesis……121

3.3. Aims……121

3.4. Methods……122

3.4.1. Investigating the effects of 5αTHB on cell migration *in vitro*……...122

3.4.1.1. Choice of cells……...122

3.4.1.2. Assessment of GR protein in cell lines……..……122

3.4.1.3. Essen bioscience cell migration scratch assay……...……123

3.4.1.3.1. Method development…….……123

3.4.1.3.2. Testing steroid effects……..……..123

3.4.2. Investigating the effects of 5αTHB in the vasculature *ex vivo*……...123

3.4.2.2. Comparing steroid effects on vessel growth…….…123

3.4.2.3. Assessing GR dependence of the effects of 5αTHB on vessel growth…...….125

3.4.2.4. Comparing steroid effects on mRNA transcript expression in aortic rings…...125

3.4.2.4. Data and statistical analysis……...127

3.5. Results……..…129

3.5.1. Assessing the effects of 5αTHB on cell migration…….129

3.5.1.1. Assessment of GR expression in cell types……...129

3.5.1.2. Optimisation of cell seeding conditions……130

3.5.1.3. Optimising assay analysis settings……131

3.5.1.4. Model assessment and time point selection……...133

3.5.1.5. Assessing steroid effects on cell migration……..…….136

3.5.2. The effects of steroids on angiogenesis…….....140

3.5.2.1. Assessment of controls…….……140

3.5.2.2. Assessment of the effect of hydrocortisone in an *ex vivo* model of angiogenesis……...145

3.5.2.3. Assessment of the angiostatic effects of 5αTHB in an *ex vivo* model……...148

3.5.2.4. Summary of the effects of 5αTHB and hydrocortisone on angiogenesis in the aortic ring assay model.……151

3.5.3. Investigation of the involvement of GR in the angiostatic effects of 5αTHB…...…152

3.5.3.1. Antagonism of the angiostatic effect of 5αTHB using equipotent doses of RU486……....152

3.5.3.2. Assessment of antagonism by a shift in the concentration-response curves….155

3.5.3.2.1. Assessment of the effect of RU486 on the concentration-response to dexamethasone……...155

3.5.3.2.2. Assessment of the effect of RU486 on the concentration response curve to 5αTHB…….158

3.5.4. The effect of steroids on gene expression in the mouse aorta……161

3.5.4.1. Retrieval of aortic rings and RNA extraction……161

3.5.4.2. Comparison of the effects of 5αTHB, dexamethasone, and hydrocortisone on gene expression in mouse aortic rings ……..……162

3.5.4.2.1. Genes involved in inflammation and signalling……162

3.5.4.2.2. Genes involved in remodelling of the extracellular matrix……...162

3.5.4.2.3. Genes involved in remodelling the vasculature……163

3.5.4.2.4. Genes known to be directly associated with GR……...163

3.5.4.3. Using RU486 to investigate the involvement of GR in the effects of steroids on gene expression in mouse aortic rings……..165

3.6. Discussion……..168

Chapter 4: Can 5αTHB act through GR?.....180

4.1. Introduction……..181

4.2. Hypotheses……...……183

4.3. Aims…….……183

4.4. Methods……185

4.4.1. Comparing steroid ability to bind GR……185

4.4.2. Assessment of 5αTHB ability to induce GR nuclear translocation……...…….185

4.4.2.1. Immunofluorescence method……..…185

4.4.2.2. Nuclear/ cytoplasmic separation method……...186

4.4.3. Assessment of 5αTHB effects on coregulator peptide recruitment to GR…….187

4.4.4. Comparing the effects of steroids on cytokine release from mouse bone marrow-derived macrophages……187

4.4.5. Data analysis……...188

4.5. Results……..……189

4.5.1. Does 5αTHB displace selective GR ligands from the isolated GR ligand binding domain?..... 189

4.5.2. Does 5αTHB translocate GR into the nucleus?.....190

4.5.2.1. Immunofluorescence method development……...190

4.5.2.2. N/C separation method development……..…202

4.5.2.3. Assessment of GR translocation using the N/C separation technique…..…….204

4.5.2.3.1. Data analysis……..204

4.5.2.3.2. Assessment of controls……..….204

4.5.2.3.3. Assessing GR translocation in response to 5αTHB…….……..204

4.5.3. Does 5αTHB induce co-regulator peptide recruitment to the GR ligand-binding domain?.....207

4.5.4. Does 5αTHB mediate its anti-inflammatory effects through GR?.....209

4.5.4.1. ELISA Quality control……...209

4.5.4.2. Effects of steroid to suppress IL6 release from BMDM stimulated with 100 ng/mL LPS ……211

4.5.4.3. The effects of steroids on suppression of IL6 release from BMDM stimulated with 3 ng/mL LPS.……213

4.5.4.4. Steroid-induced suppression of TNFα release from BMDM stimulated with 3 ng/mL LPS.……215

4.6. Discussion……217

Chapter 5: What is the mechanism of action of 5αTHB?…….227

5.1. Introduction……228

5.2. Hypothesis……..229

5.3. Aims……..229

5.4. Methods……..230

5.4.1. Sample collection and RNA analysis by microarray……..….230

5.4.2. Data analysis……231

5.4.3. Functional analysis……...233

5.5. Results……235

5.5.1. Time point assessment……235

5.5.2. Analysis of gene lists……..237

5.5.3. Enrichment analysis……239

5.5.3.1. Enrichment analyses of all genes regulated by dexamethasone and 5αTHB…240

5.5.3.1.1. Enrichment of GO biological processes……240

5.5.3.1.1.1. Enrichment of GO biological processes by all genes regulated by dexamethasone……...……240

5.5.3.1.1.2. Enrichment of GO biological processes by all genes regulated by 5αTHB……242

5.5.3.1.2. Enrichment of KEGG pathways……244

5.5.3.1.2.1. Enrichment of KEGG pathways by all genes regulated by dexamethasone……244

5.5.3.1.2.2. Enrichment of KEGG pathways by all genes regulated by 5αTHB……246

5.5.3.2. Enrichment analysis of genes only regulated by either dexamethasone or 5αTHB……248

5.5.3.2.1. Enrichment analysis of GO biological processes……248

5.5.3.2.1.1. Enrichment of GO biological processes by genes regulated only by dexamethasone……248

5.5.3.2.1.2. Enrichment of GO biological processes by genes only regulated by 5αTHB……250

5.5.3.2.2. Enrichment analysis of KEGG pathways……252

5.5.3.2.2.1. Enrichment analysis of KEGG pathways by genes regulated only by dexamethasone……252

5.5.3.2.2.2. Enrichment of KEGG pathways by genes regulated only by 5αTHB……253

5.5.3.3. Enrichment analysis of genes commonly regulated by both 5αTHB and dexamethasone……255

5.5.3.3.1. Enrichment of GO biological pathways by genes commonly regulated by both 5αTHB and dexamethasone……256

5.5.3.3.2. Enrichment of KEGG pathways by genes commonly regulated by both 5αTHB and dexamethasone……258

5.6. Discussion……259

Chapter 6: Summary and future work……268

6.1. Is 5αTHB less detrimental to wound repair processes than current glucocorticoids?.....269

6.2. Does 5αTHB work through GR?.....272

6.3. How does 5αTHB work?.....274

6.4. Summary……276

References……..278

List of Figures

Figure 1.1: Glucocorticoid (GC) chemical structures…….34

Figures 1.2: Glucocorticoid biosynthetic pathways occurring in the adrenal cortex.....36

Figure 1.3: Glucocorticoid regulation by the hypothalamic-pituitary-adrenal (HPA) axis……..……37

Figure 1.4: Domain structure of the Glucocorticoid Receptor (GR)…...……...40

Figure 1.5: Genomic signalling mechanisms of the Glucocorticoid Receptor (GR)……49

Figure 1.6: Glucocorticoid Receptor (GR) Isoforms……..58

Figure 1.7: Structures of previously investigated Selective Glucocorticoid Receptor Analogues (SEGRAs)……73

Figure 1.8: Metabolism of natural rodent glucocorticoid corticosterone (B) to produce 5α-tetrahydrocorticosterone (5αTHB)……..……75

Figure 1.9: Skin structure and the wound repair process……...…….82

Figure 1.10: Mechanisms involved in the initiation of angiogenesis……..……..84

Figure 2.1: RNA band visualization under UV light……101

Figure 2.2: Vessel counting from murine aortic rings under light microscopy……114

Figure 3.1: Human Umbilical Vein endothelial cells (HUVECs), HaCaTs and dermal fibroblasts all expressed GR…….129

Figure 3.2: The Incucyte® analysis software package was used to apply ‘confluence’ (in orange) and ‘wound’ (in yellow) masks to cell migration images at each time point…….....132

Figure 3.3: Epidermal growth factor (EGF, 25ng/ml) increased cell migration of HaCaT cells in comparison to vehicle treated cells……..134

Figure 3.4: Cell migration was successfully manipulated using the Incucyte® cell migration scratch assay, with differences between treatments becoming significant at the time point when vehicle treated scratches had 40% relative wound density (RWD)……...…135

Figure 3.5: Dermal fibroblast cell migration was unaffected by dexamethasone (a), hydrocortisone (b) and 5α-tetrahydrocorticosterone (5αTHB)…….137

Figure 3.6: Human Umbilical Vein Endothelial Cell (HUVEC) migration was unaffected by dexamethasone (a) and 5α-tetrahydrocorticosterone (5αTHB)(c) but was inhibited by hydrocortisone……...…138

Figure 3.7: HaCaT cell migration was unaffected by dexamethasone (a), hydrocortisone (b) and 5α-tetrahydrocorticosterone (5αTHB)…….139

Figure 3.8: Vessel growth was succesfully stimulated from murine aortic rings……...141

Figure 3.9: Dexamethasone (Dex) induced a concentration-dependent suppression of vessel growth from murine aortic rings.……..142

Figure 3.10: Aortic ring assay concentration response curve fit was not improved through normalisation……...143

Figure 3.11: Concentration-dependent suppression of vessel growth from aortic rings by dexamethasone (Dex)……..144

Figure 3.12: Hydrocortisone (HC) induced a concentration-dependent suppression of vessel growth from murine aortic rings.……..146

Figure 3.13: Concentration-dependent suppression of vessel growth from aortic rings by hydrocortisone (HC)……147

Figure 3.14: 5αTHB induced a concentration-dependent suppression of vessel growth from murine aortic rings.…….…149

Figure 3.15: Concentration-dependent suppression of vessel growth from aortic rings by 5αTHB.……....150

Figure 3.16: Investigation of the involvement of the glucocorticoid receptor (GR) in 5αTHB-mediated inhibition of angiogenesis.……...154

Figure 3.17: Investigation of the effect of the glucocorticoid receptor antagonist RU486 on the suppression of angiogenesis by dexamethasone ……..……157

Figure 3.18: Investigation of glucocorticoid receptor antagonist RU486 effect on the suppression of angiogenesis by 5αTHB……159

Figure 3.19: The effect of the glucocorticoid receptor antagonist RU486 on the suppression of angiogenesis by dexamethasone (Dex) and 5αTHB ……160

Figure 3.20: Combined control data from concentration-response experiments for dexamethasone and 5αTHB in combination with RU486……..……..161

Figure 3.21: Steroid effects on gene transcript abundance……...164

Figure 3.22: RU486-mediated antagonism of dexamethasone-mediated changes in gene expression in the mouse aorta …….……166

Figure 3.23: RU486-mediated antagonism of 5α-Tetrahydrocorticosterone (5αTHB)-mediated changes in gene expression in the mouse aorta ……..…..167

Figure 4.1: 5αTHB only competed for binding to the glucocorticoid receptor (GR) ligand binding domain (LBD) at high concentrations……..189

Figure 4.2: Representative images from a preliminary immunofluorescence screen of the effects of dexamethasone (dex, 100 nM) and 5αTHB (1μM, 3μM or 10μM) to cause GR nuclear translocation in serum starved A549 cells.……..191

Figure 4.3: Quantification of a preliminary immunofluorescence screen of the effects of dexamethasone (Dex, 100 nM) or 5αTHB (1μM, 3μM or 10μM) on GR nuclear translocation in serum starved A549 cells.……...192

Figure 4.4: Immunofluorescence optimisation: Comparing background signal and dynamic range between two primary antibodies……..195

Figure 4.5: Negative immunofluorescence controls demonstrate auto-fluorescence from fixed A549 cells in the green emission spectrum..……..……..…..196

Figure 4.6: Unfixed A549 cells do not auto-fluoresce in the green or red emission spectra.…….….197

Figure 4.7: Paraformaldehyde-fixed A549 cells auto-fluoresce in the green, but not the red, emission spectra.…….….198

Figure 4.8: Qualitative assessment of GR nuclear translocation in fixed A549 cells was improved using the red emission spectra for immunofluorescence analysis in comparison to green…….....200

Figure 4.9: Quantitative comparison between immunofluorescence analysis in red and green emission spectra, and of two different quantification methods....…..…..201

Figure 4.10: Method development for Western blot……..…...……203

Figure 4.11: GR nuclear translocation occurred after dexamethasone (Dex) but not 5α-tetrahydrocorticosterone (5αTHB) treatment…….……205

Figure 4.12: Dexamethasone caused glucocorticoid receptor (GR) translocation into the nucleus, whereas 5α-tetreahydrocorticosterone (5αTHB) did not..……..…..206

Figure 4.13: 5αTHB did not stimulate co-regulator peptides to interact with the glucocorticoid receptor ligand binding domain (LBD)..……..…….208

Figure 4.14: ELISA standard curves for measuring IL6 and TNFα cytokine concentrations……...210

Figure 4.15: In murine bone marrow-derived macrophages (BMDM) stimulated with 100 ng/mL LPS, hydrocortisone (HC) induced a concentration-dependent suppression of IL6 release whereas 5αTHB did not.……...…….212

Figure 4.16: In mouse bone marrow-derived macrophage cells (BMDM) stimulated with 3 ng/mL LPS, hydrocortisone (HC) induced a concentration-dependent suppression of IL6 release whereas 5αTHB had no effect.……...……...214

Figure 4.17: In mouse bone marrow-derived macrophages (BMDM) stimulated with 3 ng/mL LPS, hydrocortisone (HC) induced a concentration -dependent suppression of TNFα release, whereas 5αTHB had no effect…….……...…..216

Figure 5.1: The proportion of genes which became differentially expressed at an early, intermediate, or late time point after dexamethasone treatment of human peripheral blood-derived macrophages.……236

Figure 5.2: The proportion of genes which became differentially expressed at an early, intermediate, or late time point after 5αTHB treatment of human peripheral blood-derived macrophages.……..…236

Figure 5.3: A Venn diagram demonstrating the number of differentially expressed genes in human peripheral blood mononuclear cells after dexamethasone and 5αTHB treatments respectively.……..…...239

Figure 5.4: Gene Ontology Biological process clusters enriched for genes which were (a) differentially expressed (both up-regulated and down-regulated genes), (b) up- regulated, or (c) down-regulated in human peripheral blood-derived macrophages between 0-24 hours after dexamethasone (100 nM) treatment.……..……..241

Figure 5.5: Gene Ontology Biological process clusters which were significantly enriched ($p<0.05$) in genes which were (a) differentially expressed (either up- and down-regulated), (b) up-regulated or (c) down-regulated (both adjusted $p<0.05$) in human peripheral blood-derived macrophages between 0-24 hours after treatment with 5αTHB (1 μM)……..……243

Figure 5.6: KEGG pathways (at p value<0.05) which were significantly enriched for (a) all differentially-expressed genes, (b) up-regulated genes, and (c) down-regulated genes in human peripheral blood derived macrophages between 0-24 hours after treatment with dexamethasone (100 nM)……..…...245

Figure 5.7: KEGG pathways (at p value<0.05) which were significantly enriched for (a) all differentially expressed genes and (b) up-regulated genes in human blood derived macrophages between 0-24 hours after treatment with 5αTHB (1 μM).....247

Figure 5.8: A list of the top 20 GO Biological process clusters which were enriched in genes found to be (a) differentially expressed (in either direction), (b) up-regulated or (c) down-regulated between 0-24 hours after dexamethasone (100 nM) treatment, but not by 5αTHB treatment, in human peripheral blood macrophage cells…..….249

Figure 5.9: GO Biological process clusters which were enriched in the list of genes found to be (a) differentially expressed (in either direction), (b) up-regulated and (c) down-regulated between 0-24 hours after treatment with 5αTHB, but not by treatment with dexamethasone, in human peripheral blood macrophage cells……251

Figure 5.10: KEGG pathways which were enriched in the genes regulated only by dexamethasone (100 nM) (and not by 5αTHB) between 0-24 hours after treatment in human peripheral blood macrophages. Heat map (a) uses both up-regulated and down-regulated genes to determine enriched processes, whereas heat maps (b) and (c) use only genes which were up-regulated or down-regulated, respectively…….253

Figure 5.11: KEGG pathways which were enriched in the genes regulated only by 5αTHB (1 μM) between 0-24 hours after treatment in human peripheral blood macrophages. Heat map (a) gives the KEGG pathways which were enriched in the list of all genes differentially regulated by 5αTHB, and heat map (b) are gives the KEGG pathways which were enriched in only the up-regulated genes. There were no enriched KEGG pathways in the down-regulated genes……..……255

Figure 5.12: GO Biological process clusters which were enriched in the list of genes which were commonly differentially expressed between 0-24 hours after both 5αTHB (1 μM) and dexamethasone (100 nM) treatment. (a) are the GO Biological processes which were enriched by this total gene list, and (b) are the biological processes which were enriched only for the up-regulated genes. There were no enriched GO biological processes by the down-regulated genes.……....257

List of Tables

Table 2.1: Details of primers and probes for real-time PCR analysis of murine genes using Roche Universal Probe Library (UPL).……104

Table 2.2: Details of primary antibodies used for protein detection by Western blot……108

Table 2.3: Secondary antibodies used for fluorescence detection of proteins by Western blot...……...109

Table 2.4: Secondary antibodies used for chemiluminescence detection of proteins by Western blot…….…….110

Table 3.1: Stimulation and treatment combinations for mouse aortic ring experiments, to investigate steroid effects on angiogenesis.……..…….127

Table 3.2: The optimum cell plating conditions chosen for use with the Essen Bioscience cell migration scratch wound assay.…….……...131

Table 3.3: The optimum analysis parameters chosen for 'confluence' and 'wound' masks to be accurately applied to images, using the Incucyte® analysis software package (Essen Bioscience).…….132

Table 3.4: A summary of the effects of steroids on angiogenesis in a murine aortic ring model after 7 days……..151

Table 5.1: A description of the comparisons undertaken vs (relative to) vehicle treated cells.……..232

Table 5.2: A summary of the gene lists generated from a microarray comparing dexamethasone and 5αTHB effects on gene expression in human peripheral blood derived macrophages……238

Table of Abbreviations

11βHSD	11β Hydroxysteroid Dehydrogenase
5αR	5α Reductase
5αTHB	5α Tetrahydrocorticosterone
AF	Activation Function
ANOVA	Analysis of Variance
AP1	Activator Protein 1
BMDM	Bone Marrow Derived Macrophages
CBG	Corticosteroid-Binding Globulin
cDNA	Complementary DNA
cGR	Cytoplasmic Glucocorticoid Receptor
COL	Collagen
CXCL5	C-X-C Motif Chemokine 5
DBD	DNA Binding Domain
DMEM	Dulbecco's Modified Eagle Media
DMSO	Dimethyl Sulfoxide
DNA	Deoxyribonucleic Acid
DUSP1	Dual Specificity Phosphatase 1
EC50	Half maximal Effective Concentration
ECM	Extracellular Matrix
EDTA	Ethylenediaminetetraacetic Acid
EGF	Epidermal Growth Factor

EndMT	Endothelial-Mesenchymal Transition
FBS	Foetal Bovine Serum
FKBP4	FK506-binding protein 4
FKBP5 (or FKBP51)	FK506-binding protein 51
GABA	Gamma-Aminobutyric acid
GC	Glucocorticoid
GR	Glucocorticoid Receptor
GRdim	GR dimerisation defective mouse
GRE	Glucocorticoid Response Element
HPA	Hypothalamic Pituitary Axis
HRP	Horseradish Peroxidase
HSD11B1	11β-Hydroxysteroid dehydrogenase type 1
HSP	Heat Shock Protein
HUVEC	Human Umbilical Vein Endothelial Cells
IL6	Interleukin 6
INOS	Inducible Nitric Oxide Synthase
LBD	Ligand Binding Domain
LPS	Lipopolysaccharide
MAPK	Mitogen Activated Protein Kinase
MARCoNI	Microarray Assay for Real-time Coregulator Nuclear receptor Interaction
MCP1	Monocyte Chemoattractant Protein 1
mGR	membrane Glucocorticoid Receptor

miRNA	micro Ribonucleic Acid
MMP	Matrix Metalloproteinase
MR	Mineralocorticoid Receptor
N/C	Nuclear/Cytoplasmic
NFκB	Nuclear Factor kappa light chain enhancer of activated B cells
nGRE	negative Glucocorticoid Response Element
NLS	Nuclear Localisation Signal
NTD	N Terminal Domain
PBMC	Peripheral Blood Mononuclear Cell
PBS	Phosphate Buffered Saline
PECAM1	Platelet and Endothelial Cell Adhesion Molecule 1
PEPCK	Phosphoenolpyruvate Carboxykinase
PER1	Period circadian clock 1
qPCR	quantitative Polymerase Chain Reaction
RNA	Ribonucleic acid
rRNA	ribosomal Ribonucleic acid
RT	Room Temperature
RU486	Mifepristone
RWD	Relative Wound Density
SEGRA	Selective Glucocorticoid Receptor Agonist
SMC	Smooth Muscle Cells
STAT	Signal Transducer and Activator of Transcription proteins

TA	Transactivation
TAT	Tyrosine Aminotransferase
TBS-T	Tris-Buffered Saline supplemented with Tween 20
TF	Transcription Factor
TGFβ	Transforming Growth Factor beta 1
TLS	Tube Like Structure
TNFα	Tumor Necrosis Factor alpha
TR	Transrepression
VCAM1	Vascular Cell Adhesion Molecule 1
VEGF	Vascular Endothelial Growth Factor

Abstracts from thesis

Orals

Amber J Abernethie, A Gastaldello, C Mitchell, R Houtman, D Melchars, OC Meijer, PWF Hadoke, DEW Livingstone, BR Walker, R Andrew (2017). Safer anti-inflammatory glucocorticoids; understanding the therapeutic potential of 5α-tetrahydrocorticosterone. *Oral Presentation, BHF 4 year PhD Studentship Annual Student Meeting, April 2017.*

Posters

Amber J Abernethie, Giorgia Maltese, Dawn EW Livingstone, Annalisa Gastaldello, Ruth A Morgan, Brian R Walker, Patrick WF Hadoke, Ruth Andrew (2017). Improving the therapeutic index of topical anti-inflammatory steroids: angiostatic effects of 5α tetrahydrocorticosterone vs hydrocortisone. *Endocrine Abstracts (2017) 50 P006, Poster Presentation, Society for Endocrinology BES, November 2017.*

Amber J Abernethie, Annalisa Gastaldello, Dawn EW Livingstone, Giorgia Maltese, Brian R Walker, Patrick WF Hadoke, Ruth Andrew (2017). Understanding the therapeutic potential of 5α-tetrahydrocorticosterone. *Program of the 5th BHF Fellows Meeting, Queen's College Cambridge, UK, Poster Presentation, September 2017.*

Amber J Abernethie, Annalisa Gastaldello, Dawn EW Livingstone, Brian R Walker, Patrick WF Hadoke, Ruth Andrew (2017). 5α-Tetrahydrocorticosterone exhibits topical anti-inflammatory action with limited adverse effects on angiogenesis. *Annual Centre for Cardiovascular Science Symposium, Poster Prize Winner, June 2017.*

Amber J Abernethie, A Gastaldello, RA Morgan, C Mitchell, KJ McInnes, K Beck, A Odermatt, R Houtman, D Melchars, OC Meijer, PWF Hadoke, DEW Livingstone, BR Walker, R Andrew (2017). 5αTHB as a novel anti-inflammatory drug: The roles of the glucocorticoid and mineralocorticoid receptors. *Endocrine Abstracts (2017) 49 EP802, Poster Presentation, 19th European Congress of Endocrinology, May 2017.*

Amber J Abernethie, Annalisa Gastaldello, Dawn EW Livingstone, Brian R Walker, Patrick WF Hadoke, Ruth Andrew (2017). 5α-Tetrahydrocorticosterone exhibits anti-inflammatory action with limited adverse effects on angiogenesis. *British Cardiovascular Society Heart Journal (2017) 22, volume 103, Issue Suppl 2. Poster Prize Winner, Scottish Cardiovascular Forum, February 2017.*

Amber Abernethie, C Mitchell, A Gastaldello, RA Morgan, K Beck, A Odermatt, OC Meijer, R Houtman, M McEwan, PWF Hadoke, BR Walker, DEW Livingstone, R Andrew (2016). 5αTHB as a novel anti-inflammatory drug: GRappling for the mechanisms! *Annual Centre for Cardiovascular Science Symposium, Poster Prize Winner, June 2016.*

Publications from thesis

Gastaldello, A., D. E. Livingstone, A. J. Abernethie, N. Tsang, B. R. Walker, P. W. Hadoke and R. Andrew (2017). "Safer topical treatment for inflammation using 5alpha-tetrahydrocorticosterone in mouse models." *Biochem Pharmacol* ***129****: 73-84.*

Chapter 1:

Introduction

1. Introduction

Inflammatory and immune diseases are highly prevalent, causing significant morbidity and mortality worldwide, as well as high costs for society (Amaya-Amaya, Montoya-Sanchez et al. 2014, Straub and Schradin 2016). Examples include rheumatoid arthritis (RA), systemic lupus erythematosus (SLE) and multiple sclerosis (Straub and Schradin 2016). It is reported that almost 5% of the European population are affected by an autoimmune disease, and one of the most serious complications is the increased risk of cardiovascular disease (CVD) (Amaya-Amaya, Montoya-Sanchez et al. 2014, Generali, Folci et al. 2017). This is due both to a modulation of risk factors and to accelerated atherosclerosis and vascular damage resulting from the inflammatory condition (Amaya-Amaya, Montoya-Sanchez et al. 2014, Generali, Folci et al. 2017, Mahmoudi, Aslani et al. 2017). In fact in RA, which has an overall prevalence of 1% worldwide, an increased CVD risk is responsible for around 50% of premature deaths (Mahmoudi, Aslani et al. 2017). Inflammatory skin disease is also a huge burden, with eczema being reported to affect around 230 million people globally (Vos, Flaxman et al. 2012). The most effective anti-inflammatory agents known, for which 40 billion prescriptions are given out each year in the UK, are glucocorticoid (GC) steroid hormones (Nixon, Upreti et al. 2012, Yang, Ray et al. 2012, Newton 2013, Nixon, Andrew et al. 2013). However, GC therapy is associated with debilitating side effects, such as impaired wound healing, obesity, type 2 diabetes and osteoporosis (Wei, MacDonald et al. 2004, De Bosscher 2010, Nixon, Upreti et al. 2012, Yang, Ray et al. 2012, Nixon, Andrew et al. 2013). Much work has focused on improving GC therapies. An alternative therapy is the use of nonsteroidal anti-inflammatory drugs

(NSAIDS). However these also have adverse effects, particularly gastrointestinal (GI) toxicity characterised by GI irritation, ulcers and bleeding. NSAIDS work in different ways to GCs, mainly by inhibiting the cyclooxygenase (COX) enzymes involved in prostaglandin biosynthesis. Since the COX 1 isozyme is expressed mainly in the stomach, whereas high COX 2 levels are present in inflammatory cells, selective COX 2 inhibitors were produced in an attempt to eliminate the GI side-effects. These drugs seemed promising but later had to be withdrawn from the market when their more serious cardiovascular side effects were identified (Suthar and Sharma 2014). There remains a large unmet medical need for safer therapies that maintain anti-inflammatory properties comparable to GCs but lack adverse effects (Vandevyver, Dejager et al. 2013). This thesis will explore the properties of an alternative anti-inflammatory steroid, believed to have a better therapeutic index than conventional glucocorticoids.

1.1. Glucocorticoids

GCs (Figure 1.1) are steroid hormones composed of 21 carbon atoms and containing the general cyclo pentane perhydrophenanthrene ring structure as a scaffold. GCs such as hydrocortisone and dexamethasone are often administered pharmaceutically. However, GCs are also produced endogenously to enable the body to respond appropriately to stress (both emotional and physical) (De Bosscher 2010). GCs therefore have many roles in the regulation and maintenance of a wide variety of homeostatic and metabolic processes (De Bosscher 2010, Vandevyver, Dejager et al. 2013). One role is in the metabolism of glucose, reflected in the name glucocorticoid (glucose+ cortex+ steroid). The many functions of GCs make them essential for health, and indeed either chronic elevation or chronic reduction of endogenous glucocorticoids produce the pathological conditions Cushing's syndrome and

Addison's disease, respectively (Nixon, Upreti et al. 2012, Kadmiel and Cidlowski 2013). Tissues which possess high GC levels include the liver, adipose tissue, muscles and bone. GC function in muscle involves the breakdown of protein into amino acids. In Cushing's syndrome GC levels are chronically elevated leading to symptoms of muscle wasting, growth retardation in children, and myopathy (Stahn, Lowenberg et al. 2007). Osteoporosis is another symptom of Cushing's syndrome and occurs as a result of GC signalling in bone (Stahn, Lowenberg et al. 2007). Another important role of GCs is glucose homeostasis, since GCs stimulate gluconeogenesis and decrease glucose utilisation, acting in an antagonistic manner to insulin and ultimately increasing blood glucose levels (De Bosscher 2010). This is reflected in the common symptoms of insulin resistance and glucose intolerance in Cushing's syndrome (De Bosscher, Beck et al. 2010). GCs also have effects on fatty acid metabolism (De Bosscher 2010). These effects on glucose and fat metabolism result in a plethora of increased metabolic and cardiovascular risk factors in Cushing's syndrome, including central adiposity, dyslipidaemia, obesity, hypertension and type II diabetes (De Bosscher, Beck et al. 2010, Yang, Nixon et al. 2011).

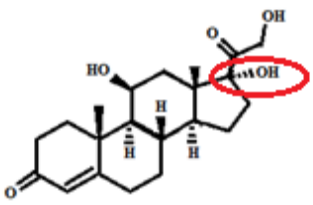

Cortisol / Hydrocortisone

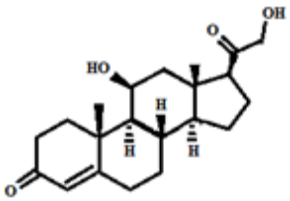

Corticosterone

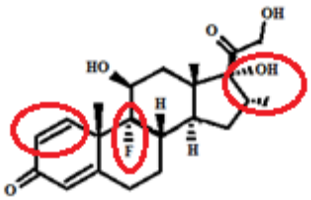

Dexamethasone

Figure 1.1: Glucocorticoid (GC) chemical structures. The endogenous GC in humans is cortisol (Nixon, Upreti et al. 2012), and in rodents is corticosterone, which is also present in human to a small extent (Nixon, Upreti et al. 2012, Chapman, Holmes et al. 2013). Dexamethasone is a synthetic GC which is commonly used pharmaceutically (Bledsoe, Montana et al. 2002, Nixon, Upreti et al. 2012, Kadmiel and Cidlowski 2013). Cortisol is also used as a pharmaceutical under the name 'Hydrocortisone'. Synthetic GCs have a similar structure to the natural GCs, but have been modified to achieve increased selectivity and binding at the glucocorticoid receptor (GR)(Nixon, Upreti et al. 2012).

Endogenous glucocorticoids are synthesised from the precursor cholesterol, in a series of enzymatic changes, known as 'steroidogenesis', mediated by hydroxysteroid dehydrogenases (HSD family) and cytochrome P450 oxidases (CYP family) (Figure 1.2)(Cain and Cidlowski 2017, Desmet and De Bosscher 2017, Clayton, Jones et al. 2018). Although local GC production has been reported in other tissue, including the thymus, intestine and skin, the major site of glucocorticoid steroidogenesis is in the cortex region of the adrenal glands (Cain and Cidlowski 2017, Clayton, Jones et al. 2018). Cortisol is the main endogenous human GC and corticosterone the main rodent GC, since rodents lack the adrenal 17α-hydroxylase enzyme. Corticosterone is also

present in humans, although it circulates at levels 10-30 times lower than cortisol (Nixon, Upreti et al. 2012). The synthesis and release of endogenous GC is controlled in a circadian and ultradian manner by the hypothalamic-pituitary-adrenal (HPA) axis (Figure 1.3) (Cain and Cidlowski 2017, Desmet and De Bosscher 2017, Clayton, Jones et al. 2018). The HPA axis can also be activated to produce GCs in response to various stressors (such as psychological distress, physical strain, tissue trauma and inflammatory cytokines) (Cain and Cidlowski 2017). In health, GCs can then act via negative feedback and limit their own production through suppression of the HPA axis (Clayton, Jones et al. 2018).

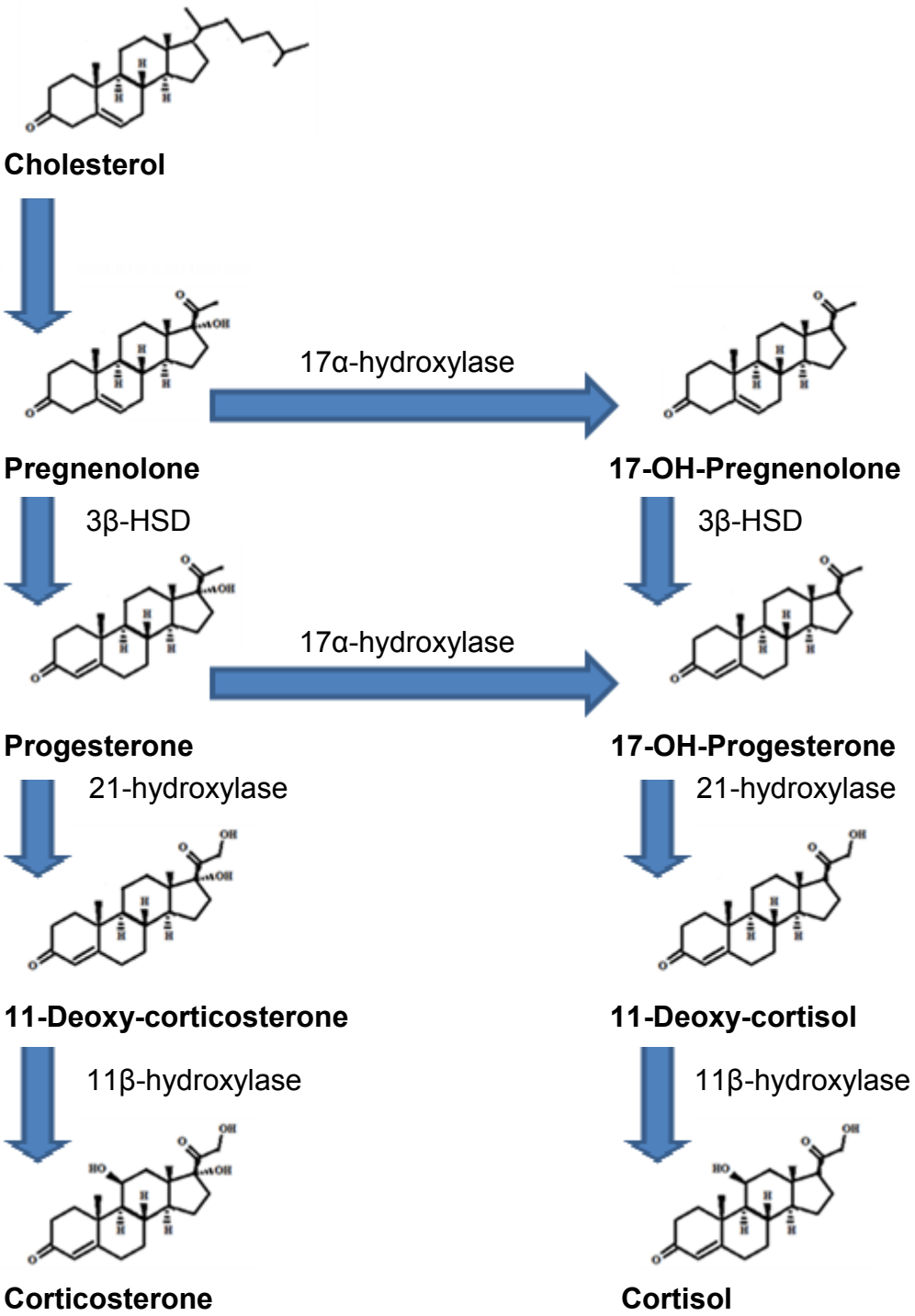

Figure 1.2: Glucocorticoid biosynthetic pathways occurring in the adrenal cortex. Glucocorticoids are synthesised from cholesterol through a series of reactions as shown. HSD = hydroxysteroid dehydrogenase.

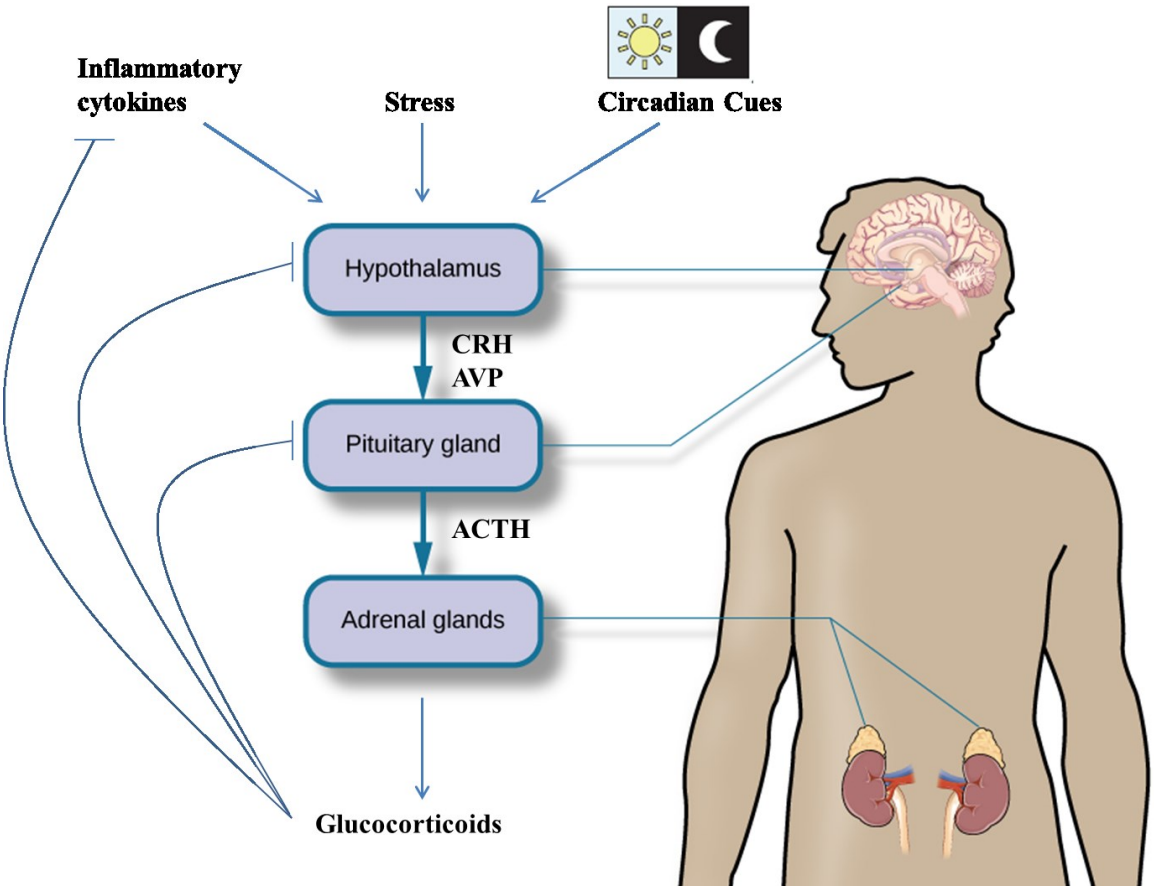

Figure 1.3: Glucocorticoid regulation by the hypothalamic-pituitary-adrenal (HPA) axis. In response to circadian cues, stress, or inflammatory cytokines, the hypothalamus produces corticotropin-releasing hormone (CRH) and arginine vasopressin (AVP), which then act on the anterior pituitary gland, causing it to synthesise and secrete adrenocorticotropin hormone (ACTH). When ACTH binds receptors on adrenocortical cells, steroidogenesis is stimulated and GC produced (Kadmiel and Cidlowski 2013, Cain and Cidlowski 2017). Image adapted from reference (Cain and Cidlowski 2017) and 'Psychology' book, 'Stress, lifestyle and health' chapter, by Eric B. Weiser, January 2014.

Once released into the circulation from the adrenal cortex, ~90% endogenous GC becomes bound to plasma proteins, mainly the plasma protein corticosteroid-binding globulin (CBG) whereas 10% remains unbound. CBG-bound GR is protected from metabolic degradation. Since GCs are small hydrophobic molecules the unbound fraction can readily diffuse across membranes and exert their biological effects (Nixon, Andrew et al. 2013), or are themselves metabolised in the liver and then excreted from either the kidney (95%) or gut (5%)(Schacke, Docke et al. 2002). However there is also evidence of selective active transport of glucocorticoids out of tissues. For example, the ATP (adenosine 5' –triphosphate)-binding cassette (ABC) transporters have been described which differentially transport cortisol and corticosterone out of target cells, providing further control over their availability (Nixon, Mackenzie et al. 2016). Although active systemic GC levels are controlled by the HPA axis, CBG protein in serum, and ABC transporters in cells, GC availability in tissues and cells can be further controlled enzymatically through the action of metabolic enzymes, best exemplified by 11β-hydroxysteroid dehydrogenases (11β HSDs). 11βHSD2 is able to convert the active GC (cortisol in human, corticosterone in rodent) into its inactive form (cortisone in human, 11-dehydrocorticosterone in rodent), whilst 11βHSD1 predominantly catalyses the reverse reaction (Draper and Stewart 2005, Walker 2007, Tiganescu, Walker et al. 2011, Chapman, Holmes et al. 2013). Differences in 11βHSD1 and 11βHSD2 abundance and activities, therefore, provide an extra control to determine GC sensitivity at a cell and tissue specific level. More recently my supervisor's group has shown that the enzyme 5α-reductase 1 (5αR1) also modulates GC activity (Livingstone, Di Rollo et al. 2014, Livingstone, Di Rollo et al. 2017). The 5α-reductases convert GCs into their 5α-reduced forms and are involved in GC

clearance in the liver as the first step of increasing polarity to promote excretion. Aside from the liver, 5αR1 is also expressed in other metabolic tissues such as adipose and skeletal muscle (Russell and Wilson 1994, Upreti, Hughes et al. 2014). The loss or inhibition of 5αR1 has been linked to an adverse metabolic phenotype in humans and rodents including development of a fatty liver, decreased insulin sensitivity, increased weight gain, as well as HPA suppression, all of which are consistent with the effects of GC excess (Livingstone, Di Rollo et al. 2014, Livingstone, Barat et al. 2015).

Once inside a target cell, GCs exert their main effects through binding to the glucocorticoid receptor (GR; unified nuclear receptor nomenclature NR3C1) which is expressed in almost all cells and tissues (De Bosscher 2010, Kadmiel and Cidlowski 2013). Endogenous GCs can also bind to the Mineralocorticoid receptor (MR, NR3C2) with a 10 fold higher affinity than they do to the GR (Schacke, Docke et al. 2002, Vandevyver, Dejager et al. 2013). However, although GC binding to MR is important for some physiological effects, GC selectivity for GR is achieved in most cellular contexts due to the more limited/ tissue specific expression of MR, and also as a result of the activity of the 11βHSD2 isozyme which is often co-expressed with MR. Hence, 11βHSD2 provides a barrier against GC binding to MR, achieving GR selectivity (Nixon, Andrew et al. 2013). Many synthetic glucocorticoids (such as dexamethasone) also exist which, in contrast, often do not bind MR since they were designed to be selective for GR.

1.2. The Glucocorticoid Receptor

The glucocorticoid receptor is a 94 kD modular protein. It is a member of the nuclear receptor superfamily of transcription factors which includes the progesterone receptor (PR), androgen receptor (AR), estrogen receptor (ER) and mineralocorticoid receptor (MR) (Kadmiel and Cidlowski 2013, Nixon, Andrew et al. 2013, De Bosscher, Beck et al. 2016). GR is activated through ligand binding, with different ligands resulting in distinct conformational changes and, hence, a different spectrum of effects. Encoded by the *NR3C1* gene, GR consists of 9 exons (Kino 2000, Cain and Cidlowski 2017). Exon 1 is an untranslated region, exon 2 encodes an N-terminal transactivation domain (NTD), exons 3 and 4 encode a DNA-binding domain (DBD), and exons 5-9 encode a ligand binding domain (LBD) as well as a hinge region which separates the DBD and LBD (Kino 2000). Like the other nuclear receptors, GR is therefore composed of three major functional domains: The NTD, DBD and LBD (Figure 1.4)(Kadmiel and Cidlowski 2013, Cain and Cidlowski 2017).

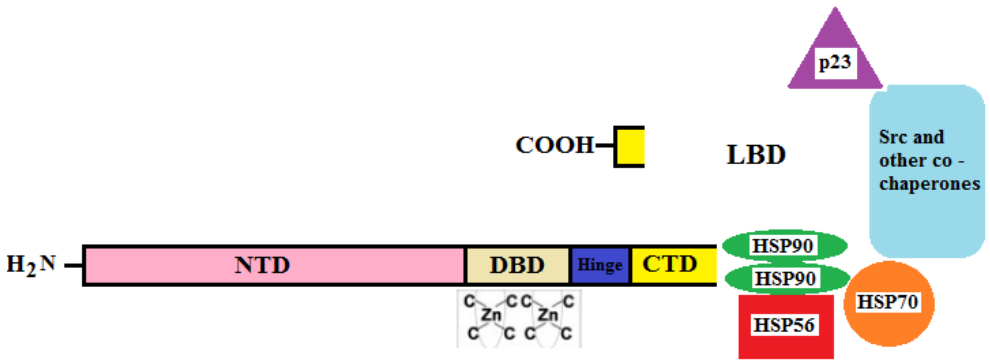

Figure 1.4: Domain structure of the Glucocorticoid Receptor (GR). GR is composed of an N-terminal domain (NTD) including the AF1 transactivation region; a central DNA binding domain (DBD) region containing 'zinc fingers' responsible for binding DNA; and a C terminal domain (CTD) separated from the DBD by a hinge region. The C terminal domain contains another transactivation region AF2 , and also interacts with various stabilising proteins (for example Heat shock proteins (HSP) 90, 56 and 70, p23 and Src) as well as folding to form a ligand binding domain (LBD) where ligand becomes bound. Figure adapted from reference (Buttgereit, Straub et al. 2004).

1.2.1. Functional domains of GR

The NTD (residues 1-417) is the least conserved domain of GR (Kadmiel and Cidlowski 2013). This contains a transcriptional activation function (AF1) which mediates binding to diverse molecules necessary for the initiation of transcription, such as coactivators, chromatin modulators, and transcriptional machinery (Kino 2000, Kadmiel and Cidlowski 2013). Whereas in its basal state AF1 is relatively unfolded, it adopts a more complex helical structure in response to binding of cofactors (Kino 2000). It also contains several serine residues (S203, S211 and S226) capable of being phosphorylated to modulate GR function (Nixon, Andrew et al. 2013).

The central DBD (residues 418-487) is the most conserved region throughout the nuclear receptor superfamily (Kino 2000, Kadmiel and Cidlowski 2013). It contains two zinc finger motifs, each composed of a zinc ion held between four cysteine residues and followed by an α-helix (Kino 2000). The zinc finger motifs mediate genomic interaction with specific DNA sequences called glucocorticoid responsive elements (Kino 2000, Kadmiel and Cidlowski 2013, Cain and Cidlowski 2017). The DBD also contains a nuclear localisation function, a dimerisation interface, and has additional roles in transcription factor interaction (Schacke, Rehwinkel et al. 2006, De Bosscher 2010, Yang, Ray et al. 2012, Vandevyver, Dejager et al. 2013).

Finally, the well conserved C terminal LBD is comprised of 11 α-helices and 4 small β-sheets that fold to form a hydrophobic pocket for high affinity binding to specific ligands (Kino 2000, Kadmiel and Cidlowski 2013, Cain and Cidlowski 2017). The LBD also contains a transcriptional activation function (AF2) to recruit

coactivators in a ligand dependent manner (Yang, Ray et al. 2012). Like the DBD, the LBD is also involved in nuclear localisation and dimer formation (De Bosscher 2010).

1.2.2. 'Classical' genomic signalling by GC

Many mechanisms exist by which GC exert their effects. These mechanisms are complex and depend on the ligand structure. The 'classical' GC signalling mechanism involves its binding to GR, followed by translocation of GR into the nucleus, where GR either binds to DNA or to other transcription factors, resulting in direct or indirect gene regulation, respectively. These components of 'classical GC signalling' are described in sections 1.2.2.1 – 1.2.2.3. However, it is now known that signalling by GC is much more complex, and additional mechanisms are described in 1.2.3.

1.2.2.1. GR binding and nuclear translocation

In the absence of ligand, GR is reported to constantly shuttle through the nuclear pore channel between the nucleus and cytoplasm but to reside predominantly in the cytoplasm (De Bosscher 2010, Yang, Ray et al. 2012, Vandevyver, Dejager et al. 2013). In the cytoplasm, GR exists as part of a multiprotein complex (Cain and Cidlowski 2017, Scheschowitsch, Leite et al. 2017, Vandewalle, Luypaert et al. 2018) consisting of GR interacting with two molecules of HSP90, additional heat shock proteins (HSP70, HSP56), members of the Mitogen-activated protein kinase (MAPK) family, and other chaperones and co-chaperones (p23, p60, Src, hop) (Stahn, Lowenberg et al. 2007, De Bosscher, Beck et al. 2010, Yang, Ray et al. 2012, Chinenov, Gupte et al. 2013, Vandevyver, Dejager et al. 2013, Keenan, Lew et al.

2016, Scheschowitsch, Leite et al. 2017, Whirledge and DeFranco 2018). These interactions are required for efficient folding of GR into a stable conformation, preventing its degradation and enhancing its affinity for ligand (Kino 2000). The region of GR responsible for forming these stabilising interactions is demonstrated in figure 1.4 and is close to the ligand binding domain (Stahn, Lowenberg et al. 2007, De Bosscher, Beck et al. 2010, Yang, Ray et al. 2012, Chinenov, Gupte et al. 2013, Vandevyver, Dejager et al. 2013). Additionally the complex contains an immunophilin, which is either FK506 binding protein 51 (FKBP4) or FK506 binding protein 52 (FKBP5)(Bekhbat, Rowson et al. 2017). FKBP4 and FKBP5 compete with each other for binding to HSP90 (Bekhbat, Rowson et al. 2017). Whereas interaction with FKBP4 stimulates GR nuclear translocation, this movement is inhibited by FKBP5, which is reported to have a reduced interaction with dynein and also to mask nuclear localisation signals (NLS) (Bekhbat, Rowson et al. 2017, Clayton, Jones et al. 2018).

Upon ligand binding to the GR LBD, a conformational change takes place in the receptor, resulting in partial dissociation of the complex, and in FKBP5 replacement with FKBP4 (Keenan, Lew et al. 2016, Cain and Cidlowski 2017, Desmet and De Bosscher 2017, Clayton, Jones et al. 2018, Vandewalle, Luypaert et al. 2018). This conformational change exposes NLS and results in GR now favouring nuclear import over nuclear export, as the NLS interacts with dynein (a motor protein) and dynein then associates with microtubules to transport the GR complex to the nuclear pore (Bekhbat, Rowson et al. 2017, Scheschowitsch, Leite et al. 2017). At the nuclear pore GR interacts with importins and nucleoporins, allowing it to enter the nucleus, dissociate from further chaperones and induce its genomic effects (Scheschowitsch,

Leite et al. 2017). The extent of GR nuclear translocation is, therefore, in part dictated by the balance of FKBP4 and FKBP5, as well as by exposure of NLS (of which there are two for GR: NL1 and NL2), which often depends on the ligand structure (Kino 2000, Bekhbat, Rowson et al. 2017, Scheschowitsch, Leite et al. 2017). Once in the nucleus GR modulates gene transcription. The ligand receptor complex is then degraded, as GR dissociates from the ligand and is cleared from DNA (Kino 2000). GR is then recycled, slowly translocating back to the cytoplasm, reportedly mediated by the Ca^{2+} binding protein calreticulin, and finally the GR chaperone complex reforms (Kino 2000, Cain and Cidlowski 2017).

1.2.2.2. Direct gene regulation by GR (Transactivation)

One of the most widely reported mechanisms of gene regulation is the direct binding of GR, using the two zinc fingers contained within its DBD, to glucocorticoid response elements (GREs) in the promoter regions of target genes (Kino 2000). Classical GREs consist of inverted repeats of hexameric half sites separated by a sequence of three base pairs, with the consensus sequence GGAACAnnnTGTTCT, where 'n' is any base (Cain and Cidlowski 2017). Each half site binds one GR molecule, and these two bound GR molecules form multiple contacts and subsequently dimerise (Kino 2000); although it is still under debate whether the dimerisation occurs prior to DNA binding and in which subcellular compartment (Scheschowitsch, Leite et al. 2017). GR binding and dimerisation results in a conformational change (Scheschowitsch, Leite et al. 2017) and leads to the recruitment of coactivator proteins via the GR activation functions AF-1 and AF-2 (Kino 2000, Keenan, Lew et al. 2016, Whirledge and DeFranco 2018). Examples of these coactivator proteins are the steroid receptor coactivator 1 (SRC1, also known as NCOA1), glucocorticoid receptor-

interacting protein 1 (GRIP1, also known as NCOA2), and p300/CBP (Keenan, Lew et al. 2016, Cain and Cidlowski 2017). The recruitment of coactivator proteins induces chromatin remodelling, subsequently allowing the pre-initiation complex to form (including the recruitment of RNA polymerase II) and resulting in the activation of gene transcription (Keenan, Lew et al. 2016, Cain and Cidlowski 2017). Variation in GRE sequences, such as the 3 non-specific spacer nucleotides, influences the 3D structure of the bound GR dimer, leading to variations in its surface conformation (Kino 2000, Scheschowitsch, Leite et al. 2017). This in turn determines which transcriptional co-activators and chromatin-remodelling complexes are recruited, and modulates the transcriptional output of GR (Kino 2000, Scheschowitsch, Leite et al. 2017). The DNA GRE sequence itself is, therefore, described to be critical in determining GR transcriptional activity (Kino 2000, Cohen and Steger 2017, Scheschowitsch, Leite et al. 2017), although other mechanisms are also involved in directing GR to these sites (Desmet and De Bosscher 2017). This mechanism of action, demonstrated in figure 1.5a, is known as transactivation (TA) and these dimeric GRE sites are mainly associated with an increase in gene expression (Cohen and Steger 2017).

1.2.2.3. Indirect gene regulation by GR (Transrepression)

GR can also indirectly regulate gene transcription, and the main mechanism through which it does this is by targeting transcription factors. This alternative mode of GR-mediated gene regulation occurs when GR monomers (Scheschowitsch, Leite et al. 2017) physically interact with, or 'tether', to another transcription factor without contacting DNA, although the TF may or may not be bound to DNA itself (Cain and Cidlowski 2017, Desmet and De Bosscher 2017, Scheschowitsch, Leite et al. 2017,

Vandewalle, Luypaert et al. 2018). This protein-protein interaction, demonstrated in figure 1.5d, alters the ability of both GR and the tethered transcription factor to influence gene transcription, such as by modulating their ability to bind DNA or to recruit co regulators and the transcriptional machinery (Kino 2000, Cain and Cidlowski 2017). The process has been termed transrepression (TR) and is usually associated with gene down-regulation (Desmet and De Bosscher 2017). It is reported to be particularly important for the suppression of inflammatory and immune responses by glucocorticoids (Kino 2000, Cain and Cidlowski 2017).

1.2.3. Additional 'non-classical' genomic GC signalling

Increases and decreases in gene expression were originally assumed to largely depend on transactivation (1.2.2.2) and transrepression (1.2.2.3) mechanisms, respectively. However, the situation is now known to be more complex. Direct GR binding to DNA can also result in *suppression* of gene expression, whereby GR interacts with repressive DNA motifs, termed negative GREs (nGREs)(figure 1.5b)(Kino 2000, Cain and Cidlowski 2017, Cohen and Steger 2017, Scheschowitsch, Leite et al. 2017). nGREs consist of an inverted palindrome separated by 0-2 nucleotide pairs, with the consensus sequence CTCC(n)$_{0\text{-}2}$GGAGA (Kino 2000, Cain and Cidlowski 2017). Two monomers bind to nGREs with inverted polarity compared to how they bind GREs (Bekhbat, Rowson et al. 2017). Whereas at GRE the GR monomers bind on the same side of the DNA strand in a head to head fashion, at a nGRE they bind in a head to tail fashion on opposite sides of DNA (Kino 2000, Bekhbat, Rowson et al. 2017, Vandewalle, Luypaert et al. 2018). This orientation prevents GR dimerization (Bekhbat, Rowson et al. 2017, Scheschowitsch, Leite et al. 2017), ensuring that two single monomers are bound to nGREs (Scheschowitsch, Leite

et al. 2017), and leading to the formation of a repressing complex through the recruitment of histone deacetylases and of co-repressors such as nuclear receptor co-repressor 1 (NCOR1) and silencing mediator of retinoid and thyroid hormone receptors (SMRT) (Keenan, Lew et al. 2016, Cain and Cidlowski 2017, Vandewalle, Luypaert et al. 2018). This results in the suppression of gene transcription (Keenan, Lew et al. 2016, Scheschowitsch, Leite et al. 2017). In addition to GREs and nGREs, half site GREs are now also known to exist (figure 1.5c). These consist of only half of the classic GRE binding sequence (Desmet and De Bosscher 2017). GR binds to half site GREs as a monomer (Cohen and Steger 2017, Desmet and De Bosscher 2017, Scheschowitsch, Leite et al. 2017, Clayton, Jones et al. 2018), and has already been shown to drive transcription in both liver and primary macrophages in this way (Scheschowitsch, Leite et al. 2017). Interestingly, it was demonstrated in mouse liver that, under physiological conditions, GR monomer binding to half site motifs occurs more frequently than GR dimer binding to GREs (De Bosscher, Beck et al. 2016, Scheschowitsch, Leite et al. 2017), whilst administration of exogenous GCs causes a preference for GR homodimer binding at GRE sites, which occurs at the cost of monomer binding to half site GREs (De Bosscher, Beck et al. 2016, Vandewalle, Luypaert et al. 2018). It has, therefore, been suggested that GR monomers are more important for the physiological roles of GCs, and GR dimers for the pharmaceutical and stress functions (Vandewalle, Luypaert et al. 2018). Another layer of complexity is added by the fact that GR has also recently been reported to form heterodimers with MR and regulate gene expression this way (Trapp, Rupprecht et al. 1994, Liu, Wang et al. 1995, Savory, Prefontaine et al. 2001, Mifsud and Reul 2016). Furthermore, as well as translocating into the cell nucleus (Kino 2000) the ligand bound GR is also

reported to translocate into mitochondria and bind to mitochondrial DNA, stimulating gene expression and mediating apoptosis (Cain and Cidlowski 2017).

Additionally, indirect methods of gene regulation other than transrepression exist. GR may compete with other TFs for essential co-activators, preventing TF activity (Cain and Cidlowski 2017). Furthermore, in a slight variation of the TR mechanism, GR may interact with transcription factors whilst itself bound to DNA. This typically occurs at DNA sites containing both a responsive element for a distinct transcription factor as well as a half site GRE (Figure 1.5e) (Kino 2000, Cain and Cidlowski 2017, Whirledge and DeFranco 2018). This type of site is known as a 'composite element' (Kino 2000, Cain and Cidlowski 2017, Vandewalle, Luypaert et al. 2018) and monomer binding at these sites has also been suggested to stabilise the interaction between monomer and nearby TFs in a process known as 'half site facilitated tethering' (Cohen and Steger 2017, Desmet and De Bosscher 2017). Binding at composite elements can lead to gene repression due to an interruption in TF-DNA binding, as described for the TR mechanism. However, it can also lead to gene activation in some cases, and this has been explained in terms of the bound TFs acting as pioneer factors in order to facilitate access of GR to the GRE half site. This mechanism is known as 'assisted loading' and alternatively (depending on the binding site composition and local chromatin conditions) may involve GR acting as the pioneer factor to aid TF binding to its response element (Kino 2000). Whether gene induction or suppression occurs at a composite element often depends on the TF subunit composition, with both directions of GR regulation being described for various STAT family members as well as for AP1 depending on the context (Cain and Cidlowski 2017).

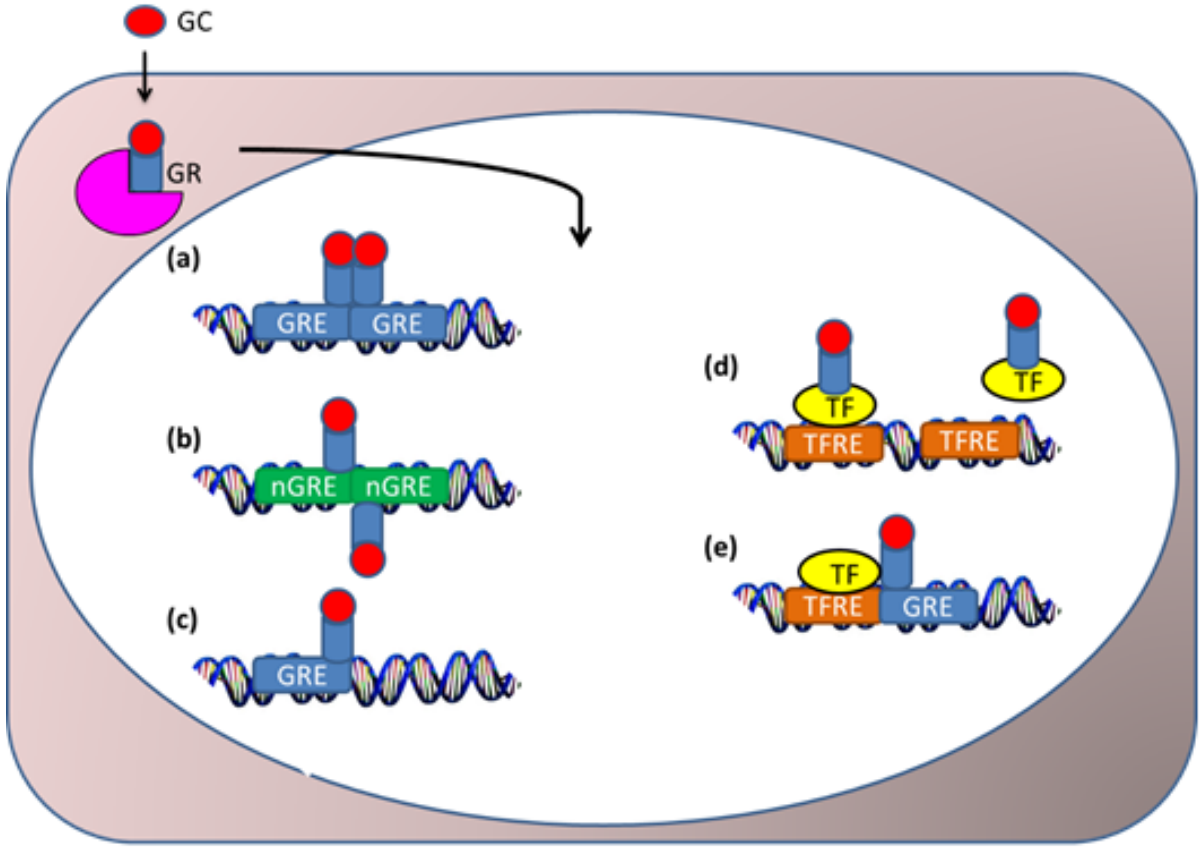

Figure 1.5: Genomic signalling mechanisms of the Glucocorticoid Receptor (GR): Glucocorticoids (GC) diffuse through cell membrane and bind to GR, causing it to dissociate from a stabilising complex and translocate into the nucleus to exert its effects. In a mechanism known as Transactivation (a) GR may bind as a homodimer to glucocorticoid response elements (GRE) in the promoter region of target genes, which is usually associated with gene activation. It may also bind negative GRE (nGRE) as two GR monomers (b), usually associated with gene down regulation, or may bind as a monomer to a half-site GRE (c). Alternatively, GR monomers may tether to and suppress the activity of transcription factors (TF)(d) which are either unbound or bound to TF response elements (TFRE) on target genes. They may also bind at a 'composite element' € which has both a GRE for a GR monomer, and a TFRE for a TF. DNA helices are modified from the following source: http://www.funkidslive.com/events/its-dnas-60th-birthday/#

1.2.4. Non-genomic signalling of GCs

Aside from genomic mechanisms which target DNA or transcription factors to regulate transcription/translation, *non-genomic* GC signalling is also known to occur and is thought to be particularly important for rapid GC effects. Whereas genomic GC effects usually occur within a few hours, more rapid GC actions have been demonstrated which, in contrast, occur within minutes. Non-genomic effects are reported to clearly contribute to the physiological and pharmaceutical effects of GCs, including the suppression of inflammation, as described in detail in section 1.3. GC modulation of brain function and behaviour is known to involve non-genomic mechanisms (Haller, Mikics et al. 2008) as is HPA axis regulation (Song and Buttgereit 2006). The mechanisms underpinning these non-genomic effects are diverse and vary according to the cell, tissue, species and steroid. However, they do appear to overlap and share some common signalling pathways; for example often involving calcium ions, protein kinase C (PKC), phospholipase C (PLC), cyclic adenosine monophosphate (cAMP), mitogen-activated protein kinases (MAPK), and tyrosine kinases (Wehling 1997, Falkenstein, Tillmann et al. 2000, Losel and Wehling 2003). Although a crossover between non-genomic and genomic mechanisms is known to exist it has not been widely explored (Haller, Mikics et al. 2008), and the genomic effects later arising from non-genomic signalling may be very important for function. (Losel and Wehling 2003).

One non-genomic mechanism involves non-specific interactions with cell membranes, during which steroids intercalate into cell and mitochondrial membranes, thus influencing their physiochemical properties, although very high concentrations of GC are often required for this (Stahn, Lowenberg et al. 2007, Strehl and Buttgereit

2013). However, non-genomic GC effects may alternatively involve GC binding to the cytoplasmic GR (cGR) or to a membrane bound receptor (Buttgereit and Scheffold 2002, Buttgereit, Straub et al. 2004, Song and Buttgereit 2006, Stahn, Lowenberg et al. 2007, Haller, Mikics et al. 2008, Strehl and Buttgereit 2013). cGR-mediated non-genomic effects are based on the fact that GC binding causes the stabilised GR-multi protein complex to dissociate (Strehl and Buttgereit 2013). This promotes the release of cofactors (including of Src, HSPs, kinases such as MAPKs, and immunophilins) which mediate non-genomic intra-cellular signalling (Buttgereit and Scheffold 2002, Buttgereit, Straub et al. 2004, Stahn, Lowenberg et al. 2007, Haller, Mikics et al. 2008, Strehl and Buttgereit 2013). Alternatively, specific non-genomic effects of GCs can also occur through binding to receptors other than the classical GR. One example is the membrane variant of this receptor termed membrane GR (mGR)(Stahn, Lowenberg et al. 2007). mGR originates from the same gene as cGR but is suggested to vary through differential splicing, promoter switching or post translational editing (Stahn, Lowenberg et al. 2007). mGR was originally only known to exist in amphibian neuronal membranes, lymphoma and leukaemia cells (Buttgereit and Scheffold 2002, Buttgereit, Straub et al. 2004, Song and Buttgereit 2006, Stahn, Lowenberg et al. 2007). It was later identified in PBMCs (monocytes and B lymphocytes) with the use of a high sensitivity immunofluorescence technique (Buttgereit, Straub et al. 2004, Stahn, Lowenberg et al. 2007). mGR exerts rapid effects through phosphorylation and dephosphorylation processes (Strehl and Buttgereit 2013). cGR and mGR have a similar capacity for binding to HSP and DNA binding, and they also possess similar phosphorylation patterns (Mitre-Aguilar, Cabrera-Quintero et al. 2015). However, there are also differences between mGR and cGR (as well as the difference in location)

such as different molecular weights and, interestingly, different ligand binding specificities. An example is that, whereas mGR was reported to bind dexamethasone and aldosterone but not hydrocortisone, cGR is known to bind hydrocortisone (Powell, Watson et al. 1999, Mitre-Aguilar, Cabrera-Quintero et al. 2015).

A receptor other than the classical GR and mGR, through which non-genomic effects have been proposed to be mediated, is a 63 kDa acidic glycoprotein (Mitre-Aguilar, Cabrera-Quintero et al. 2015), possessing completely different pharmacological characteristics from mGR, and originally described to share similarities with opioid receptors (Losel and Wehling 2003). Interestingly, cortisol and corticosterone bind to this receptor with high affinity and specificity, but other classical GR ligands such as dexamethasone and aldosterone do not (Rose and Moore 1999, Falkenstein, Tillmann et al. 2000, Mitre-Aguilar, Cabrera-Quintero et al. 2015). However, a whole series of membrane proteins capable of GC binding appear to exist not just on the plasma membrane but also on other membranes such as the endoplasmic reticulum, intra cytoplasmic vesicles and mitochondria (Haller, Mikics et al. 2008). Glucocorticoid effects are also known to be mediated through allosteric actions at receptors for other hormones, and this has been reported for the GABA receptor (Tasker, Di et al. 2006). GABA receptors are proteins with allosteric binding sites not just for GABA neurotransmitters but also for benzodiazepines and barbiturates (Falkenstein, Tillmann et al. 2000). 3α,5α-tetrahydroprogesterone (3α5αTHP) and 3α,5α-tetrahydrodeoxycorticosterone (3α,5αTHDOC) were the first steroids demonstrated to modulate neuronal excitability through interaction with GABA (Falkenstein, Tillmann et al. 2000) and a 3α OH group in the steroid A ring seems to allow the positive allosteric interaction.

1.4. Achieving cell- and tissue-specific regulation by GR

Despite ubiquitous expression of GR, and the fact that all cells have the same set of genes, the effects of GR are cell, tissue, context, and ligand specific (Cohen and Steger 2017, Vandewalle, Luypaert et al. 2018). This is because multiple factors determine responsiveness to GCs, hence leading to this specificity in GR transcriptional regulation.

1.4.1. Chromatin Accessibility

Chromatin accessibility is one factor contributing to cell and tissue specificity of GC effects. Section 1.2.3 described the various types of GR binding sites on DNA, however the accessibility of the binding sites for GR and TF depends on the local chromatin structure (Cohen and Steger 2017, Scheschowitsch, Leite et al. 2017, Clayton, Jones et al. 2018). In eukaryotic cells, DNA associates with various nuclear proteins such as histones and chromatin modifying factors. It wraps 1.67 turns around a histone octamer to form the smallest structural unit called a 'nucleosome', which then compacts further into a higher order chromatin (Kino 2000). It has been shown that up to 95% of GR occupancy occurs in pre-existing regions of accessible chromatin. However, this takes up only a subset of the existing binding sites, as the rest are inaccessible due to being buried in repressive chromatin structures (Cohen and Steger 2017, Vandewalle, Luypaert et al. 2018). Chromatin structure is organised differently depending on the tissue and cell type, and this is one reason why GR binds and regulates different genes in a cell specific manner (Cohen and Steger 2017, Scheschowitsch, Leite et al. 2017, Vandewalle, Luypaert et al. 2018). *In vivo* work suggests that GR on its own cannot remodel chromatin in order to access DNA in nucleosomes (Cohen and Steger 2017). However once bound to DNA it can further

remodel chromatin and, therefore, stimulate binding of other TFs (or vice versa) in a mechanism known as 'assisted loading' described to occur at 'composite elements' in section 1.2.3.2 (Cohen and Steger 2017).

1.4.2. GR Isoforms

Alternative splicing and transcription initiation of the *NR3C1* gene gives rise to a variety of mRNA species. This and a further variety in translation initiation sites mean that many heterogeneous GR isoforms are produced, perhaps contributing to tissue specific functions (Kino 2000, Bekhbat, Rowson et al. 2017, Cain and Cidlowski 2017, Cohen and Steger 2017, Desmet and De Bosscher 2017, Clayton, Jones et al. 2018).

The human *GR* gene contains 9 exons, and alternative splicing of the terminal exon (exon 9) generates the two major and most widely studied isoforms, the classic GRα and the non-ligand binding GRβ, with molecular weights of 97 and 94 kilo-Daltons, respectively (Kino 2000, De Bosscher, Beck et al. 2016, Bekhbat, Rowson et al. 2017, Vandewalle, Luypaert et al. 2018). GRα and GRβ are both ubiquitously expressed and are highly homologous. They differ only after amino acid 727, after which GRα has an additional 50 amino acids in its C terminal region, whereas GRβ has an additional-non homologous 15 amino acids (Kino 2000).

GRα is the traditional receptor isoform (Kino 2000) which acts as a transcription factor to influence gene expression and accounts for the classical functions of GR (Kino 2000, Bekhbat, Rowson et al. 2017, Scheschowitsch, Leite et al. 2017, Vandewalle, Luypaert et al. 2018). In contrast, the GRβ isoform, does not bind glucocorticoid and cannot induce gene transcription in response to GC (Kino 2000, De Bosscher, Beck et

al. 2016, Bekhbat, Rowson et al. 2017, Vandewalle, Luypaert et al. 2018). This is because, whereas the NTD and DBD are the same in both isoforms, their LBD are different (Kino 2000). Specifically, helix 11 and 12 are disrupted in the LBD of GRβ, and these helices are crucial for forming the ligand binding pocket (Kino 2000, Cohen and Steger 2017). GRβ is able to interact with GREs in the nucleus using its DBD, and it is thought to negatively regulate the activity of the GRα isoform (De Bosscher, Beck et al. 2016, Bekhbat, Rowson et al. 2017, Cohen and Steger 2017, Scheschowitsch, Leite et al. 2017). Consistent with this, GRβ attenuated GRα-mediated transrepression of IL6 and TNFα genes (Kino 2000) and was also shown to have a negative effect on GRE-mediated transactivation by GCs, such as of the MKP-1 and PEPCK genes (Kino 2000). Clinical studies have also provided evidence that GRβ inhibits GRα activity, and increased GRβ expression is thought to be a mechanism of glucocorticoid resistance in inflammatory disease (Bekhbat, Rowson et al. 2017). Cytokine signalling increases expression of GRβ relative to GRα, and increased GRβ expression is associated with reduced sensitivity to GCs in patients with various inflammatory and immune system diseases (Kino 2000, Cohen and Steger 2017, Vandewalle, Luypaert et al. 2018). GRβ has been proposed to act as an inhibitor through several mechanisms. This includes competing with GRα for GRE sites, binding directly to GRα to prevent its activity, or by using its AF1 domain to compete for co-activator proteins (Kino 2000). However, due to the low expression of GRβ in comparison to GRα, its inhibitory effect has been doubted by some and is not universally accepted (Bekhbat, Rowson et al. 2017). Interestingly, it was recently shown that GRβ has intrinsic transcriptional activity, independent of its effects to inhibit GRα-activity (Kino 2000, Keenan, Lew et al. 2016, Cain and Cidlowski 2017, Scheschowitsch, Leite et al. 2017).

For example, GRβ has been shown to stimulate STAT1 expression through GREs, and was shown to modulate gene expression both in GRα-dependent and -independent manners in the liver (Kino 2000). However, the physiological role of this activity is not yet known (Kino 2000). Furthermore, although currently there are no known endogenous ligands for GRβ, it has recently been demonstrated that it can bind the GR antagonist mifepristone (RU486) in the same ligand binding pocket and orientation as GRα (Lewis-Tuffin, Jewell et al. 2007, Ligr, Li et al. 2012, Min, Perera et al. 2018). Although GRβ is located predominantly in the nucleus (Bekhbat, Rowson et al. 2017, Cohen and Steger 2017, Vandewalle, Luypaert et al. 2018), RU486 also stimulates cytoplasmic GRβ to undergo nuclear translocation and to regulate gene expression in an antagonistic manner (Lewis-Tuffin, Jewell et al. 2007, Min, Perera et al. 2018). This is because despite the lack of helix 12, the GRβ/ RU486 complex preferentially interacts with a co-repressor, but not with a coactivator, with an affinity similar to that of the GRα/RU486 complex (Min, Perera et al. 2018).

As well as alternative splicing, further GR isoforms are produced due to the presence of 8 different translation initiation sites, beginning at amino acids 1 (GRα-A), 27 (GRα-B), 86 (GRα-C1), 90 (GRα-C2), 98 (GRα-C3), 316 (GRα-D1), 331 (GRα-D2) and 336 (GRα-D3). Since all initiation sites are present on the NTD, both GRα and GRβ are thought to give rise to a similar amount of isoforms (Kino 2000). With regard to the GRα isoforms, whilst all are capable of nuclear translocation in response to ligand, in the absence of ligand they have different cytoplasmic and nuclear distribution patterns (Kino 2000). Furthermore, the isoforms vary in their ability to transactivate and transrepress genes, reported to be in part due to distinct chromatin modulatory activity (Kino 2000, Bekhbat, Rowson et al. 2017). Differences in

expression of these diverse isoforms could partly explain the cell-specific responses to GCs (Cain and Cidlowski 2017, Vandewalle, Luypaert et al. 2018).

The various splice variants and translational isoforms of GR are demonstrated in figure 1.6.

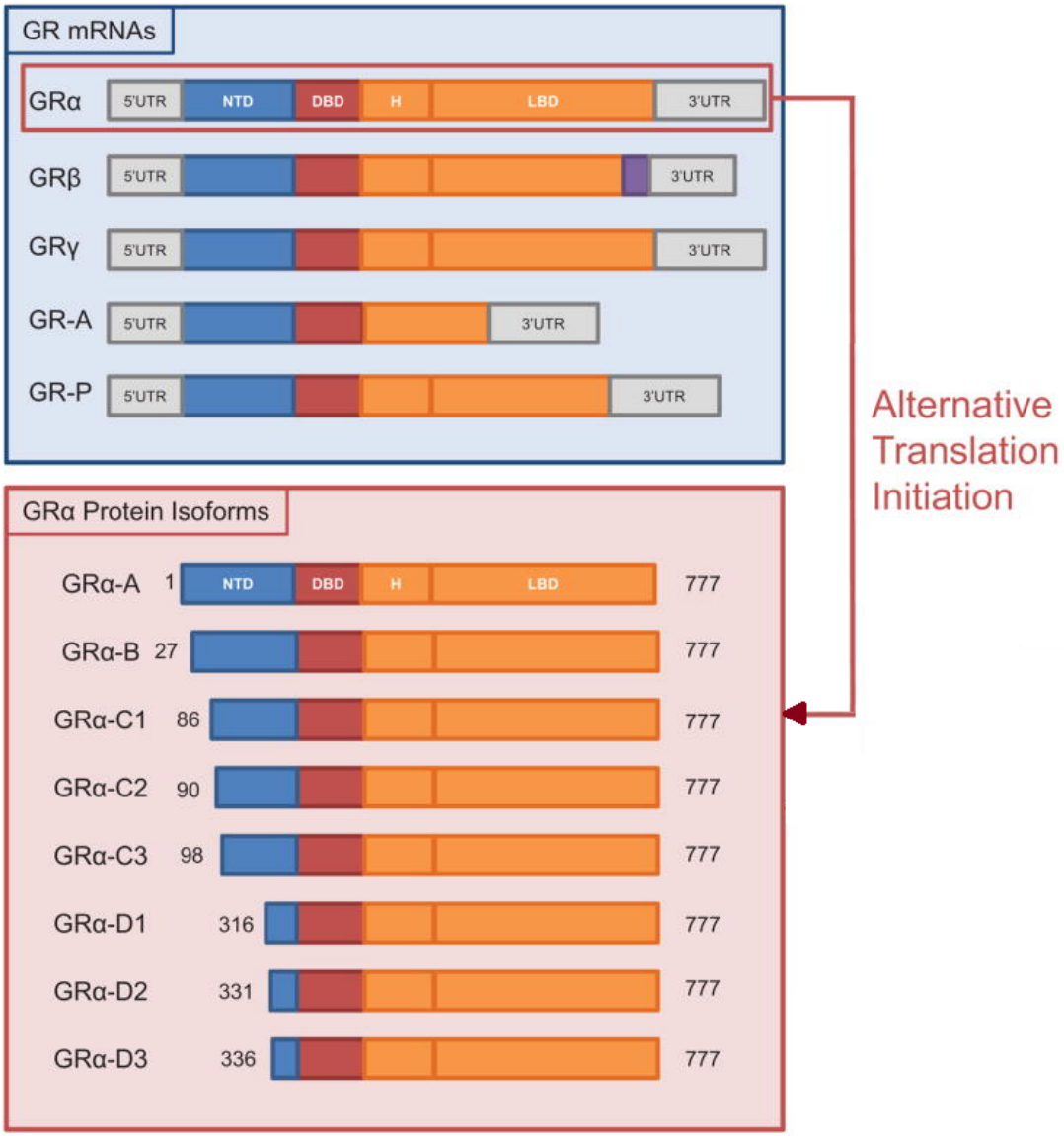

Figure 1.6. Glucocorticoid Receptor (GR) Isoforms: Alternative splicing and translation initiation of a single GR primary transcript give rise to diverse GR isoforms. Five splice variants (GRα, GRβ, GRγ, GR-A, and GR-P) have been identified, each with 8 potential translational protein isoforms (A, B, C1, C2, C3, D1, D2, and D3). Image adapted from (Cain and Cidlowski 2015).

1.4.3. Post Translational Modifications

Post translational modifications (PTM) of GR also contribute to the diversity of glucocorticoid signalling, by regulating GR activity (Keenan, Lew et al. 2016). Aspects of GR activity which are influenced by PTM include nuclear translocation, effects on gene transcription, protein interactions and receptor degradation (Cain and Cidlowski 2017, Whirledge and DeFranco 2018).

Phosphorylation is a commonly reported post-translational modification. The NTD of GR is extensively phosphorylated, and contains at least 5 phosphorylation sites (Kino 2000, Cohen and Steger 2017, Clayton, Jones et al. 2018) whereby a serine residue can be phosphorylated in response to GC (Bekhbat, Rowson et al. 2017). Several kinases phosphorylate GR, including mitogen activated protein kinases (MAPKs), cyclin-dependent kinases (CDKs), and glycogen synthase kinase 3 (GSK3)(Kino 2000, Cohen and Steger 2017). Phosphorylation can alter GR transcriptional activity either globally or in a gene specific manner, by influencing GR recruitment to target genes (Bekhbat, Rowson et al. 2017, Clayton, Jones et al. 2018). As mentioned in section 1.2.1, many serine residues located inside the AF1 domain of GR can be phosphorylated, which alters its interaction with cofactors and its subsequent transcriptional regulation (Kino 2000). GR phosphorylation at certain residues is often ligand selective, and has been shown to correlate with GR transcriptional activity (Keenan, Lew et al. 2016). Various GR phosphorylation sites have been functionally characterised (Clayton, Jones et al. 2018). GR Serine211 residue can be phosphorylated by p38 MAPK and this is associated with increased nuclear translocation, cofactor recruitment and an enhancement of transcriptional activity (Kino 2000, Grose, Werner et al. 2002, Bekhbat, Rowson et al. 2017, Cohen

and Steger 2017). Adenosine 5'monophosphate-activated protein kinase (AMPK) activates p38 MAPK, and is therefore able to indirectly phosphorylate GR (Kino 2000). In contrast, phosphorylation of the GR Serine226 residue by c-Jun N-terminal kinases (JNKs) suppresses transcriptional activity, and this is reported to be due to its increased nuclear export (Kino 2000, Cohen and Steger 2017).

1.4.4. Micro RNAs

Further GR regulation appears to be mediated by microRNAs (miRNAs) which are short single stranded RNAs, around 19-22 nucleotide bases long (Kino 2000, Clayton, Jones et al. 2018). miRNAs are transcribed mainly by RNA polymerase II either from miRNA clusters or from within protein-coding or non-coding genes (Kino 2000, Clayton, Jones et al. 2018). They can interact with mRNA causing its degradation, or can inhibit transcriptional initiation, both resulting in post-transcriptional down-regulation of protein expression (Clayton, Jones et al. 2018). It is estimated that miRNAs can regulate as much as 60% of the mammalian transcriptome, and although individual mRNAs only have subtle effects on gene expression, the cumulative effects of several miRNAs on a biological process may be much more profound (Clayton, Jones et al. 2018). miRNAs are known to negatively regulate steroidogenesis, and to also influence GC availability through modulating 11βHSD enzyme expression (Clayton, Jones et al. 2018). Furthermore, it is reported that several miRNAs regulate inflammatory and immune responses, some of which are induced by GCs (De Bosscher, Beck et al. 2016, Clayton, Jones et al. 2018). mRNAs may, therefore, influence GR signalling through effects on its ligand, or alternatively by associating with GR itself to influence signalling (De Bosscher, Beck et al. 2016).

1.4.5. Ligand Selectivity

Crucially, the spectra of effects which result from GR activation depend on the ligand structure. Different ligands can activate distinct GR-regulated genes and signalling pathways, resulting in different pharmacological outcomes (De Bosscher, Beck et al. 2016, Keenan, Lew et al. 2016). This results from the fact that GR exhibits a high level of flexibility, and, therefore, the conformational change which results from their activation is highly ligand-dependent (De Bosscher, Beck et al. 2016, Vandewalle, Luypaert et al. 2018). Consequently, different ligands lead to varying patterns of GR co-factor recruitment, dimerization, nuclear translocation and transcriptional activity (De Bosscher, Beck et al. 2016, Scheschowitsch, Leite et al. 2017). This raises the possibility of designing ligands which selectively activate some GR effects over others, in order to improve the safety and effectiveness of GCs (Keenan, Lew et al. 2016). This theme is discussed further in sections 1.6 onwards, since the focus of this thesis is a particular compound which provides promise as a selective GR ligand to treat inflammatory diseases.

1.4. Pharmaceutical use of GCs to treat inflammation

1.4.1. Introduction to inflammation

Inflammation is fundamental to the immune system's response to infection, irritation or injury. It is normally initiated with the binding of a foreign molecule (which may be a protein, nucleic acid or an endotoxin such as LPS) to a specific pattern recognition receptor (PRR) such as a Toll like receptor (TLR) on the surface of immune and neighbouring cells. Binding to these receptors activates signalling cascades which ultimately lead to activation of key inflammatory transcription factors

such NFκB, AP1, IRF and STAT. Activation of pro-inflammatory transcription factors is a crucial step during an inflammatory response as it leads to increased expression of many key anti-inflammatory molecules, such as the IL6, IFNα and TNFα cytokines. These inflammatory mediators then induce changes in, for example, vascular permeability and immune cell recruitment, which ultimately lead to the successful clearance of infection (Chinenov, Gupte et al. 2013).

1.4.2. History of anti-inflammatory GC use

Hench and co-workers, in 1948, were the first to demonstrate the therapeutic use of glucocorticoids to suppress inflammation, when they used cortisone in the treatment of rheumatoid arthritis (Hench 1950). For this work they later won a Nobel Prize, and since then it has become commonplace to use GCs for the treatment of a wide range of acute and chronic inflammatory and immune diseases (Schacke, Schottelius et al. 2004, Yang, Ray et al. 2012). Cortisol is now regularly administered under the name of 'hydrocortisone' which was first introduced in the early 1950s (Schacke, Docke et al. 2002). However, since GR signalling underpins many processes other than just inflammation, any exogenously administered GC not only targets inflammatory cells but all others in which GCs are active, hence resulting in the detrimental side effects. Consequently, the long term use of GCs is associated with increased risk of death from cardiovascular disease (Souverein, Berard et al. 2004, Wei, MacDonald et al. 2004) with phenotypes strongly resembling those in patients with Cushing's syndrome in whom endogenous GC levels are high (Nixon, Upreti et al. 2012). In addition to these increased disease risks, long term administration of GCs is also known to suppress the HPA axis, in turn resulting in maladaptive behaviour and increased susceptibility to future inflammatory insult (Stahn, Lowenberg et al. 2007). It is, therefore, clear that

new drugs, which retain anti-inflammatory ability but do not cause these side-effects, or at least have a reduced side-effect profile, are urgently required. Many synthetic glucocorticoids have been developed over the years, a common one being dexamethasone (Figure 1.1). Synthetic GCs generally possess a similar steroid scaffold but have structural modifications to improve potency as well as specificity for the GR over MR since 11βHSD2 often does not metabolise synthetic GCs in the same way as endogenous GCs. Importantly, some synthetic GCs are even predominantly reduced by 11βHSD2 rather than oxidised. As a result the co expression of 11βHSD2 with MR is often not sufficient for synthetic GCs to achieve GR selectivity (Best, Nelson et al. 1997, Wamil, Andrew et al. 2008, Nixon, Upreti et al. 2012, Kadmiel and Cidlowski 2013). Additional attention has also been paid to the pharmacokinetics of drugs in order to reduce side-effects and improve the therapeutic index (Schacke, Schottelius et al. 2004, Schacke, Rehwinkel et al. 2006). A big improvement in synthetic topical GC use was marked by the development of drugs which are less stable and can be delivered directly to the site of inflammation, therefore undergoing degradation before they can exert systemic effects (Schacke, Rehwinkel et al. 2006, Stahn, Lowenberg et al. 2007). Especially in the context of skin inflammatory conditions such as eczema, the therapeutic index has been greatly improved in drugs such as mometasone furoate (MF) and methylprednisolone aceponate (MPA) which rarely have systemic effects. However local side effects such as skin atrophy and decreased wound healing still exist and cannot be ignored (Schacke, Zollner et al. 2009). Improvements based on drug design principles have almost reached their limit and the remaining problems now appear to lie within the molecular mechanism of these drugs, namely the fact that they stimulate a wide range of GR mediated processes

other than just the desired anti-inflammatory effects. Understanding this phenomenon may open doors to new strategies for drug design.

1.4.3. Dissociating between GR mechanisms

For decades, an attractive idea has been that the anti-inflammatory effects of GCs are mainly a consequence of GR tethering to transcription factors (TR), whereas the side-effects arise because of an increase in gene expression due to direct binding of GR to GREs (TA)(Cain and Cidlowski 2017, Vandewalle, Luypaert et al. 2018). This was because the GR is known to suppress the activity of pro-inflammatory transcription factors via the TR mechanism, leading to downregulation of pro-inflammatory genes such as intracellular adhesion molecule (ICAM1), interleukin 6 (IL6), monocyte chemoattractant protein 1 (MCP1), and tumour necrosis factor α (TNFα)(De Bosscher, Beck et al. 2016, Keenan, Lew et al. 2016). In contrast, genes up-regulated as a consequence of the TA mechanism included those involved in carbohydrate, protein and fat metabolism (which lead to the common GC side-effects), such as tyrosine amino transferase (TAT), phosphoenolpyruvate carboxykinase (PEPCK), and fatty acid synthase (Grose, Werner et al. 2002, De Bosscher, Beck et al. 2010, De Bosscher, Beck et al. 2016, Vandewalle, Luypaert et al. 2018). From this idea arose the hypothesis that the anti-inflammatory effects of GCs could be separated from the adverse effects, by selectively targeting TR, and avoiding TA mechanisms (De Bosscher, Beck et al. 2016). The concept of an improved ‘dissociated steroid’ has therefore arisen. A dissociated steroid would bind to GR to induce its TR effects, but without affecting the TA mechanism. Since TA is assumed to rely on GR dimers and TR on monomers, a skewing towards GR monomers has been the avenue explored in order to create a ‘dissociated steroid’. This idea was explored with the help of a GR

dimerisation defective mouse (GRdim). The GRdim mouse model was generated by an A458T (alanine-to-threonine) single point mutation introduced by gene targeting using the Cre/loxP system (Reichardt, Kaestner et al. 1998). This mutation is in the second zinc finger of the DBD (De Bosscher, Beck et al. 2016, Scheschowitsch, Leite et al. 2017, Vandewalle, Luypaert et al. 2018). Dimer binding to a typical GRE is reported to be stabilised by protein-protein interactions of two GR monomers through a dimerization interface within the second zinc finger of the DBD (Adams, Meijer et al. 2003). The A458T mutation therefore compromises the ability of GR to form homodimers, and impairs any process dependent on homodimerisation, such as GRE driven TA (De Bosscher, Beck et al. 2016, Vandewalle, Luypaert et al. 2018). Indeed, the authors reported a loss of TA and impaired DNA binding of GR in GRdim mice, however the mutated GR was still able to repress the activity of other transcription factors such as AP1 (Reichardt, Kaestner et al. 1998). The GRdim mouse model therefore demonstrated that TA and TR activities could be separated *in vivo,* and that any action of GCs remaining in these mice were independent of GR binding to DNA (Reichardt, Kaestner et al. 1998). The authors also concluded that DNA binding of GR is not essential for survival, since unlike GR-/- mice which die shortly after birth due to atelectasis of the lungs, GRdim mice are viable (Reichardt, Kaestner et al. 1998). Further studies have since been performed using the GRdim mouse model, confirming that TR functions mediated by GR tethering to TFs remain intact in GRdim mice (Vandewalle, Luypaert et al. 2018). In both wild and mutant animals, TR mechanisms mediated through AP1 and NFκB were retained, and cytokines under the control of these transcription factors, such as IL6 and TNFα, were suppressed to the same extent after LPS stimulation in macrophages (Schacke, Docke et al. 2002, Nixon, Andrew et

al. 2013). However whilst retaining anti-inflammatory ability, the DNA interaction and transcriptional activity of the mutated GR appears to be impaired at classical GRE binding sites (Vandewalle, Luypaert et al. 2018). Indeed, the GRdim mice have demonstrated an impaired ability to upregulate certain GRE containing genes such as TAT, glutathione-3-peroxidase and PEPCK, in comparison with wild type mice (Schacke, Rehwinkel et al. 2006, Nixon, Andrew et al. 2013, Vandevyver, Dejager et al. 2013). Furthermore, in the GRdim mice, in contrast to wild types, after exogenous GC treatment there was an enrichment of GR at half site GRE motifs due to a lack of GR redistribution from monomeric to dimeric GRE sites (De Bosscher, Beck et al. 2016, Vandewalle, Luypaert et al. 2018). This is consistent with impaired gene regulation in GRdim mice. These studies, therefore, provided strong evidence that the anti-inflammatory effects of GCs were strongly dependent on the TR mechanism, and were capable of occurring in the absence of direct DNA interaction with GR dimers. The search for improved GR ligands has, hence, moved in recent years to focus on dissociating between different mechanisms of the GR, and this idealised type of ligand has been given the term a Selective Glucocorticoid Receptor Agonist (SEGRA).

However, a ligand which dissociates TA and TR is an oversimplification of what needs to be achieved. Indeed, the GRdim model itself has been criticised. Evidence has suggested the requirement of other residues for dimerization, and it has been questioned whether the single point mutation is sufficient to eliminate GR dimerization and TA. It has been suggested that, independent of the DBD dimer interface, other 'alternative' types of dimer can form in GRdim mice and that these can bind DNA but in a reduced manner dependent on the cell type and gene promoter. Examples given have included multimers or even GR/MR dimers (Nixon, Andrew et al. 2013,

Vandevyver, Dejager et al. 2013). Indeed whilst the A458T point mutation (contained within the GR of the GRdim mouse) prevents GR binding at a single GRE, it is now suggested that on some GR responsive promoters GR can form distinct multimers independently of the DBD dimer interface (Adams, Meijer et al. 2003). The PNMT gene promoter for example contains five regions where GR could bind (in contrast to TAT which contains a single GRE). Furthermore a dimerization defective GR was reported to bind to the PNMT promoter and in fact stimulated its transcription more strongly than wild type GR *in vitro.* This report demonstrated that typical GR dimer binding to GRE is not essential for regulation of PNMT. The authors of this latter paper therefore proposed that in fact, DNA binding of GR might be essential for survival (Adams, Meijer et al. 2003)

Furthermore, although the separation of GRE-dependent TA and protein-protein interaction-dependent TR initially provided considerable optimism (De Bosscher, Beck et al. 2016), understanding of GR mechanisms and their complexity has now improved (Keenan, Lew et al. 2016) and achieving a dissociation of the side-effects and anti-inflammatory effects of GCs in this way is now considered unrealistic (Vandewalle, Luypaert et al. 2018). For example, GR is able to enhance, rather than repress, transcriptional activity through interaction with some transcriptional factors, such as with members of the signal transducer and activator of transcription (STAT) family (Keenan, Lew et al. 2016). Likewise, recent observations suggest that GR bound to canonical GREs can lead to negative regulation of genes in some cases, rather than cause TA (Keenan, Lew et al. 2016). Importantly, many genes up-regulated by the TA mechanism encode anti-inflammatory proteins, such as glucocorticoid induced leucine zipper (GILZ), inhibitor of NFκB (IκBα), interleukin 10 (IL10), MAP kinase

phosphatase 1 (MKP-1) and lipocortin 1(De Bosscher, Beck et al. 2016, Keenan, Lew et al. 2016, Cain and Cidlowski 2017, Desmet and De Bosscher 2017). These are often essential, particularly in acute inflammatory conditions, to completely resolve inflammation (De Bosscher, Beck et al. 2016, Vandewalle, Luypaert et al. 2018), making GR dimerization a requirement in some conditions for responding to exogenous GCs and suppressing inflammation (Vandewalle, Luypaert et al. 2018). In fact, GRdim mice are significantly more susceptible to several models of acute inflammation (such as septic shock induced by LPS, and TNF lethality) than wild type mice (Desmet and De Bosscher 2017, Vandewalle, Luypaert et al. 2018). Whereas wild type mice are well-protected by exogenous GCs in acute inflammation, GRdim mice are not (Vandewalle, Luypaert et al. 2018). Interestingly, this is in contrast to chronic models (such as irritative skin inflammation) in which wild type and GRdim mice are equally protected by exogenous GCs (Schacke, Schottelius et al. 2004). It has, therefore, been suggested by De Bosscher *et al.* (2016) that for chronic conditions, where long term treatment is required and GR dimers are most likely to result in side-effects, skewing the balance towards GR monomers would be of benefit (De Bosscher, Beck et al. 2016, Desmet and De Bosscher 2017); whereas a skewing towards GR dimers over monomers may be beneficial to treat acute inflammatory diseases for which the long term effects are less of a consideration due to the short term and lifesaving nature of the treatment (De Bosscher, Beck et al. 2016, Vandewalle, Luypaert et al. 2018). De Bosscher *et al.* have proposed that new compounds that maximally stimulate GR dimerization could be designed for acute conditions, whereas compounds which selectively form monomers could be used for chronic conditions. They have termed these compounds SEDIGRAMs (selective dimerising GR agonists

or modulators) versus SEMOGRAMs (selective monomerising GR agonists or modulators) (De Bosscher, Beck et al. 2016, Vandewalle, Luypaert et al. 2018). However, this approach may also be overly simplistic. An alternative approach may be based on designing ligands which when bound to GR, result in a modified GR-ligand structure, in turn affecting interaction of the GR-ligand complex with cofactors and, hence, influencing gene expression. Indeed, upon GR binding, the agonist dexamethasone induces a conformational change within helix-11, leading to interaction with TIF2 coactivator. Binding of the GR antagonist RU486, however, caused helix-11 to adopt an alternative conformation with co-repressor NCoR instead being recruited (Nixon, Andrew et al. 2013). It may, therefore, be that SEGRAs bind to GR and cause differences in gene transcription through distinct cofactor recruitment.

1.4.4. The development of a Selective Glucocorticoid Receptor Agonist (SEGRA)

In recent years there has been an immense effort in both pharmaceutical and academic settings to develop a SEGRA. This is a compound capable of binding to GR and activating its anti-inflammatory mechanisms (which are thought to largely depend on TR by GR monomers) whilst not affecting mechanisms underpinning the side effects (many of which involve TA by GR dimers). The first compounds which appeared to be able to 'dissociate' between these two mechanisms of GR activity were the RU compounds (RU24782, RU24858 and RU40066) (Schacke, Rehwinkel et al. 2006, Stahn, Lowenberg et al. 2007). The RU compounds, which were developed by Roussel Uclaf (now Sanofi Aventis, Paris, France) have a steroidal core and demonstrate strong GR binding affinity (Figure 1.7) (Schacke, Rehwinkel et al. 2006, McMaster and Ray 2007). In contrast to conventional GCs, the RU compounds showed

a reduced *in vitro* ability to cause TA of target genes and, hence, were thought to distinguish between TA and TR mechanisms (McMaster and Ray 2007). However, while these data were tantalising *in vitro*, when tested *in vivo* it was evident that this was not the case, since the same side effects arose as with conventional GCs, with no therapeutic advantage (Rosen and Miner 2005, McMaster and Ray 2007).

Since the RU compounds, various other SEGRAs, both steroidal and non-steroidal, have been proposed. Examples of non-steroidal candidates are AL-438 and Compound A (Figure 1.7). AL-438 is a quinolone-based compound which binds strongly to GR and which was synthesised by modification of the progestin scaffold (McMaster and Ray 2007, Reeves, Rayavarapu et al. 2012). Developed by Ligand Pharmaceuticals (San Diego, CA, USA) and Abbott Laboratories (Abbott Park, IL, USA) this compound demonstrated anti inflammatory effects with a reduced side effect profile, especially in relation to glucose metabolism and bone reabsorption. This was evident *in vivo* as well as *in vitro* (Schacke, Rehwinkel et al. 2006, Reeves, Rayavarapu et al. 2012). Rather than completely dissociating TA from TR mechanisms, AL-438 is reported to reduce the interaction between GR and coactivators involved in the development of certain side effects (Schacke, Rehwinkel et al. 2006).

Compound A was the first proposed SEGRA to be derived from a natural source (Reeves, Rayavarapu et al. 2012). It is a synthetic analog of a non-steroidal compound identified from the Namibian shrub *Salsola tuberculatiformmis Botschantev,* by Haegman and colleages (De Bosscher, Vanden Berghe et al. 2005, Reeves, Rayavarapu et al. 2012). Compound A is a high affinity GR ligand and can induce GR nuclear translocation (De Bosscher, Vanden Berghe et al. 2005, Reeves,

Rayavarapu et al. 2012, Reuter, Grunwitz et al. 2012). It has been reported to favour a monomeric GR conformation and also did not appear to increase Ser-211 phosphorylation in a similar way to Dex as described in sections 1.2.1. and 1.2.4.3 (De Bosscher, Vanden Berghe et al. 2005, Reeves, Rayavarapu et al. 2012). It, therefore, appeared to have low TA potential and, indeed, this was demonstrated in comparison to conventional GCs *in vitro* and *in vivo* (De Bosscher, Vanden Berghe et al. 2005, Reeves, Rayavarapu et al. 2012). However, at high doses of compound A, toxic aziridine breakdown products are formed, resulting in apoptosis of various cell types, and death of mice (Reeves, Rayavarapu et al. 2012, Reuter, Loitsch et al. 2012).

Another series of promising SEGRA compounds are the ZK compounds by Bayer Schering Pharma AG (Berlin). Of special interest has been compound ZK216348 which is a non-steroidal compound synthesised from dihydrobenzofurane (Schacke, Rehwinkel et al. 2006, Reeves, Rayavarapu et al. 2012). This compound was identified as the (+) enantiomer of a racemic compound (ZK 209614) during a screening process specifically for selective glucocorticoid modulators. Although the (-) enantiomer did not bind GR, ZK216348 was found to be a high affinity GR agonist (Schacke, Schottelius et al. 2004). In addition to binding GR, ZK 216348 was also able to induce GR nuclear translocation (Reuter, Loitsch et al. 2012) and exert anti-inflammatory effects both *in vitro* and *in vivo* (Schacke, Schottelius et al. 2004). Furthermore, this compound has demonstrated a reduced side-effect profile compared to conventional GCs, especially in relation to dermal applications (Reuter, Loitsch et al. 2012). ZK216348 reduced skin thickness and skin breaking strength significantly less than prednisolone *in vivo* (Schacke, Schottelius et al. 2004). *In vitro*, ZK216348 did not inhibit the closure of wounds made in a non-transformed rat small intestine

epithelial cell line (IEC-6), nor in HaCaT cells (a skin-derived keratinocyte cell line), whereas dexamethasone significantly reduced migration of cells in comparison to control (Reuter, Loitsch et al. 2012). However ZK216348 also binds to the MR and to PR which may limit its use due to unwanted effects. Another compound in this series, Compound ZK245186, is currently in phase 2 clinical trials for atopic dermatitis (Reeves, Rayavarapu et al. 2012).

It seems that the SEGRA quest is moving forward since the focus has been put on finding drugs which dissect between different GR signalling mechanisms. These synthetic drugs have real promise for dramatically reducing side-effects. However, although much focus has been paid to synthesising these dissociative compounds, it may now appear that compounds like this, which were previously ignored, may already be in existence physiologically. Indeed, 5α-reduced glucocorticoids, which have been known since the 1970s. are now coming to light as potential SEGRAs.

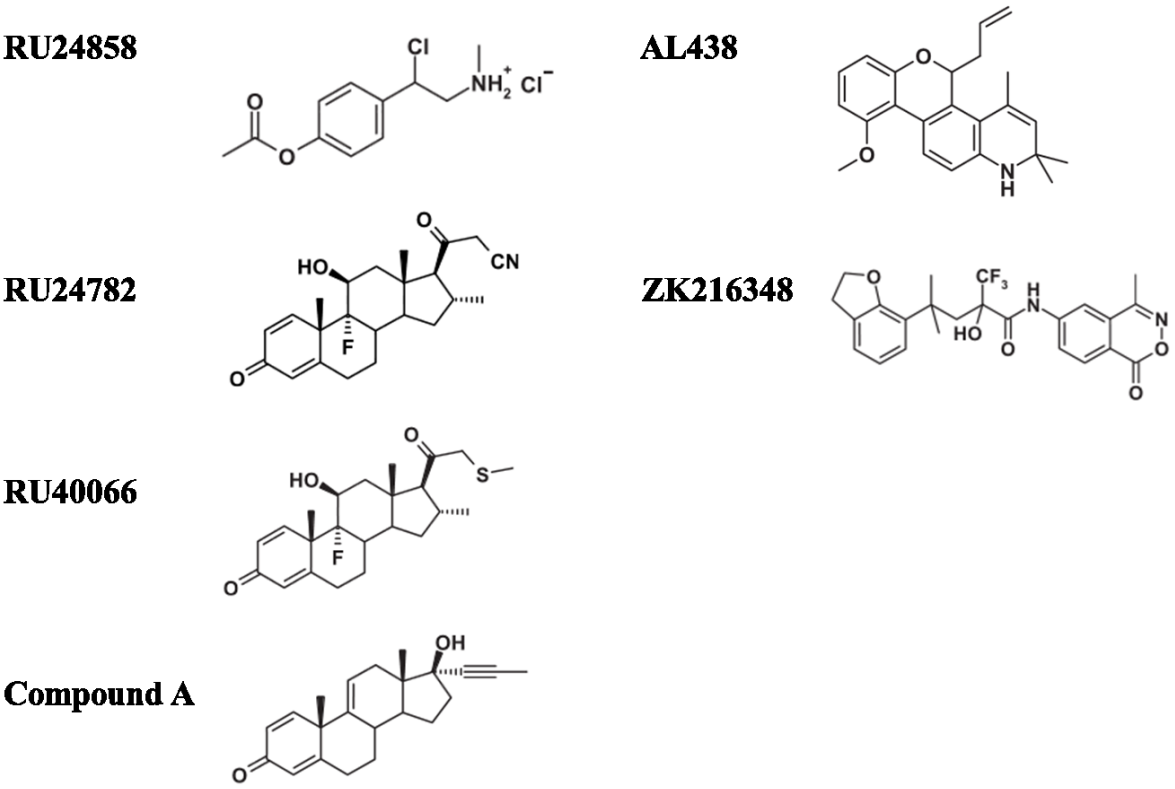

Figure 1.7: Structures of previously investigated Selective Glucocorticoid Receptor Analogues (SEGRAs). Image adapted from (Schacke, Rehwinkel et al. 2006).

1.4.5. 5α reduced Glucocorticoids

5α reduced glucocorticoids are formed via a series of reductions that occur naturally in the liver as part of the elimination process for glucocorticoids. In the rate limiting step, 5α reductase enzymes catalyse reduction of the Δ4,5 double bond in the glucocorticoid A ring (Stahn, Lowenberg et al. 2007) to form a 5α dihydrometabolite. The 3-ketone group is then rapidly reduced either by 3α-hydroxysteroid dehydrogenase (3α-HSD) to give the major 3α,5α-tetrahydro-metabolite or by 3β-hydroxysteroid dehydrogenase (3β-HSD) to give the minor 3β,5α-tetrahydrometabolite (McInnes, Kenyon et al. 2004, Nixon, Upreti et al. 2012), as

shown in Figure 1.7. These reactions provide a GC clearance route since the polar end products can be more easily cleared by the kidneys (Nixon, Upreti et al. 2012). Since disruption of 5αR activity shares adverse effects with alterations in GC activity, it does appear that 5α reduced GCs may be physiologically relevant in tissues other than the liver (Livingstone, Barat et al. 2015), although the relative contributions of increased product and decreased substrate are hard to dissect.

The 5α reductase enzymes are hydrophobic membrane bound enzymes identified in rodent work during the 1950s. They are expressed not only in the liver but also in other tissues such as the skin, lungs, GI tract, adipose tissue and reproductive tissue (McInnes, Kenyon et al. 2004, Nixon, Upreti et al. 2012). In addition to binding GCs, 5α reductase enzymes also bind a range of 3-oxo-4-ene steroids, including the androgens, progestogens, and mineralocorticoids. The 5α reduced metabolites of these other steroids are known to have biological activity (Yang, Nixon et al. 2011, Nixon, Upreti et al. 2012). For example, 5α reduced androgens (such as dihydrotestosterone) bind the AR with greater affinity than the parent androgens. 5α reduced progesterones, which bind PR and are suggested to be neurosteroids, are actually the main progestogen in some species. Although with weaker activity, 5α reduced aldosterone metabolites also bind the MR (Nixon, Upreti et al. 2012). In contrast, 5α reduced GCs were assumed inert metabolites since they only very weakly activated metabolic gene transcription (such as TAT) which was known to be an important effect of the parent GCs. They were thus deemed a 'suboptimal inducer' and remained largely ignored (Nixon, Upreti et al. 2012). However, recently there has been renewed interest in 5α reduced GCs since they have been shown to possess some previously unexplored anti-inflammatory activity. If able

to be used as an anti-inflammatory treatment, the fact that 5α reduced GCs only weakly activate metabolic gene expression is actually highly desired in order to prevent side effects. Due to our better understanding of GR mediated mechanisms, we can now postulate that 5α reduced GCs may be SEGRAs, capable of activating TR processes with limited effects on TA. This could be explained in terms of the more planar Δ4,5 trans double bond of parent GCs which is likely to interact with GR in a different manner to the reduced forms with all single bonds. This may therefore affect the final conformation of the ligand bound GR, and hence its ability to induce downstream processes (Nixon, Upreti et al. 2012).

1.4.6. 5α Tetrahydrocorticosterone (5αTHB)

Of particular interest, is the 5α reduced metabolite of corticosterone (the main rodent GC), 5alpha tetrahydrocorticosterone (5αTHB) (Figure 1.8 iii). 5αTHB has a reduced side-effect profile *in vitro* and *in vivo* in comparison to its parent GC corticosterone, alongside its anti-inflammatory effects. Accumulating evidence suggests that the mechanisms of action of 5αTHB are different from those of conventional GCs.

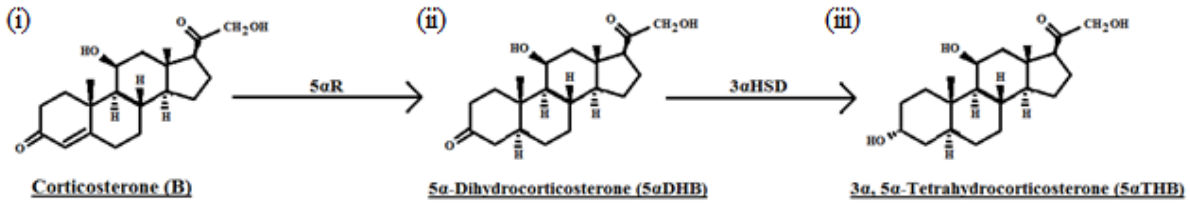

Figure 1.8: Metabolism of natural rodent glucocorticoid corticosterone (B) to produce 5α-tetrahydrocorticosterone (5αTHB). The conversion of B (i) to 5αTHB occurs naturally in the liver to increase polarity and, therefore, enable easier excretion. In the rate-limiting step, B is reduced by the 5α-reductase enzyme (5αR) to form the dihydrometabolite 5αDHB (ii)(McInnes, Kenyon et al. 2004, Nixon, Upreti et al. 2012). Further reduction by 3α-hydroxysteroid dehydrogenases (3αHSDs) then follows rapidly to form 5αTHB (iii) (McInnes, Kenyon et al. 2004, Yang, Nixon et al. 2011, Nixon, Upreti et al. 2012).

Evidence of 5αTHB having anti-inflammatory effects *in vitro* and *in vivo* has been collated. In LPS-stimulated mouse bone marrow-derived macrophages (BMDM), 5αTHB suppressed IL6 and TNFα cytokine release although to a lower extent than dexamethasone and corticosterone (Yang, Nixon et al. 2011). Dose-dependent effects of 5αTHB to suppress cytokine release were also demonstrated in RAW264.7 macrophages (Nixon, 2011), again with a weaker suppressive effect than corticosterone. This work also provided evidence that the cytokine suppression is due to direct effects of 5αTHB on transcription factors by demonstrating that both 5αTHB and corticosterone suppressed phosphorylation of JNK and p38; two MAPK family members which once phosphorylated, lead to AP1 and NFκB activation. Unlike corticosterone, 5αTHB did not have a significant effect on the amount of IKβα, which could be suggestive of effects mediated by 5αTHB solely through the MAPK family. Anti-inflammatory effects to suppress IL6 and TNFa cytokine release *in vivo* were confirmed in mouse whole blood, and in peritoneal lavage fluid from a mouse model of thioglycollate-induced peritonitis 5αTHB suppressed IL6 and MCP1 (TNFα was not tested)(Yang, Nixon et al. 2011). Furthermore, in the latter model inflammatory cell infiltration into the peritoneum was also measured, and 5αTHB suppressed neutrophil and inflammatory monocyte cell infiltration. However, recent work suggests interesting modes of action (Gastaldello, Livingstone et al. 2017). In a mouse model of dermatitis (induced with croton oil) 5αTHB appeared to mediate anti-inflammatory effects in a different manner to corticosterone. Whereas the anti-inflammatory effects of corticosterone (decreased cell infiltration, ear swelling and neutrophil activity) were evident after 6 hours, 5αTHB demonstrated (at concentrations 5 fold higher than corticosterone) a different time course of action with

these effects only evident after 24 hours. In addition to this difference in time course, Gastaldello (2014) demonstrated that 5αTHB increased transcripts of the anti-inflammatory *Dusp1* (also known as *Mkp-1*) in two different mouse models, whereas interestingly corticosterone did not. This is strongly suggestive of 5αTHB acting to suppress inflammation through different mechanisms to those of conventional GCs. Further evidence to suggest differences exerted by 5αTHB is that when HE293 cells were co-transfected with GR, 5αTHB actually increased NFκB and AP1 mediated luciferase activity (Nixon, 2011). This is contrary to the effects of corticosterone and 5αDHB and to what would be expected if 5αTHB suppressed inflammation through the conventional TR mechanism.

It, therefore, appears that 5αTHB is anti-inflammatory but with different mechanisms of actions and reduced adverse metabolic effects in comparison to conventional GCs. The *in vivo* anti-inflammatory effects of 5αTHB were first demonstrated in a murine model of thioglycollate-induced peritonitis, in which 5αTHB suppressed neutrophil infiltration with a similar efficacy to corticosterone (McInnes, Kenyon et al. 2004). In this model the drugs had to be administered subcutaneously, since 5αTHB was rapidly cleared from the circulation when infused systemically, indicative of poor systemic bioavailability and difficulty in maintaining an effective dose. This, therefore, suggested that 5αTHB would not be suitable for oral use and instead should be developed as a topical treatment. For topical use, the rapid clearance is actually a positive feature, reducing the likelihood of systemic side effects occurring. Evidence that 5αTHB could suppress inflammation when applied topically was subsequently tested. Indeed, in a murine croton oil ear model of dermal inflammation, 5αTHB reduced swelling and cell infiltration to a similar extent to corticosterone,

without inducing systemic side-effects (42)(Dawn Livingstone, personal communication). 5αTHB is now being investigated as a safer topical glucocorticoid and, therefore, its adverse effects locally on the skin (e.g. impaired wound healing) need to be explored.

1.4.7. 5αTHB as a SEGRA with decreased adverse effects on wound healing

With eczema estimated to affect 230 million people worldwide, inflammatory skin diseases are highly prevalent and are most commonly treated with topical GCs. Absorption of these drugs into the circulation leads to the systemic side effects previously described. This is a particular problem for babies with a low body volume to skin ratio. Therefore, in the context of topical treatments, the high clearance rate of 5αTHB may actually be an advantage, reducing the potential for systemic effects. However topical GC treatments are additionally plagued by local adverse effects of delayed wound healing and skin atrophy. For patients with a skin barrier which is already delicate and compromised, such as in the elderly or in diabetic patients who are more likely to experience chronic non healing wounds, this is a particular concern (Brandt, Grunler et al. 2015, Briquez, Hubbell et al. 2015, Holmes, Plichta et al. 2015, Rosique, Rosique et al. 2015). Therefore, more needs to be known about the effects of 5αTHBs on wound repair. Delayed wound healing as a result of GC exposure is not only a problem for skin treatments but also for systemic use, where GCs may delay internal wound healing (for example in vascular repair processes). The wound repair process is surprisingly similar in different tissues and after various insults, with internal repair mechanisms (occurring after, for example myocardial infarction, reperfusion injury or tissue ischaemia) strongly resembling those following skin

wounding (Gurtner, Werner et al. 2008). The skin, hence, provides a very useful model for studying effects on wound healing processes in general, and 5αTHB could not only provide a safer topical anti-inflammatory treatment, but through an understanding of its mechanisms may also help to provide a prototype for a safer drug which could regulate internal inflammation at sites of vascular injury and repair, without some of the adverse effects.

1.10. Mechanisms of wound repair in the skin

The skin is the largest organ of the body, composed of two main layers (Bayo, Sanchis et al. 2008, Hopkinson, Hamill et al. 2014, Holmes, Plichta et al. 2015, Rosique, Rosique et al. 2015). The inner layer is the dermis consisting mainly of fibroblasts and connective tissue. The outer layer, the epidermis, is a stratified squamous epithelium containing multilayers of keratinocytes (Hopkinson, Hamill et al. 2014). The dermis and epidermis are joined together through a basement membrane of many extracellular matrix (ECM) proteins (Hopkinson, Hamill et al. 2014). Due to the skin's crucial function as a protective barrier, it is very important that when a wound is formed and this barrier is broken, that the healing process occurs as quickly as possible.

The wound healing process involves many cell types, pathways, proteins, growth factors, and ECM components (Eming, Brachvogel et al. 2007, Jiang, Zhang et al. 2013, Sinno and Prakash 2013, Ding and Tredget 2015). It can be divided into four main phases of haemostasis, inflammation, new tissue formation, and tissue remodelling (Eming, Brachvogel et al. 2007, Giusti, Rughetti et al. 2013, Sinno and Prakash 2013, Johnson and Wilgus 2014, Martinez, Smith et al. 2015, Portou, Baker

et al. 2015, Rosique, Rosique et al. 2015). Haemostasis initiates the wound healing process (Ding and Tredget 2015, Portou, Baker et al. 2015, Rosique, Rosique et al. 2015). Platelets released from damaged vessels form a 'haemostatic plug' in the wound, and release biomolecules important for later stages of tissue repair (Giusti, Rughetti et al. 2013, Sinno and Prakash 2013, Hopkinson, Hamill et al. 2014, Ding and Tredget 2015, Martinez, Smith et al. 2015, Rosique, Rosique et al. 2015). The haemostatic plug provides a protective barrier, prevents haemorrhage and serves as a temporary matrix for early cell migration (Sinno and Prakash 2013, Hopkinson, Hamill et al. 2014, Briquez, Hubbell et al. 2015, Ding and Tredget 2015). Inflammation is then activated whereby increased vascular permeability, capillary dilation, and expression of endothelial adhesion molecules, result in leucocyte recruitment (Sinno and Prakash 2013, Ding and Tredget 2015). Neutrophils arrive first, followed by macrophages after a few days and later T lymphocytes (Eming, Brachvogel et al. 2007, Barrientos, Stojadinovic et al. 2008). The immune cells clean the wound of foreign material and provide further growth factors and cytokines for later stages of wound repair (Portou, Baker et al. 2015). The proliferative stage of wound healing involves the migration and proliferation of many cell types including fibroblasts, keratinocytes and endothelial cells. Fibroblasts migrate to the wound site and differentiate into myofibroblasts, which contract to help close the wound and secrete ECM components such as collagen (Barrientos, Stojadinovic et al. 2008, Briquez, Hubbell et al. 2015, Rosique, Rosique et al. 2015) (Eming, Brachvogel et al. 2007, Portou, Baker et al. 2015, Rosique, Rosique et al. 2015). In a process called reepithelialisation keratinocytes from the side of the wound migrate, proliferate and differentiate in order to cover the wound site and restore the epidermis (Martinez-Mora, Mrowiec et al.

2012, Jiang, Zhang et al. 2013, Hopkinson, Hamill et al. 2014, Portou, Baker et al. 2015). Finally, angiogenesis occurs. This is the formation of new blood vessels from the pre-existing vasculature and is vital for wound repair to give a temporary increase in blood vessels, providing oxygen and nutrients at the injury site (Eming, Brachvogel et al. 2007, Sinno and Prakash 2013, Johnson and Wilgus 2014, Martinez, Smith et al. 2015). During angiogenesis the vessel basement membrane degrades, and the vessel dilates and becomes more permeable to allow proliferation and migration of endothelial cells, leading to the sprouting of new vessels (Hwang and Heath 2010, Johnson and Wilgus 2014, Lee, Lin et al. 2015). The final stage in wound repair, which overlaps with the end of the proliferative phase, is the remodelling phase during which the ECM is remodelled into a more permanent scar tissue (Sinno and Prakash 2013). The wound healing process is demonstrated in figure 1.9.

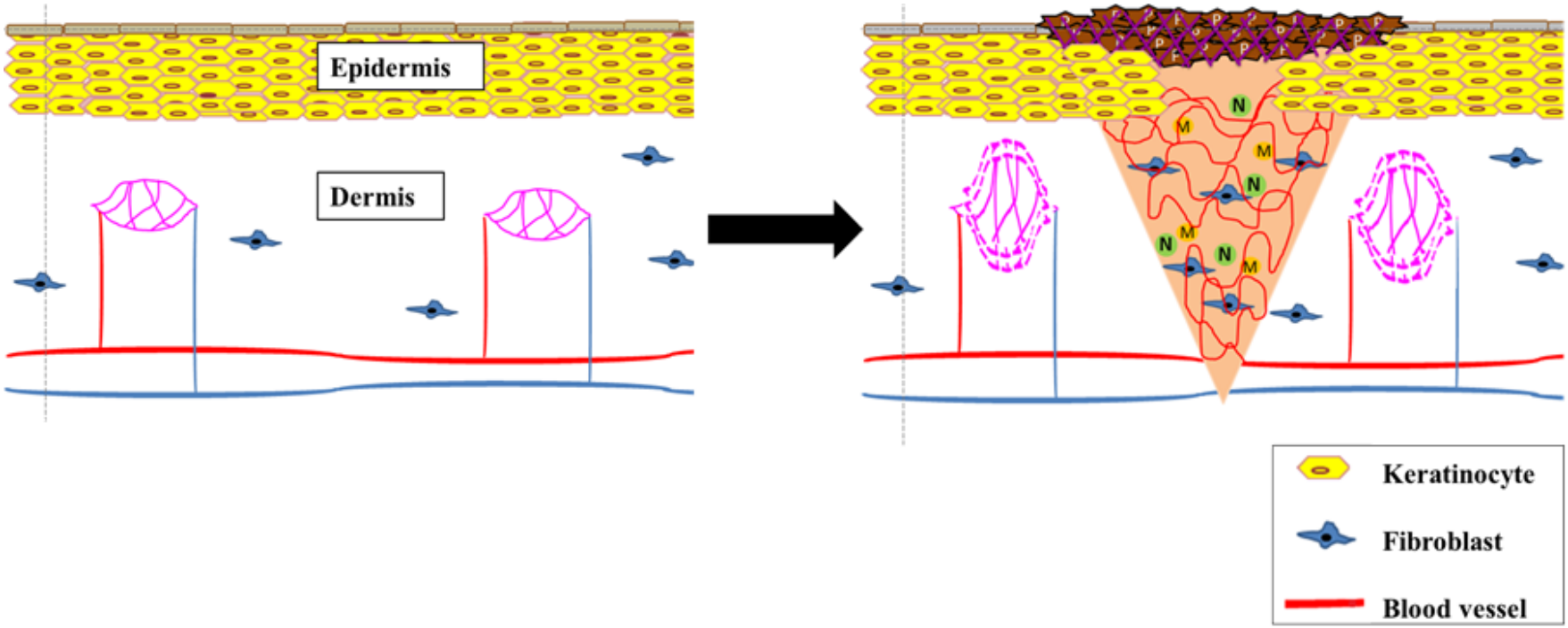

Figure 1.9: Skin structure and the wound repair process. The skin consists of the epidermis (mainly keratinocytes) and the dermis (fibroblasts, blood capillaries and connective tissue). When a wound is formed the repair process involves: the formation of a haemostatic plug by platelets (P); dilation and increased permeability of blood vessels, and the subsequent infiltration of neutrophil (N) and monocyte (M) inflammatory cells; the growth of new blood vessels (angiogenesis) into the wound to supply it with oxygen and nutrients; and finally, the migration of fibroblasts and keratinocytes for wound contraction, connective tissue formation, and epithelialisation.

1.6. Mechanism of angiogenesis

Angiogenesis is the formation of new blood vessels from the pre-existing vasculature (Johnson and Wilgus 2014). Since oxygen can only diffuse up to 200μM through tissues this process is vital for wound repair to give a temporary increase in blood vessels at the injury site and, hence, provide nutrients and oxygen for granulation tissue formation (Eming, Brachvogel et al. 2007, Logie, Ali et al. 2010, Sinno and Prakash 2013, Johnson and Wilgus 2014, Martinez, Smith et al. 2015).

Blood vessels in healthy tissue exist in a quiescent state, with tight cell-cell adhesions between endothelial cells, and surrounded by a basement membrane which is important for stabilisation as well as for endothelial cell function. Mature vessels are further stabilised due to the pericytes and smooth muscle cells surrounding them (Johnson and Wilgus 2014). The blood vessels are held in this quiescent state in adult tissues, due to production of more inhibitors of angiogenesis than activators in the microenvironment (Johnson and Wilgus 2014). However, during wound repair, many proangiogenic molecules are released, such as from platelets and macrophages (Martinez, Smith et al. 2015). This tips the balance in favour of angiogenic activation, and the point at which the proangiogenic factors dominate is known as the 'angiogenic switch' (8, 11, 18, 19). Angiogenesis then proceeds through several stages, demonstrated in figure 1.9. The existing vessel first dilates and becomes more permeable - Pericytes and SMCs detach from the vessel and endothelial cell-cell contacts loosen, transforming them from their quiescent state into proliferative and migratory cells (Hwang and Heath 2010, Zhu, Yao et al. 2015). Degradation of the basement membrane and surrounding ECM by matrix metalloproteinases (MMPs) and serine and cysteine proteases then provides a gap for migration of ECs to occur and

form a sprout (Johnson and Wilgus 2014) (Hwang and Heath 2010, Lee, Lin et al. 2015). Proliferation and migration of cells within the sprout, and subsequent remodelling, forms a 'lumen' or 'tube'. Finally, maturation of the vascular network occurs. Whilst excessive blood vessels regress in a process known as 'vessel pruning' (Korn and Augustin 2015), other vessels are stabilised through formation of a new basement membrane, and for larger vessels, also the reattachment of smooth muscle cells and pericytes (Eming, Brachvogel et al. 2007).

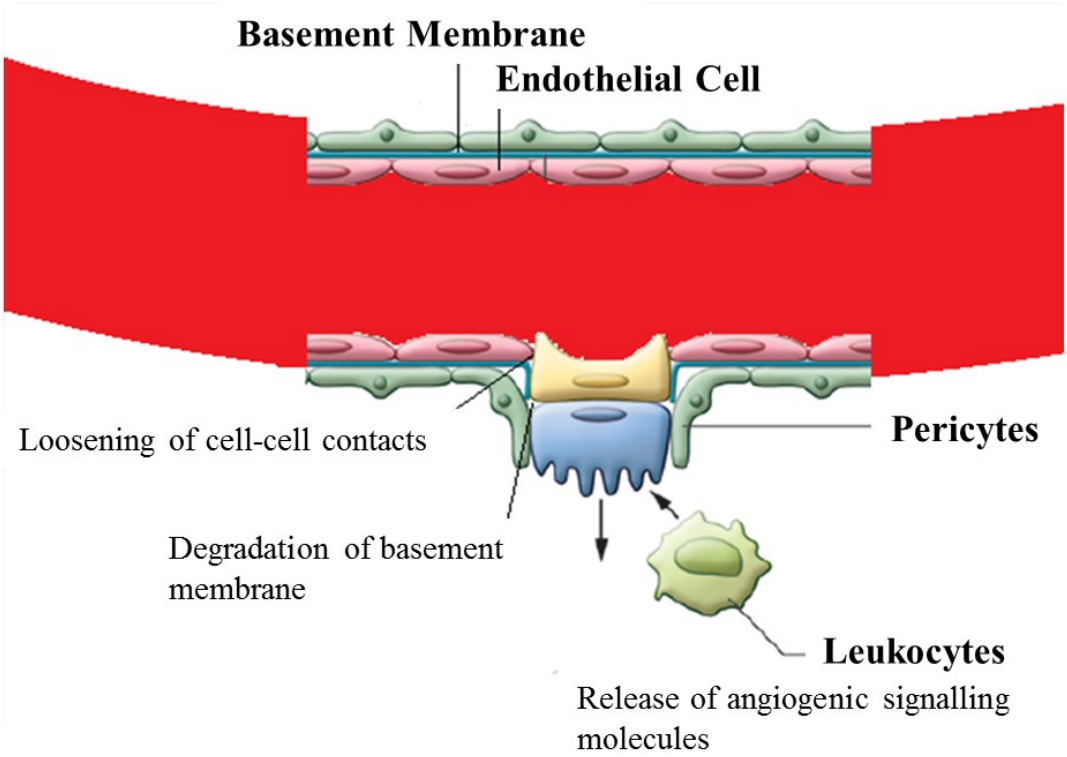

Figure 1.10: Mechanisms involved in the initiation of angiogenesis. Angiogenesis is initiated by an alteration in the presence of angiogenic signalling molecules. These signals stimulate degradation of the basement membrane, and also activate endothelial cells to loosen their cell-cell contacts, in preparation for cell migration through the gap in the basement membrane. Image adapted from (*Welti, Loges et al (2013) J Clin Invest 123(8):3190-200).*

1.7. Glucocorticoid-mediated effects on wound repair and angiogenesis

Glucocorticoids impair wound healing through effects on both the epidermal and dermal skin layers, as well as causing a flattening of the junction between these two layers (Schoepe, Schacke et al. 2006, Tiganescu, Walker et al. 2011, Tiganescu, Tahrani et al. 2013). Keratinocytes and fibroblasts are both targets of GCs, with growth factor signalling and cross-talk between the two cell types also being affected (Schoepe, Schacke et al. 2006, Tiganescu, Hupe et al. 2014). With regard to keratinocytes, their migration and proliferation is inhibited by GCs (Schoepe, Schacke et al. 2006, Tiganescu, Walker et al. 2011, Jozic, Vukelic et al. 2017, Tiganescu, Hupe et al. 2018). Their size is also decreased, assumed to be mediated by reduced synthesis of macromolecules (Schoepe, Schacke et al. 2006). There is also a reduced synthesis of epidermal lipids. The consequences of these effects are epidermal thinning, impaired epithelialisation, with increased permeability and water loss (Schoepe, Schacke et al. 2006, Schoepe, Schacke et al. 2010, Tiganescu, Hupe et al. 2014) resulting in disrupted barrier function of the skin (Schoepe, Schacke et al. 2006). Fibroblasts are also affected by GCs due to a reduction in proliferation (Schoepe, Schacke et al. 2006, Guo and Dipietro 2010) and in particular their synthesis of ECM proteins is inhibited by GCs (Schoepe, Schacke et al. 2006, Guo and Dipietro 2010) GCs have direct effects on gene expression involved in collagen turnover (Tiganescu, Tahrani et al. 2013) and reduce both major skin collagens – type 1 (making up around 80% of skin collagen) and type III (10-15%) (Schoepe, Schacke et al. 2006, Terao, Tani et al. 2014, Terao and Katayama 2016). Other ECM proteins, such as elastin, are also affected by GCs (Guo and Dipietro 2010). This results in a thinning of the dermis,

with decreased tensile strength and elasticity (Schoepe, Schacke et al. 2006). The combined effects of GC on the epidermis and dermis results in skin with a reduced barrier function and reduced structural integrity (Tiganescu, Walker et al. 2011). It is thinner, dryer, and has a reduced ability to heal. Wound healing is further impaired by GCs due to a suppression of angiogenesis (Gastaldello, Livingstone et al. 2017).

GCs are well known to inhibit angiogenesis, both at physiological concentrations and in chronic excess (Small, Hadoke et al. 2005, Logie, Ali et al. 2010, Morgan, Keen et al. 2018). This has been demonstrated *in vitro*, *in vivo* and during wound repair, and is reported to be mediated via GR (Small, Hadoke et al. 2005, Logie, Ali et al. 2010, Morgan, Keen et al. 2018). Pharmacological inhibition of GCs has been suggested as a possible treatment to enhance angiogenesis and improve healing during both topical and internal wound repair (Logie, Ali et al. 2010, McSweeney, Hadoke et al. 2010). The mechanisms through which GCs affect vascular function are diverse and are still not completely understood, but they appear to act at multiple stages of the angiogenesis process (Small, Hadoke et al. 2005, Logie, Ali et al. 2010, Morgan, Keen et al. 2018). It is well known that GCs suppress inflammation, and this itself is detrimental to angiogenesis due to the pro-angiogenic cytokines released from inflammatory cells (McSweeney, Hadoke et al. 2010). GCs also modify secretion of angiogenic factors from other cell types. For example, they are suggested to inhibit VEGF transcription and nitric oxide production by endothelial cells themselves (Small, Hadoke et al. 2005). Furthermore, in a recent study they modified the secretion of factors from myofibroblasts, which caused an indirect suppression of angiogenesis and also prevented endothelial cell migration and ability to form tube like structures (Drebert, MacAskill et al. 2017). Another indirect mode in which GCs can suppress

angiogenesis is through effects on the basement membrane. GCs can cause degradation of the ECM, and this can affect cell behaviour such as to inhibit endothelial cell migration and proliferation (Drebert, MacAskill et al. 2017, Morgan, Keen et al. 2018). The ECM is often reported as the key component in the effects of GCs on angiogenesis. Next generation RNA sequencing analysis recently assessed gene expression changes in the mouse aorta in response to cortisol. Of 13 enriched KEGG pathways for with genes downregulated in cortisol-treated aorta, 9 were associated with inflammatory responses and 4 were associated with ECM or cytoskeletal function (Morgan, Keen et al. 2018). Aside from indirect effects, there is also evidence that GCs exert direct effects on endothelial cells themselves. This is perhaps expected since endothelial cells express both GR and MR (Logie, Ali et al. 2010). Indeed, GCs have been shown to directly inhibit TLS formation by cultured isolated endothelial cells. This TLS formation was inhibited in a concentration- and time-dependent manner, and was prevented by the GR antagonist RU486. It was demonstrated that the GCs achieved this by reducing the formation of cell-cell contacts rather than increasing the degradation of existing tubes. Furthermore, the GCs did not impair endothelial cell proliferation, migration or viability but instead caused alterations in the cytoskeletal structure of the endothelial cells, hence interfering with their morphology and ability to form cell-cell connections (Logie, Ali et al. 2010). Finally, GCs are also reported to act on vascular smooth muscle cells which surround the vessels. For example they can inhibit production of matrix metalloproteinases, and also prevent their migration and proliferation (Small, Hadoke et al. 2005, Logie, Ali et al. 2010, Drebert, MacAskill et al. 2017).

1.8. Introduction Summary

In summary, glucocorticoids (GCs) thin the skin and prevent wound repair. Along with adverse metabolic effects, these are the major side effects associated with the use of GCs topically to treat inflammatory skin disease. The GC metabolite 5αTHB may reduce inflammation with fewer side effects than GCs. However the mechanisms of action of 5αTHB are unknown. This thesis will compare the effects of 5αTHB and the topical GC hydrocortisone to prevent wound repair. It will also investigate the mechanisms of action of 5αTHB, in particular whether its effects are mediated through the glucocorticoid receptor. This work may bring us closer to the development of a safer topical anti-inflammatory therapy, preventing much suffering and healthcare costs.

1.11. Hypotheses and Aims

Our group is interested in developing 5αTHB as a topical anti-inflammatory agent, necessitating studies of the effects of 5αTHB on wound repair processes. Further studies are also required to decipher its mechanism of action which appears different from that of conventional GCs.

The hypotheses explored in this thesis are:

1. 5αTHB is suitable for use as a safer topical anti-inflammatory treatment.
2. 5αTHB acts through GR.
3. 5αTHB is a SEGRA, dissociating between different GR- mediated molecular mechanisms.

The corresponding aims are:

1. To assess whether 5αTHB is less detrimental to wound repair processes than conventional GCs.
2. To investigate whether the anti-inflammatory effects of 5αTHB are GR-dependent.
3. To assess whether gene regulation by 5αTHB and conventional GCs differs in inflammatory cells.

Chapter 2:

Materials and Methods

2. Materials and Methods

2.1 Materials and reagents

Room temperature is abbreviated as RT. Overnight is abbreviated as O/N.

2.1.1. Source and maintenance of animals

Male C57Bl/6 mice, 8-12 weeks old, were purchased from Harlan Laboratories Ltd. (Bicester, UK). They were allowed to acclimatise for one week after arrival prior to being used for experiments. Mice were maintained under controlled conditions of temperature (18-22^{0}C) and light (lights on between 0700-1900 hours). They were allowed free access to standard chow (RMI 801002; Special Diet Services, Witham, UK) and drinking water. All experiments were approved by Veterinary Services at the University of Edinburgh and performed under the guidelines of the UK Home Office, and the following project licences: PW Hadoke, PPL No: 60/4523 and KE Chapman, PPL No: 60/7874. Animals were killed by asphyxiation with CO_2.

2.1.2. Outsourced reagents and chemicals

All cell culture reagents, including for washing cells and for the preparation of media, were from Lonza (Berkshire, UK) unless otherwise stated. All laboratory chemicals and reagents are from Sigma Aldrich (Dorset, UK) unless otherwise stated. Steroids, including the GR antagonist RU486, were from Steraloids (Newport, RI, USA).

2.1.3. Sources of cultured cells

2.1.3.1. Cell lines

hTERT immortalised human dermal fibroblasts were a gift from Andrew Campell, Beatson Institute for Cancer Research (Glasgow, UK); The human keratinocyte cell line HaCaT was from, and is considered proprietary to, the German Cancer Research

Centre (DKFZ, Heidelberg, Germany). The HaCaTs were formed by spontaneous transformation to immortality of a long term primary culture of human adult skin keratinocytes, originally obtained from a male skin melanoma specimen (Boukamp, Petrussevska et al. 1988). Human umbilical vein endothelial cells (HUVECs) were from PromoCell GmbH (Heidelberg, Germany). Each batch had been pooled from multiple donors from the supplier, and cells were used between passage number 2 and 6 in all experiments. A549 cells were from the European Collection of Cell Cultures (ECACC, distributor Sigma-Aldrich) and are transformed human type II alveolar epithelial cells, initiated from the lung carcinoma of a 58 year old Caucasian male (Lieber, Smith et al. 1976). L292 cells were also obtained from ECACC (distributor Sigma- Aldrich) and are transformed fibroblast cells derived from normal subcutaneous areolar and adipose tissue of a 100 day old male C3H/An mouse.

2.1.3.2. Murine bone marrow-derived macrophages (BMDM)

Primary BMDMs were freshly isolated from murine tibia and femur according to a published protocol (Weischenfeldt and Porse 2008), using mice which had been maintained and culled as described in (2.1.1.), as follows:

2.1.3.2.1. Removal of femur and tibia bones:

Hip joints were dislocated from culled mice which had previously been partially dissected for the aortic ring assay described in (2.2.3). Posterior limbs were removed and cleared of skin and soft tissues to reveal the bones. Femur and tibia bones were then detached, immersed in sterile ice cold PBS and stored at 4ºC for a maximum of 24 hours, until required, since the cells do not loose viability in this time period (personal communication from Professor Karen Chapman).

2.1.3.2.2. BMDM cell isolation, plating, and differentiation

Femur and tibia bone ends were removed with a scalpel (Swann-Morton, Sheffield, UK) to expose the marrow. Holding the bone at one end with sterile forceps, the marrow was flushed out into a Falcon tube (Falcon, Fischer Scientific, Loughborough, UK) with a syringe (Medisave, Dorset, UK) containing normal serum medium for BMDM (2.1.4.1.1, 5 mL), attached to a needle (22 G; Medisave, Dorset, UK). The cell suspension, resulting from the contents of all 4 bones of the mouse, was passed gently ten times through a larger needle (18 G; Medisave, Dorset, UK) to break cell clumps, and then filtered through a 40 μM Falcon^{TM} cell strainer to remove bone fragments and debris. The suspension was then adjusted to 20 mL with medium, and transferred to a T25 ultra low-attachment flask (Corning, Flintshire, UK) which was incubated (37 °C, 7 days) to allow for monocyte-macrophage differentiation. Every 2 days, 1/3rd of the medium was replaced, and one week after plating the cells, they were detached from the bottom of the flask by firmly hitting it from the side. The resulting cell suspension was transferred into a 50 mL Falcon tube, and the flask washed with PBS (no calcium, no magnesium)(4°C 20 mL)(Thermo Fisher Scientific, Paisley, UK) and subjected to another round of firm hitting on its side to remove any remaining cells. The PBS containing the remaining cells was added to the suspension in the 50 mL tube, which was centrifuged (400 G, 5 min, RT) to collect the cells as a pellet. The cell pellet was then resuspended in serum free medium. Cells were then plated 5x10^5 cells/mL per well in 12 well plates (Corning, Flintshire, UK) and left to settle at 37 °C for 24 hours before treatment.

2.1.4. Preparation of reagents and solutions

2.1.4.1. Cell culture medium

2.1.4.1.1. Normal serum medium:

Normal serum medium for murine bone marrow derived macrophage (BMDM) cells consisted of DMEM/Nutrient mixture F-12 (DMEM F-12) supplemented with penicillin (100 IU/mL), streptomycin (100 µg/ mL), L-glutamine, FBS (10% v/v) and L929 cell cultured medium described in 2.1.4.2 (15%). L929 cells were cultured in DMEM/F-12 supplemented with HI-FBS (10% v/v), penicillin (100 IU/mL) and streptomycin (100 µg /mL). For HaCaTs, Fibroblasts, and A549 cells normal serum medium consisted of Dulbecco's modified Eagle's medium supplemented with a high concentration of glucose (4.5 g/L, glucose), HI-Foetal Bovine Serum (HI-FBS, 10% v/v), penicillin (100 IU/ml), streptomycin (100 µg/mL) and L-glutamine (2 mM). For HUVECs normal serum medium consisted of endothelial basal medium-2 (EBM-2) with all the supplements and growth factors added from the ECM-2 SingleQuot kit.

2.1.4.1.2. Serum free medium:

Serum free medium for BMDM consisted of normal serum medium in the absence of FBS and L929 cultured medium.

2.1.4.1.3. Stripped serum medium:

For HaCaTs and fibroblasts, stripped serum medium consisted of normal serum medium with the same volume of charcoal stripped FBS (Sigma Aldrich) in place of HI-FBS. For HUVECs, stripped serum medium consisted of normal serum medium minus the addition of the hydrocortisone aliquot from the ECM-2 SingleQuot kit.

2.1.4.2. L929 fibroblast-conditioned medium for BMDMs.

L929 cells were cultured until confluent and then left for 10 days without the medium being changed. The medium was then collected, sterilised by filtration (0.22 μM, Millipore, Hertfordshire, UK) and frozen (-20 °C) for subsequent use during the culture of BMDMs.

2.1.4.3. Freezing medium

This was composed of 10% dimethyl sulphoxide (DMSO; Sigma Aldrich) in FBS.

2.1.4.4. Steroid solutions

Steroids were dissolved in ethanol to obtain stock solutions 1000 times more concentrated than required. 1 μL of these stock steroid solutions was added for every 1 mL of medium, at the time of treatment, minimising the amount of ethanol which was present in the final solution (and hence exposed to cells) to 0.1%.

2.1.5. Cell culture

2.1.5.1. Cell thawing

Aliquots of cells were stored frozen in liquid nitrogen. Frozen cells were thawed in a water bath maintained at 37 °C and then transferred to a 15 mL Falcon tube (Falcon, Fisher Scientific, Loughborough, UK) containing normal serum medium (2.1.3.1.1) and collected as a pellet by centrifugation (1000xg, 5 min, RT). The cell pellet was resuspended in normal serum medium and plated in 75 cm^3 flasks (Corning, Flintshire, UK). The flasks used for HUVECs were coated in gelatin (as described in 2.1.5.4.) representing an adjustment of the standard protocol.

2.1.5.2. Maintenance and passaging of cells

The thawed cells were maintained at 37 °C in a 5% CO_2 incubator, and were passaged when confluent. To passage cells, they were first washed with phosphate buffered saline (PBS) and detached from the flask by treatment with trypsin (5 mL, 5 min, 37 °C)(Gibco by Life Technologies, Thermo Fisher Scientific, Paisley, UK). For HaCaT cells which adhere strongly to cell culture plates, the trypsin was replaced with TrypLE Express Enzyme (1X) phenol red (gibco, life technologies, Thermo fisher scientific, Paisley, UK) and incubated for 10, instead of 5, minutes. Once the cells had detached, an equal volume of medium was added in order to inactivate the trypsin, followed by centrifugation (1000xg, 5 min, RT) to collect the cells as a pellet. The pellet was re suspended in medium and separated into 5 - 10 new flasks, which already contained medium so that the final volume of medium in each flask was 12 mL. The cells were then returned to 37 °C.

2.1.5.3. Cell freezing

To freeze, cells were washed with sterile PBS and detached from the flask by treatment with trypsin (5 mL, 5 min, 37 °C) or TrypLE Express in the case of HaCaTs (5 mL, 10 min, 37 °C). An equal volume of fresh culture medium was then added to counteract the trypsin, and the cells were collected as a pellet by centrifugation (1000xg, 5 min, RT). The cell pellet was re suspended in freezing medium and separated into 1 mL aliquots. Aliquots were gradually frozen, primarily at -80°C inside a polystyrene box (24 h) before moving into liquid nitrogen.

2.1.5.4. Coating of culture flasks and plates

Gelatin-coating: To coat the 75 cm^2 cell culture flasks in gelatin (Sigma Aldrich, Dorset, UK), gelatin was first diluted in PBS to give a 0.1% solution, and 10 mL of this was added to the cell culture flask. The flask was incubated (37 °C, 0.5 hours) and then transferred to a sterile hood with the lid left ajar, for 3 hours. To coat 96 well plates with gelatin, 50 µL of the 0.1% gelatin solution was pipetted into each well, and the same protocol followed as for the flasks.

Collagen-coating: To coat 96 well plates with collagen-type 1 (rat tail, Millipore, Hertfordshire, UK), collagen was diluted 1:4 in 70 % ethanol then vortexed until it had solubilised. 25 µl of this was then transferred to each well, and the plate gently shaken. The cell culture plate was then left ajar to allow airflow and prevent condensation, for 3 hours. This protocol was taken from the Merck Millipore website (http://www.merckmillipore.com/GB/en/life-science-research/cellculturesystems/cellgrowth/hanging/IyGb.qB.y1MAAAFBNgdb3.rV,nav?ReferrerURL=http%3A%2F%2Fwww.google.co.uk%2Furl%3Fsa%3Dt%26rct%3Dj%26q%3D%26esrc%3Ds%26source%3Dweb%26cd%3D12%26ved%3D2ahUKEwiQ0N_GkaPcAhXDKcAKHTEoA_oQFjALegQIBRAB%26url%3Dhttp%253A%252F%252Fwww.merckmillipore.com%252FTW%252Fzh%252Flife-science-research%252Fcell-culture-systems%252Fcell-growth%252Fhanging%252FIyGb.qB.y1MAAAFBNgdb3.rV%252Cnav%26usg%3DAOvVaw0rgnMZhr3BLU7oTb-KTn, last accessed on 16.07.2018).

2.2. Laboratory protocols

2.2.1. RNA analysis

2.2.1.1. Materials

2.2.1.1.1. Tris-Borate-Ethylenediamine tetra acetic acid (TBE) 10X Buffer solution:

1.0 M Tris, 0.9 M Boric acid, 0.01 M ethylenediamine tetra acetic acid *(*EDTA)

2.2.1.1.2. TBE 0.5X Buffer Solution:

10X Buffer Solution diluted 1/20 using de-ionised water.

2.2.1.2. RNA extraction from aorta

A protocol which had previously been used for RNA extraction (Morgan, Keen et al. 2018) was adapted in order to obtain sufficient amounts of RNA at the desired concentration range (10-100 ng/µL) and of adequate quality. In comparison to the original protocol, tissue homogenisation was altered to be performed at the lowest speed (4000 *x g*) and for the shortest time (30 sec) possible, to avoid degradation. The modified protocol consisted of adding Qiazol lysis reagent (250 µL/well; Qiagen, Manchester, UK) to each well of a 96 well plate on ice, and using a pipette to mix this with the collagen, to release the aortic rings. The mixture of Qiazol, collagen and aortic rings was then transferred from the well to a 1.5 mL Eppendorf tube and stored frozen at -80°C. Four rings which had been treated in the same way, together with the collagen and QIAzol solution, were then pipetted into a MagNA lyser green beads tube (Roche Diagnostics, Mannheim, Germany) for tissue homogenization with Precellys 24 tissue

homogeniser (Bertin Technologies, Montigny le Bretonneux, France) (4000 x *g*, 30 sec). Total RNA was extracted by using an RNeasy mini kit and its reagents (Qiagen). Briefly, chloroform (200 µL) was added to the MagNA lyser tubes, which were shaken and then incubated (2 min, RT). Centrifugation (21130 x *g*, 15 min, 4 °C) followed and the upper transparent layer containing the total RNA (approximately 700 µL) was transferred to an equal volume of ethanol (70%) in a new 2 mL Eppendorf tube. After gentle mixing, the solution was transferred to an RNeasy Mini Spin Column, centrifuged (8000 x *g*, 30 sec, RT), and the flow-through discarded. The column was then sequentially washed with RWI buffer (700 µL), RPE buffer (500 µL), and finally ethanol (500 µL, 80 %), with centrifugation (8000 x *g*, 30 sec, RT) after each step, discarding the flow-through each time. A final centrifugation step (8000 x *g*, 1 min, RT) was then conducted in order to remove any residual ethanol, and the column was placed into a 1.5 mL Eppendorf tube. Finally, RNase-free water (30 µL) was added to the column which was incubated (2 min, RT) and then centrifuged (8000 x *g*, 1 min, RT) in order to elute RNA. The RNA was then added again to the same column and centrifuged again (8000 x *g*, 1 min, RT) to maximise recovery of the RNA from the column.

2.2.1.3. RNA quantification

RNA Quantification was performed using the Qubit™ RNA HS (High Sensitivity) Assay Kit (Invitrogen, Thermo Fisher Scientific) in order to obtain accurate quantification with the low concentrations of RNA. The Qubit™ working solution was prepared by diluting the Qubit™ RNA HS Reagent in Qubit™ RNA HS Buffer (1:200). The two standards required by the assay were prepared by adding 190 µL of

the working solution and 10 µL of both Qubit™ standard #1 and of Qubit™ standard #2 in two separate 0.5 µL Qubit™ assay tubes. The working solution was added to the individual assay tubes together with 2 µL of the samples so that the final volume in each tube was 200 µL. All the tubes were mixed by vortexing (2-3 sec) and allowed to incubate (2 min, RT). Standards were read using a Qubit™ 2.0 Fluorometer (Invitrogen Life Technology, Thermo Fisher scientific, Paisley, UK) to calibrate the instrument. Then the sample concentrations were measured and reported by the instrument as ng/mL. RNA samples with concentrations equal or higher than 6.25 ng/µL were accepted for real-time qPCR analysis. Four RNA samples were discarded since their RNA concentrations were lower than this. The excitation wavelength of the Qubit™ 2.0 Fluorometer is 644 nm, and the emission wavelength of the fluorophore used by the Qubit™ RNA HS Assay Kit is 673 nm. The fluorescence emission intensity is the indicator of the RNA concentration.

2.2.1.4. Evaluation of RNA quality

RNA quality and integrity were assessed, using gel electrophoresis, by the visibility of two bands, corresponding to 28S and 18S ribosomal RNA (rRNA). Agarose gel (1 %w/v) was prepared by dissolving agarose in TBE buffer solution (0.5X; section 2.2.1.1.2) followed by the addition of the Biotum GelRed™ Nucleic acid stain (Cambridge Bioscience, Cambridge, UK). When solidified, 2 µg RNA together with Loading Buffer Orange (VWR International Ltd, Leicestershire, UK) was loaded onto the gel and run in TBE buffer (0.5X) with an electrophoresis Power Supply POWER 350 (Fischer Scientific, Thermo Fisher Scientific) (200 V, 1 h, RT). The gel was imaged under Ultra-Violet (UV) radiation (306 nm) using UVDOC HD6

(UVITEC, Cambridge, UK) with the band for the 28S rRNA being approximately twice as intense as the band for the 18S rRNA. Samples that separated into two visible bands in a 2:1 ratio (figure 2.1) were deemed acceptable. This was the case for all samples taken forward.

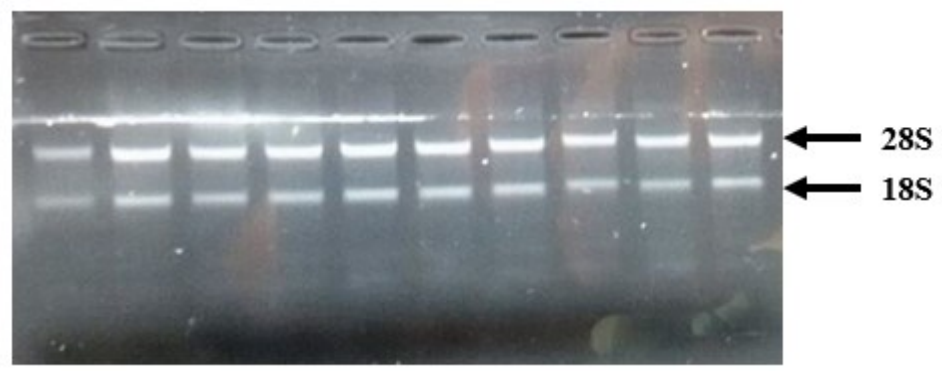

Figure 2.1: RNA band visualisation under UV light. RNA was extracted from mouse aortic rings and assessed for quality and integrity using gel electrophoresis. The 28S and 18S ribosomal RNA bands were clearly visible in approximately a 2:1 ratio, indicating the total RNA samples were intact. Representative from images of all samples.

2.2.1.5. Reverse Transcription

RNA samples were diluted to a concentration of 6.25 ng/µL using nuclease free water. Reverse transcription of these RNA samples to give complementary DNA (cDNA) was performed with an applied biosystems High Capacity cDNA Reverse Transcription Kit (Thermo Fisher Scientific, Paisley, UK) using the kit reagents and protocol. Briefly, 75 ng of each RNA sample was added to RNAse Inhibitor (1 µL) to prevent RNA degradation, 10X RT buffer (2 µL) to maintain a favourable reaction pH and ionic strength, 25X deoxyribonucleotide triphosphate (dNTP) Mix (100 mM, 0.8 µL), 10X RT Random Primers (2 µL), Multiscribe^{TM} Reverse Transcriptase (1 µL) and nuclease free water (1.2 µL). Two negative controls were also prepared: one consisted of adding nuclease free water in place of the Multiscribe^{TM} Reverse Transcriptase, in order to identify contamination with genomic DNA. The other consisted of replacing

the RNA sample with nuclease free water, to identify any contamination with RNA. Reverse transcription was performed using a thermal cycler (Techne, Staffordshire, UK) which involved incubating the samples at 25 °C for 10 min first to allow the primers to anneal, then at 37 °C for 2 h for DNA polymerisation to occur, followed by 85 °C for 5 min for enzyme deactivation. Finally, temperature was reduced to 4 °C and samples were stored at -20 °C until needed.

2.2.1.6. Real-time qPCR

For quantification of genes by real-time PCR, a LightCycler® 480 (Roche Diagnostics, Mannheim, Germany) was used. Primers (Table 2.1) were designed to match intron-spanning probes with the Roche Universal Probe Library (UPL) using the online software Universal ProbeLibrary Assay Design Center (https://lifescience.roche.com/en_gb/brands/universal-probe-library.html#assay-design-center, 2017). Primers were stored at concentrations of 100 pmol/ µL in Tris-EDTA buffer solution for stability (100 µM) and diluted in nuclease free water to 20 µM for use. The primer concentrations required by the assay was of 200 nM, therefore 0.1 µL of each 20 µM primer was used in 10 µL of reaction. Each newly made cDNA was diluted 1/20 in nuclease free water for analysis. In parallel, for each gene tested, a standard curve was generated: representative cDNA samples from each group were pooled and diluted 1/5 to give a starting solution, from which serial dilutions were prepared until 1/320 standard was achieved. Assay mix for each gene of interested was prepared as follows: each well contained LightCycler® 480 Probes Master (5 µL), primers (0.1 µL forward primer and 0.1 µL reverse primer), the corresponding UPL probe (0.1 µL) and nuclease free water (2.7 µL). Standards (2 µL) or samples (2 µL)

were mixed with the 8 μL of the master mix in the 384-well qPCR plate. A negative control to assess for potential contamination of reagents was prepared by using nuclease free water instead of sample. Samples were heated for initial denaturation (95 °C, 30 sec), followed by 50 cycles of PCR amplification, consisting of denaturation (95 °C, 10 sec), and annealing and extension (60 °C, 30 sec). Once the PCR programme was complete, samples were cooled (40 °C, 30 sec). All samples were analysed in triplicate and amplification curves plotted (x axis = cycle number, y axis = fluorescence). Crossing points (Cp) were determined by the LightCycler® software v1.5.3, using the maximum point of the second derivative of the amplification plot. Triplicates were accepted if the standard deviation of their crossing points (Cp) was lower or equal to 0.4 cycles. If the standard deviation was higher than 0.4 cycles then the replicates were checked for consistency and any outliers excluded. A standard curve was generated for each gene (x axis = log concentration, y axis = crossing point), fitted with a straight line of best fit and accepted if reaction efficiency was between 1.7 and 2.1. Negative controls were accepted as negative if there was no amplification for at least 10 cycles after the most dilute point on the standard curve. There were no statistical differences in transcript abundance of the housekeeping genes *Actβ* or *Tbp* between treatment groups. This was the case both for their individual transcript abundances measured alone (P=0.139 and P=0.226 respectively), and for the mean of their transcript abundances (P=0.122). This confirmed that the mean transcript abundance of these two genes was an appropriate reference in order for normalisation of the subsequent data.

Gene symbol, full name	Primers sequence	UPL
Actβ (Actin, beta)	5'-accagaggcatacagggaca-3' 3'-ctaaggccaaccgtgaaaag-5'	64
Col4a1 (Collagen, type IV, alpha 1)	5'-agttggaggaatgggcttg-3' 3'-ccagggacaccctgtgag-5'	80
Col14a1 (Collagen, type XIV, alpha 1)	5'-atgtggattccggtctatgg-3' 3'-agagtcctgttcttctttgaggtc-5'	79
Cxcl5 (C-X-C motif chemokine ligand 5)	5'-cagtgggtttgagaacaccata-3' 3'-ctggaggctcattgtggac-5'	25
Dusp1 (Dual specificity phosphatase 1)	5'-tggttcaacgaggctattgac-3' 3'-ggcaatgaacaaacactctcc-5'	89
Fkbp51 (FK506 binding protein 5)	5'-ccttcttgctccgagcttt-3' 3'-tgttcaagaagttcgcagagc-5'	69
Hsd11b1 (Hydroxysteroid 11-beta dehydrogenase 1)	5'-tctacaaatgaagagttcagaccag-3' 3'-gccccagtgacaatcacttt-5'	1
Mcp1 (Chemokine (C-C motif) ligand 2)	5'-catccacgtgttggctca-3' 3'-gatcatcttgctggtgaatgagt-5'	62
Mmp9 (Matrix metallopeptidase 9)	5'-cagaggtaacccacgtcagc-3' 3'-gggatccaccttctgagactt-5'	7
iNOS (Nitric oxide synthase 2, inducible)	5'-ctttgccacggacgagac-3' 3'-tcattgtactctgagggctgac-5'	13
Pecam1 (Platelet/endothelial cell adhesion molecule 1)	5'-actcgacaggatggaaatcac-3' 3'-cggtgttcagcgagatcc-5'	45
Per1 (Period circadian clock 1)	5'-acagcagccacggttctc-3' 3'-ggacccaggagtgcacag-5'	71
Tbp (TATA-binding protein)	5'-gatgggaattccaggagtc-3' 3'-gggagaatcatggaccagaa-5'	97
Vcam1(Vascular cell adhesion molecule 1)	5'-tcttacctgtgcgctgtgac-3' 3'-gacctccacctgggttctct-5'	47
Wnt5a (Wingless-type MMTV integration site family, member 5A)	5'-acgcttcgcttgaattcct-3' 3'-cccgggcttaatattccaa-5'	55

Table 2.1: Details of primers and probes for real-time PCR analysis of murine genes using Roche Universal Probe Library (UPL). The forward primer (5' → 3') for each gene is the upper sequence, the reverse primer (3' → 5') is the lower. Reference genes were beta-Actin (*Actβ*) and TATA-binding protein (*Tbp)*. Primers were designed to match the given intron-spanning probes with the Roche Universal Probe Library UPL using the online software Universal ProbeLibrary Assay Design Center (https://lifescience.roche.com/en_gb/brands/universal-probe-library.html#assay-design-center, 2017).

2.2.2. Protein analysis

2.2.2.1. Western blotting

2.2.2.1.1. Materials and buffers

Hypotonic buffer: Hepes (20 mM, pH 7.6), glycerol (20 %; BD Laboratory supplies, Nottingham, UK), NaCl (10 mM), $MgCl_2$ (1.5 mM), EDTA (0.2 mM), Triton (0.1% in distilled water). The following reagents were added immediately before use: Pefabloc (1 mM) and aprotinine (10 µL/mL, Thermo Scientific).

Hypertonic buffer: Hypotonic buffer + NaCl (5 M).

Running buffer 1X: Tris Base (1 M), Sodium dodecyl sulphate (SDS, 0.035 M), Hepes (1 M) in distilled water.

Transfer Buffer 1X: 0.025 M Tris Base (0.025 M), 0.2 M glycine (0.2 M), methanol (10% v/v in distilled water).

TBS-T: TBS prepared with Tris-HCl (50 mM) and NaCl (150 mM) plus Tween-20 (0.1% v/v, in distilled water).

2.2.2.1.2. Whole protein extraction

To extract protein from the cells, the RIPA lysis buffer system (Santa Cruz biotechnology, Heidelberg, Germany) was prepared using kit reagents as follows: Per mL of 1x RIPA lysis buffer, 10 µL PMSF, 10 µL sodium orthovonadate solution and 20 µL protease inhibitor cocktail solution was added. Media was removed from the flask and cells washed (12 mL cold PBS) before incubating with complete RIPA buffer (1 mL, cold, shaker, 5 min). With the flask tilted on ice, cells were scraped from the

surface of the flask and the RIPA buffer containing these cells was transferred into an Eppendorf, rotated (15 min) to complete the lysis, before subjecting to centrifugation (15 min, 13 *x g*, 4 °C) and transferring the supernatant (containing protein) to a fresh Eppendorf for concentration measurement.

2.2.2.1.3. Protein extraction of separated nuclear and cytoplasmic components

Cells in 6 well plates were washed (2x PBS) and allowed to swell on ice in hypotonic buffer (700 µL/ well, ice cold, 5 min). Cells were then detached from the well plate by scraping, and the cells from 3 separate wells were combined and transferred into 15 mL Falcon tubes. These were then centrifuged (100 *x g*, 15 min, 4ºC) after which the supernatant (containing the cell cytoplasm) was transferred into an Amicon ultra- 2 mL centrifugal filter (Millipore, Hertfordshire, UK) and spun (800 *x g*, 4 ºC, around 30-60 min) until around 400 µL cytoplasmic protein solution was obtained. The cell pellets (containing the nuclear fraction) were resuspended in 5 x their volume of hypertonic buffer and transferred to Eppendorfs. They were then rotated (1 hour, 4ºC) and centrifuged (16000 *x g*, 5 min, 4 ºC) and the supernatant containing the nuclear protein was transferred into fresh Eppendorfs. Protein concentration measurements and Western blot were then performed on nuclear and cytoplasmic fractions.

2.2.2.1.4. Protein quantification

Protein was quantified using the Bio-rad DC Protein Assay kit according to manufacturer's instructions (Bio-Rad Laboratories Ltd, Hertfordshire, UK). Bovine serum albumin (BSA, fraction V) at concentrations of 0.25, 0.5, 1 and 2 mg/mL, was used to generate the standard curve. Water was used as a blank (0 mg/mL). Samples and standards (5 µL) were added in duplicate to a 96 well plate before addition of Bio-

Rad's alkaline copper tartrate solution (25 µl), followed by Bio-Rad's dilute Folin reagent (200 µl). The plate was gently agitated to mix the reagents and after 15 minutes the absorbance was measured at 750 nm using an OPTImax tunable microplate reader (Molecular Devices, Wokingham, UK). The standard curve was deemed acceptable if r^2 >0.98. The samples were accepted if the standard deviation between values was less than 10 % of the mean. The concentration of each protein sample was calculated from its absorbance value, using the line of best fit from the standard curve.

2.2.2.1.5. Western blot sample preparation

Western blot samples were prepared by adding 20 µg protein to appropriate volumes of 4x NuPAGE LDS Sample buffer (Life Technologies, Paisley, UK) and 10x NuPAGE sample reducing agent (Life Technologies). These samples were frozen at -20°C until required.

2.2.2.1.6. Gel electrophoresis and protein transfer to membrane

Protein samples were denatured (95 °C, 5 min) and separated on 4-12 % w/v gradient gels (Thermo Fischer Scientific) in running buffer for 2 hours at 80 V. Separated protein was then transferred to 0.45 µm nitrocellulose blotting membrane (GE Healthcare, Buckinghamshire, UK) using transfer buffer (1.5 hours, 60 V, 4°C). Transfer was confirmed by visualising protein on the membrane using Ponceau S solution which was washed off using 0.1 M NaOH as described in the manufacturer's instructions. Membranes were then blocked with 5% blotting-grade blocker (Bio-rad, Hertfordshire, UK) in TBS-T (1 h, 37 °C) before washing (TBS-T, 5 minX3) and incubation with primary antibody (4 °C, O/N unless otherwise stated) diluted in 5% BSA in TBS-T. Primary antibodies and the dilutions used are given in Table 2.2.

Membranes were again washed (TBS-T, 5 minX3) and incubated with secondary antibody (1h, RT) diluted in 5% blocking solution in TBS-T, and matched to the species in which the primary antibody was raised. Membranes were then washed again in the same way before being viewed.

Protein detected	**Code of antibody used**	**Antibody dilution**	**Species**
GR	Sc-1003, Santa Cruz	1/500	Rabbit
GR	Sc-1004, Santa Cruz	1/500	Rabbit
GR	Sc-8992, Santa Cruz	1/500	Rabbit
β-Tubulin	Sc-101527, Santa Cruz	1/500	Mouse
GRB2	Sc-255, Santa Cruz	1/1000	Rabbit
PARP	556494, BD Pharmingen	1/1000	Mouse

Table 2.2. Details of primary antibodies used for protein detection by Western blot. Primary antibodies were for binding to the Glucocorticoid receptor (GR), β-Tubulin, Growth factor receptor bound protein 2 (GRB2), and Poly (ADP-ribose) polymerase (PARP) proteins.

2.2.2.1.7. Visualisation and quantification of protein on membrane

2.2.2.1.7.1. Fluorescence

Secondary antibodies used in 2.2.2.1.6 when being visualised by the fluorescence method were those listed in Table 2.3. The membrane was scanned using an Odyssey Imaging System (LICOR Biosciences, Cambridgeshire, UK): the fluorescence intensity was measured at an emission wavelength of 795 nm (excitation wavelength 778 nm), and the band intensity was then quantified using Image studio-lite software (Odyssey Imaging Systems, LI-COR Biosciences, Cambridgeshire, UK).

Antibody	Code of antibody	Antibody dilution
Goat anti-mouse IR Dye800 CW	926-32210, Licor Biosciences	1/10,000
Goat anti-rabbit IR Dye800 CW	926-32211, Licor Biosciences	1/10,000

Table 2.3. Secondary antibodies used for fluorescence detection of proteins by Western blot.

2.2.2.1.7.2. Chemiluminescence

Secondary antibodies used in 2.2.2.1.6 when being visualised by the chemiluminescence method were those listed in Table 2.4. Membranes were prepared for X-ray development using Immobilon Western Chemiluminescent Horse Radish Peroxidase (HRP) substrate kit (Millipore, Watford, UK) and its reagents. Briefly, the membrane was incubated (5 min, RT) in a mixture containing equal amounts of HRP substrate luminol and a HRP substrate peroxide solution. The membrane was then exposed to X ray film (CL-XPosure™ Film, 34088, Thermo Scientific)(5 min, RT) and film developed using an X

ray developer (Konica Minolta). The HRP-conjugated secondary antibody present on the protein of interest initiates luminol oxidation by peroxide, which then creates a signal on the film due to the emission of light as it decays to the ground state.

Antibody	Code of antibody	Antibody dilution
Anti-mouse IgG (whole molecule)- Peroxidase	A5906, Sigma	1/10,000
Anti-rabbit IgG (whole molecule)- Peroxidase	A0545, Sigma	1/10,000

Table 2.4. Secondary antibodies used for chemiluminescence detection of proteins by Western blot.

2.2.2.2. Quantification of cytokines by ELISA

IL6 and TNFα cytokines were measured in cell medium by following the manufacturer's instructions and using kit reagents of the Mouse IL-6 and Mouse TNF alpha ELISA Ready-SET-Go! Kits (Invitrogen, Thermo Fischer Scientific, Paisley, UK). Briefly, the 96 well ELISA plate was prepared by shaking with capture antibody (100 µL/well, 4 °C, O/N). The plate was then washed three times by soaking it in wash buffer (>250 µL, 1 min) which consisted of 0.05 % Tween-20 in PBS. Wells were then blocked by shaking with assay diluent (200 µL/ well, RT, 1 hour). They were then washed (>250 µL wash buffer, 1 min, RT) and samples were loaded in duplicate (100 µL/ well). Standard curve samples were prepared in diluent, and diluent was also used as a blank. The samples were shaken (4 °C, O/N) before washing 5 times with wash buffer as described above. Detection antibody (100 µL/ well) was added and incubated (1 hour, RT) then the plate washed 5 times as above. Then 100 µL / well Avidin-HRP enzyme was added (30 min, RT) and washed 7 times soaking for 2 minutes each time. Wells were incubated with TMB substrate solution (100 µL/ 15 min/ RT) and the reaction stopped with 1 M H_2SO_4 (50 µL/ well). The plates were analysed

spectrophotometrically using SoftMaxPro software (Molecular Devices, Berkshire, UK). The absorbance difference between 570 nM and 450 nM was measured, in order to correct for background. The standard curve, which was fitted according to manufacturer's instructions, was accepted if r^2 >0.98 and duplicates if the standard deviation was <10% of the mean.

2.2.2.3. Visualisation of protein by immunofluorescence

A549 cells were plated at 200,000 cells/4 ml/ well on glass coverslips in 6 well plates. After 24 hours the cells were washed (3 X PBS) and incubated in serum free medium for 24 hours. Treatments followed, and then treated cells were washed (2x PBS, RT) and fixed (2% v/v paraformaldehyde in PBS, 10 min, RT, 800 µL). Fixed cells were washed twice with PBS (RT) and then twice again with a solution of PBS containing 0.1% v/v Triton X100). Excess liquid was subsequently removed from coverslips by holding their edges to tissue, and cells were permeabilised (ice cold methanol, Scientific laboratory supplies, Nottingham, UK) (3 min, wet ice) and left to air-dry (1-3 min). Coverslips were blocked with 1% w/v heat-shock fraction BSA in PBS (4 mL/well, 1 hour, RT), washed (2x PBS, RT), and incubated with primary antibody (100 µL, dark, ON, 4 °C). They were then washed (3x PBS + 0.05% v/v TritonX100) and incubated with secondary antibody (100 µL, dark, 2 hours, RT). After a further wash (3x PBS+0.05% TritonX100) coverslips were stained with DAPI (30 min, RT) then washed again (3x PBS+ 0.05% Triton, then 3x PBS) and placed on glass slides using mountant (Thermoscientific, Cheshire, UK). Slides were then air-dried in the dark and stored in the dark at 4 ºC until cells were visualised with fluorescence microscopy, using a Zeiss Axioskop microscope (HB050/HC, Germany) fitted with a microcolour liquid crystal tunable RGB filter and a photometrics Coolsnap camera. 5

images were taken randomly of each slide in blue (400-550nm), green (470-630nm) and red (550-700nm) channels, and then 10 cells were randomly chosen within each image to have their fluorescence quantified. Two approaches were taken for fluorescence quantification. A 'scoring method' required a qualitative measurement of the fluorescence in each cell according to the extents of fluorescence between the nucleus (N) and cytoplasm (C). Possible scores were 5 (N>>C), 4 (N>C), 3 (N=C), 2 (N<C) and 1 (N<<C) and the mean score for each treatment were calculated. The other method of quantification was analysis using 'ImageJ' software, in which the corrected total cell fluorescence (CTCF) was quantified. The operator was blinded to treatment in all cases.

2.2.3. *Ex vivo* aorta angiogenesis assay

2.2.3.1. Aorta dissection from mouse

The aortic ring assay was used to measure steroid effects on angiogenesis. Animals were maintained and killed as described in (2.1.1). The mouse was then pinned down by its paws, in the supine position, and cleaned with ethanol (70%, VWR Chemicals, Leicestershire, UK). The skin was cut along the ventral midline with sterile tweezers and scissors. The ribcage was cut open, and organs and tissues removed to expose the aorta. The aorta was subsequently cut at the distal end, and then cleared of blood by flushing serum free DMEM through it from the heart, using a syringe and 27G needle (BD Microlance, Medisave, Dorset, UK). The heart was subsequently removed, and the aorta isolated by detaching it from the surrounding upper and lower layer of adipose and connective tissue. Following dissection, the aorta was placed in DMEM and stored on ice for up to 4 hours until used.

2.2.3.2. Aortic ring plating and culture

Aortas were cut into rings approximately 0.5 mm in length. Aortic rings were embedded one ring/well (96 well plate) in an ice cold solution of Collagen Type 1 (1 mg/mL; Millipore, Hertfordshire, UK) in DMEM (ice cold, and adjusted with 0.1 M NaOH until the solution is pink, indicating a basic pH). Once embedded, the plate was left at RT (15 min) before transferring to 37ºC (1 hour). Opti-MEM (Life Technologies, Paisley, UK) was then added (150 μL/well) containing either no treatment, a growth stimulating treatment, or the growth stimulating treatment plus the appropriate steroid. The growth stimulating treatment consisted originally (day 0) of 1% FCS and was then changed to 5 ng/mL Recombinant Murine Vascular Endothelial Growth Factor (VEGF) (PeproTech, London, UK) on days 3 and 5. In our laboratory this combination had previously been found to provide optimum conditions for vessel growth (personal communication from Dr Junxi Wu and Dr Robert Ogley). Medium was replaced on days 3 and 5.

2.2.3.3. Quantification and analysis of angiogenesis

Aortic rings were assessed, by light microscopy, for cells migrating out from the rings in response to FCS at day 3, and for vessel growth in response to VEGF at day 7. The rings that did not respond to the FCS and VEGF treatments, which lacked both a cell migration and vessel growth response, were assumed dead and were discarded (on average this was the case for one ring per two complete assays (of 20 rings each)). Angiogenesis was assessed by counting the new vessels which had grown from aortic rings, by direct light microscopy (x50). This vessel counting method is commonly used to quantify angiogenesis in the literature (Rohan *et al*. 2000, Nicosia & Ottinetti 1990).

Small (2005) had compared the accuracy and consistency of this method with a computer-assisted analysis method, which involved taking images of aortic rings from a live feed camera and then using the Microcomputer Imaging Device (MCID)(Imaging Research Inc, Canada) to measure the area of growth, maximum and average diameter of growth and vessel density. While measurement of vessel density proved to be unreliable and inconsistent, similar patterns of vessel growth were detected using the other 3 methods. However since they offered no major improvements Small *et al.* chose the counting method to quantify angiogenesis based on the fact that it is technically less demanding and requires only the use of light microscopy whilst still being reliable. The same decision was also made here, and vessels were counted originally both on days 5 and 7. Each segment sprouting from both the aortic ring and the new vessels, were considered as an individual vessel (Figure 2.2). Images of rings were captured on days 5 and 7 using an Axiovert 25 Microscope (Zeiss, Cambridge, UK) fitted with a Photometrics Coolsnap camera.

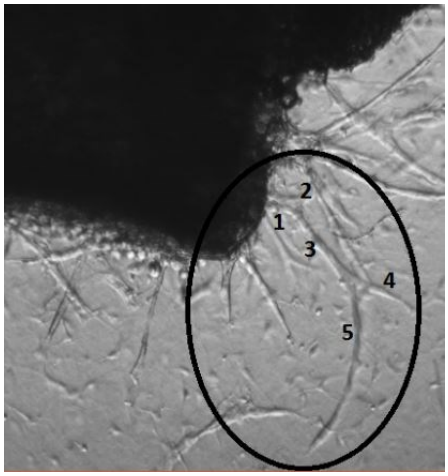

Figure 2.2: Vessel counting from murine aortic rings under light microscopy. Representative example showing that each segment sprouting from both the aortic ring and the new vessels was considered as an individual vessel during vessel counting.

2.2.4. *In vitro* cell migration assay

Cell lines (Human dermal fibroblasts, HaCaTs, and HUVECs) were grown to confluence in normal serum medium, as detailed in 2.1.5. Cells were plated in stripped serum medium in specialised 96 well Image Lock Microplates (Essen bioscience, Hertforshire, UK). Cells were grown for 8-16 hours in a standard incubator. Scratches were then made using the Essen Bioscience 96 pin wound maker, which was specially developed to create precise and reproducible wounds. Medium was immediately removed and wells washed twice (100 µl PBS), to remove dead cells, before replacing with fresh stripped serum medium (100 µl/well) with or without treatment. The ImageLock plate was then placed in the Incucyte (Essen Bioscience, Hertfordshire, UK) and the proprietary software used to record images to monitor wound closure. The metric chosen for quantification of cell migration was Relative Wound Density (RWD, %). This metric relies on measuring the spatial cell density in the wound area relative to the spatial cell density outside the wound area, at every time point (therefore the RWD should be 0% at t=0, and 100% when the cell density inside the wound is the same as the cell density outside the initial wound). Because of this it is self-normalising for cell density changes occurring outside the wound due to cell proliferation and/or pharmacological effects, and is reported to be robust across multiple cell types (Incucyte ZOOM Scratch Wound Processing Overview Technical Note, Essen Bioscience).

2.2.5. Measurement of co-regulator peptide recruitment to nuclear receptors

This was performed in collaboration with Professor Onno Meijer (Leiden University Medical Centre) and René Houtman (PamGene International) using the PamGene

Microarray Assay for Real-time Coregulator Nuclear Receptor Interaction (MARCoNI). Steroids were first prepared in DMSO, and were then added to a buffered solution of the isolated GST-tagged ligand binding domain (LBD-GST, 10 nM, AB vector, San Diego, CA) of a human nuclear receptor (either GR or MR) and a fluorescent Anti-GST alexa 488 antibody (25 nM). Each assay mix was subsequently added to all wells of an individual PamChip array, where each well contained a different coregulator peptide immobilised in a porous microarray membrane. Binding of nuclear receptors to the coregulator peptides was visualised by detecting the fluorescence signal using a PamStation 12 processing platform. The changes in binding in response to steroid, relative to DMSO control, were made using Student's unpaired t-tests. The experiment was repeated 3 times.

2.2.6. Assessment of steroid ability to bind GR ligand binding domain

This was performed by the Drug Discovery core (College of Medicine and Veterinary Medicine, University of Edinburgh) using a PolarScreen Glucocorticoid Receptor Competitor Assay kit (Fisher Scientific, Loughborough, UK). This kit is a displacement assay utilising a commercial fluorescent ligand, called Fluormone GS1. Since Fluormone GS1 is a specific ligand for the hGR LBD, it binds at this site to form a GS1/GR complex. However, an effective competitor may also bind to the hGR LBD and prevent this GS1/GR complex from forming. This results in a shift in the fluorescence polarisation value, and the extent of this shift is used to determine the relative affinity of test compounds for GR. The assay was performed in accordance with the manufacturer's protocol. This involved adding the GR, fluormone GS1 and steroid to a micro well plate. The fluorescence polarisation (mP) was then measured at 535 nm and 590 nm using a TECAN infinite 1000 microplate reader (TECAN,

Reading, UK). Graphs were plotted using Graphpad 4, with the logIC curves plotted with a fitted four parameter equation.

2.3. Data analysis

Data analysis was performed using GraphPad Prism 6 (CA, USA) and was presented as mean ± SEM. Data were analysed using the statistical tests described in the legend of each figure. Statistical significance was taken at $p<0.05$, and when a trend is described this indicates a p value of $0.05<p<0.1$.

Chapter 3:

Is 5αTHB less detrimental during wound repair than current glucocorticoid administration?

Chapter 3: Is 5αTHB less detrimental during wound repair than current glucocorticoid administration?

3.1. Introduction

As mentioned in the introduction, 5α-Tetrahydrocorticosterone (5αTHB) is now being investigated as a safer topical anti-inflammatory treatment which is less detrimental during wound repair than current glucocorticoids (GCs). Wound repair is a complex process involving inflammatory signalling, formation of granulation tissue (composed largely of extracellular matrix proteins and myofibroblasts), angiogenesis, and epithelialisation (Eming, Brachvogel et al. 2007, Giusti, Rughetti et al. 2013, Sinno and Prakash 2013, Johnson and Wilgus 2014, Martinez, Smith et al. 2015, Portou, Baker et al. 2015, Rosique, Rosique et al. 2015). The process relies on the action of keratinocytes, fibroblasts, and endothelial cells. GCs are known to be detrimental to multiple stages occurring during wound repair (Schoepe, Schacke et al. 2006, Tiganescu, Walker et al. 2011, Tiganescu, Tahrani et al. 2013). They are anti-inflammatory, both by suppressing pro-inflammatory signalling and by remodelling the vasculature to prevent inflammatory cell recruitment to the wound site. They also cause decreased expression of many molecules involved in extracellular matrix (ECM) formation (such as collagen and matrix metalloproteinases (MMPs)), and inhibit the migration and proliferation of keratinocytes and fibroblasts (Small, Hadoke et al. 2005, Schoepe, Schacke et al. 2006, Tiganescu, Walker et al. 2011). Importantly, GCs inhibit angiogenesis (the formation of new blood vessels from the pre-existing vasculature) with defective angiogenesis being largely responsible for impaired wound healing in many cases (Johnson and Wilgus 2014).

Initial studies suggest that 5αTHB is less detrimental to angiogenesis and ECM component formation, than conventional GCs (Gastaldello, Livingstone et al. 2017). In a mouse subcutaneous sponge implantation model of angiogenesis, 5αTHB suppressed vessel growth only to a limited extent whereas growth was substantially decreased by corticosterone. Transcript analysis of mRNA from these sponges revealed that corticosterone decreased expression of many factors important during vessel formation, whereas 5αTHB reduced only a small subset. Furthermore, 5αTHB did not reduce deposition of collagen (an important ECM component of granulation tissue) in sponges whereas corticosterone did. This work provided initial evidence that 5αTHB would have fewer adverse effects on wound healing processes than conventional GCs, and would, hence, be suitable as an improved topical anti-inflammatory treatment.

3.2. Hypothesis

The hypothesis addressed in this chapter is that 5αTHB is suitable for use as a safer topical anti-inflammatory agent. It is less harmful to the skin than conventional GCs, with decreased effects on skin thinning and wound repair processes. In particular:

1. 5αTHB has fewer adverse effects on migration of cells important during the wound repair process.
2. 5αTHB is less angiostatic than conventional glucocorticoids.

3.3. Aims

1. To determine whether 5αTHB impairs migration of fibroblasts, keratinocytes and endothelial cells and compare its effects to those of dexamethasone and hydrocortisone.
2. To assess the effects of 5αTHB on the vasculature using a mouse *ex vivo* aortic ring assay, and to compare with the effects of dexamethasone and hydrocortisone. The model will be used to:
    I. Compare steroid effects on vessel growth.
    II. Compare steroid effects on gene expression in the aorta.
3. To determine whether the effects of 5αTHB are GR dependent.

3.4. Methods

3.4.1. Investigating the effects of 5αTHB on cell migration in vitro

3.4.1.1. Choice of cells

HaCaT cells were chosen as the human keratinocyte cell model since they were known from the literature to be GC responsive, since dexamethasone impaired cell migration in an *in vitro* scratch wound assay (Reuter, Loitsch et al. 2012). Human umbilical vein endothelial cells (HUVECs) were used as the endothelial cell model since glucocorticoids had previously inhibited tube-like structure formation in these cells (Logie, Ali et al. 2010). Finally, hTERT immortalised human dermal fibroblasts were chosen as a relevant skin fibroblast model since they are taken from the skin and so are likely to be appropriate for studying effects on wound repair mechanisms; however, there was no literature available on steroid responsiveness of this particular cell line.

3.4.1.2. Assessment of GR protein in cell lines

The presence of GR protein was assessed in HaCaT, HUVEC, and dermal fibroblast cells. Cells were grown to confluence and complete protein extracted as described in 2.2.2.1.2. Protein was subsequently quantified (2.2.2.1.4) and visualised as a band using Western blot (2.2.2.1.5 – 2.2.2.1.6). Primary antibodies used were GR (sc-1003, rabbit polycloncal IgG) and β-tubulin (sc-101527, mouse monoclonal IgG) (both 1:500 dilution and from Santa Cruz, Heidelberg, Germany). Secondary antibodies used were goat anti-rabbit IR Dye 800 CW (926-32211) and goat anti-mouse IR Dye 800 CW (926-32210) (both 1:10000 dilution and from Licor Biosciences, Cambridge, UK) matched to the species of the primary antibody. The blots were developed and band

intensity quantified with the fluorescence method (2.2.2.1.7.1) using an Odyssey® Imaging Systems and ImageStudioLite software (both LI-COR Biosciences, Cambridge, UK).

3.4.1.3. Essen bioscience cell migration scratch assay

3.4.1.3.1. Method development

The scratch assay was utilised as described in (2.2.4) in order to compare steroid effects on HUVEC, HaCaT or dermal fibroblast migration. Initial assays were performed in the absence of steroid treatment in order to find the optimum conditions required for confluent monolayers to have formed after 8-16 hours, from which reproducible scratches could be made. Seeding densities of between 10000 and 60000 cells/ well were tested, and the effect of coating the plate with collagen type 1 or gelatin (protocols in 2.1.5.4) was also investigated in the case of fibroblasts and HUVECs, respectively, in order to increase adherence of cells to the plate surface. Pharmacological manipulation of the optimised assay was subsequently tested by treating HaCaT cells with epidermal growth factor (EGF, 25 ng/ml) as this had consistently been reported to increase HaCaT cell migration (Charvat, Chignol et al. 1998, Tochio, Tanaka et al. 2010).

3.4.1.3.2. Testing steroid effects

Dexamethasone, hydrocortisone and 5αTHB concentration responses were performed in triplicate, and repeated on three independent cell preparations, using the following concentration range: 1 nM, 10 nM, 100 nM, 1 μM, and 10 μM, according to the method described in (2.2.4) with previously optimised conditions stated in table 3.2. The

negative control for all experiments consisted of the addition of ethanol as vehicle in the absence of steroid.

3.4.2. Investigating the effects of 5αTHB in the vasculature ex vivo

3.4.2.1. Comparing steroid effects on vessel growth

Angiogenesis was examined using the mouse *ex vivo* aortic ring assay model (Baker, Robinson et al. 2012). As described in (2.2.3), vessel growth was stimulated from aortic rings, and the ability of steroids to suppress this was investigated. Day 7 was determined by Small *et al*. (Small, Hadoke et al. 2005) to be the optimal time-point to assess effects on vessel growth. Small *et al.* (Small, Hadoke et al. 2005) reported that new vessel growth increased from days 3 to 7, then reached a plateau after day 7 (Small, G.R, 2005). In this thesis, vessel growth was stimulated with growth factors and it was therefore anticipated that a plateau of vessel growth may be reached in less than 7 days. For this reason the vessels were originally counted both on days 5 and 7. However more vessels had grown on day 7 than on day 5, leading to an increased power to detect suppression of vessel growth at this later time point. Therefore, subsequent comparisons were made using day 7 data. Power calculations using PS: Power and Sample size calculation software (WD Dupont and WD Plummer, Jr) indicated that a sample size of n=8 was required in order to achieve sufficient power in this assay. Therefore n=8 was achieved in duplicate. Steroid concentration responses were performed, with treatments consisting of dexamethasone (1 nM, 3 nM, 10 nM, 30 nM, 100 nM, 300 nM, and 1 μM), hydrocortisone (10 nM, 30 nM, 100 nM, 300 nM, 1 μM, 3 μM, and 10 μM), or 5αTHB (same dose range as hydrocortisone).

3.4.2.2. Assessing GR dependence of the effects of 5αTHB on vessel growth

Effects mediated via GR were also investigated using the GR antagonist RU486, initially using concentrations of 30 nM or 3 μM RU486 (equal to the doses used of dexamethasone and 5αTHB), either alone or in combination with dexamethasone (30 nM) or 5αTHB (3 μM). Dexamethasone was chosen as the positive control due to its GR selectivity, and the concentrations used of dexamethasone (30 nM) and 5αTHB (3 μM) were those previously calculated from their concentration response curves to be required for significant suppression of vessel growth. Subsequently, the effect of RU486 to shift the steroid concentration-response curves was investigated, by re-performing the concentration response experiments described in (3.4.2.1) in the presence of 30 nM RU486.

3.4.2.3. Comparing steroid effects on mRNA transcript expression in aortic rings

After counting, on day 7, the new vessels that had grown from aortic rings used in the experiments described in (3.4.2.1) and (3.4.2.2), RNA was extracted from the rings and reverse transcribed for qPCR using the protocols described in (2.2.1.2 – 2.2.1.5). Four rings (of the same treatment group) were combined for RNA extraction to produce each RNA sample. Treatment groups consisted of unstimulated control, stimulated aortic ring (with FCS followed by VEGF as described in 2.2.3.2.), or aortic ring which had been stimulated and then treated with either 5αTHB (3 μM), dexamethasone (30 nM), hydrocortisone (1 μM), or RU486 (30 M or 3 M) either alone or in combination with 5αTHB (3 μM) or dexamethasone (30 nM). Table 3.1 demonstrates these treatment combinations for clarification. The steroid doses were

chosen based on the results of the experiments described in (3.4.2.1). Since aortic rings were only treated with specific drug concentrations in order to achieve the concentration responses described in 3.4.2.1, it was not possible to compare EC_{50}s of each steroid. Furthermore the EC_{50} of dexamethasone did not significantly suppress vessel growth. Consequently, the lowest concentrations of each steroid required to significantly suppress vessel growth were chosen to compare effects on gene expression in the aorta. At these concentrations vessel growth was suppressed to 35±11%, 30±7% and 26±14% of stimulated controls by hydrocortisone, dexamethasone, and 5αTHB, respectively. RNA transcript abundance across the treatment groups was assessed by real-time qPCR (2.2.1.6). To ensure reliability of results, two reference genes (*Tbp* and *Actβ*) were used, and transcript abundance of each gene was normalised to the mean of the two for each sample, due to the lack of significant changes in the abundance of transcripts among groups. Next generation RNA sequencing analysis had recently been performed to identify gene expression changes in the murine aortic ring model in response to hydrocortisone, and genes of interest were selected from this study (Morgan, Keen et al. 2018), as well as from real-time PCR analysis of transcripts in the sponge implantation model performed by Gastaldello (Gastaldello, Livingstone et al. 2017).

	Unstimulated	Stimulated
Vehicle	√	
Vehicle		√
5αTHB		√
Hydrocortisone		√
Dexamethasone		√
RU486		√
RU486 + 5αTHB		√
RU486 + Hydrocortisone		√
RU486 + Dexamethasone		√

Table 3.1: Stimulation and treatment combinations for mouse aortic ring experiments, to investigate steroid effects on angiogenesis.

3.4.2.4. Data and statistical analysis

qPCR samples with RDS < 10 % different between analytical triplicates were deemed acceptable. All data were analysed using GraphPad Prism6 software and presented as mean with error bars representing the standard error of the mean (SEM). Data were analysed by one-way ANOVA and either Dunnett's or Tukey's multiple comparison test, depending on whether every mean was being compared with every other mean (Tukey's test) or every mean was being compared to a control mean (Dunnett's test). To fit the concentration response curves, a non-linear regression analysis was performed using the log (inhibitor) vs response (three parameters) equation and using

the least squares fitting method. Curves were fitted to the mean data and due to the inherent variability in the aortic ring assay, EC_{50} values were calculated from the mean data. Statistical analysis was performed using GraphPad Prism 6.

3.5. Results

3.5.1. Assessing the effects of 5αTHB on cell migration

3.5.1.1. Assessment of GR expression in cell types

The presence of GR protein in the dermal fibroblast, HaCaT and HUVEC cell lines was assessed by Western blot. A similar intensity of bands for β-tubulin demonstrated equal loading of protein from each cell type and provided a control between slight deviations in sample loading. Bands were quantified and expressed relative to β-tubulin loading control. All cell types expressed GR (figure 3.1a and b).

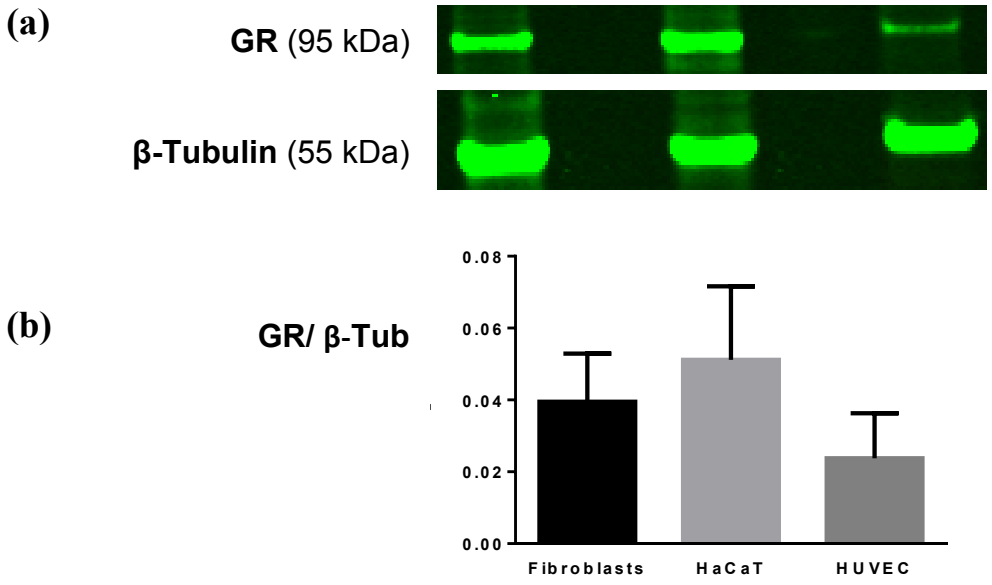

Figure 3.1: Human Umbilical Vein Endothelial cells (HUVECs), HaCaTs and dermal fibroblasts all expressed GR. Whole protein was extracted from cells and visualised by Western blot with β-tubulin, the latter demonstrating equal loading of protein (a). GR band intensities were quantified and expressed relative to the band intensity of their β-tubulin loading control (b). GR protein was present in all cell types. Graph is mean ± SEM of n=3.

3.5.1.2. Optimisation of cell seeding conditions

During initial preliminary assays with each cell type, the importance of selecting the correct seeding density became apparent. With too low a seeding density, cell monolayers were not completely formed due to the presence of gaps between cells. This meant that there was a lot of variability in the rate of wound closure between replicates, as cells often moved in other directions in order to fill the gaps, rather than to close the wounds. With too high a seeding density, cells would attach too tightly to each other, often forming clumps and detaching from the well surface. This prevented reproducible scratches from being formed, and also led to the presence of cell debris (which as well as blocking the pathway of migrating cells, also interfered with the computer's ability to distinguish between 'cell' and 'scratch' areas). As an additional measure to prevent the formation of cell debris, it was also determined that both fibroblasts and HUVECs required a coating in order to increase their adherence to the surface of the well plates. This was achieved with collagen-1 and gelatin, respectively. Since collagen-1 is the major collagen in the skin (providing around 80% of skin collagen (Schoepe, Schacke et al. 2006)) this mimics well the granulation tissue present in the wound into which the fibroblasts migrate (Schoepe, Schacke et al. 2006, Terao, Tani et al. 2014, Terao and Katayama 2016). In contrast, the basement membrane of blood vessels, which forms around the endothelial cells, is a dense polymeric sheet composed of ECM proteins but with a slightly different composition to the skin ECM (Eming, Brachvogel et al. 2007). The main collagen present is collagen IV, and this forms a scaffold together with separate polymers of laminin, held together by linker proteins such as nidogens and the heparin sulphate proteoglycan perlecan (Eming, Brachvogel et al. 2007, Briquez, Hubbell et al. 2015). Gelatin is a

heterogeneous mixture of water-soluble proteins present in collagen, and is extracted from skin, tendons, ligaments and bones. It is, therefore, often used mimic the basement membrane of blood vessels in order to test the mobility of endothelium cells *in vitro* (https://www.sigmaaldrich.com/catalog/product/sigma/g1393?lang=en&region=GB, last accessed 21/07/2018).

Ultimately, the conditions which were deemed optimum in order to study cell migration in this assay for each cell type are given in table 3.2.

	Seeding Density:	**Plates coated with:**
HaCaT	40000	Uncoated
Fibroblast	15000	1 mg/mL collagen-type 1
HUVEC	45000	0.1% gelatin

Table 3.2: The optimum cell plating conditions chosen for use with the Essen Bioscience cell migration scratch wound assay. Human umbilical cord endothelial cells (HUVEC), HaCaTs, and dermal fibroblasts were plated in 96 well plates under the conditions in this table, 8-16 hours before scratch formation.

3.5.1.3. Optimising assay analysis settings.

After scratch formation, cell migration was continuously monitored and well-images taken every 2 hours by the Incucyte® analysis software package. From these images, cell migration was quantified using the relative wound density (RWD) metric previously described (2.2.4). To compute RWD the Incucyte® software relies on the formation of various masks – a 'confluence mask' covering the cells and a 'wound mask' covering the scratch area, demonstrated in figure 3.2, as compared to without the masks as seen in figure 3.3. It was therefore vital for these masks to be accurately applied and 'processing definitions' were made for each cell type, with various

parameters altered to optimise this as far as possible. Table 3.3 gives the optimised parameters for each cell type.

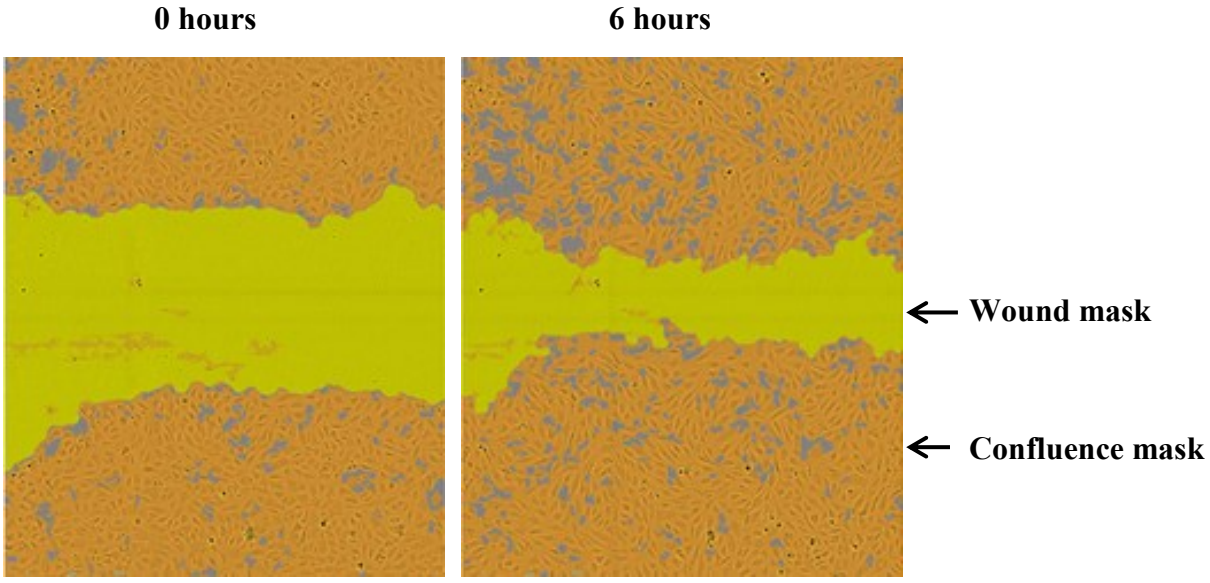

Figure 3.2: The Incucyte® analysis software package was used to apply 'confluence' (in orange) and 'wound' (in yellow) masks to cell migration images at each time point. From these masks, progress of the cells to migrate and cover the scratch area was computed by the software in terms of relative wound density (RWD). Image (a) is a representative original scratch at zero hours (0 hours) made by the Incucyte Wound maker tool in human umbilical vein endothelial cells (HUVECs). Cell migration to cover the scratch after 6 hours (the time at which vehicle-treated HUVECs had 40% RWD) can be visualised in image (b).

		HaCaT	Fibroblasts	HUVEC
Segmentation adjustment		1.2	1.3	2
Clean up	Hole fill (μm^2)	500	4000	300
Filters	Minimum area (μm^2)	700	3500	900

Table 3.3: The optimum analysis parameters chosen for 'confluence' and 'wound' masks to be accurately applied to images, using the Incucyte® analysis software package (Essen Bioscience). These parameters were optimised separately for each cell type, ensuring reliable mask formation and subsequent cell migration quantification. Only the settings listed in this table were applied.

3.5.1.4. Model assessment and time point selection

To assess whether the scratch wound model was suitable for studying pharmacological effects on cell migration, endothelial growth factor (EGF) was used, which is widely reported to stimulate HaCaT cell migration. Vehicle treatment did not influence cell migration in comparison to untreated control cells (figure 3.4). EGF treatment increased HaCaT cell migration as assessed visually and after RWD quantification (figures 3.3 and 3.4). For vehicle-treated scratches the average wound closure times were calculated as well as the time required for the scratch to reach 20, 40, 60 and 80% RWD. RWDs of EGF-treated scratches were subsequently compared at each time point. EGF increased cell migration in comparison to vehicle-treated cells at time-points when vehicle treated cells had 40, 60 and 80% RWD. This indicated that cell migration changes could be detected by the model and, hence, that it is suitable for assessing the effects of other compounds. The difference between vehicle- and EGF-treated scratches became significant when vehicle-treated scratches had 40% RWD (occurring after 12 hours in HaCaTs). The time for vehicle-treated scratches to reach 40% RWD was therefore the time point chosen to quantify further pharmacological effects.

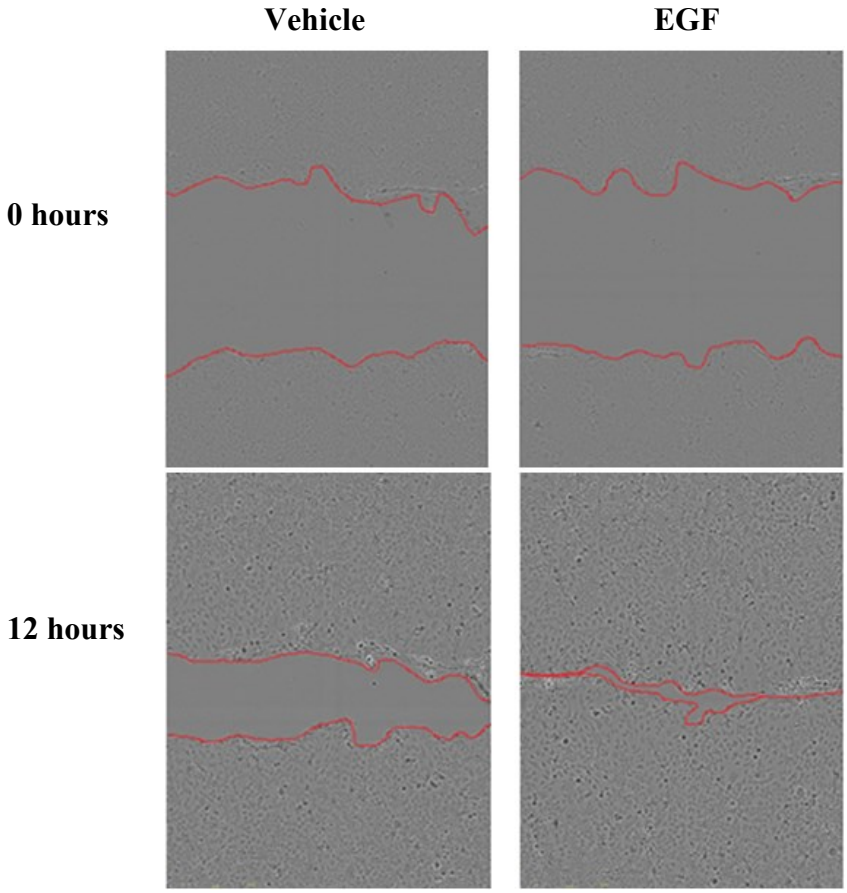

Figure 3.3: Epidermal growth factor (EGF, 25ng/ml) increased migration of HaCaT cells in comparison to vehicle-treated cells. HaCaTs were plated in stripped serum medium and grown to confluence in 96 well ImageLock Microplates. A scratch was made and media replaced with either vehicle or EGF. Images (a) and (b) demonstrate original wounds zero hours (0h) after scratch formation. Cell migration occurred over time to cover the scratch area, and masks applied by the Incucyte® analysis software were used to compute relative wound density (RWD, %). After 12 hours RWD of vehicle-treated cells was 43% (c) whereas in EGF-treated cells it was 78% (d). Images are representative of three replicates.

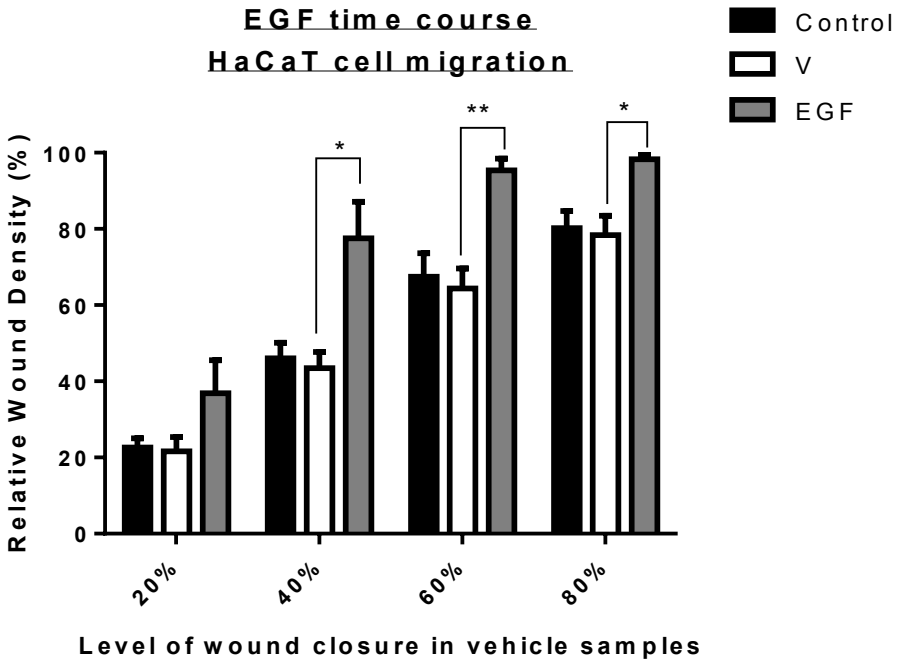

Figure 3.4: Cell migration was successfully manipulated using the Incucyte® cell migration scratch assay, with differences between treatments becoming significant at the time point when vehicle treated scratches had 40% relative wound density (RWD). Scratches were made in confluent HaCaT monolayers and stripped serum media replaced either with no treatment (Control), with ethanol vehicle (V) or with epidermal growth factor (EGF, 25ng/ml). Wound closure was then monitored using Essen Bioscience Incucyte® analysis software. RWD was compared between the two treatment groups at the time when vehicle treated cells had 20, 40, 60 and 80% RWD. Vehicle treatment did not influence wound closure in comparison to untreated control. EGF increased RWD of scratches in comparison to vehicle treatment, at the time points when vehicle treated scratches had 40, 60 and 80% RWD. Data from each time point were individually analysed by one-way ANOVA with Dunnett's multiple comparisons test. *=P<0.05 vs V, **=P<0.01 vs V.

3.5.1.5. Assessing steroid effects on cell migration

Cell seeding densities optimised as described in section 3.4.1.2 were successful in creating confluent monolayers from which reproducible wounds could be made. Processing definitions using the chosen parameters described in section 3.4.1.3 allowed the Incucyte® software to distinguish clearly between open scratch areas and those containing cells for each cell type. The time taken for vehicle-treated scratches to close to 40% RWD occurred in a consistent manner, requiring 16 hours for fibroblasts, 12 hours for keratinocytes and 6 hours for HUVECs. Comparisons to assess steroid effects were subsequently made at these time points.

The GR-selective glucocorticoid dexamethasone did not have a significant effect on fibroblast, HUVEC, or HaCaT migration, at any concentration tested from 1nM to 10μM. This can be seen visually (appendices figures A1, A4 and A7) and was confirmed through quantification (figures 3.5a, 3.6a and 3.7a). Hydrocortisone did not have any effect on fibroblast or HaCaT migration (figures 3.5b and 3.7b), but did suppress HUVEC migration (figure 3.6b), reaching significance at doses of 1 nM and 10 nM. 5αTHB also did not affect cell migration of any cell type, at any dose tested (figures 3.5c, 3.6c and 3.7c, and appendices figures A3, A6 and A9).

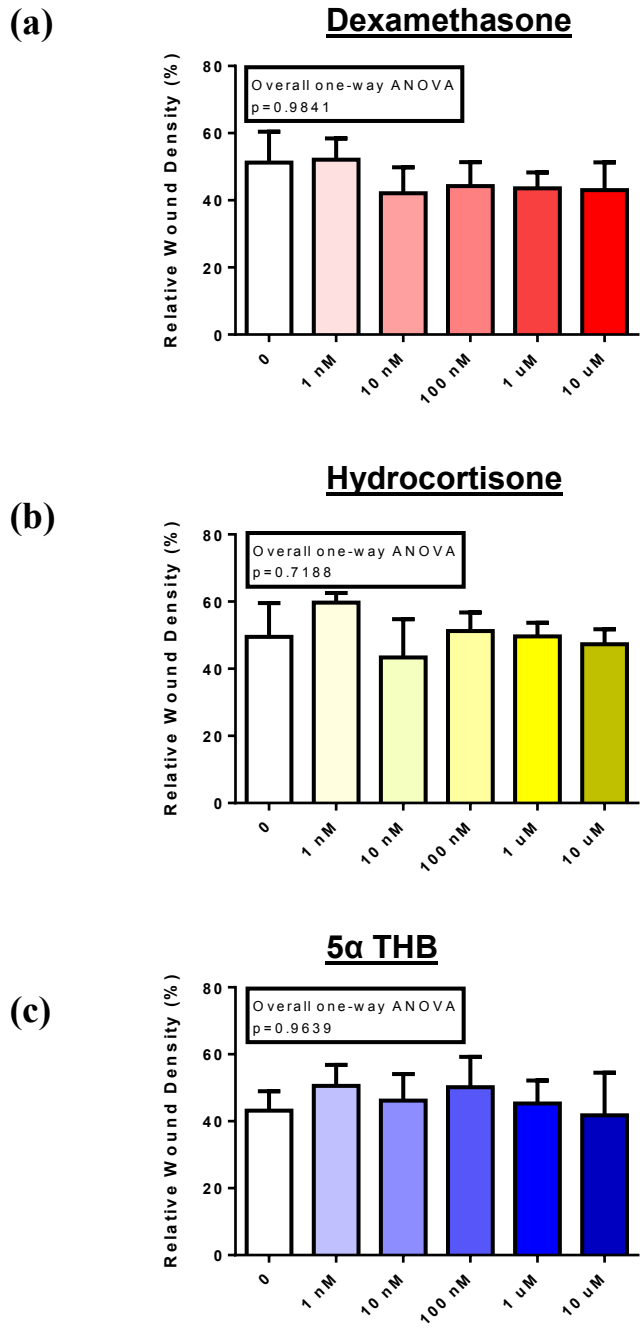

Figure 3.5: Dermal fibroblast cell migration was unaffected by dexamethasone (a), hydrocortisone (b) or 5α-tetrahydrocorticosterone (5αTHB)(c). Cell migration was assessed using the Incucyte® cell migration scratch assay (Essen Bioscience). Cells were plated in stripped serum medium. Scratches were made in confluent cell monolayers and media replaced containing vehicle (ethanol) or either dexamethasone, hydrocortisone or 5αTHB concentrations ranging from 1 nM to 10 μM. Cell migration to cover the scratch area (or 'wound') was then assessed every 2 hours as the 'relative wound density' (RWD), a measurement of the spatial cell density in the wound area relative to the spatial cell density outside of the wound area at every time point. RWD was compared between treatments at the time when RWD of vehicle-treated cells was 40%. The steroids tested did not cause any difference in fibroblast cell migration in comparison to vehicle-treated control. Graphs are mean ± SEM, n=3. Data were analysed by one-way ANOVA.

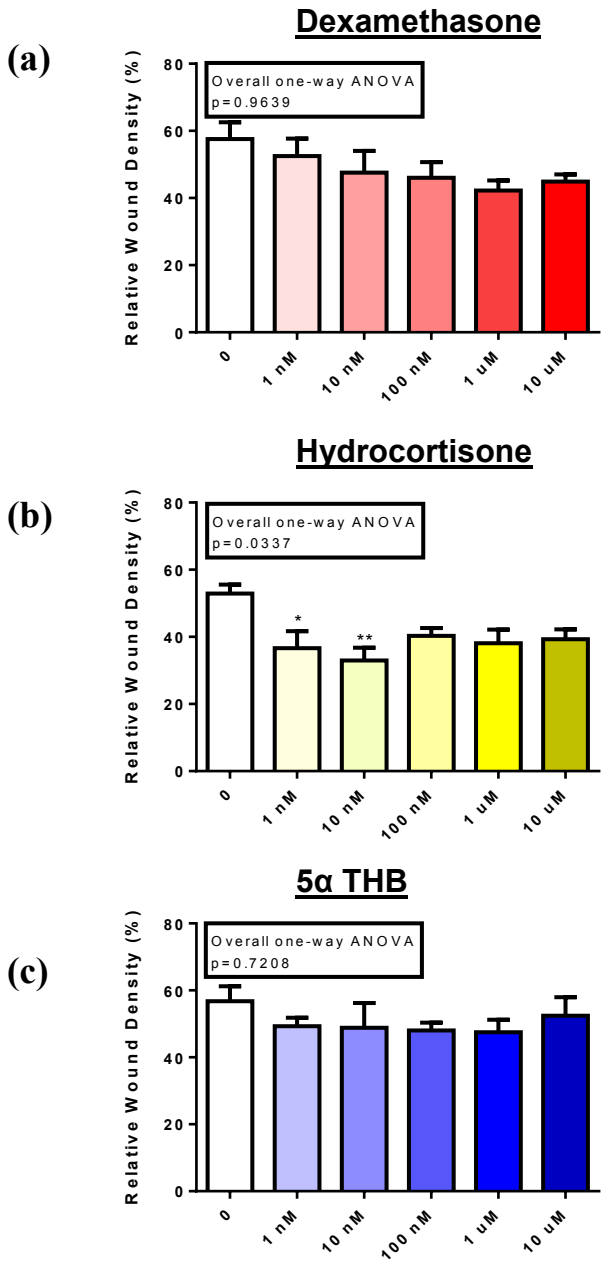

Figure 3.6: Human Umbilical Vein Endothelial Cell (HUVEC) migration was unaffected by dexamethasone (a) or 5α-tetrahydrocorticosterone (5αTHB)(c) but was inhibited by hydrocortisone (b). Cell migration was assessed using the Incucyte® cell migration scratch assay (Essen bioscience). Cells were plated in stripped serum medium. Scratches were made in confluent cell monolayers and media replaced containing vehicle (ethanol), or either dexamethasone, hydrocortisone or 5αTHB at concentrations ranging from 1 nM to 10 μM. Cell migration to cover the scratch area (or 'wound') was then assessed every 2 hours and the 'relative wound density' (RWD) measured: the spatial cell density in the wound area relative to the spatial cell density outside the wound area at every time point. RWD was compared between treatments at the time when RWD of vehicle-treated cells was 40%. RWD of dexamethasone (a) and 5αTHB (c) treated wounds was unchanged relative to control. RWD was decreased by hydrocortisone (b) at doses of 1 nM and 10 nM, indicative of reduced HUVEC cell migration. Comparisons were made with Dunnett's multiple comparisons test. Graphs are mean ± SEM, n=3. Data were analysed by one-way ANOVA. * = P<0.05, ** = P<0.01 vs control.

(a)

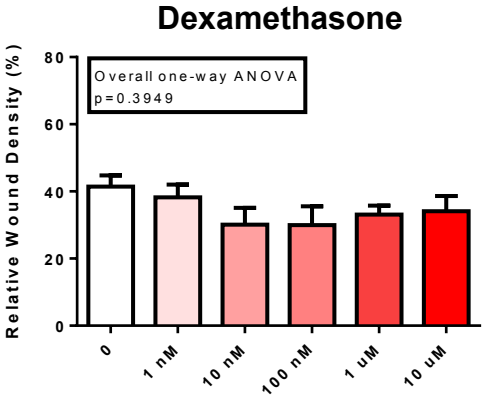

(b)

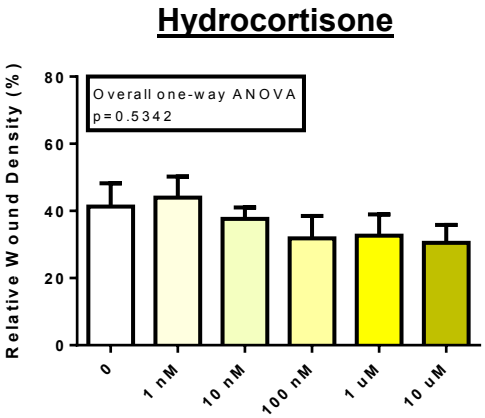

(c)

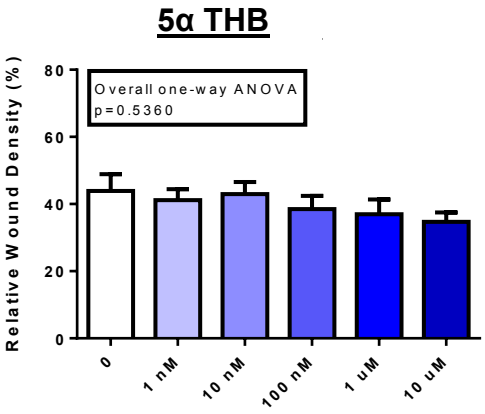

Figure 3.7: HaCaT cell migration was unaffected by dexamethasone (a), hydrocortisone (b) or 5α-tetrahydrocorticosterone (5αTHB) (c). Cell migration was assessed using the Incucyte® cell migration scratch assay (Essen bioscience). Cells were plated in stripped serum medium. Scratches were made in confluent cell monolayers and media replaced containing vehicle (ethanol) or either dexamethasone, hydrocortisone or 5αTHB concentrations ranging from 1 nM to 10 μM. Cell migration to cover the scratch area (or 'wound') was then assessed every 2 hours as the 'relative wound density' (RWD), a measurement of the spatial cell density in the wound area relative to the spatial cell density outside the wound area at every time point. RWD was compared between treatments at the time when RWD of vehicle-treated cells was 40%. None of the drugs caused any difference in HaCaT cell migration in comparison to control, as analysed with Dunnett's multiple comparisons test. Graphs are mean ± SEM, n=3. Data were analysed by one-way ANOVA

3.5.2. The effects of steroids on angiogenesis

3.5.2.1. Assessment of controls

A growth stimulus (FCS followed by VEGF) increased the number of vessels that sprouted from aortic rings in comparison to unstimulated negative controls (figure 3.8). This effect was significant after both 5 and 7 days (white panels in figures 3.9a and b, respectively). However, the magnitude of growth was greater at 7 days, justifying this as the correct time to assess the effects of steroids on vessel growth, as a greater suppression in the number of vessels could be possible at this time point. Dexamethasone (positive control) suppressed vessel growth in a concentration-dependent manner (figures 3.9 and 3.11). There was a pattern indicating dexamethasone-induced suppression of growth at day 5 (figure 3.9a), with significant suppression achieved at 300 nM. However, this concentration-dependent suppression became more apparent at day 7, when several concentrations (30 nM, 100 nM, 300 nM and 1 μM) of dexamethasone significantly suppressed vessel growth. The EC50 dose for suppression of vessel growth by dexamethasone at day 7 was 7.66 nM. However suppression of vessel growth by 10 nM dexamethasone (just higher than the EC50 dose) did not reach significance. Therefore a concentration of 100 nM was chosen as the positive control for future experiments; this was slightly higher than the first concentration required to reach significance (30 nM), in order to ensure demonstration of inhibition.

Power calculations performed using PS: Power and Sample size calculation software (by WD Dupont and WD Plummer, Jr) supported day 7 as the best time point to robustly detect the observed suppression (by 69%) of vessel growth by

dexamethasone. In order to achieve power of 90%, a sample size of 8 was required when assessing vessel growth at day 7.

The large error bars (particularly at lower concentrations of dexamethasone when the mean vessel numbers are high, and hence the standard deviations, are large) demonstrate an inherent variability in this assay. In an attempt to reduce this inter assay variability, the effect of normalising the data to the number of vessels which grew in response to the stimulus alone, was investigated. Curves were fitted to the mean raw data, and the mean data expressed as % stimulus (figure 3.10). However there was no major improvement in the parameters describing the quality of the curve fit by normalising the data to the stimulus. It was, therefore, decided to continue assessing vessel growth using the raw number of vessels.

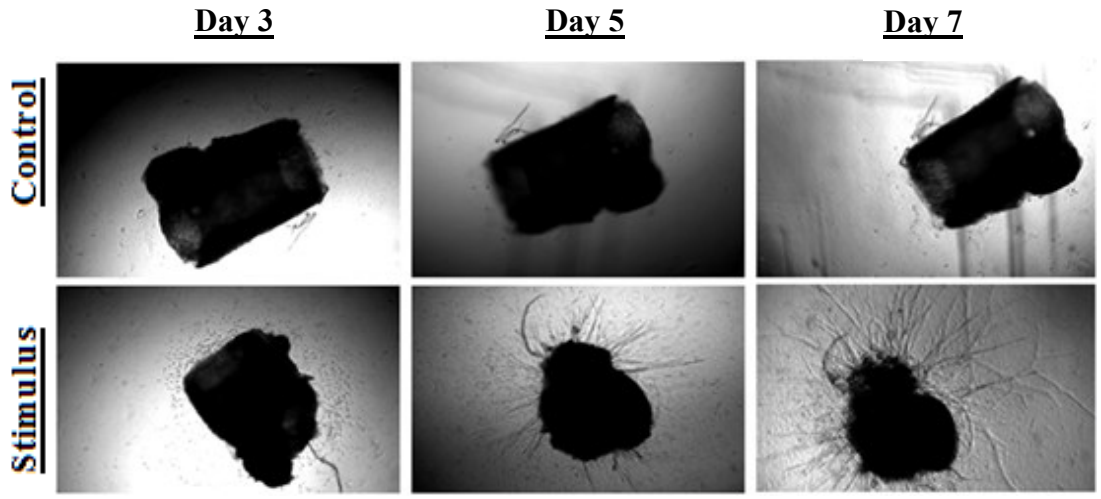

Figure 3.8: Vessel growth was succesfully stimulated from murine aortic rings. Rings were plated in collagen and cultured in medium originally containing 1% Foetal calf serum (FCS, day 0). Medium was replaced on days 3 and 5, with the addition of vascular endothelial growth factor (VEGF, 5 ng/mL) in place of FCS. Rings treated with this stimulus treatment (FCS followed by VEGF) produced many more vessels than control rings, evident on days 5 and 7. Images are representative of n=8.5X magnification.

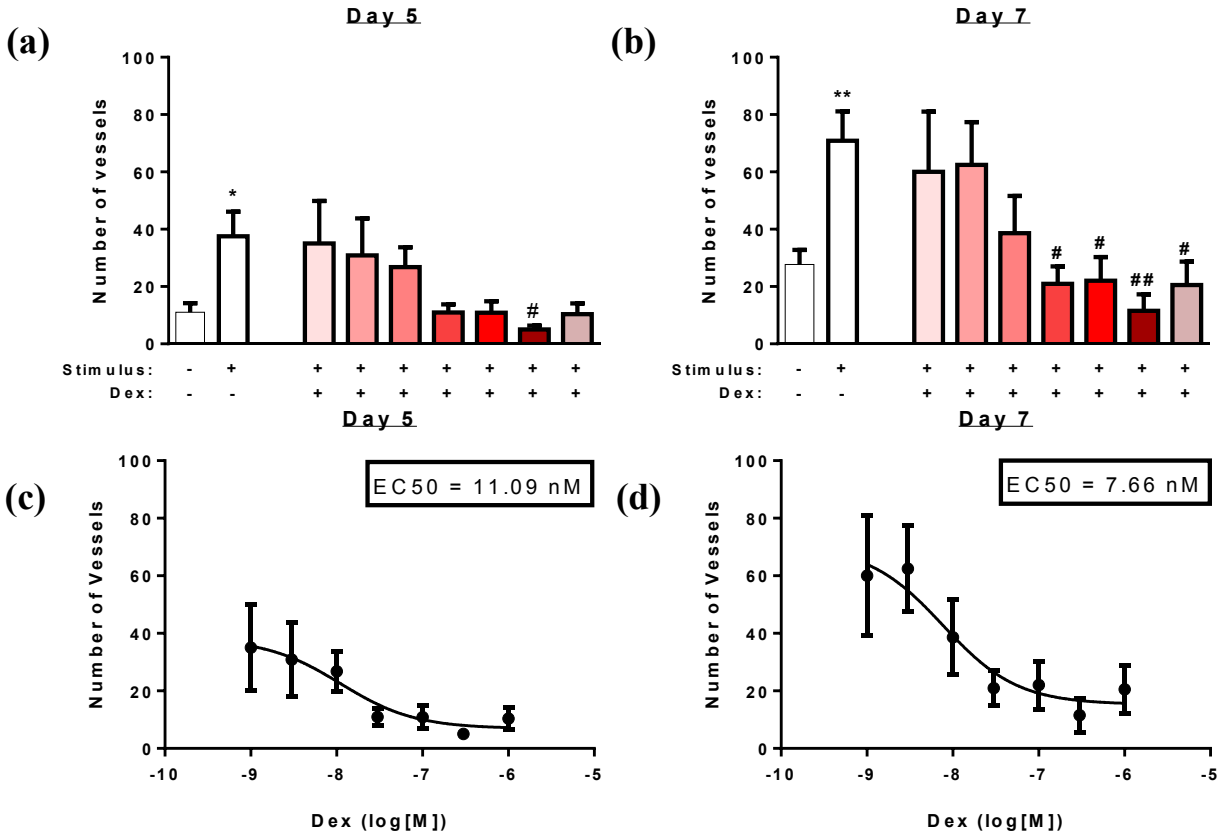

Figure 3.9: Dexamethasone (Dex) induced a concentration-dependent suppression of vessel growth from murine aortic rings. Aortic rings were maintained in medium containing vehicle (control), a stimulus for vessel growth, or a combination of the stimulus plus one of the following concentrations of dexamethasone: 1, 3, 10, 30, 100, 300 or 1000 nM (left to right on graphs). The stimulus consisted of foetal calf serum on day 0, followed by vascular endothelial growth factor on days 3 and 5. Vessels which had grown from aortic rings were counted on day 5 (graphs a and c) and on day 7 (b and d) after plating. The stimulus significantly increased vessel growth from aortic rings after 5 (a) and 7 (b) days, but more vessels had grown at the later time point. Dexamethasone induced a concentration-dependent suppression of this vessel growth, requiring a concentration of 300 nM to reach significance at day 5, and a lower concentration(30 nM) at day 7. Concentration- response curves were then plotted for data at both day 5 (c) and day 7 (d). From these the concentration of dexamethasone required to inhibit vessel growth by half (EC50) was found to be 11.1 nM at day 5, and 7.7 nM at day 7. EC50 values were calculated from mean data due to inherent variability in the aortic ring assay. Graphs show mean ± SEM of n=8. *=P<0.05, **=P<0.01 vs control as analysed by an unpaired t-test. #=P<0.05, ##=P<0.01 vs stimulus as analysed by one-way ANOVA, followed by Dunnett's multiple comparisons test.

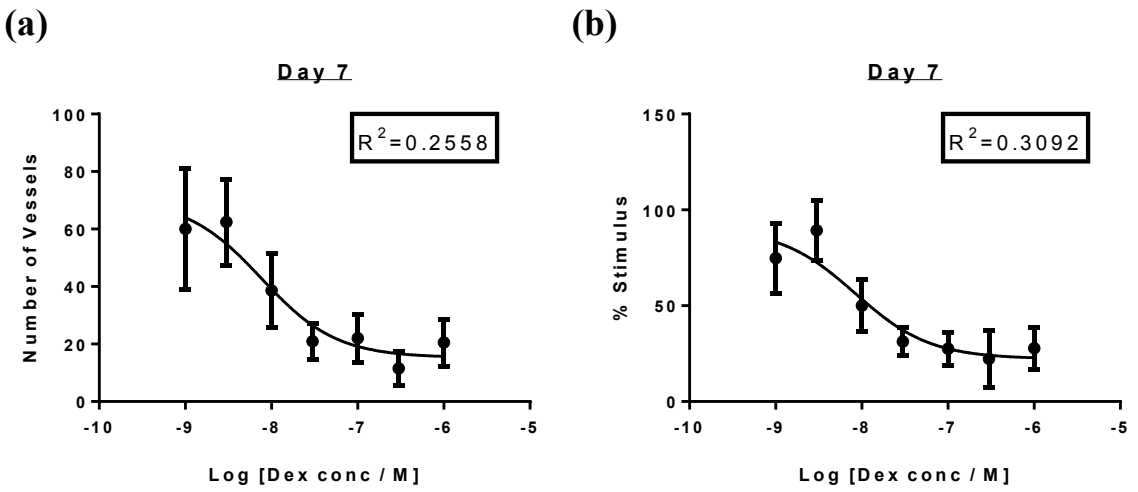

Figure 3.10: Aortic ring assay concentration-response curve fit was not improved through normalisation. Murine aortic rings were maintained in medium containing vehicle (control), a stimulus for vessel growth, or a combination of the stimulus plus dexamethasone (1, 3, 10, 30, 100, 300 or 1000 nM). After 7 days the vessels which had grown from the rings were counted and a concentration-response curve of these raw values was plotted (a). In addition, a concentration-response curve was also plotted of these vessel numbers normalised to the number of vessels which had grown from rings treated with the stimulus alone (set to 100%)(b). The R^2 value for the curve generated by normalising the data was not much different, since the shape stayed the same, so this does not control well for inter assay variability. Data is mean of n=8.

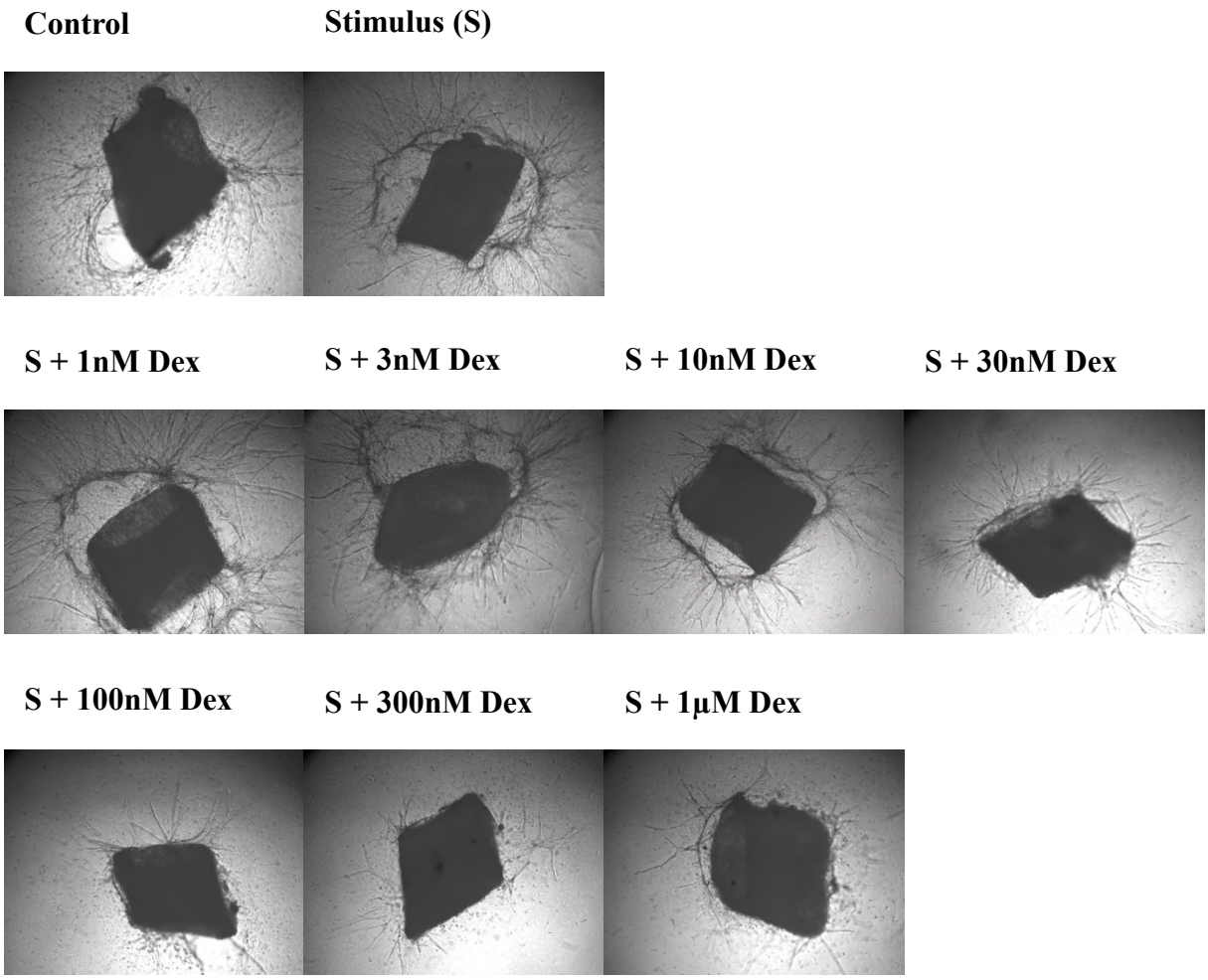

Figure 3.11: Concentration-dependent suppression of vessel growth from aortic rings by dexamethasone (Dex). Aortic rings were plated in collagen and cultured in medium either alone, containing a stimulus (S) for vessel growth, or with a combination of the stimulus plus a dexamethasone concentration ranging from 1 nM to 1 µM. The stimulus increased the number of vessels which had sprouted from aortic rings after 7 days. Dexamethasone induced a concentration-dependent suppression of this vessel growth with 7.7 nM required for half-maximal effect (EC50). The EC50 was calculated from mean data due to inherent variability in the aortic ring assay. Images are representative of n=8. 5X magnification.

3.5.2.2. *Assessment of the effect of hydrocortisone in an* ex vivo *model of angiogenesis*

As demonstrated by the white panels in figure 3.12a, the stimulus (FCS followed by VEGF) was successful in stimulating the growth of vessels from murine aortic rings after 7 days of culture. This was consistent with the previous experiments given in figure 3.9, in which a similar number of vessels grew after treatment with the stimulus. This vessel growth was inhibited by the positive control, dexamethasone, once again demonstrating that angiogenesis can be manipulated in this assay and, hence, its appropriateness for assessing steroid effects.

Further rings were treated with a combination of the stimulus and hydrocortisone. Hydrocortisone induced a concentration-dependent suppression of vessel growth from murine aortic rings. However, it was less potent than dexamethasone; the suppression of vessel growth became significant in comparison to stimulated controls (not treated with steroid) at a concentration of 1 μM (figure 3.12a) and the EC50 for suppression by hydrocortisone was 867 nM (figure 3.12b).

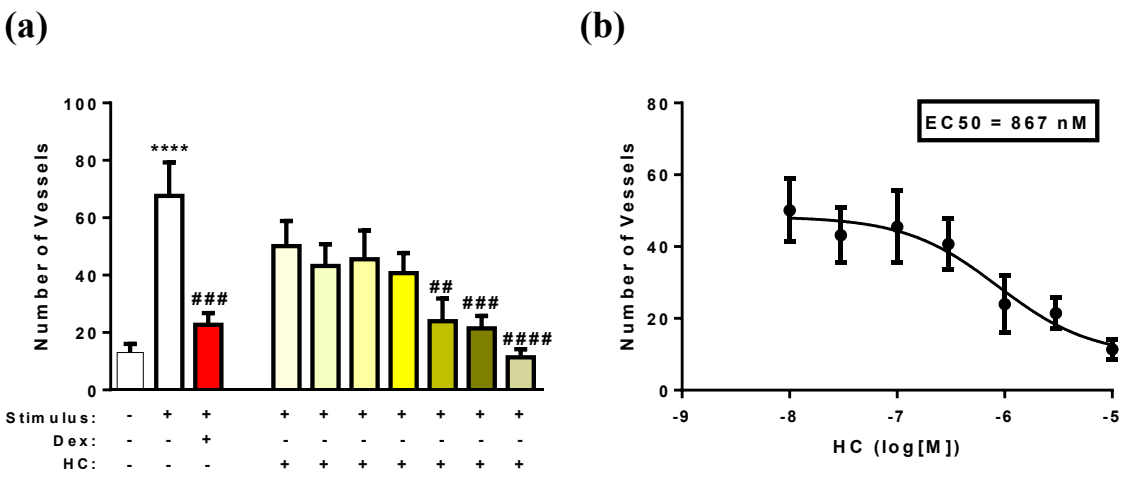

Figure 3.12: Hydrocortisone (HC) induced a concentration-dependent suppression of vessel growth from murine aortic rings. Aortic rings were maintained in medium either containing vehicle (control), a stimulus for vessel growth, or a combination of the stimulus plus dexamethasone (Dex) positive control (100 nM) or a HC concentration of 10, 30, 100, 300, 1000, 3000 or 10,000 nM (left to right on graphs). The stimulus consisted of foetal calf serum on day 0 followed by vascular endothelial growth factor on days 5 and 7. Vessels which had grown from aortic rings were counted 7 days after plating. By day 7, the stimulus had caused a significant increase in vessel growth from aortic rings (graph a). HC induced a concentration--dependent suppression of this vessel growth, with the effect becoming significant at 1 μM. A concentration-response curve (R^2=0.2891) was plotted (b) and from this the concentration of HC required to inhibit vessel growth by half (EC50) was 867 nM. The EC50 was calculated from mean data due to inherent variability in the aortic ring assay. Graphs show mean ± SEM of n=8. ****=P<0.0001 vs control, ##=P<0.01, ###=P<0.001, ####=P<0.0001 vs stimulus as analysed by one-way ANOVA followed by Dunnett's multiple comparisons test.

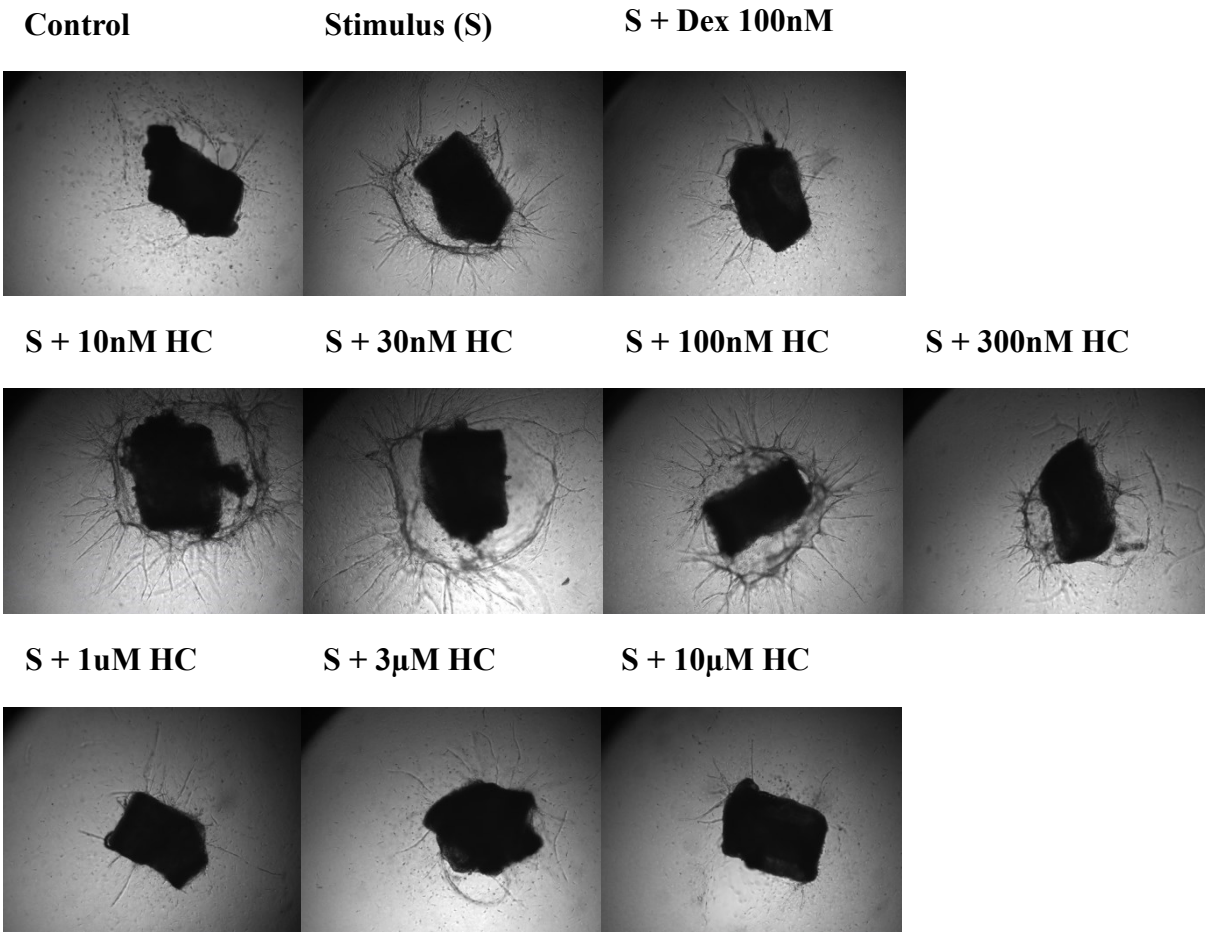

Figure 3.13: Concentration-dependent suppression of vessel growth from aortic rings by hydrocortisone (HC). Aortic rings were plated in collagen and cultured in medium either alone, containing a stimulus (S) for vessel growth, or with a combination of the stimulus plus 100 nM dexamethasone (Dex) or a HC concentration ranging from 10 nM to 10 µM. The stimulus increased the number of vessels which had sprouted from aortic rings after 7 days. Dexamethasone (positive control) suppressed this vessel growth. HC also induced a concentration-dependent suppression of vessel growth with 867 nM required for half-maximal effect (EC50). The EC50 was calculated from mean data due to inherent variability in the aortic ring assay. Images are representative of n=8. 5X magnification.

3.5.2.3. Assessment of the angiostatic effects of 5αTHB in an ex vivo model.

As demonstrated in figure 3.14a, during experiments with 5αTHB the growth stimulus (FCS followed by VEGF) significantly increased the number of vessel outgrowths which had sprouted from mouse aortic rings after 7 days. This is consistent with the stimulus effect previously described (figures 3.9 and 3.12). Dexamethasone (positive control; 100 nM) significantly suppressed this vessel growth, demonstrating a functional and reliable assay.

5αTHB also suppressed vessel growth from aortic rings. This suppression was evident at higher concentrations than required with the other steroids tested, reaching significance in comparison to stimulated control at 3 μM and 10 μM (figure 3.14a). However, at lower concentrations the effect of 5αTHB was less clear, and the concentration-response curve was flatter in comparison to those for dexamethasone and hydrocortisone. This is reflected in the higher EC50 of 2399 nM for suppression of vessel growth by 5αTHB in this model (figure 3.14b).

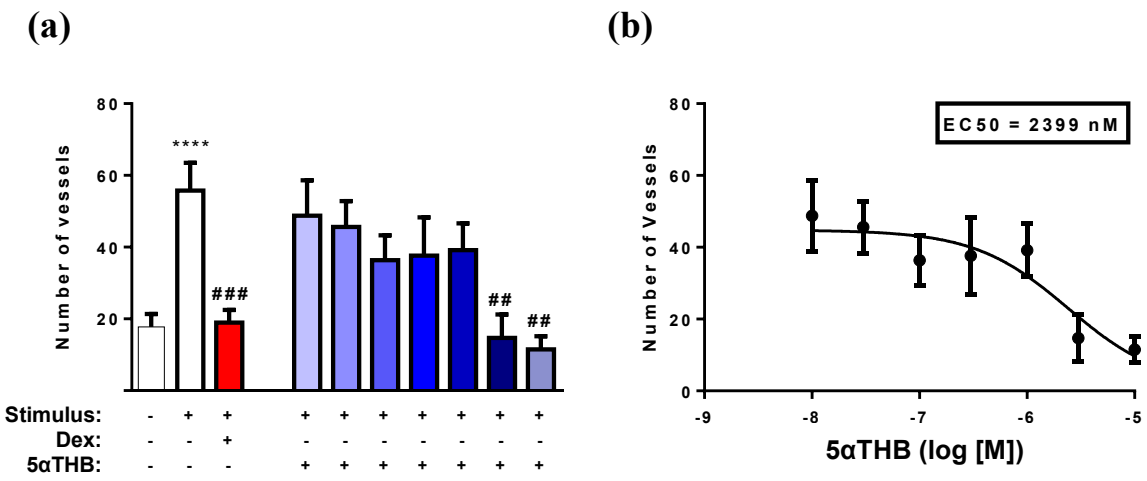

Figure 3.14: 5αTHB induced a concentration-dependent suppression of vessel growth from murine aortic rings. Aortic rings were maintained in medium either containing vehicle (control), a stimulus for vessel growth, or a combination of the stimulus plus dexamethasone (Dex; positive control) or 5αTHB at a concentration of 10, 30, 100, 300, 1000, 3000 or 10,000 nM. The stimulus consisted of foetal calf serum on day 0 followed by vascular endothelial growth factor on days 5 and 7. Vessels which had grown from aortic rings were counted 7 days after plating. At day 7, the stimulus had caused a significant increase in vessel growth from aortic rings. 5αTHB induced a concentration-dependent suppression of this vessel growth, with the effect becoming significant at 3 μM. A concentration-response curve (b) was subsequently plotted (R^2=0.2512) and from this the concentration of 5αTHB required to inhibit vessel growth by half (EC50) was determined as 2399 nM. The EC50 was calculated from mean data due to inherent variability in the aortic ring assay. Graphs show mean ± SEM of n=8. ****=P<0.0001 vs control, #=P<0.05, ##=P<0.01, ###=P<0.001 vs stimulus as analysed by one-way ANOVA followed by Dunnett's multiple comparisons test.

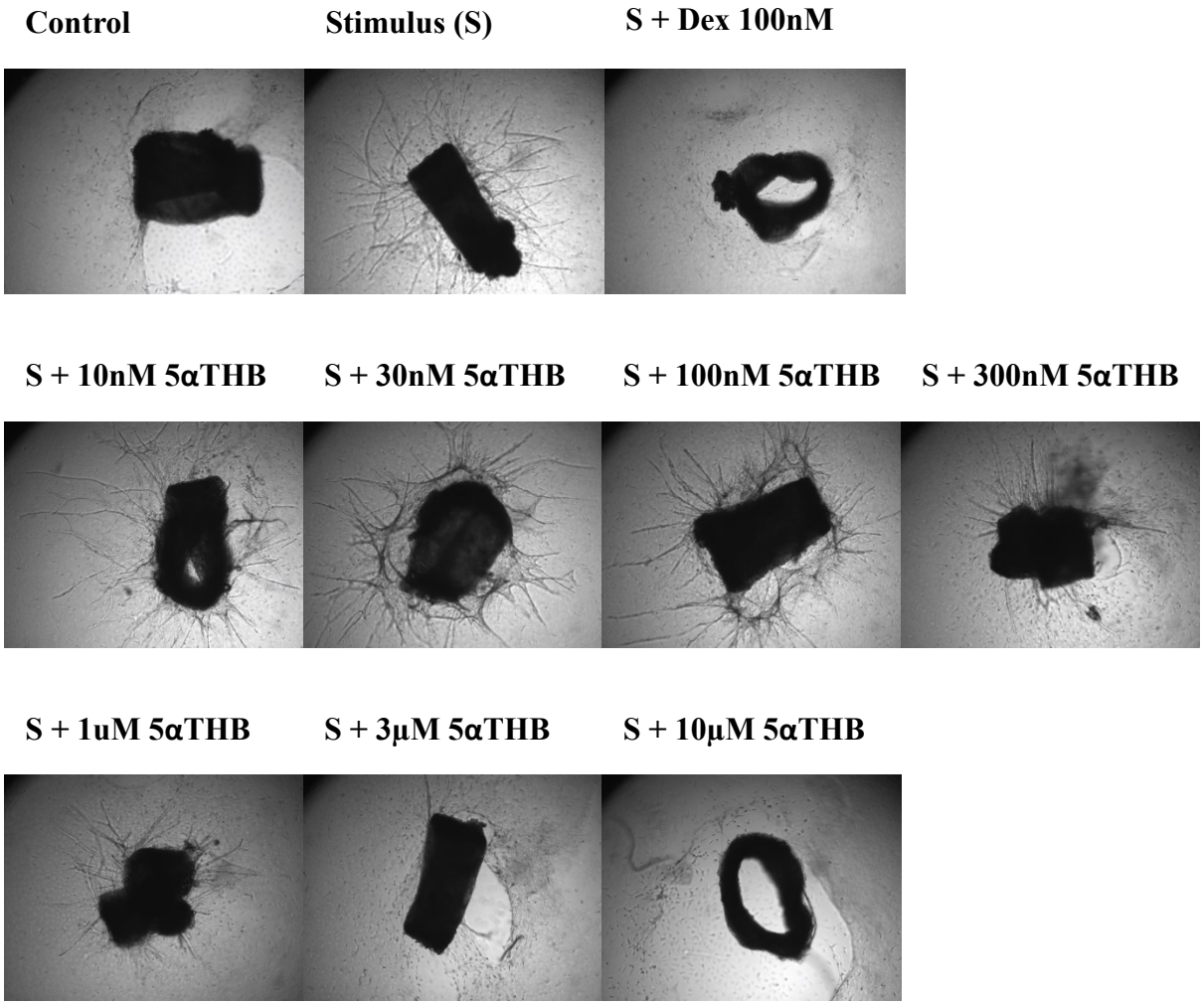

Figure 3.15: Concentration-dependent suppression of vessel growth from aortic rings by 5αTHB. Aortic rings were plated in collagen and cultured in medium either alone, containing a stimulus (S) for vessel growth, or with a combination of the stimulus plus 100 nM dexamethasone (Dex) as a positive control, or plus 5αTHB at a concentration ranging from 10 nM to 10 μM. The stimulus increased the number of vessels which had sprouted from aortic rings after 7 days. Dexamethasone suppressed this vessel growth. 5αTHB induced a concentration-dependent suppression of vessel growth with 2399 nM required for half-maximal effect (EC50). The EC50 was calculated from mean data due to inherent variability in the aortic ring assay. Images are representative of n=8. 5X magnification.

3.5.2.4. Summary of the effects of 5αTHB and hydrocortisone on angiogenesis in the aortic ring assay model.

As evident from figures 3.12 and 3.14, hydrocortisone and 5αTHB both induced concentration- dependent suppression of vessel outgrowth from mouse aortic rings. Hydrocortisone did this with an EC50 of 867 nM and achieved a significant suppression with doses 1 μM and above. 5αTHB was less potent than hydrocortisone to suppress vessel growth. It had a higher EC50 of 2399 nM and required a larger dose of 3 μM in order for its suppression of vessel growth to reach significance. A summary of the angiostatic effects of the steroids tested in this model, including that of the positive control dexamethasone, is given in table 3.4.

Steroid	**EC50 for angiostasis**	**Lowest dose for significant angiostatic effect, and suppression achieved versus stimulated control.**
Dexamethasone	7.7 nM	30 nM, achieving 65±11% suppression.
Hydrocortisone	867 nM	1 μM, achieving 70±7% suppression.
5αTHB	2399 nM	3 μM, achieving 74±14% suppression.

Table 3.4: A summary of the effects of steroids on angiogenesis in a murine aortic ring model after 7 days. Murine aortic rings were plated in collagen and cultured in medium with a stimulus for vessel growth plus either vehicle (ethanol, 1 μL per 1 mL), or dexamethasone, hydrocortisone or 5αTHB at concentrations ranging from 1 nM to 10 μM. All steroids induced concentration-dependent suppression of the stimulated vessel growth, with the half-maximal doses (EC50) given in the middle column. EC50 values were calculated from mean data due to the inherent variability in the aortic ring assay. The dose of each steroid required for the suppression of vessel growth to reach significance against stimulated controls (not treated with steroid) is given in the right hand column. Data were determined from mean of n=8 experiments.

3.5.3. Investigation of the involvement of GR in the angiostatic effects of 5αTHB

In section 3.4.2. it was determined that 5αTHB induced a concentration-dependent suppression of angiogenesis in the murine aortic ring assay, albeit with a lower potency than either hydrocortisone or dexamethasone. To understand the underlying mechanism, the GR antagonist RU486 was used to determine whether this suppression of angiogenesis was mediated through GR. A GR-selective agonist, dexamethasone, was used as the positive control (hydrocortisone being a ligand for both MR and GR).

3.5.3.1. Antagonism of the angiostatic effect of 5αTHB using equipotent doses of RU486

N=12 was selected to increase power, since a concentration-response was no longer being performed. Equal concentrations of RU486 and steroid were used, since in previous preliminary work by McInnes (2003) this was sufficient for RU486 to antagonise the effect of 5αTHB in the same assay. The lowest concentrations required of dexamethasone and 5αTHB (as determined in sections 3.4.1.2 and 3.4.1.3) in order to significantly suppress vessel growth, were chosen in order to assess antagonism by RU486. At these doses it was anticipated that any antagonism would clearly be evident.

Once again, aortic rings responded well to the stimulus with vessel growth successfully increased to an average of 98 sprouts per ring (figure 3.16). Dexamethasone (30 nM) suppressed this vessel growth (figure 3.16a) consistent with previous data. Low concentration (30 nM) RU486, in the absence of steroid, did not

alter vessel growth but the high concentration (3 μM) induced a significant suppression of growth. For this reason the combined effects of the steroids with this high concentration of RU486, could not be interpreted. Whereas dexamethasone (30 nM) suppressed vessel growth alone, in combination with the lower concentration of RU486 (30 nM, concentration equivalent to dexamethasone) it did not, suggesting some antagonism. Power calculations indicated that N=117 were required to detect (with 90% power) a significant difference between dexamethasone- mediated suppression of vessel growth in the presence of RU486, and in the absence of RU486. With regard to 5αTHB, in contrast to the previous concentration-response data, suppression of vessel growth by a concentration of 3 μM did not achieve significance (figure 3.16b). Power calculations based on this data demonstrated that N=41 would be required for the effect to become significant (for a power of 90%).

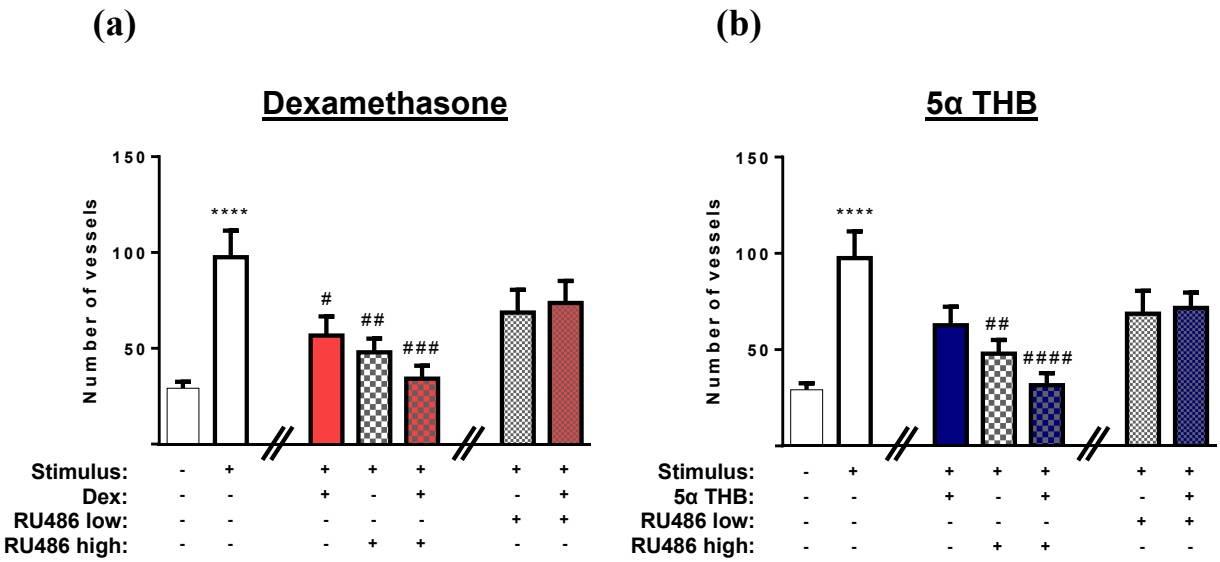

Figure 3.16: Investigation of the involvement of the glucocorticoid receptor (GR) in 5αTHB-mediated inhibition of angiogenesis. The GR antagonist RU486 was used to assess whether the suppression of vessel growth by (a) dexamethasone (Dex; positive control), or (b) 5αTHB, is mediated via GR. Murine aortic rings were cultured in medium either with vehicle (control), with a stimulus for vessel growth, or with a combination of the stimulus plus either dexamethasone (30 nM) or 5αTHB alone or in combination with RU486 at low (30 nM) or high (3 μM) concentrations. The stimulus increased the number of vessels which grew from aortic rings. High concentration RU486 alone suppressed this vessel growth, making its effects in combination with the steroids difficult to interpret. Graphs are mean ± SEM of n=12. ****=P<0.0001 vs control as analysed by unpaired t-test, #=P<0.05, ##=P<0.01, ###=P<0.001, ####=P<0.0001 vs stimulus, as analysed by one-way ANOVA followed by Dunnett's multiple comparisons test.

3.5.3.2. Assessment of antagonism by a shift in the concentration-response curves.

In section 3.5.3.1 single doses of steroid (30 nM of dexamethasone and 3 μM of 5αTHB) were used to suppress vessel growth, and antagonism of this suppression was assessed using RU486. However due to the inherent variability in the aortic ring assay, the sample sizes required to detect significant effects and gain definitive answers in this previous section would be very high, requiring many mice. In this current section, in order to better interpret the effects of RU486, the steroid concentration- responses were re performed in the presence of RU486 (30 nM). The EC50 values were then compared for steroid dose responses in the presence and absence of RU486, to assess whether the EC50 values were altered by RU486.

3.5.3.2.1. Assessment of the effect of RU486 on the concentration-response to dexamethasone

The stimulus significantly increased vessel growth from aortic rings in comparison to unstimulated controls (figure 3.17a). However there was less vessel outgrowth formation from rings in general in this assay compared to previous experiments. For example, during the original dexamethasone concentration-response (figure 3.9b) an average of 28 vessel outgrowths formed from unstimulated control rings, in comparison to an average of 15 vessel outgrowths in this experiment (figure 3.17a). Likewise, an average of 71 vessel outgrowths formed from stimulated controls in the original dexamethasone concentration-response, compared to an average of 34 in this experiment. Also in contrast, the suppression of vessel outgrowth formation by dexamethasone alone at 100 nM (positive control) in this current assay did not reach

significance (p=0.2). This is likely related to the assay variability as well as the lower number of vessel outgrowths, resulting in reduced sensitivity of the assay to allow detection of small effects. Power calculations revealed that a sample size of 47 would be required to detect a significant suppression of vessel growth by dexamethasone with 90% power. This reflects problems with this experiment in comparison to the previous concentration-response experiment where n=8 was sufficient to achieve high power. An additional problem was that RU486 itself suppressed vessel growth, even at this lower dose of 30 nM, further complicating the interpretation of the experiment and indicating that further methods of answering the question should instead be sought. In spite of these issues, in the presence of 30 nM RU486, dexamethasone still induced a concentration-dependent suppression of vessel growth in this experiment. A higher dose (1 μM) was required to reach significance in comparison to 30 nM required previously (figure 3.9b) in the absence of RU486. In addition the EC50 had increased to 287.7 nM (in comparison to 7.7 nM in the absence of RU486). A rightward shift was therefore induced in the dexamethasone concentration response curve by RU486. Raw vessel numbers were normalised to stimulated controls and concentration-responses in the presence and absence of RU486 were superimposed on the same graph (figure 3.19a). Although the error bars do overlap at the lowest and highest doses of dexamethasone, they do not for the middle doses. Again this is suggestive of some antagonism by RU486, however it is not definitive due to the lack of power in this assay.

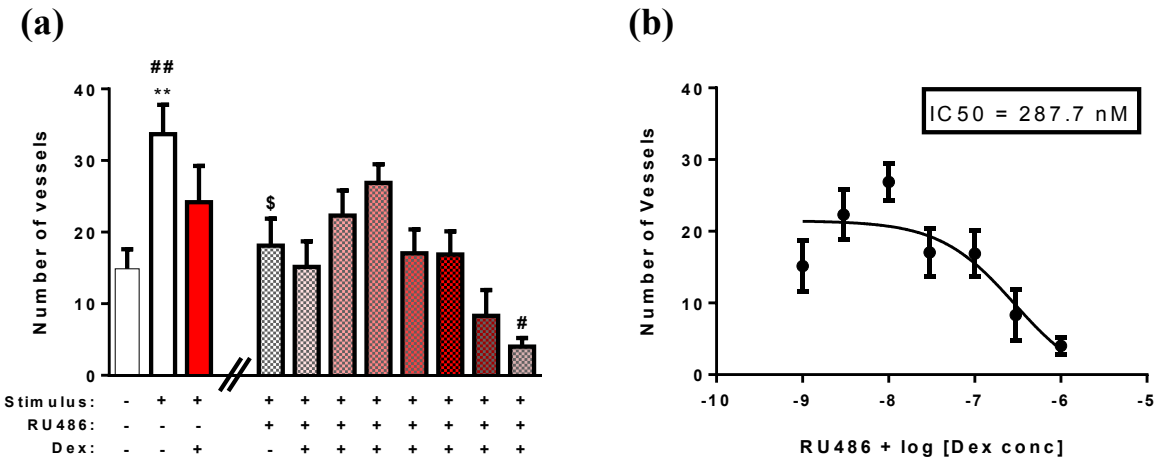

Figure 3.17: Investigation of the effect of the glucocorticoid receptor antagonist RU486 on the suppression of angiogenesis by dexamethasone. Murine aortic rings were cultured in medium either with vehicle (control), with a stimulus for vessel growth, or with a combination of the stimulus plus RU486 (30 nM) alone or together with one of the following concentrations of dexamethasone: 1, 3, 10, 30, 100, 300 or 1000 nM (left to right on graphs). After 7 days vessels which had grown from the rings were counted. The stimulus (foetal calf serum on day 0, followed by vascular endothelial growth factor on days 3 and 5) increased the number of vessels which grew from aortic rings in comparison to control. RU486 when given alone suppressed this vessel growth, and dexamethasone had an additional effect, achieving significance in comparison to RU486 alone at a dose of 1 μM (a). In the presence of RU486 the concentration of dexamethasone required to inhibit vessel growth by half (EC50) was 287.7 nM (b). EC50 values were calculated from mean data. Graphs show mean ± SEM of n=8. **=P<0.01 vs control, #=P<0.05, ##=P<0.01 vs Stimulus + RU486, $=P<0.05 vs Stimulus, as analysed by one-way ANOVA followed by Dunnett's multiple comparisons test.

3.5.3.2.2. Assessment of the effect of RU486 on concentration response curve to 5αTHB

The stimulus significantly increased vessel growth from aortic rings in comparison to unstimulated controls (figure 3.18a) from an average of 12 to an average of 32. Again, this assay has a lower power than the previous 5αTHB concentration response curve in the absence of RU486 (figure 3.14a) in which vessel growth was increased to an average of 56 from an average of 18. Just as in the dexamethasone concentration-response curve in the presence of RU486 (figure 3.17a), the dexamethasone positive control did not suppress the stimulated vessel growth in this experiment (figure 3.18a). As suggested previously, this is likely to be a consequence of the low power of this experiment; indeed when the control data from both experiments are combined (to achieve n=16; figure 3.20) the suppression by dexamethasone becomes significant. Suppression of vessel growth by 5αTHB was also not statistically significant (figure 3.18a). From the concentration-response curve (figure 3.18b) a higher EC50 of 3110 nM was evident, in comparison to 2399 nM in the absence of RU486 (figure 3.14b). Again, this could be interpreted as a rightward shift of the concentration-response curve by RU486; however, when the normalised concentration-response curves in the presence and absence of RU486 were superimposed on the same graph (figure 3.19b) the error bars overlapped for all concentrations of 5αTHB. This suggests that RU486 did not antagonise the effect of 5αTHB. However again due to the lack of power this is not conclusive.

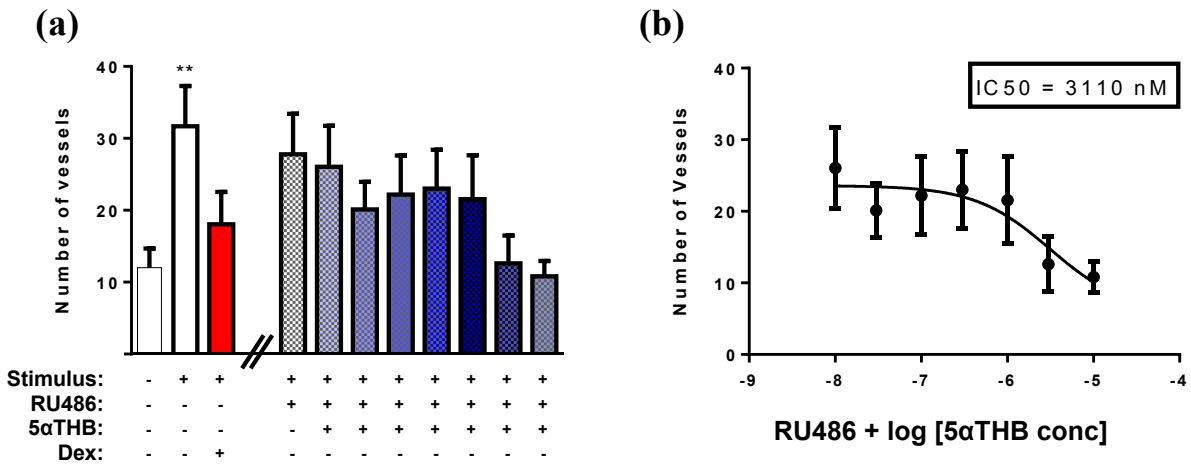

Figure 3.18: Investigation of glucocorticoid receptor antagonist RU486 effect on the suppression of angiogenesis by 5αTHB. Murine aortic rings were cultured in medium either with vehicle (control), with a stimulus for vessel growth, or with a combination of the stimulus plus RU486 (30 nM) alone or together with one of the following concentrations of 5αTHB: 10, 30, 100, 300, 1000, 3000 or 10000 nM (left to right on graphs). After 7 days, vessels which had grown from the rings were counted. The stimulus (foetal calf serum on day 0, followed by vascular endothelial growth factor on days 3 and 5) increased the number of vessels which grew from aortic rings in comparison to control. Suppression of this by dexamethasone (Dex) positive control did not achieve significance, demonstrating a lack of power in this assay and making further interpretation difficult. Graphs show mean ± SEM of n=8. **=P<0.01 vs control as analysed by one-way ANOVA followed by Dunnett's multiple comparisons test.

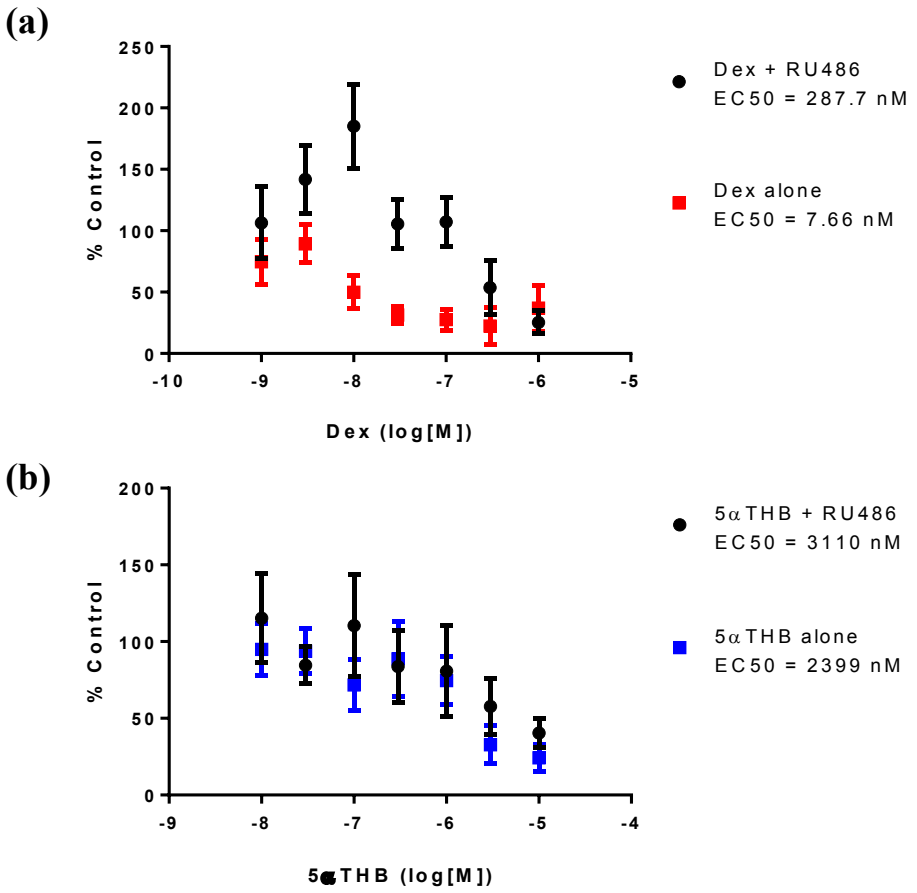

Figure 3.19: The effect of the glucocorticoid receptor antagonist RU486 on the suppression of angiogenesis by dexamethasone (Dex) and 5αTHB. Steroid-induced suppression of vessel growth from mouse aortic rings was compared in the presence and absence of RU486 (30 nM). The number of vessels which grew from rings was normalised to stimulated controls, and normalised data were used to superimpose concentration-response curves in the presence and absence of RU486 for (a) dexamethasone, and (b) 5αTHB. Whereas RU486 appears to antagonise the effect of low concentrations of dexamethasone, it did not antagonise the effect of 5αTHB. Graphs show mean ± SEM of n=8.

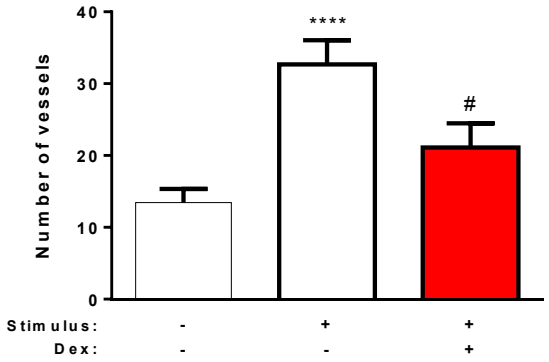

Figure 3.20: Combined control data from concentration-response experiments for dexamethasone and 5αTHB in combination with RU486. Graphs show mean ± SEM of 16. ****=P<0.0001 vs control, #=P<0.05 vs stimulus, as analysed by one-way ANOVA followed by Dunnett's multiple comparisons test.

3.5.4. The effect of steroids on gene expression in the mouse aorta

In addition to investigating the mechanisms of 5αTHB by antagonism with RU486 (section 1.4.3), in this section the effects of 5αTHB on gene expression in the aorta were compared to those of hydrocortisone and dexamethasone.

3.5.4.1. Retrieval of aortic rings and RNA extraction.

In sections 1.4.2 and 1.4.3, aortic ring assays were performed, from which aortic rings were available for RNA extraction and subsequent gene expression analysis. Additional experiments were also performed to increase the availability of rings as they needed to be pooled. It was established, whilst using the protocol for RNA extraction described in section (2.2.1.2), that it was necessary to combine four aortic rings for RNA extraction in order to obtain sufficient RNA for analysis by qPCR. An initial power calculation revealed that a sample size of 5 was required in order to detect a 362% induction of *Per1* by dexamethasone with 90% power. Therefore a sample size of at least N=5 was ensured for all treatment groups. The

number of RNA samples produced varied according to the aortic rings available, and were as follows: Stimulus only N=11, Dexamethasone N=8, Hydrocortisone N=5, 5αTHB N=9, RU486 N=6, RU486 + Dex N=5, RU486 + 5αTHB N=5.

3.5.4.2. Comparison of the effects of 5αTHB, dexamethasone, and hydrocortisone on gene expression in mouse aortic rings

3.5.4.2.1. Genes involved in inflammation and signalling

Exposure to dexamethasone decreased the abundance of transcripts for *Cxcl5* (figure 3.21a) and produced a trend (p=0.053) to increase transcripts for *Dusp1* (figure 3.21b) in mouse aortic rings undergoing angiogenesis. Hydrocortisone decreased transcript abundance of *Cxcl5* (figure 3.21a) and increased that of *Dusp1* (figure 3.21b)(30). 5αTHB did not affect transcript abundance of these genes. There was a trend (p=0.07) for 5αTHB to increase transcripts of *Mcp1* versus control (figure 3.21c). *Mcp1* transcripts were significantly increased (P<0.01) by 5αTHB in comparison to aortic rings exposed to dexamethasone or hydrocortisone, both of which had no effect. Therefore the trend for 5αTHB to increase *Mcp1* transcripts would likely become significant with increased power. *iNOS* expression was not altered by any treatment (figure 3.21d).

3.5.4.2.2. Genes involved in remodelling of the extracellular matrix (ECM)

The transcript abundance of *Col4a1* was increased by hydrocortisone and there was a trend (p=0.0501) for an increase with dexamethasone (figure 3.21e). Both dexamethasone and hydrocortisone decreased abundance of *Mmp9* transcripts (figure 3.21f). There was a trend (p=0.09) for hydrocortisone to reduce the expression of

Col14a1 (figure 3.21g). 5αTHB did not alter abundance of any of these gene transcripts.

3.5.4.2.3. Genes involved in remodelling the vasculature

5αTHB decreased the abundance of *Pecam1* transcripts, and hydrocortisone also exhibited a trend (p=0.07) to decrease them (figure 3.21h). *Vcam1* expression was not altered by any treatment (figure 3.21i).

3.5.4.2.4. Genes known to be directly associated with GR

Dexamethasone and hydrocortisone both increased the abundance of *Per1, Hsd11b1,* and *Fkbp51* transcripts (figures 3.21j, k, and l). 5αTHB only increased the abundance of *Per1* transcripts; however this was to a lesser extent than hydrocortisone or dexamethasone (figure 3.21j).

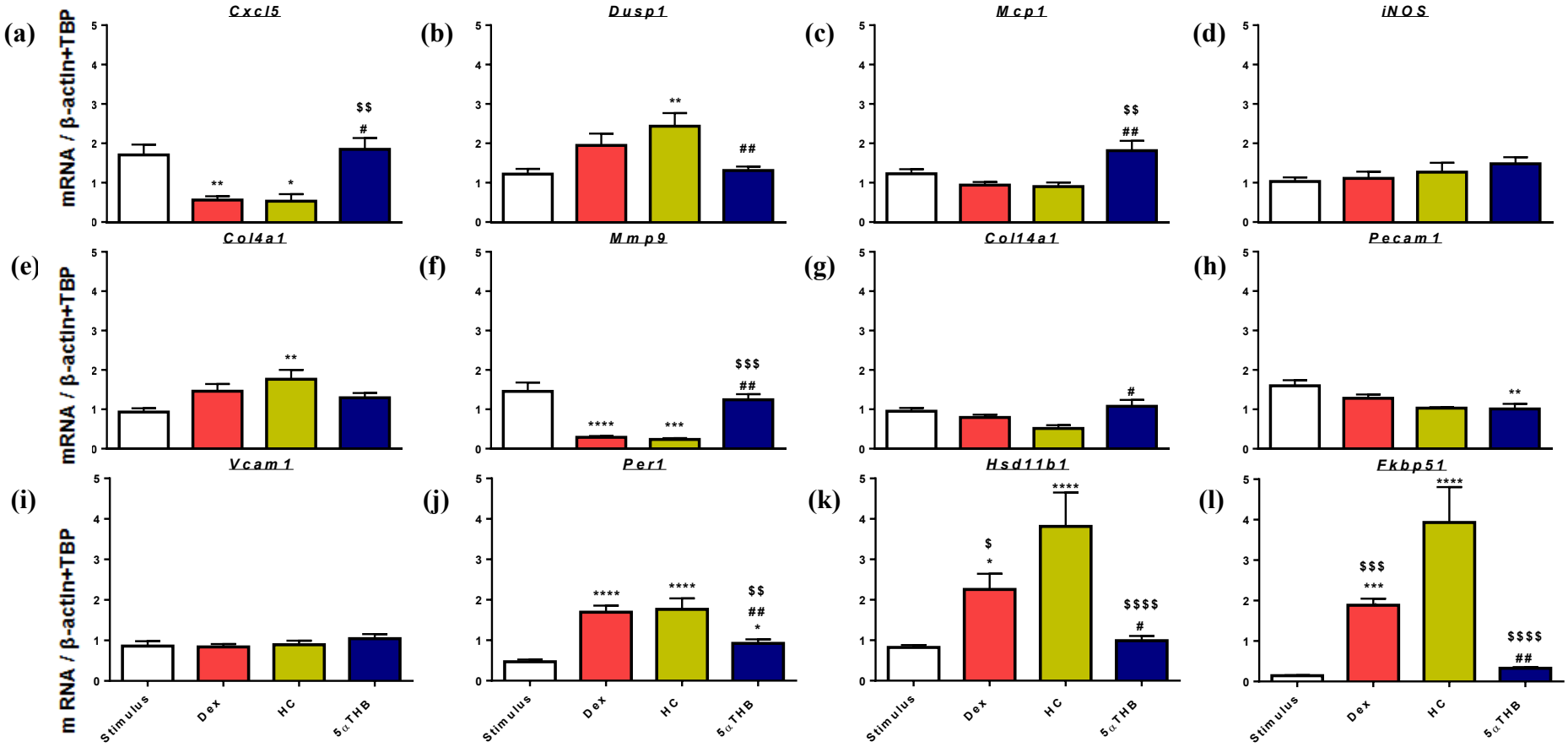

Figure 3.21: Steroid effects on gene transcript abundance: RNA was extracted from stimulated mouse aortic ring sections treated with either vehicle (stimulus only), dexamethasone (Dex; 30 nM), hydrocortisone (HC; 1μM) or 5αTHB (3 μM). The RNA was reverse transcribed into cDNA and analysed by real-time PCR for expression of genes involved in inflammation and signalling ((a) *Cxcl5*, (b) *Dusp1*, (c) *Mcp1*, and (d) *iNOS), extracellular matrix (ECM) remodelling ((e) Col4a1, (f) Mmp9, (g) Col14a1), vasculature remodelling ((h) Pecam1, (i) Vcam1) as well as typical GR responsive genes ((j) Per1, (k) Hsd11b1 and (l) Fkbp51))* . n=11 for stimulus- only treated group, n=8 for Dex, n=5 for HC, and n=9 for 5αTHB. Graphs (mean ± SEM) were analysed by one-way ANOVA followed by Tukey's multiple comparison test, *=p<0.05, **=p<0.01, ***=p<0.001, ****=p<0.0001 vs Stimulus; #=p<0.05, ##=p<0.01, ####=p<0.0001 vs HC; $=p<0.05, $$=p<0.01, $$$=p<0.001, $$$$=p<0.0001 vs Dex.

3.5.4.3. Using RU486 to investigate the involvement of GR in the effects of steroids on gene expression in mouse aortic rings.

In order to test the contribution of GR to transcript regulation by 5αTHB, the ability of RU486 to antagonise the effect was assessed. It should be kept in mind that this experiment is compromised by my demonstration that RU486 had a direct effect on vessel growth in this assay. Dexamethasone was used as a positive control in this experiment, since it is a selective GR agonist. Dexamethasone no longer caused differential expression of *Cxcl5*, *Mmp9*, and *Hsd11b1* when co-administered with RU486 (figures 3.22a, b and d). RU486 also tended to antagonise dexamethasone-induced up-regulation of *Per1* (P=0.06) and *Fkbp51* (P=0.08)(figures 3.22c and e). Interestingly, RU486 alone actually down-regulated *Mmp9* (figure 3.22b). Whilst this makes interpretation difficult, it is interesting that rather than having an additive effect, dexamethasone no longer had an effect in the presence of RU486.

In contrast to the genes influenced by dexamethasone, RU486 did not antagonise the effect of 5αTHB on *Pecam1* and *Per1* transcripts (figure 3.33a and b). RU486 did decrease *Pecam1* transcript expression on its own, complicating the interpretation regarding this gene. However it did not alter transcript abundance of *Per1* (figure 3.33b).

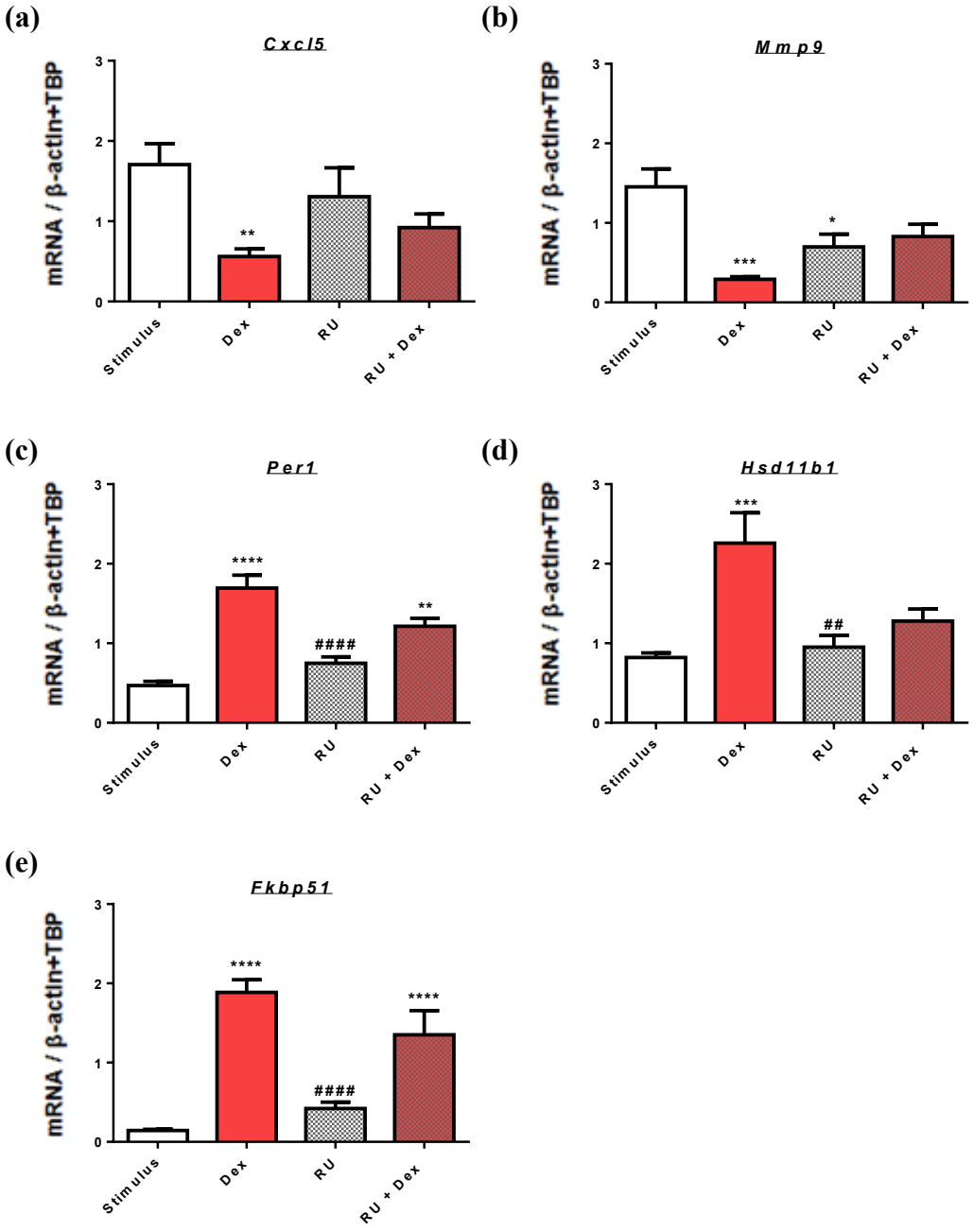

Figure 3.22: RU486-mediated antagonism of dexamethasone-mediated changes in gene expression in the mouse aorta. RNA was extracted from mouse aortic ring sections, which had been treated with stimulus (1% FCS on day 0, followed by 5 ng/ mL VEGF on days 3 and 5) in combination with either dexamethasone (Dex, 30 nM), the glucocorticoid receptor antagonist RU486 (RU, 30 nM), or a combination of the two (RU + Dex). The RNA was reverse transcribed into cDNA, and real-time PCR was used to measure transcript abundance of (a) *Cxcl5*, (b) *Mmp9*, (c) *Per1*, (d) *Hsd11b* and (e) *Fkbp51*. Dex altered transcript abundance of all the genes tested. When given in combination with RU486 it no longer altered transcript abundance of *Cxcl5*, *Mmp9* and *Hsd11b1*. RU486 tended (0.05<P<0.1) to antagonise the effect of Dex on transcript abundance of *Mmp9* (P=0.089), *Per1* (P=0.058), *Hsd11b1* (P=0.063) and *Fkbp51* (P=0.081). n=11 for stimulus-only treated group, n=8 for Dex, n=6 for RU, and n=5 for RU+Dex. Graphs (mean ± SEM) were analysed by one-way ANOVA followed by Tukey's multiple comparisons test, *=p<0.05, **=p<0.01, ***=p<0.001, ****=p<0.0001 vs stimulus, ##=p<0.01, ####=p<0.0001 vs Dex.

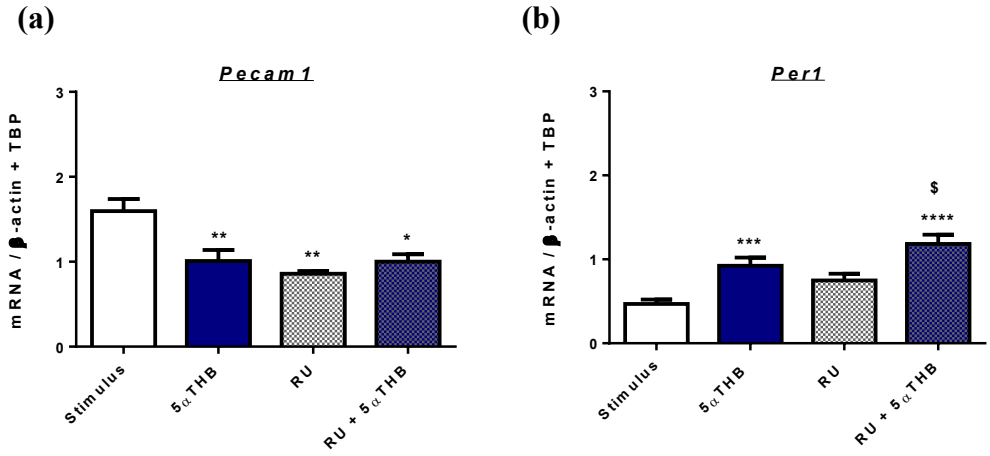

Figure 3.23: RU486-mediated antagonism of 5α-Tetrahydrocorticosterone (5αTHB)-mediated changes in gene expression in the mouse aorta. RNA was extracted from mouse aortic ring sections, which had been treated with stimulus (1% FCS on day 0, followed by 5 ng/ mL VEGF on days 3 and 5) in combination with either 5αTHB (3 μM), the glucocorticoid receptor antagonist RU486 (RU, 30 nM), or a combination of the two (RU + 5αTHB). The RNA and was reverse transcribed into cDNA, and real-time PCR was used to measure transcript abundance of (a) *Pecam1* and (b) *Per1*. 5αTHB altered transcript abundance of both genes, both in the presence and absence of RU486. RU486 alone decreased expression of *Pecam1,* but had no effect on *Per1.* n=11 for stimulus-only treated group, n=9 for 5αTHB, n=6 for RU, and n=5 for RU+5αTHB. Graphs (mean ± SEM) were analysed by one-way ANOVA followed by Tukey's multiple comparisons test, *=p<0.05, **=p<0.01, ***=p<0.001, ****=p<0.0001 vs Stimulus, $=p<0.05 vs RU486.

3.6. Discussion

The investigations described in this chapter were designed to assess the potential of 5αTHB as a potential novel topical anti-inflammatory treatment. 5αTHB had previously suppressed skin inflammation *in vivo* (Gastaldello, Livingstone et al. 2017). However the local adverse effects of 5αTHB on the skin had not been fully investigated, and the effects of 5αTHB on wound repair were of particular interest. GCs are known to inhibit wound repair (Sevilla and Perez 2018). During wound repair the migration of keratinocytes, fibroblasts, and endothelial cells is important for epithelialisation, to secrete ECM/ close the wound, and for angiogenesis, respectively (Lee, Lin et al. 2015, Martin and Nunan 2015). Since each cell regulates a different stage of the wound healing process, steroid effects were compared on the migration of keratinocyte (HaCaT), fibroblast (dermal fibroblast), and endothelial (HUVEC) cell lines, hence providing a good overall broad model. However unexpectedly in this assay, migration of these cell lines was unaffected by the positive control dexamethasone, the topical glucocorticoid hydrocortisone, and by 5αTHB. One exception was a small effect on migration of the HUVEC endothelial cell line by low (but not high) doses of hydrocortisone which may be due to effects mediated via MR, or alternatively due to assay variability. Endothelial cells are known to express MR, and effects through MR may be dominant at lower doses when affinity for GR is low. Although MR expression was not tested here it has been reported in HUVECs (Oberleithner, Schneider et al. 2003, Yang and Zhang 2004, Logie, Ali et al. 2010). However, since the effect was lost at higher doses, and since the average RWD for vehicle -treated cells in this assay appears particularly high, the apparent effect is likely to result from small differences in the original scratch sizes and in the accuracy of

mask formation by the software. The effect could, hence, disappear with increasing sample size and could be tested in this way.

Although migration of keratinocyte migration is described in the literature to be GC responsive (Lee, Vouthounis et al. 2005, Vukelic, Stojadinovic et al. 2010, Reuter, Loitsch et al. 2012), there are conflicting reports regarding the effect of GCs on endothelial cell and fibroblast migration (Huang, Liu et al. 2001, Eming, Brachvogel et al. 2007, Drebert, MacAskill et al. 2017). A lack of effect by dexamethasone on migration of this particular HUVEC endothelial cell line has been reported previously (Huang, Liu et al. 2001, Drebert, MacAskill et al. 2017) whereas GCs have inhibited migration of other types of endothelial cell such as porcine aortic endothelial cells and rat skeletal muscle microvascular endothelial cells (Fyfe, Rosenthal et al. 1995, Shikatani, Trifonova et al. 2012). The effect of GC on endothelial cell migration may, therefore, differ between species, due to species-specific differences in GR. Indeed species differences are already known to exist regarding glucocorticoid effects on vascular smooth muscle cell (VSMC) migration, which dexamethasone is known to inhibit in rodent, but not in human cells (Pross, Farooq et al. 2002). There are also known to be tissue specific differences in endothelial cells, and reports describing the limitations of using HUVECs as a model (Jaffe, Nachman et al. 1973, Alby and Auerbach 1984, Nolan, Ginsberg et al. 2013). If more time was available perhaps a more relevant cell model would be explored such as Human Dermal Microvascular Endothelial Cells (Markiewicz, Panneerselvam et al. 2016). Interestingly in one of the previous studies in which dexamethasone did not suppress HUVEC migration, it did *indirectly* inhibit migration through a modification of the secreted factors from myofibroblasts (Drebert, MacAskill et al. 2017). Therefore

another likely reason for the lack of GC effects on endothelial cells in this chapter may, therefore, be because the cells were studied in isolation, when actually wound repair is a very complex process requiring communication between many cell types. The *indirect* effects of 5αTHB on HUVEC cell migration, may therefore be investigated in the future.

Literature is sparse for the effects of GCs on fibroblast migration. In a previous study dexamethasone had no effect on migration of primary human normal dermal fibroblasts (Syed, Singh et al. 2013) but inhibited primary human *keloid* fibroblasts, which is interesting because keloids result from excessive fibrosis and are, thus, likely to contain more myofibroblasts (Eming, Brachvogel et al. 2007). As mentioned in section 1.9.2, fibroblasts differentiate into myofibroblasts during wound healing, therefore perhaps myofibroblasts would be a more relevant model. However unlike endothelial and fibroblast cells, keratinocyte cell migration is consistently inhibited by dexamethasone in the literature, including both the HaCaT cell line (Reuter, Loitsch et al. 2012) and primary human keratinocytes (Lee, Vouthounis et al. 2005, Vukelic, Stojadinovic et al. 2010). The lack of effect in this current work, therefore, is not in agreement with the literature in this case. It may be possible that the assay was not able to detect GC- mediated alterations in migration. However EGF positive control increased HaCaT migration in this assay consistent with the literature, demonstrating that the model was reliable for measuring pharmacological effects to upregulate cell migration (Charvat, Chignol et al. 1998, Tochio, Tanaka et al. 2010). Consistent positive controls to assess pharmacological manipulation of the fibroblast and endothelial cell lines could not be found, and ideally it would have been good to have a positive control for each cell type which is a critique I have of the work. Since the

cell migration assay was not responsive to even the conventional GCs, the effects of 5αTHB could not be compared in this 'broad' model of wound healing. Instead the steroid effects were compared on angiogenesis; one particular stage of the wound repair process already known to be inhibited by GCs (Small, Hadoke et al. 2005) .

Angiogenesis is crucial during wound repair. Since 1983 it has been known that GCs suppress angiogenesis (Folkman, Langer et al. 1983) and it is now known that even physiological GC concentrations can cause this inhibition (Small, Hadoke et al. 2005). The aortic ring assay model of angiogenesis was adopted here which had responded to GCs in past work (Small, Hadoke et al. 2005). Considerable intra-assay variability was noted in the data generated by this assay, caused by many factors such as variations in ring size, ring handling, and also the exact location of the aorta from which rings were taken from. However in spite of this variability, dose dependent suppression of vessel growth occurred in response to all three steroids (dexamethasone, hydrocortisone, and 5αTHB). Hydrocortisone required a concentration (1 μM) around 33x the concentration required of dexamethasone (30 nM) in order to reduce vessel growth significantly. This is broadly consistent with a chick embryo chorioallantoic membrane bioassay performed in 1987, in which hydrocortisone was reported to be around 25x less angiostatic than dexamethasone (Folkman and Ingber 1987). In the current work, 5αTHB was less potent than hydrocortisone to suppress vessel growth, with a higher EC50 (2399 nM) in comparison to that of hydrocortisone (867 nM) and requiring a higher concentration (3 μM) in order for the suppression of vessel growth to reach significance. In a previous experiment using the aortic ring assay model, 5αTHB suppressed vessel growth at a lower dose than in the current work (1μM; McInnes 2003). However, in

that assay the vessel growth was not stimulated by growth factors whereas in my assay it was, which was important since during wound repair many growth factors are present and are known to initiate the process of angiogenesis. The results from this current study, therefore, suggest that 5αTHB is less detrimental to angiogenesis than hydrocortisone. In a mouse *in vivo* model of skin inflammation it has been demonstrated that 5αTHB has anti-inflammatory effects equipotent to those of hydrocortisone (Yang, Nixon et al. 2011). Combined with the results in this chapter, this suggests that 5αTHB would provide a safer topical anti-inflammatory treatment than GC, less detrimental to wound repair processes. However, it should be acknowledged that these were two separate models. Furthermore, since angiogenesis is just one stage of wound repair, additional processes involved in the healing process would need to be studied in order to make a definitive conclusion regarding the therapeutic profile of 5αTHB. In particular an *in vivo* mouse model of skin wound healing, which is known to be glucocorticoid responsive, would be a suitable approach (Duan, Patyna et al. 2006, Xie, Gao et al. 2009).

In the recent *in vivo* sponge implantation model of angiogenesis 5αTHB was also less detrimental to vessel density than corticosterone, even at high doses (Gastaldello, Livingstone et al. 2017). During the wound healing process *in vivo,* inflammation precedes angiogenesis, and inflammatory cells such as neutrophils and macrophages are recruited into the wound site (Sinno and Prakash 2013). The growth factors and cytokines released from inflammatory cells, in particular from monocytes/macrophages, promote angiogenesis (Barrientos, Stojadinovic et al. 2008). However the aortic ring assay provides an excellent model for studying the effects of glucocorticoids directly on angiogenesis, whilst excluding their indirect effects on the

infiltration of inflammatory cells into the wound site. This current work using the aortic ring assay therefore expands on the findings of Gastaldello, by demonstrating that 5αTHB is also able to suppress angiogenesis through direct effects on the vasculature. Other steroids have been reported to suppress angiogenesis independent of their ability to reduce cytokine production, and are known as 'angiostatic' steroids (Hori, Hu et al. 1996). Indeed, in the literature the potencies of steroids in terms of their ability to suppress angiogenesis and inflammation do not necessarily appear correlated. It should not be ignored that, whilst less potent than hydrocortisone, 5αTHB still did induce a clear concentration-dependent suppression of angiogenesis, and this may be important physiologically. Importantly, in 1987, angiogenesis was inhibited by epicortisol (a stereoisomer of hydrocortisone)(Folkman and Ingber 1987) which lacks both GR and MR activity. This is particularly relevant here since there remains doubt over whether effects of 5αTHB are mediated through GR. Investigations into the mechanisms through which 5αTHB suppresses angiogenesis have been performed in this chapter, including mediation through GR.

As described in 1.7.7.3, the mechanisms through which GCs affect vascular function are diverse and are still not completely understood (Small, Hadoke et al. 2005, Logie, Ali et al. 2010, Morgan, Keen et al. 2018). It is well known that GCs suppress inflammation, and thus indirectly suppress angiogenesis due to the proangiogenic cytokines released from inflammatory cells (McSweeney, Hadoke et al. 2010). Another indirect mode in which GCs can suppress angiogenesis is through effects on the vessel basement membrane, causing degradation of the ECM and affecting cell behaviour such as to inhibit endothelial cell migration and proliferation (Drebert, MacAskill et al. 2017, Morgan, Keen et al. 2018). Finally there is also evidence that

GCs exert direct effects on endothelial cells themselves, remodelling the vasculature by altering the ability of endothelial cells to form cell-cell connections (Logie, Ali et al. 2010). A functional analysis of next generation RNA sequencing data has recently been published to study the effect of hydrocortisone on gene expression changes in the mouse aorta. Of 13 KEGG pathways which were down-regulated in cortisol-treated aorta, 9 were associated with inflammatory responses and 4 were associated with ECM or cytoskeletal function (Morgan, Keen et al. 2018). It was concluded from this study that hydrocortisone mainly suppressed angiogenesis through effects on the basement membrane ECM (Morgan, Keen et al. 2018). In this chapter, the effects of steroids were compared on gene expression involved in ECM remodelling (*Col4a1, Mmp9,* and *Col14a1*) as well as in inflammatory signalling (*Cxcl5, Dusp1, Mcp1,* and *iNOS)*, and vasculature remodelling (*Pecam1, Vcam1*). In relation to genes involved in inflammation and signalling, dexamethasone and hydrocortisone both caused down-regulation of *Cxcl5,* and increased (hydrocortisone) or tended to increase (dexamethasone) expression of *Dusp1*. This is consistent with the effects of hydrocortisone on expression of these genes in the published next generation RNA sequencing analysis (Morgan, Keen et al. 2018). However, unlike dexamethasone and hydrocortisone, 5αTHB had no effect on expression of *Cxcl5* and *Dusp1* in this work. Instead it had a trend to increase *Mcp1* expression, whereas dexamethasone and hydrocortisone had no effect.

In relation to genes involved in ECM remodelling, while there was no effect on *Col14a1*, *Mmp9* expression was decreased by both dexamethasone and hydrocortisone, whereas hydrocortisone increased, and dexamethasone tended to increase, *Col4a1* expression. *Col4a1* encodes the α1 chain of collagen IV, the main

collagen present in the basement membrane surrounding endothelial and vascular smooth muscle cells (Vahedi and Alamowitch 2011). Likewise MMP9 (encoded by *Mmp9*) is one of the most commonly studied MMP proteins in blood vessels, where it degrades both collagens and gelatins, causing increased migration of vascular endothelial cells (Chen, Jin et al. 2013). A decrease in *Mmp9* and increase in *Col4a1* is, therefore, consistent with a suppression of angiogenesis. The effects of hydrocortisone and dexamethasone here are consistent with the effects of hydrocortisone on expression of these genes in the RNA sequencing analysis previously published (Morgan, Keen et al. 2018). However, in contrast, 5αTHB had no effect on *Col4a1* or *Mmp9* expression in the mouse aorta in our current study.

The work presented in this chapter is consistent with reports that hydrocortisone suppresses angiogenesis mainly through effects on the ECM and on inflammatory signalling (Folkman and Ingber 1987, Morgan, Keen et al. 2018). However, the results suggest that 5αTHB does not suppress angiogenesis through these same mechanisms. This is in agreement with previous *in vivo* work using the sponge implantation model of angiogenesis, where 5αTHB had more limited effects than corticosterone on altering transcript abundance involved in ECM homeostasis, and, in contrast to corticosterone, did not decrease collagen staining in sponges (Gastaldello, Livingstone et al. 2017). The increase in *Mcp1* expression seen here in response to 5αTHB is also in agreement with the sponge implantation model, where *Mcp1* expression was also increased by 5αTHB but not by corticosterone (Gastaldello, Livingstone et al. 2017). *Mcp1* stimulates the recruitment of monocytes into tissues, and is described to have a key role in the development of an inflammatory response (Madrigal, Garcia-Bueno et al. 2010). Interestingly, in our current study

dexamethasone had no effect on expression of the genes investigated involved in vascular remodelling; whereas 5αTHB decreased, and hydrocortisone had a trend to decrease, expression of *Pecam1*. In the sponge implantation model *Pecam1* expression was also suppressed by both corticosterone and 5αTHB. *Pecam1,* also known as CD31, is a cell adhesion molecule with pro-angiogenic and pro-inflammatory activity. A cell surface glycoprotein, it is expressed by endothelial cells and concentrated mainly at sites of cell-cell contact, where it has adhesive properties (Park, Sorenson et al. 2015). *Pecam1* is also expressed to a lesser extent by platelets and leukocytes, and plays a role in the migration of leukocytes through junctions between adjacent endothelial cells (Woodfin, Voisin et al. 2007). A decrease in *Pecam1* is consistent with reduced endothelial cell adhesion, and impaired TLS formation and angiogenesis. Since hydrocortisone also had a trend to decrease *Pecam1*, it could be that both hydrocortisone and 5αTHB have another mode of action which dexamethasone does not share. This may involve MR since hydrocortisone binds to both MR and GR, whereas dexamethasone is GR-specific. A decrease in *Pecam1* may indicate that the suppression of angiogenesis is mediated by a decrease in endothelial cell adhesion in newly forming vessels. Alternatively it may suggest that the endothelial cells are being induced to undergo endothelial-to-mesenchymal transition, which is also associated with reduced angiogenesis.

This suggestion that 5αTHB may act through different mechanisms to suppress angiogenesis is further supported by the fact that dexamethasone and hydrocortisone increased expression of all GR responsive genes tested (*Per1, Hsd11b1,* and *Fkbp51*) whereas 5αTHB only increased *Per1 e*xpression, which can also be increased by MR. The GR antagonist RU486 was used to further investigate whether the angiostatic

effects of 5αTHB were mediated through GR. RU486 is a competitive GR antagonist with a binding affinity for GR 3 times greater than that of dexamethasone, and 10 times that of hydrocortisone (Castinetti, Brue et al. 2012, Fleseriu, Biller et al. 2012, Nguyen and Mizne 2017). In addition, it also antagonises the progesterone receptor (binding affinity more than twice that of progesterone) and the androgen receptor (binding affinity less than one third that of testosterone)(Castinetti, Brue et al. 2012, Sun, Fang et al. 2014) but does not bind the MR or to the estrogen receptor (Castinetti, Brue et al. 2012, Fleseriu, Biller et al. 2012). Out of the two doses of RU486 originally tested in this work, the higher concentration suppressed vessel growth alone, which was not entirely unexpected since RU486 also has some agonist activity (Peeters, Ruigt et al. 2008). The lower RU486 concentration partially-blocked dexamethasone-induced suppression of angiogenesis, suggesting that dexamethasone was acting through GR. Furthermore when dexamethasone concentration-response curves in the presence and absence of RU486 were normalised and superimposed on the same graph, the error bars often did not overlap, again suggesting some antagonism, although it did not hold true for all data points. In contrast when 5αTHB concentration-response curves, in the presence and absence of RU486, were normalised and superimposed, the error bars overlapped for every concentration of 5αTHB. This suggests that RU486 did not shift the concentration-response curve of 5αTHB, and hence that the suppression of vessel growth by 5αTHB was independent of GR. However, these results should be interpreted with caution and no firm conclusions can be made as there was a lack of power in both the dexamethasone and 5αTHB concentration-response curves in the presence of RU486. This was due to poor vessel growth which may have resulted from the fact that, in comparison to previous assays, the experiments with RU486 were

performed around a year later than the original dose responses where vessel growth was much better. Although all medium was used prior to its expiration date, different batches may have caused variations in the extent of vessel growth from aortic rings. In line with this, the suppression of vessel growth by dexamethasone alone at 100 nM (positive control) did not reach significance for either of the 5αTHB or dexamethasone concentration–response curves in combination with RU486. This was due to the lack of power since when the 5αTHB and dexamethasone data were combined, the suppression by dexamethasone at this concentration reached significance. Power calculations indicated that this could only be resolved by using a high number of mice. Therefore the results from these experiments are only speculative and no firm conclusions can be made, both due to the lack of power and the fact that RU486 had an effect alone in this assay. Keeping the above limitations in mind, the low dose of RU486 (30 nM) was used to assess the role of GR on steroid-mediated alterations in gene expression in the mouse aortic rings. The effects on gene expression by 5αTHB were not blocked by RU486 and, therefore, may have been mediated through a receptor other than GR. This is in agreement with the previous concentration-response data.

In summary, the work presented in this chapter provides further evidence that 5αTHB is less detrimental to wound repair than current GCs. The work suggests that 5αTHB is acting through alternative mechanisms than glucocorticoids to suppress angiogenesis, perhaps by preventing endothelial cell adhesion in newly forming vessels, or by inducing endothelial-to mesenchymal transition (EndMT). Both explanations are consistent with a decrease in angiogenesis. Future work will investigate whether 5αTHB is able to induce EndMT by assessing its effects on further

gene expression related to this process. Crucially, this work suggests that not only does 5αTHB work through different signalling pathways but also via a distinct receptor. Since 5αTHB did influence *Per1* transcripts one alternative receptor through which 5αTHB may act through to suppress angiogenesis is the MR. Future work will address this by investigating whether the MR antagonist spironolactone antagonises the effects of 5αTHB, aldosterone, and hydrocortisone on angiogenesis and gene expression.

Chapter 4:
Can 5αTHB act through GR?

4. Can 5αTHB act through GR?

4.1. Introduction

It has been demonstrated that 5αTHB has *in vitro* and *in vivo* effects to suppress inflammation, and now also to inhibit angiogenesis, although to a lesser extent than corticosterone and hydrocortisone (McInnes, Kenyon et al. 2004, Yang, Nixon et al. 2011). However it has been difficult to determine whether or not these effects are mediated in the same way as for classical GCs.

Of particular interest has been whether the effects of 5αTHB are mediated via GR. McInnes *et al.* showed that corticosterone and 5αTHB were similarly effective in displacing tritiated dexamethasone from binding sites in rat hepatocytes, with a Kd in the nM range (McInnes, Kenyon et al. 2004). However, it has been difficult to show that the anti-inflammatory actions of 5αTHB are GR dependent. In previous work, whereas the GR antagonist RU486 prevented 5αTHB-induced cytokine suppression in LPS-stimulated RAW264.7 cells (Nixon, M ,2011), it actually increased inhibition induced by 5αTHB in LPS-stimulated murine bone marrow-derived macrophages (BMDM)(Gastaldello, 2014; Yang, 2009). Later work revealed that RU486 alone suppressed cytokine release, making RU486 a poor tool for these studies (Gastaldello, 2014). *In vivo* RU486 given systemically, antagonised the suppression of dermatitis by topical administration of corticosterone in mice but did not attenuate the anti-inflammatory effects of 5αTHB (Gastaldello, Livingstone et al. 2017). Additional experiments are, therefore, required to address the question of whether the anti-inflammatory effects of 5αTHB are GR mediated.

Although a simplified model, the classical mechanism by which GCs are reported to work is by binding to GR and stimulating its translocation into the nucleus, where ligand bound GR regulates the expression of target genes through direct DNA binding (mechanism a in figure 1.4). Ligand-dependent co-regulator proteins become recruited to GR during this process to assist with DNA binding. Alternatively GR may tether to other transcription factors and modulate their activity (mechanism d in figure 1.4). This chapter addresses the ability of 5αTHB to stimulate these classical activities of GR.

4.2. Hypotheses

The conclusion in chapter 3 is that 5αTHB acts on the vasculature through different mechanisms from conventional glucocorticoids. It is thought that perhaps 5αTHB binds to GR to target alternative mechanisms to those targeted by the glucocorticoids currently in use. Therefore, the hypothesis tested by the work described in this chapter is that 5αTHB acts through GR but with alternative downstream effects. In particular, the sub-hypotheses tested here are that:

1. 5αTHB is able to bind GR.
2. 5αTHB can cause nuclear translocation of GR.
3. 5αTHB can stimulate co-regulator peptide recruitment to GR.
4. The anti-inflammatory effects of 5αTHB are dependent on GR.

4.3. Aims

The aim is to use model systems to investigate whether 5αTHB can stimulate the above GR mechanisms. The individual aims are to:

1. Assess whether 5αTHB is able to displace selective GR ligands from the isolated human GR ligand binding domain (hGR LBD).
2. To quantify nuclear translocation of human GR after treatment with 5αTHB in A549 cells.
3. To compare effects of 5αTHB and dexamethasone on co-regulator peptide recruitment to the isolated hGR LBD.

4. Investigate whether GR knockdown prevents 5αTHB suppression of inflammatory cytokine release in mouse bone marrow-derived macrophages (BMDM).

4.4. Methods

4.4.1. Comparing steroid ability to bind GR

Steroid binding to human GR ligand binding domain (hGR LBD) was measured using a PolarScreen Glucocorticoid Receptor Competitor Assay Kit (Fisher Scientific, Loughborough, UK) as described in 2.2.6. This was performed by the Drug Discovery core (College of Medicine and Veterinary Medicine, University of Edinburgh). For each steroid a concentration-response was performed, using concentrations of 0.5, 1, 5, 10, 50, 100, 500 and 1000 nM for dexamethasone, 0.5, 1, 5, 10, 50, 100, 500, 1000, 5000 and 10000 nM for hydrocortisone, and 5, 10, 50, 100, 500, 1000, 5000 and 10000 nM for 5αTHB.

4.4.2. Assessment of 5αTHB ability to induce GR nuclear translocation

A549 cells were chosen for the study of GR nuclear translocation due to the fact that they had also been used previously by Gastaldello (2014) to investigate whether 5αTHB induces phosphorylation of the GR Serine 211 residue. Phosphorylation of GR at this residue is associated with GR nuclear translocation; therefore for completeness the work was performed in the same cell type.

In order to investigate GR nuclear translocation, two alternative methods were evaluated: 'Immunofluorescence' and 'Nuclear/Cytoplasmic (N/C) separation'.

4.4.2.1. Immunofluorescence method

The immunofluorescence protocol described in (2.2.2.3) was followed to visualise GR in A549 cells and to qualitatively and quantitatively assess the effects of steroids on GR nuclear translocation. Cells were treated in duplicate on days 3 (for 24 hour

treatment) and 4 (30 minute treatment) with dexamethasone (positive control; 100 nM) or 5αTHB (1, 3 or 10 μM). The negative control consisted of either vehicle (ethanol, 1 μL per 1 mL) or no treatment. The primary antibody was either GR sc-8992 or sc-1003 (both 1/150 dilution in PBS) in combination with Goat-anti-rabbit AlexaFluor488 or AlexaFluor555 conjugate secondary antibody (Thermo scientific, 1/800 dilution in PBS, 100μL, 2h, dark, RT). Negative controls were also performed with no primary antibody, no secondary antibody, or in the absence of both primary and secondary antibodies, as described in (4.4.3.1), to check for non-specific antibody binding and cell autofluorescence.

4.4.2.2. Nuclear/Cytoplasmic separation method

A549 cells were plated 350000 cells/ well in 6 well plates (day 1) and treated in triplicate on days 3 (24 hour treatment) and 4 (6 hours and 30 minute treatment). Treatment consisted of vehicle (ethanol, 1 μL per 1 mL; negative control), dexamethasone (positive control; 100 nM) or 5αTHB (1, 3 or 10 μM). Separate nuclear and cytoplasmic protein was then extracted from the cells and its concentration measured according to the protocols described in (2.2.2.1.3) and (2.2.2.1.4). The amount of GR was then quantified and compared between the two fractions using Western blot, as described in (2.2.2.1.5). The primary antibody for GR visualisation by Western blot was sc-1003; however, during optimisation sc-8992 and sc-1004 were also tested (all 1/500 dilution). Both sc-1003 and sc-8992 had previously been used my members of our group, and sc-1004 had been recommended to give clear GR bands by another group, although they were not using human tissue. Primary antibodies for GRB2 (sc-255) and PARP (BD Pharmingen, 556494) were used as nuclear and

cytoplasmic controls respectively (2 hours, RT, 1/1000 dilution) since they are only expressed in either the nucleus or cytoplasm respectively so could confirm the clear separation of the two fractions. Secondary antibodies used were either Goat Anti-rabbit (926-32211) or Goat Anti-mouse (926-32210)(both Licor Biosciences, 1/10000 dilution) diluted in a milk solution (5% w/v in TBS-T). Finally, protein was detected on the membrane using fluorescence method as described in (2.2.2.1.7.1).

4.4.3. Assessment of 5αTHB effects on coregulator peptide recruitment to GR.

PamGene's MARCoNI assay was used as described in (2.2.5) to compare the effects of dexamethasone (1 μM) or 5αTHB (1 μM) on co-regulator peptide recruitment to the isolated GR GST-tagged ligand binding domain (GR-LBD-GST, 10 nM, AB vector, San Diego, CA). Experiments were performed using n=3.

4.4.4. Comparing the effects of steroids on cytokine release from mouse bone marrow-derived macrophages

Primary BMDM were freshly isolated from mouse tibia and femur bones, and then plated as described in section 2.1.4.2. Cells were treated 24 hours later with either hydrocortisone (at concentrations of 10, 30, 100, 300 or 1000 nM) or 5αTHB (at concentrations of 100, 300, 1000, 3000 or 10000 nM). Since there were not enough cells per mouse to treat in duplicate, cells were treated in singlicate. One hour after steroid treatment the cells were then stimulated with LPS (either 3 or 100 ng/mL; lipopolysaccharides from Escherichia coli, Sigma). A vehicle control was included which consisted of cells treated with ethanol and PBS in place of steroid and LPS, respectively. In addition, a stimulus control was performed which had ethanol (1 μL

per 1 mL) in place of steroid but was still stimulated by LPS (either 3 or 100 ng/mL). 24 hours after LPS stimulation (or control treatment) medium was collected, and frozen at -20 °C for quantification of IL6 or TNFα cytokines by ELISA, performed as described in 2.2.2.2. ELISA standard curves were accepted with relative standard deviations (RSD) within 15%.

4.4.5. Data analysis

Data produced using methods 4.3.1 and 4.3.3.2 were analysed using GraphPad Prism6 software and presented as mean with error bars representing the standard error of the mean (SEM). Data were analysed by one-way ANOVA and comparisons made using Dunnett's multiple comparisons test. To fit the concentration-response curves, a non-linear regression analysis was performed using the log (inhibitor) vs response (three parameters) equation and using the least squares fitting method.

4.5. Results

4.5.1. Does 5αTHB displace selective GR ligands from the isolated GR ligand binding domain?

A model GR expression system was used in order to assess whether 5αTHB is able to displace selective GR ligands from the isolated GR LBD (figure 4.1). Dexamethasone and hydrocortisone both decreased the fluorescence polarisation of the GR-selective ligand, with EC50 values of 0.00421 μM and 0.019 μM, respectively. 5αTHB, however, only displaced the selective GR ligand to a very limited extent, and at high concentrations. This is reflected in its EC50 value of 480 μM.

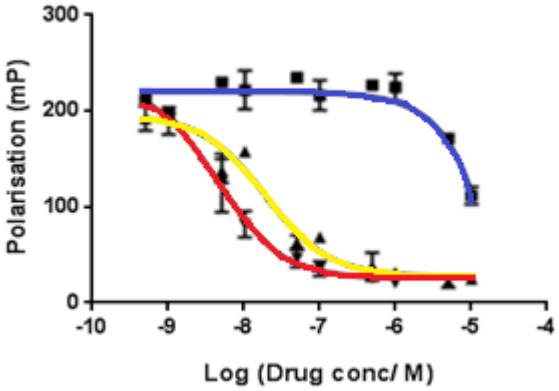

	EC50 values (μM)
Dexamethasone	0.00421
Hydrocortisone	0.019
5αTHB	480

Figure 4.1: 5αTHB only competed for binding to the glucocorticoid receptor (GR) ligand binding domain (LBD) at high concentrations. A competitor assay was performed using the isolated GR LBD and a fluorescent ligand selective for the GR LBD. Dexamethasone and hydrocortisone both displaced the fluorescent ligand from GR, with EC50s of 0.00421 μM and 0.019 μM, respectively. 5αTHB however did this only to a very small extent at high concentrations. Its EC50 was 480 μM. Data are mean ± SEM of n=3.

4.5.2. Does 5αTHB translocate GR into the nucleus?

In order to investigate nuclear translocation of GR two alternative methods, 'immunofluorescence' and 'Nuclear/Cytoplasmic (N/C) separation', were evaluated to determine receptor localisation.

4.5.2.1. Immunofluorescence method development

As a preliminary screen, the immunofluorescence protocol and quantification procedure (described in 2.2.2.3) was performed in A549 cells either treated with ethanol vehicle, 5αTHB (1, 3 or 10 μM) or dexamethasone (positive control; 100 nM). Images of slides are given in figure 4.2 and graphs of quantification to assess nuclear translocation in figure 4.3. At all time-points (30 minutes, 6 hours and 24 hours) the quantification score for dexamethasone-treated cells was higher than for cells treated with vehicle, although only slightly and this was not significant. However, it is evident from the score, and also from visual inspection, that vehicle-treated cells already had high signal in the nucleus. This background signal created difficulties in measuring an increase in score after dexamethasone treatment, and, hence, the causes of this high background were explored to improve the dynamic range of the assay.

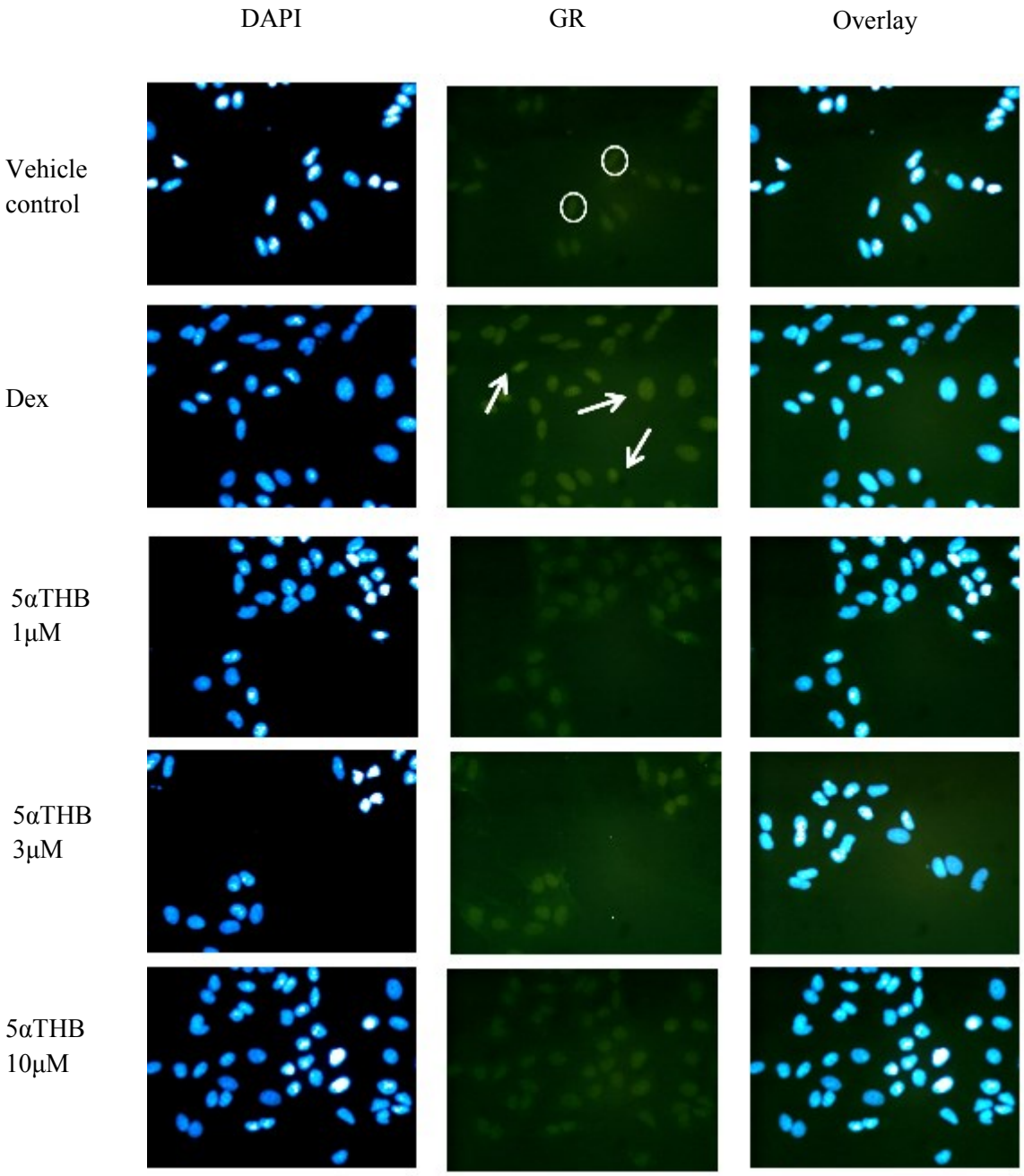

Figure 4.2: Representative images from a preliminary immunofluorescence screen of the effects of dexamethasone (dex, 100 nM) and 5αTHB (1μM, 3μM or 10μM) to cause GR nuclear translocation in serum-starved A549 cells. DAPI stain indicates cell nuclei, and GR is visualised by secondary detection of a GR antibody (in green). Additionally, overlay of the images is shown. White arrows highlight examples of nuclei with increased signal after dexamethasone treatment, indicating increased nuclear GR translocation. However, a high level of background signal in the nucleus is already present in control vehicle-treated slides. Examples of cells with high background signal are circled. Nuclear signal is also evident in 5αTHB-treated cells, although this is less pronounced than in dexamethasone-treated cells.

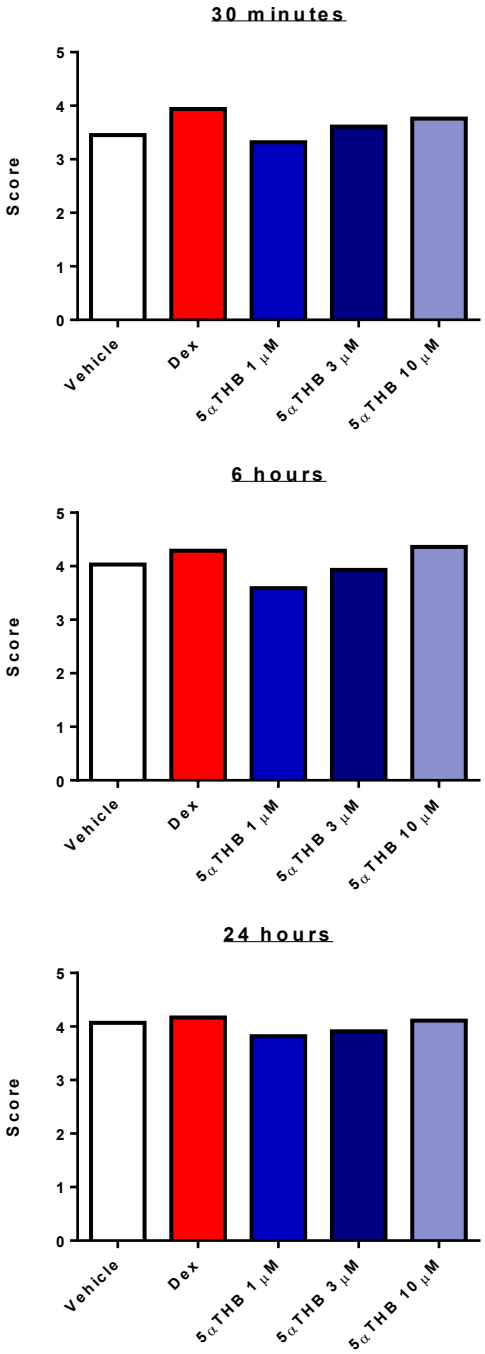

Figure 4.3: Quantification of a preliminary immunofluorescence screen of the effects of dexamethasone (Dex, 100 nM) or 5αTHB (1μM, 3μM or 10μM) on GR nuclear translocation in serum-starved A549 cells. Quantification was originally performed using the following scoring method: 5: much more fluorescence signal in the nucleus (N) in comparison to cytoplasm (C) (N<<C), 4: more fluorescence signal in the N in comparison to C (N<C), 3: an equal amount of fluorescence signal in the N and C; N=C, 2: more fluorescence signal in the N than the C (N>C) and 1: much more fluorescence signal present in the N in comparison to the C (N>>C). Dexamethasone (positive control) only produced a slightly higher score in comparison to vehicle at all time-points. However, high nuclear background meant that vehicle-treated cells already had a high score; consequently, the dynamic range between vehicle and positive control was small.

Decreased background had already been achieved in Western blots using an alternative antibody (sc-1003) in comparison to sc-8992. These two antibodies were, therefore, compared using the current immunofluorescence protocol (figure 4.4). However, with both antibodies the score remained high for vehicle-treated cells. Furthermore, the background signal remained even in the absence of primary antibody. This can be visualised in figure 4.5a, in which in the green channel, cell nuclei can be seen in the absence of primary antibody. In further negative controls with no secondary antibody (figure 4.5c, green channel) and in the absence of both primary and secondary antibody (figure 4.5d, green channel) the fluorescence signal persisted. This eliminated the possibility of non-specific antibody binding, and hence suggested that the background was caused by auto-fluorescence from the cells themselves. Interestingly, no fluorescence was evident when live cells were viewed down the microscope before being fixed (figure 4.6). This was indicative of the fixing procedure causing the fluorescence. To avoid auto-fluorescence in the green emission spectrum, an alternative secondary antibody with a fluorophore which emits in the red emission spectrum (Fluorophore red 555) was compared with that previously used (Fluorophore green 488). In contrast to the green emission spectrum, auto-fluorescence from cell nuclei was not visible in the red channel in the absence of secondary antibody (figure 4.5c and 4.5d). Quantification supported these improvements: a lack of signal in the red emission spectrum in the absence of secondary antibody meant that no score could be given to cells (figure 4.7d) in contrast to when viewed in the green emission spectrum where a score could still be given (figure 4.7c). It is evident from controls with no primary antibody that there was some non-specific binding of both the green and the red secondary antibodies, as a score could be given to the cells in both cases

(figures 4.7a and b). However, in the green channel there was additional nuclear background signal (figure 4.5a, green channel) leading to a score > 3 for vehicle-treated cells (figure 4.7a), whereas in the red channel there was no extra background signal in the nucleus – just a general background fluorescence signal equally dispersed in the image (figure 4.5b, red channel), leading to a score < 3 for vehicle treated cells as desired (figure 4.7b).

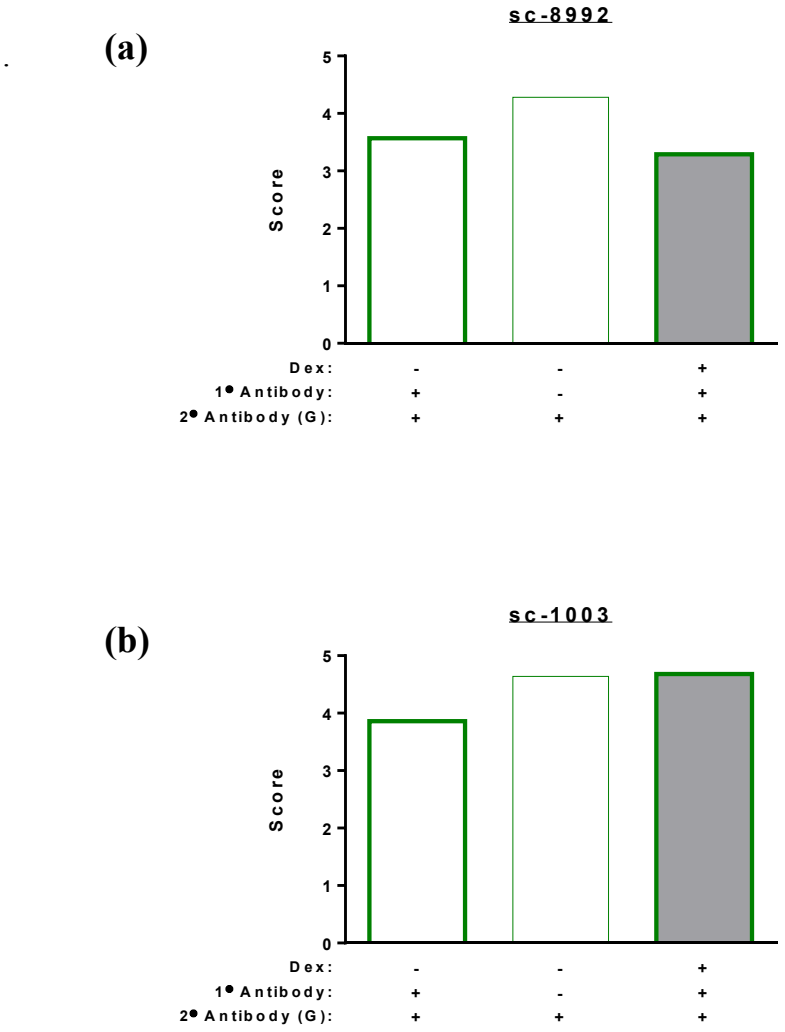

Figure 4.4: Immunofluorescence optimisation: Comparing background signal and dynamic range between two primary antibodies. A549 cells were serum starved and then treated with vehicle (ethanol, 1 µL per 1 mL) alone or combined with dexamethasone (Dex, 100 nM) for 24 hours. The cells were then fixed and stained for immunofluorescence analysis, using primary antibody combined with a green (G) fluorescent secondary antibody. Fluorescence was quantified in each cell according to the extent of fluorescent signal between the nucleus (N) and cytoplasm (C). Possible scores were 5 (N>>C), 4 (N>C), 3 (N=C), 2 (N<C) and 1 (N<<C). High background was evident previously using the sc-8992 antibody (a). An alternative antibody, sc-1003, (b) was compared in an attempt to reduce background signal in vehicle-treated cells. However, the background signal remained, and the vehicle-treated cells continued to have high scores. As a result the difference in score between vehicle- and dexamethasone-treated cells remained small. Furthermore, even with no primary antibody a fluorescence signal was evident. Single experiment; data are an average of 10 cells per image, from 5 images per slide, in duplicate.

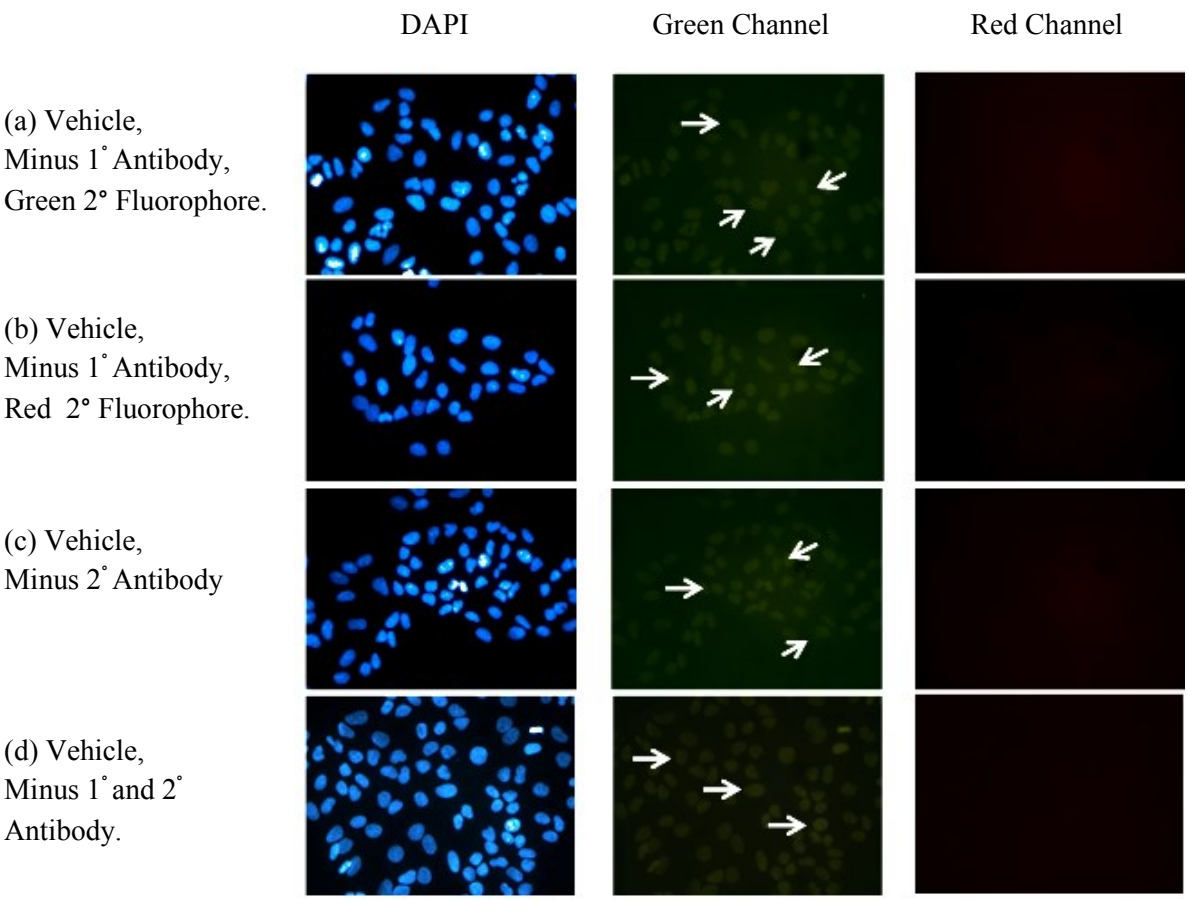

Figure 4.5: Negative immunofluorescence controls demonstrate auto-fluorescence from fixed A549 cells in the green emission spectrum. A549 cells were serum starved, treated with vehicle, and then fixed for immunofluorescence analysis. Background signal in cell nuclei was evident in controls minus primary antibody (a, green channel) suggesting unspecific secondary antibody binding. In further controls with no secondary antibody (c) and with neither primary nor secondary antibody (d) signal was still evident from cell nuclei in this channel, indicating auto-fluorescence in the green emission spectrum. White arrows indicate areas with high background signal. Using an alternative secondary antibody emitting in the red emission spectrum, background signal was not evident in cell nuclei (b, red channel). Therefore, in contrast, fixed A549 cells do not auto-fluoresce in the red emission spectrum and it is more accurate to perform immunofluorescence analysis in this channel. Images are 40X magnification.

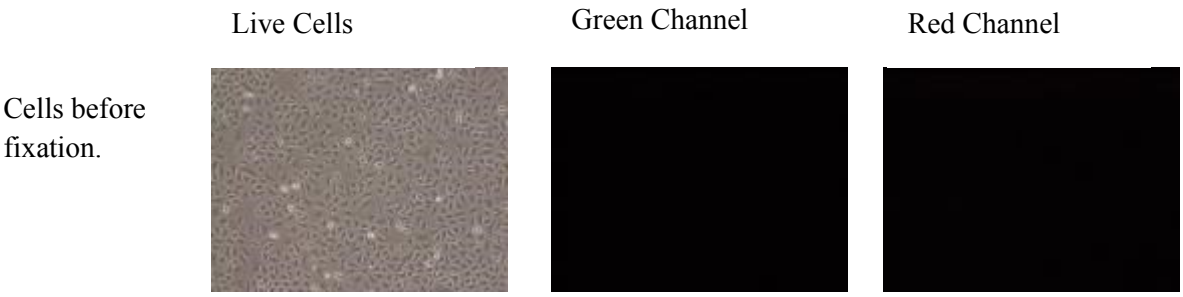

Figure 4.6: Unfixed A549 cells do not auto-fluoresce in the green or red emission spectra. Live A549 cells were viewed under a microscope before the fixing and immunofluorescence analysis procedure. Fluorescence signal was studied from both the green and red emission spectra, and fluorescence signal was not detected in either.

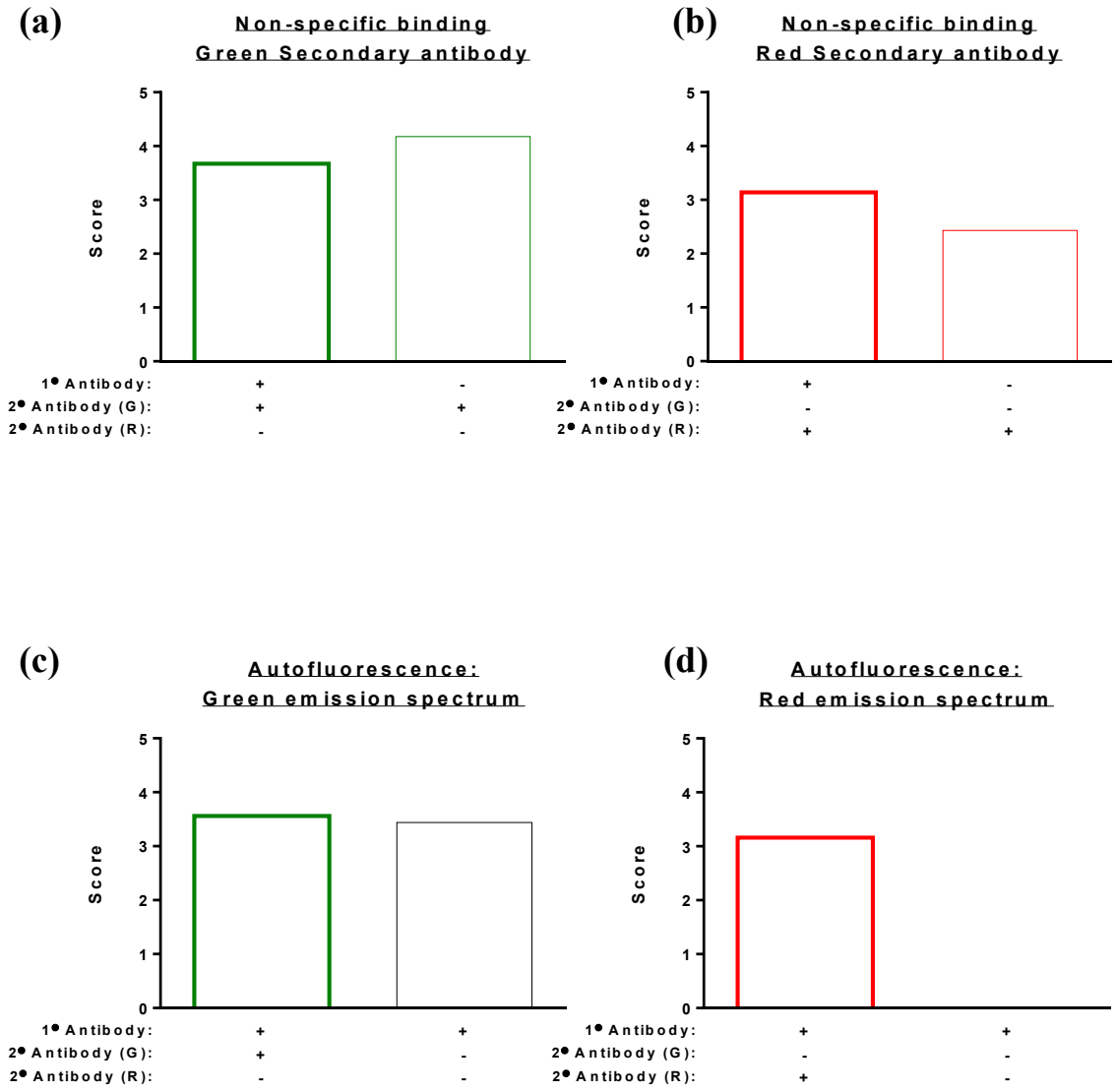

Figure 4.7: Paraformaldehyde-fixed A549 cells auto-fluoresce in the green, but not the red, emission spectra. Immunofluorescence analysis of vehicle (ethanol, 1 µL per 1 mL)-treated serum-starved A549 cells was performed in the absence of primary antibody, to assess non-specific binding of green (a) and red (b) emitting secondary antibodies. Auto-fluorescence in each emission spectrum was also assessed by the absence of secondary antibody. In the absence of primary antibody a fluorescence signal remained in both the green (a) and red (b) emission spectra, indicating non-specific binding of the secondary antibody. In the absence of secondary antibody, fluorescence signal persisted in the green emission spectra (c) but not the red (d). Vehicle groups indicate the presence of both primary and secondary antibodies. Single experiment, data are average of 10 cells per image, from 5 images per slide, in duplicate.

Following improvements gained from viewing the slides in the red emission spectrum, the immunofluorescence analysis was re-performed using the red 555 secondary antibody to compare vehicle- and dexamethasone-treated cells. Experiments with the green 488 secondary antibody were performed alongside for comparison. As seen previously in the red emission spectrum, in the absence of red 555 secondary antibody (figures 4.8a and c, red channel) no cell nuclei could be visualised. Again this is in contrast to the green emission spectra in which cell nuclei could be seen auto-fluorescing in the absence of the green secondary antibody (figures 4.8b and d, green channel). In addition to the autofluorescence, the signal in the green channel in figure 4.8d may have also arisen (to some extent) from overlap of emission spectra between the green and red secondary antibodies, demonstrated in figure 4.8e. Using a far red fluorophore with an emission spectrum further from the green wavelength could help to resolve this; however this was not attempted since despite the qualitative improvements, when quantified the dynamic range between vehicle- and dexamethasone-treated cells was still very narrow (figure 4.9a and b).

A continuous quantification method, whereby the fluorescence signal is measured by ImageJ, was used (figure 4.9c and d) to re-quantify the assessment of positive controls, in a final attempt to widen the dynamic range. No major improvements were seen in comparison to the scoring method (figures 4.9a and b). Therefore, it was decided to focus on the N/C separation method as an alternative quantifiable technique.

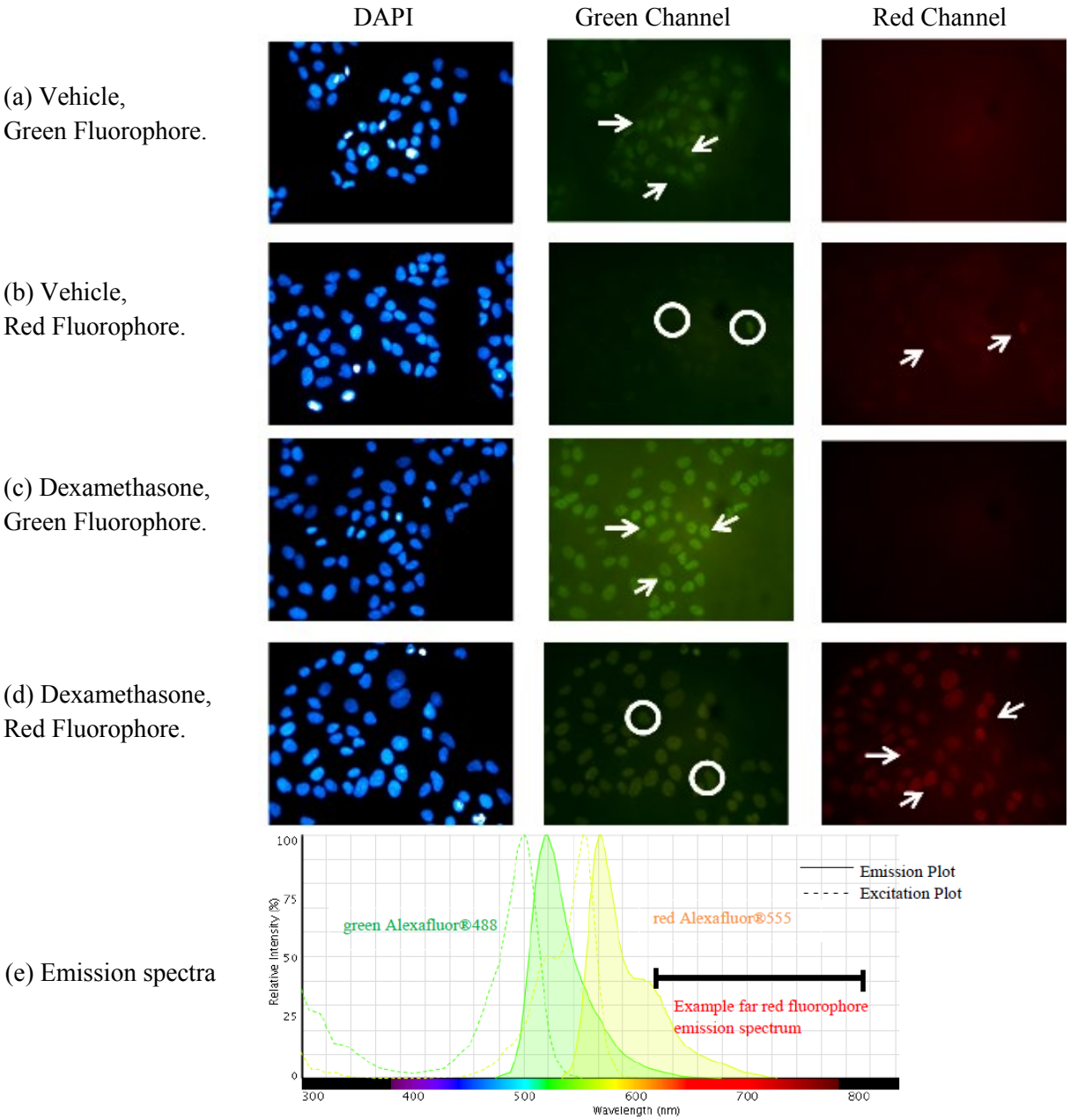

Figure 4.8: Qualitative assessment of GR nuclear translocation in fixed A549 cells was improved using the red emission spectra for immunofluorescence analysis in comparison to green. A549 cells were serum starved and then treated for 24 hours with vehicle (ethanol, 1 µL per 1 mL) (a, b) or dexamethasone (100 nM, positive control) (c, d). The cells were then fixed and analysed using immunofluorescence. Secondary antibodies absorbing in the green emission spectra (green 2^0 antibody; a and c) and red emission spectra (red 2^0, b and d) were compared. Cell nuclei auto-fluoresced in the green channel (b and d, green channel) whereas they did not in the red channel (a and c, red channel). This meant that there was a larger dynamic range between immunofluorescence of vehicle- and dexamethasone-treated cells when viewed using the red channel (b and d, respectively, red channel) than when viewed using the green channel (a and c, respectively, green channel). The signal in the green channel in (d) may arise from a combination of autofluorescence and the overlap between emission spectra for the green Alexafluor®488 and red Alexafluor®555 conjugate secondary antibodies (shown in e).

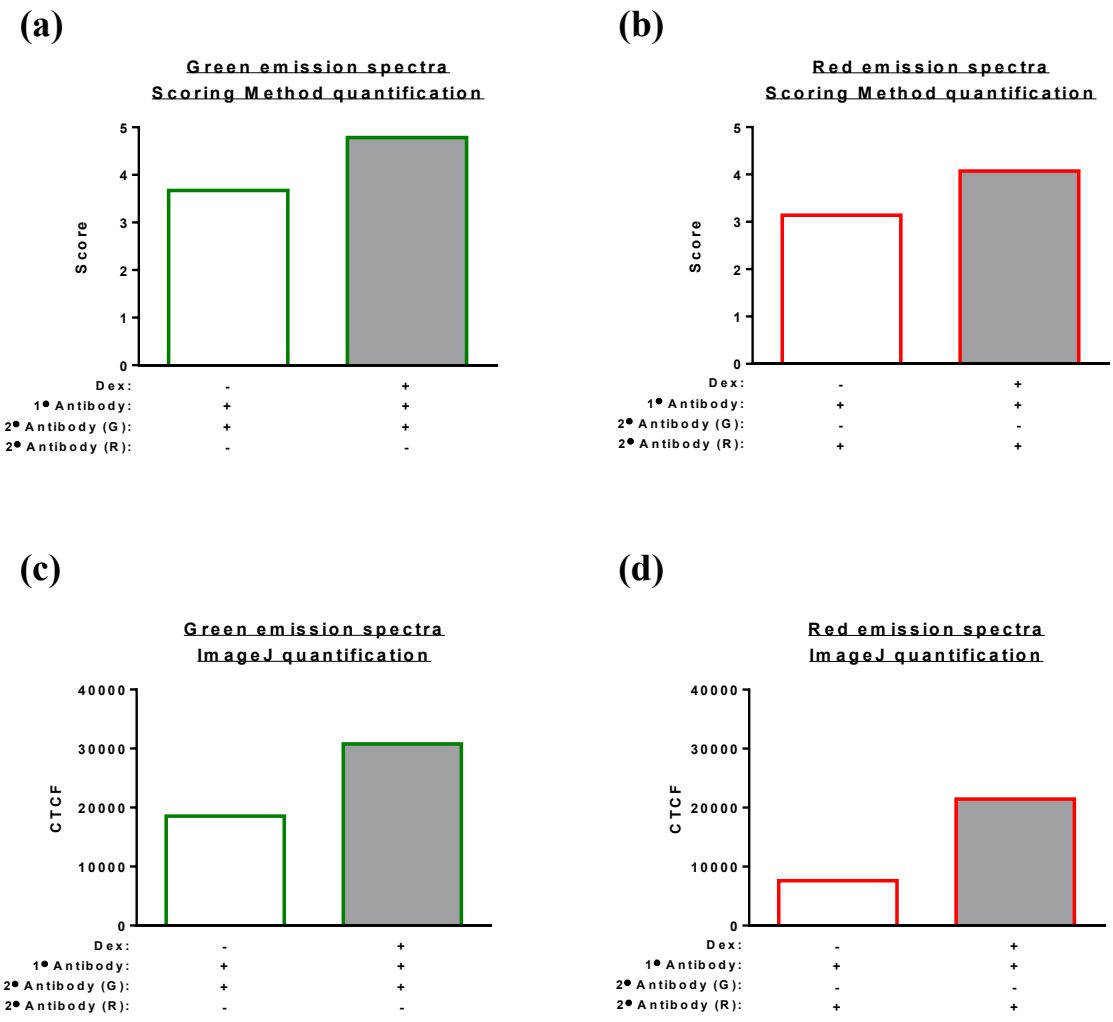

Figure 4.9: Quantitative comparison between immunofluorescence analysis in red and green emission spectra, and of two different quantification methods. The dynamic range between dexamethasone positive control and vehicle immunofluorescence was narrow after analysis in both the green (a) and red (b) emission spectra when quantified using the scoring method. An alternative ImageJ quantification (c and d) of the corrected total cell fluorescence (CTCF) was investigated to improve the dynamic range. Single experiment, data are average of duplicate slides, and of 5 images per slide. For (a) and (b) the average score was taken for 10 cells per image.

4.5.2.2. N/C separation method development

High background was evident in the initial Western blot performed using the sc-8992 antibody (figure 4.10a). Alternative antibodies and detection methods were, therefore, compared (figure 4.10b and c). Sc-1004 gave non-specific bands and, therefore, sc-1003 was chosen as the preferred antibody, giving clear GR bands at the correct size, 95kDa. Using this antibody both chemiluminescence (figure 4.10b) and fluorescence (fig 4.10c) detection methods gave the clear specific band at 95kDa. However, since fluorescence detection has a broader dynamic range for quantitative measurement, this was the method selected (Quantitative, Two- Color Western Blot Detection With Infrared Fluorescence, LI-COR Biosciences, May 2004).

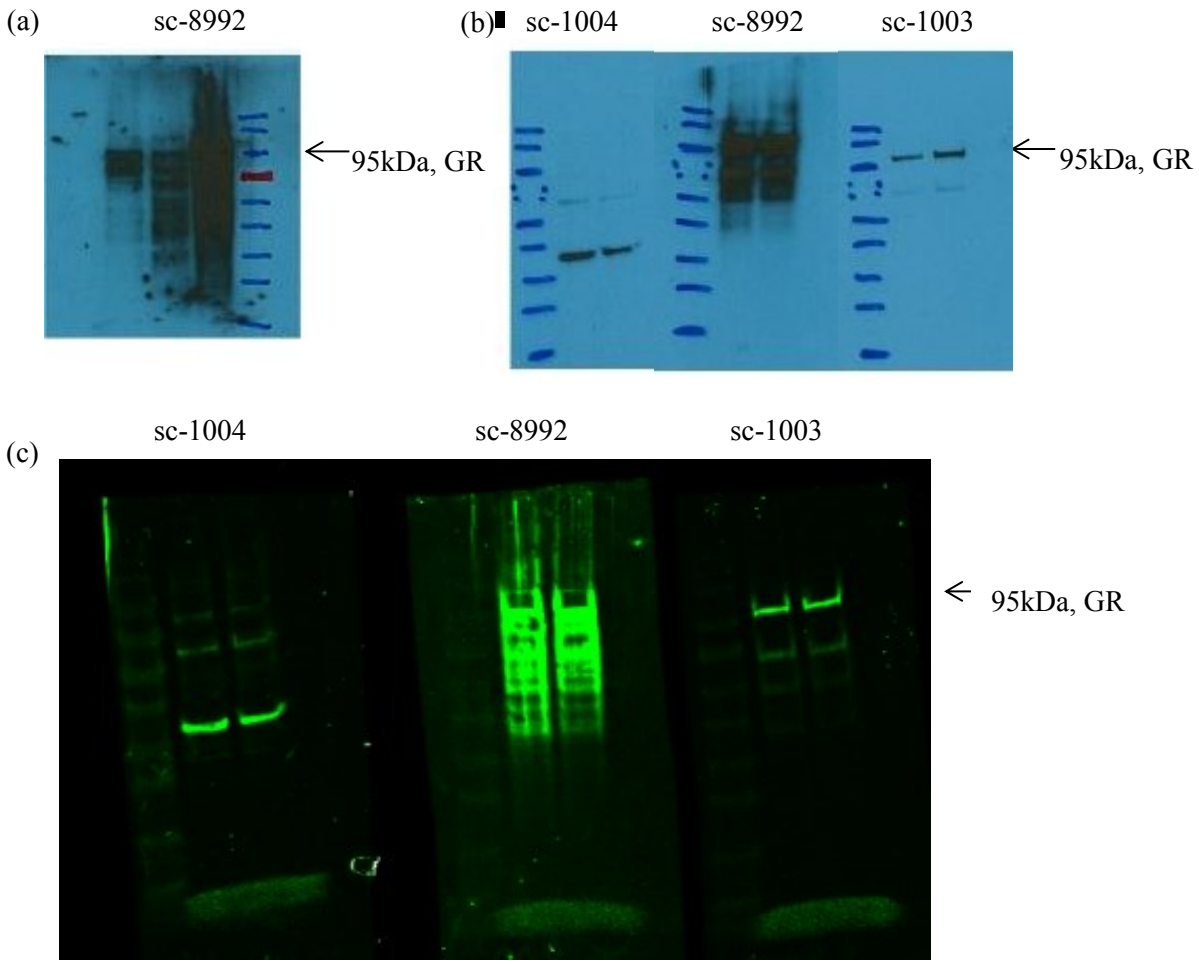

Figure 4.10: Method development for Western blot. Primary antibody optimisation followed the initial Western blot where sc-8992 antibody gave high background signal (a). This antibody was subsequently compared with alternative primary antibodies sc-1004 and sc-1003 using both chemiluminescence (b) and Licor fluorescence (c) detection methods. Sc-1004 gave non-specific bands whereas sc-1003 produced clear GR bands at 95kDa, with only a small level of non-specific binding.

4.5.2.3. Assessment of GR translocation using the N/C separation technique

4.5.2.3.1. Data analysis

Nuclear (PARP) and cytoplasmic (GRB2) loading controls indicated successful separation of nuclear and cytoplasmic fractions from A549 cells (figure 4.11). Since the two fractions had different loading controls, the raw GR intensities were used to calculate N/C values, rather than intensities normalised to a loading control. For this reason n=6 was attempted as an initial sample size in order to account for any variations in sample loading.

4.5.2.3.2. Assessment of controls

Dexamethasone (100 nM, positive control) significantly increased the N/C ratio in comparison to vehicle (negative control) at all time-points (figure 4.12), indicating increased GR nuclear translocation. This was also evident from visual inspection and was seen more easily in the cytoplasmic fraction, as a less intense GR band for dexamethasone-treated samples (figure 4.11).

4.5.2.3.3. Assessing GR translocation in response to 5αTHB

The N/C ratio for cells treated with 5αTHB (at doses of 1, 3 and 10 μM) was not different from vehicle-treated cells at any time point (figure 4.12). 5αTHB gave a significantly smaller N/C ratio than dexamethasone at all doses and time points. This suggests that GR remained predominantly in the cytosol. Again this was supported visually as no change in band intensity relative to vehicle control (figure 4.11).

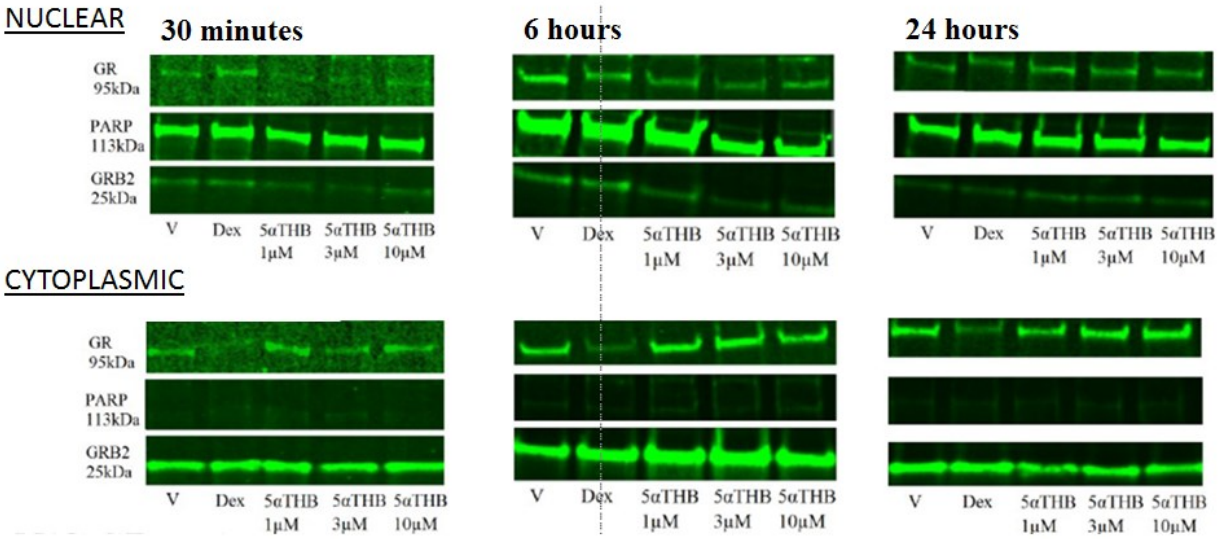

Figure 4.11: GR nuclear translocation occurred after dexamethasone (Dex) but not 5α-tetrahydrocorticosterone (5αTHB) treatment. A549 cells were cultured in serum-containing medium for 48 hours and then treated for 30 minutes, 6 hours or 24 hours with vehicle (ethanol, 1 μL per 1 mL), Dex (100nM), or 5αTHB (1, 3 or 10μM). Nuclear and cytoplasmic protein fractions were then separated and the amount of GR compared between treatments using Western blot. Clear nuclear/cytoplasmic separation was achieved as seen by PARP and GRB2 restricted to nuclear and cytoplasmic fractions respectively. Cytoplasmic GR bands of Dex treated cells were less intense at all time points (in comparison to vehicle) indicative of GR nuclear translocation. Differences were not apparent with any dose of 5αTHB. Images are representative of n=6.

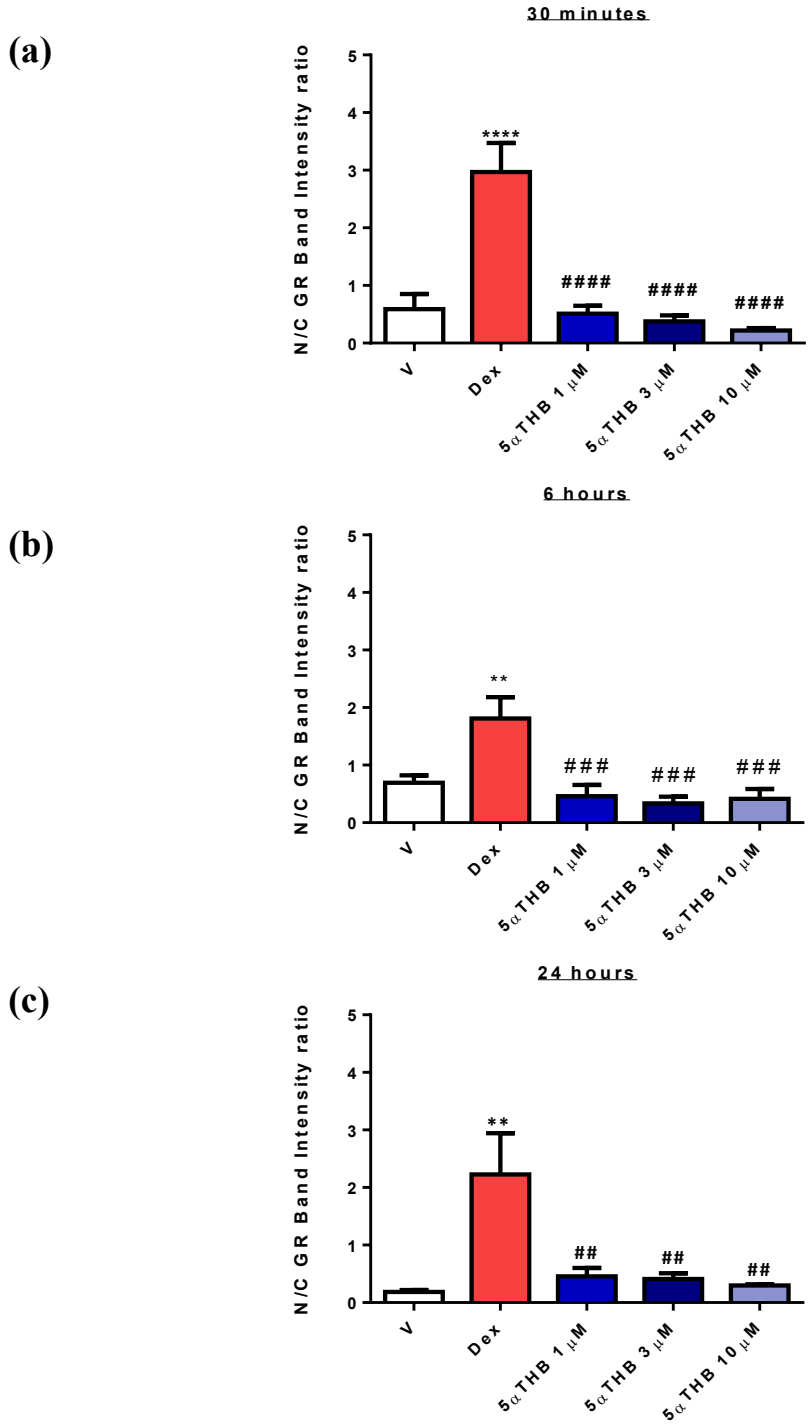

Figure 4.12: Dexamethasone caused glucocorticoid receptor (GR) translocation into the nucleus, whereas 5α-tetreahydrocorticosterone (5αTHB) did not. A549 cells were cultured in serum-containing medium for48 hours and then treated for 30 minutes (a), 6 hours (b) or 24 hours (c) with vehicle (ethanol, 1 μL per 1 mL), dexamethasone (Dex, 100 nM), or 5αTHB (1, 3 or 10μM). Nuclear and cytoplasmic protein fractions were then separated and the amount of GR compared between treatments using Western blot. GR band intensities were quantified and nuclear/cytoplasmic (N/C) ratios assessed. At all time-points the N/C ratio was increased by dexamethasone relative to vehicle control. 5αTHB, however, did not influence the N/C ratio at any concentration or time point. Data are mean ±SEM of n=6. Data were analysed by one-way ANOVA and comparisons made using Dunnett's multiple comparisons test. **=P<0.01, ****=P<0.0001 vs vehicle control. ##=P<0.01, ###=P<0.001, ####=P<0.0001 vs Dex.

4.5.3. Does 5αTHB induce co-regulator peptide recruitment to the GR ligand-binding domain?

Dexamethasone (1 μM, positive control) caused clear increases and decreases in the interaction between GR and many of the co-regulator peptides investigated (right panel, figure 4.13). 5αTHB (1 μM) however did not affect the interaction between GR with any of the co-regulator peptides (left panel, figure 4.13).

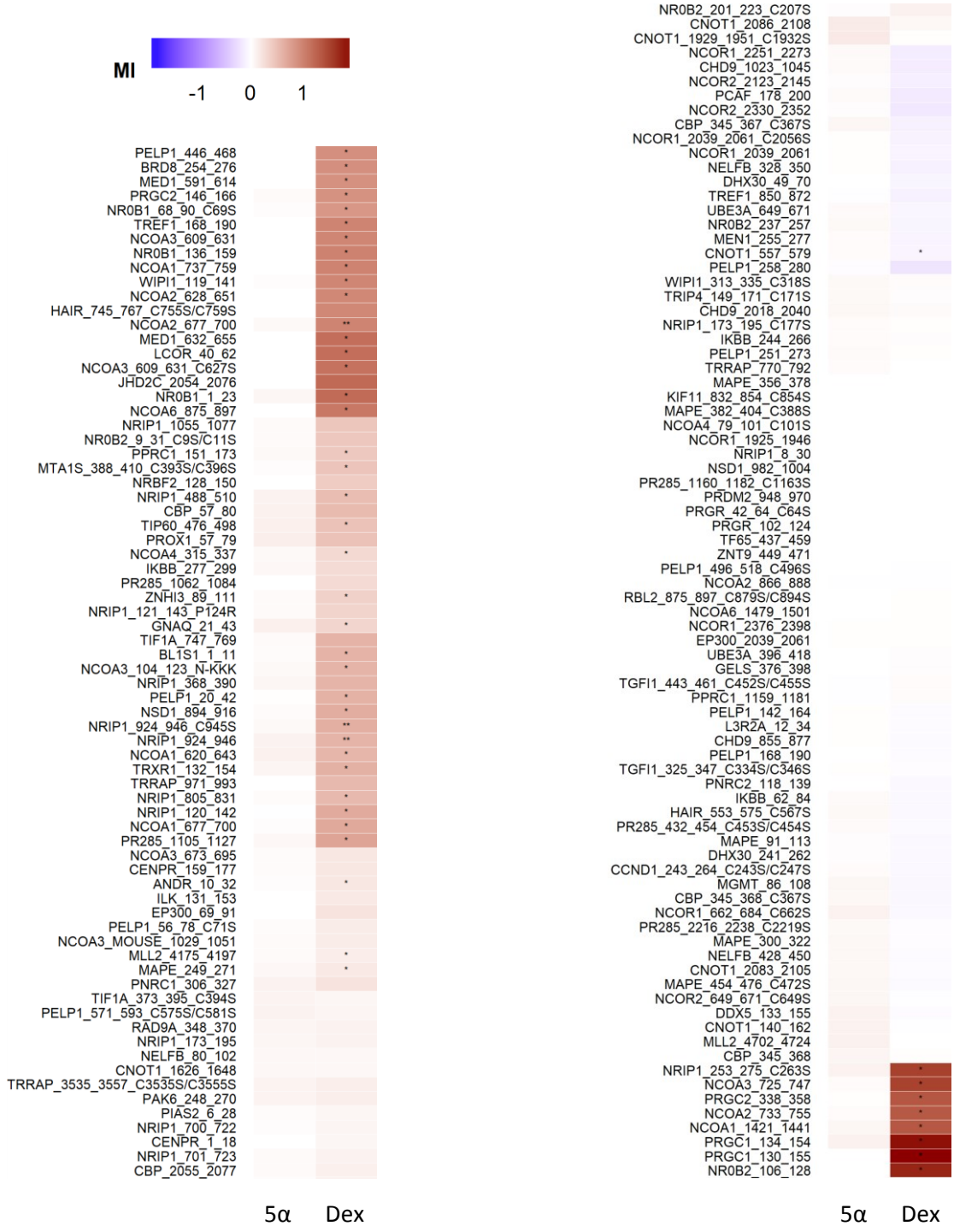

Figure 4.13: 5αTHB did not stimulate co-regulator peptides to interact with the glucocorticoid receptor ligand binding domain (LBD). PamGene's Microarray Assay for Real-time Coregulator-Nuclear Receptor Interaction (MARCoNI) was used to compare the effects of 5αTHB (1 μM) or dexamethasone (1 μM) on co-regulator recruitment to the GR ligand-binding domain (LBD). The heat map demonstrates increases (in red) and decreases (in blue) in interactions between GR with each co-regulator peptide studied. In contrast to 5αTHB, dexamethasone induced clear changes in co-regulator recruitment, consistent with its effects to bind GR, stimulate GR-DNA binding and alter gene expression. Comparisons relative to control (dimethyl sulfoxide) were made using Student's unpaired t-tests. Correction for multiple testing was performed using the Benjamin and Hochberg method. *=P<0.05, **=P<0.01, ***=P<0.001 V Control.

4.5.4. Does 5αTHB mediate its anti-inflammatory effects through GR?

In previous work 5αTHB suppressed IL6 release from murine BMDM (Yang, Nixon et al. 2011). However, the GR antagonist RU486 was shown to be a poor tool to assess whether this suppression of cytokine release by 5αTHB was mediated through GR. Therefore, as an alternative, we designed a GR knockdown experiment, in the same cell type, to assess whether GR knockdown would prevent the suppression of cytokine release by 5αTHB. First for comparison, hydrocortisone and 5αTHB concentration-response curves were performed in order to determine the IC50 for steroid-induced suppression of cytokine in the presence of GR, before the knockdown was carried out.

4.5.4.1. ELISA Quality control

ELISA was used to measure cytokine levels in cell media. Quality control samples were not provided by the manufacturer's kits, and insufficient BMDM cells were available from individual mice to produce quality control samples for comparison between each experiment. However, the RSD was calculated for each data point on the IL6 and TNFα standard curves, and curves were only accepted with RSDs within 15%. The mean standard curves and RSD values are given in figure 4.14.

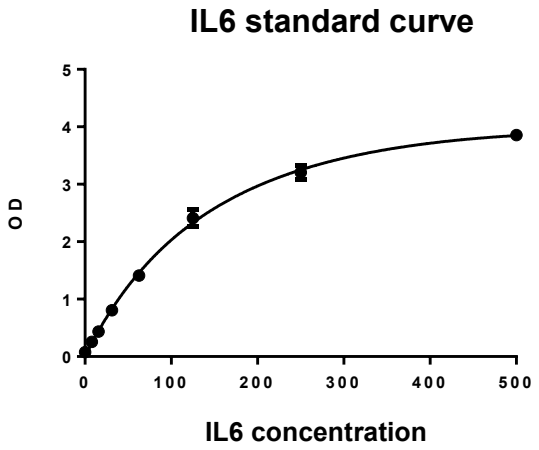

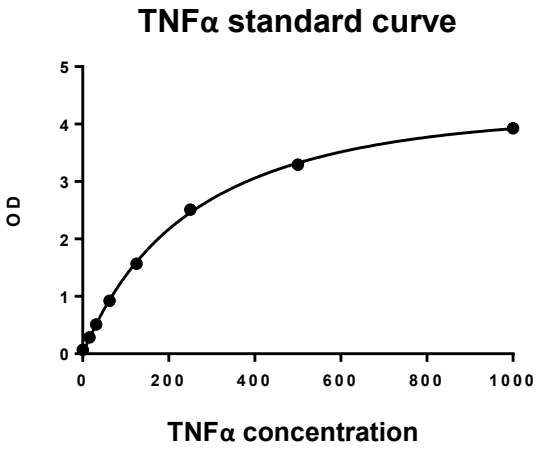

IL6 concentration	RSD
500	0.0439
250	0.0488
125	0.0989
62.5	0.102
31.25	0.1154
15.615	0.1196
7.81	0.1048
0	0.0638

TNFα concentration	RSD
1000	0.0151
500	0.0355
250	0.0578
125	0.0428
62.5	0.0385
31.25	0.0411
15.625	0.0492
0	0.0668

Figure 4.14: ELISA standard curves for measuring IL6 and TNFα cytokine concentrations. Standard curves were accepted when the relative standard deviation (RSD) for each data point was within 15%. Data is mean ± SEM of N=5 (TNFα) and N=8 (IL6).

4.5.4.2. Effects of steroid to suppress IL6 release from BMDM stimulated with 100 ng/mL LPS.

Originally, mouse BMDM were stimulated with 100 ng/mL LPS. This concentration was chosen based on the work of Gastaldello (2014) and Yang (2009), who successfully suppressed IL6 release from mouse BMDM using glucocorticoid. In an initial experiment N=4 was achieved; however, using the raw data there was not a significant increase in IL6 concentration in cell media after stimulation with 100 ng/mL LPS (figure 4.15a). Furthermore, a significant concentration-dependent effect of HC treatment was not observed (overall P=0.65), although this was likely due to variability. In order to account for inter-assay variability, the data in each individual experiment was normalised to the IL6 concentration present in the media of LPS-only treated cells (figure 4.15b). This normalisation was successful in decreasing the variability, and after normalisation the differences in IL6 concentrations between groups were significant (overall P=0.0001). From the normalised data it was evident that LPS did successfully stimulate an inflammatory response from the cells, as there was a significant increase in the IL6 release in comparison to vehicle-only treated cells. Hydrocortisone induced a concentration-dependent suppression of this IL6 release. Suppression was seen from concentrations greater than 300 nM, and complete suppression was achieved by 1 μM. A concentration-response curve was plotted (figure 4.15c) from which it was calculated that the IC50 for suppression was 151.7 nM. However, in contrast to hydrocortisone, and to the work performed previously (Yang, Nixon et al. 2011), 5αTHB did not suppress IL6 release from BMDM after stimulation with 100 ng/mL LPS.

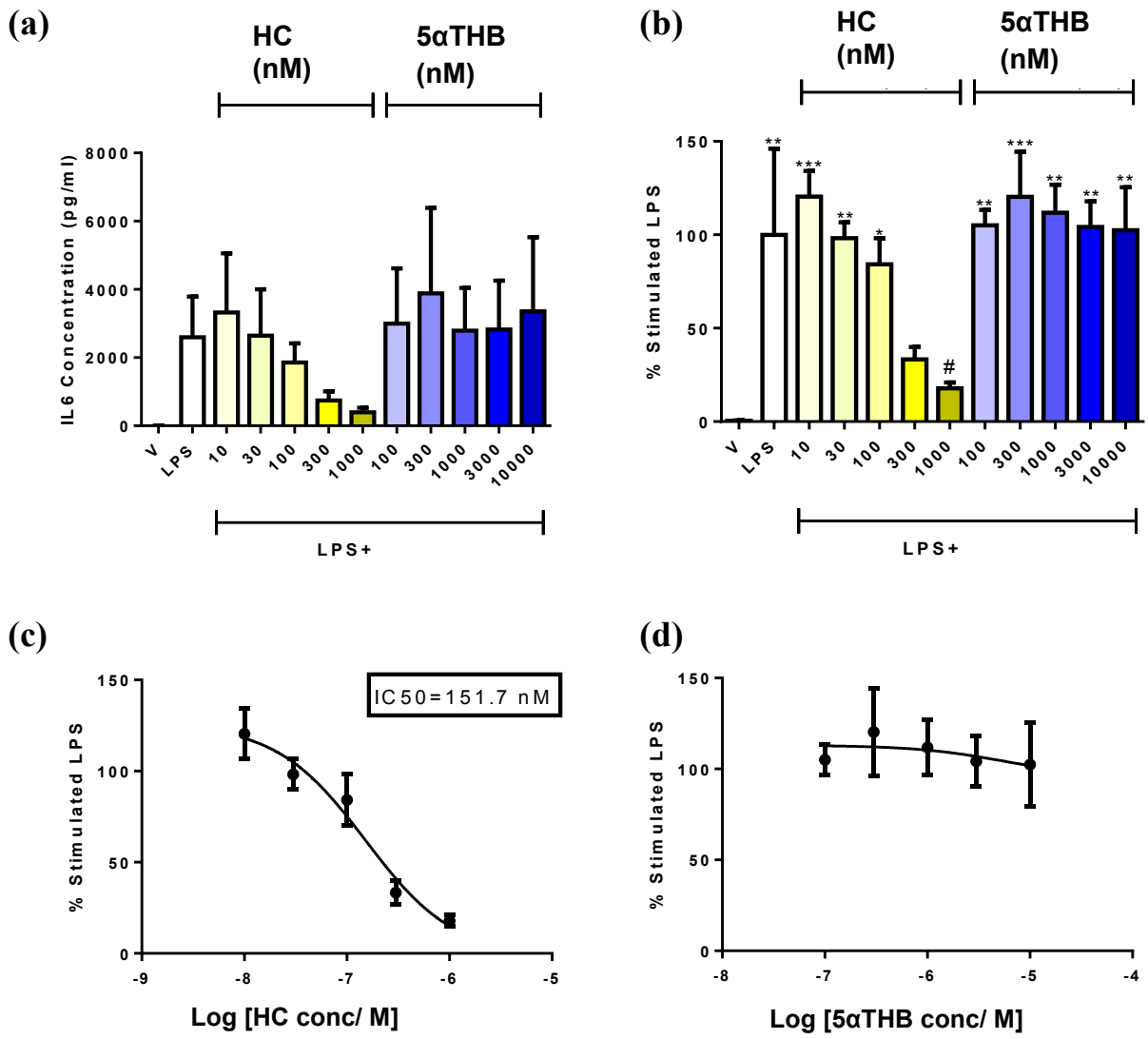

Figure 4.15: In murine bone marrow-derived macrophages (BMDM) stimulated with 100 ng/mL LPS, hydrocortisone (HC) induced a concentration-dependent suppression of IL6 release whereas 5αTHB did not. BMDM were treated with lipopolysaccharide (LPS; 100 ng/mL) to stimulate an inflammatory response, or with ethanol vehicle (V, 1 µL per 1 mL) as a negative control. One hour prior to this the cells had been primed with either vehicle (ethanol) (LPS), a HC concentration between 10 nM and 1000 nM, or a 5αTHB concentration between 100 nM and 10000 nM. The cells were incubated for 24 hours, and then their media removed for measurement of IL6 concentration by ELISA. The concentration of IL6 released from BMDM after each treatment was plotted as a bar chart (a). LPS increased the concentration of IL6 released from BMDM. Hydrocortisone induced a concentration-dependent suppression of this IL6 release, achieving a significant suppression at a concentration of 1000 nM in comparison to LPS-stimulated cells which were not exposed to HC. 5αTHB did not have an effect on IL6 release. Concentration-response curves were plotted to show the effects of HC (b) and 5αTHB (c) on IL6 release. The IC50 for HC-induced suppression of IL6 release was determined as 151.7 nM. Data are mean ± SEM of n=4. Data were analysed by one-way ANOVA and comparisons made using Dunnett's multiple comparisons test; ***=P<0.001, **=P<0.01, *=P<0.05 vs V. #=P<0.05 vs LPS.

4.5.4.3. The effects of steroids on suppression of IL6 release from BMDM stimulated with 3 ng/mL LPS.

Although 100 ng/mL was the LPS concentration used previously by Gastaldello (2014) and Yang (2009), a more significant suppression of IL6 with 5αTHB was seen when the cells were stimulated with a lower concentration of LPS; the most significant suppression was seen with an LPS concentration of 3 ng/mL in the work of Gastaldello (2014), and with an LPS concentration of 10 ng/mL in the work of Yang (2009). Therefore, it was thought that perhaps 100 ng/mL LPS was too high a concentration, and that, after this stimulation, 5αTHB is no longer able to suppress IL6 cytokine release. It was, therefore, decided to stimulate mouse BMDM with a lower dose of LPS (3 ng/mL), and increase groups to n=8 in order to account for the variability seen in preliminary experiments (figure 4.16).

After stimulation of BMDM with 3 ng/mL LPS, the concentration of IL6 released from cells was again increased in comparison to vehicle– treated cells (figure 4.16a). Hydrocortisone induced a concentration-dependent suppression of IL6 release, with an IC50 of 167 nM (figures 4.16a and b). Again, suppression was seen at concentrations of 300 nM and above, this time also achieving complete suppression with 300 nM. However, 5αTHB did not suppress the release of IL6 from BMDM stimulated with 3 ng/mL LPS (figures 4.16a and c).

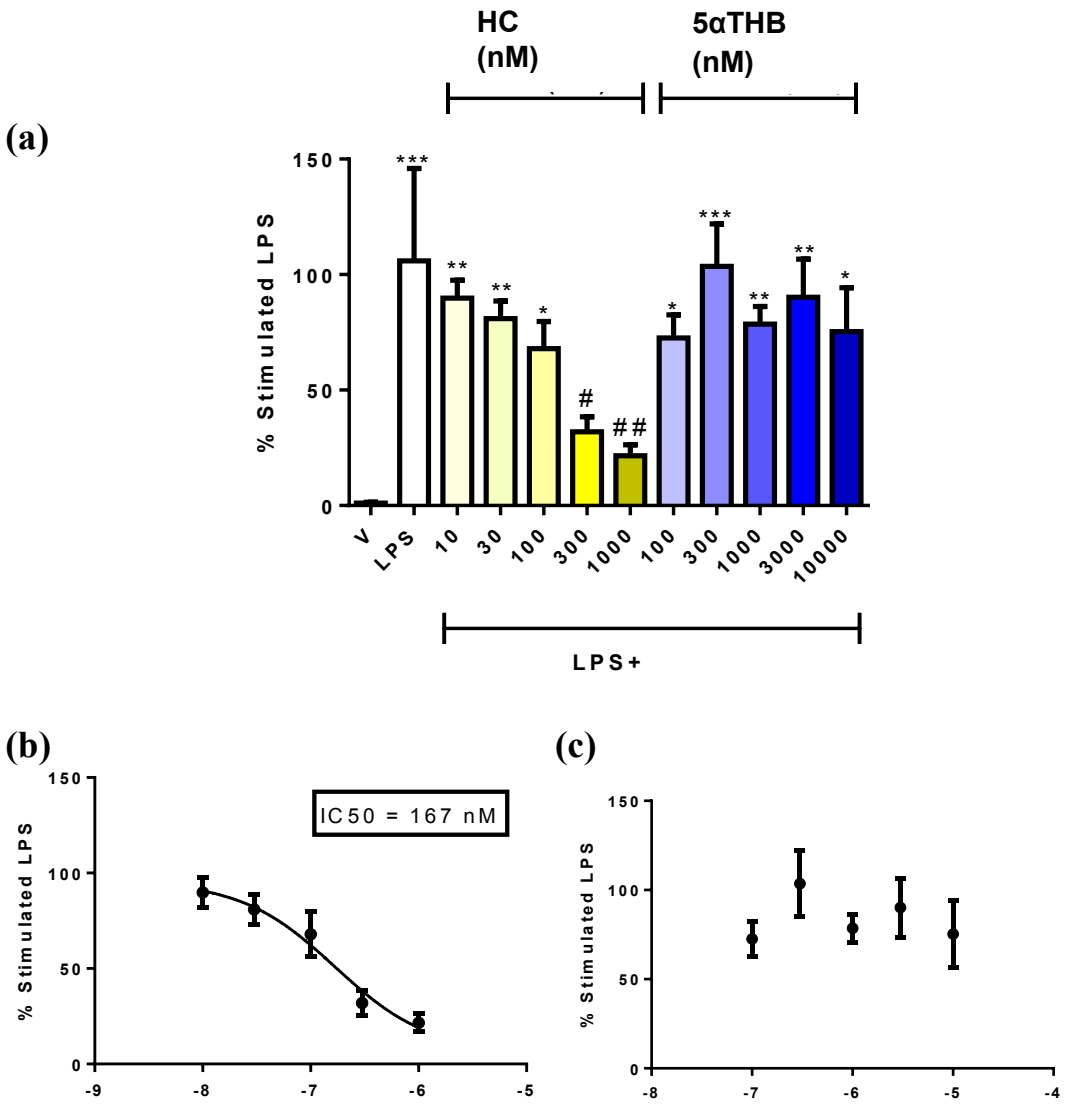

Figure 4.16: In mouse bone marrow-derived macrophage cells (BMDM) stimulated with 3 ng/mL LPS, hydrocortisone (HC) induced a concentration-dependent suppression of IL6 release whereas 5αTHB had no effect. BMDM were treated with lipopolysaccharide (LPS; 3 ng/mL) to stimulate an inflammatory response, or with vehicle (V) as a negative control. One hour prior to this the cells had been primed with either vehicle (ethanol) (LPS), a HC dose between 10 nM and 1000 nM, or a 5αTHB dose between 100 nM and 10000 nM. The cells were incubated for 24 hours, and then their media removed for measurement of IL6 concentration by ELISA. The concentration of IL6 released from BMDM after each treatment was plotted as a bar chart (a). LPS increased the concentration of IL6 released from BMDM. Hydrocortisone induced a concentration-dependent suppression of this IL6 release, achieving a significant suppression at a concentration of 300 nM in comparison to stimulated cells which were left untreated. 5αTHB did not have a significant effect on IL6 release. Concentration-response curves were plotted to show the effects of HC (b) or 5αTHB (c) on IL6 release. The IC50 for HC-induced suppression of IL6 release was determined as 167 nM. Data are mean ± SEM of n=8. Data were analysed by one-way ANOVA and comparisons made using Dunnett's multiple comparisons test; ***=P<0.001, **=P<0.01, *=P<0.05 vs V. #=P<0.05 vs LPS.

4.5.4.4. Steroid-induced suppression of TNFα release from BMDM stimulated with 3 ng/mL LPS.

5αTHB not only suppressed IL6 release from BMDM in previous work, but also TNFα release (Yang, Nixon et al. 2011). Therefore, since the suppression of IL6 could not be recapitulated in this work, the ability of 5αTHB to suppress TNFα release from the same cells was also assessed.

As with experiments investigating release of IL6, stimulation with 3 ng/mL LPS caused a significant increase in TNFα release from BMDM in comparison to unstimulated cells (figure 4.17a). Hydrocortisone induced a concentration-dependent suppression of this stimulated TNFα release with an IC50 of 313 nM (figures 4.17a and b). Complete suppression was observed with concentrations of 300 nM and above. 5αTHB however, did not significantly suppress TNFα release in comparison to stimulated controls at any concentration tested (figures 4.17a and c). A small effect was evident at the highest concentration of 5αTHB (1000 nM) which caused a significant decrease in TNFα released from cells in comparison to the lowest concentration (100 nM). However, since there was no difference in comparison to stimulated controls, and since no significant difference between these two concentrations of 5αTHB was evident in the previous IL6 concentration-response curves, the GR knockdown was not performed.

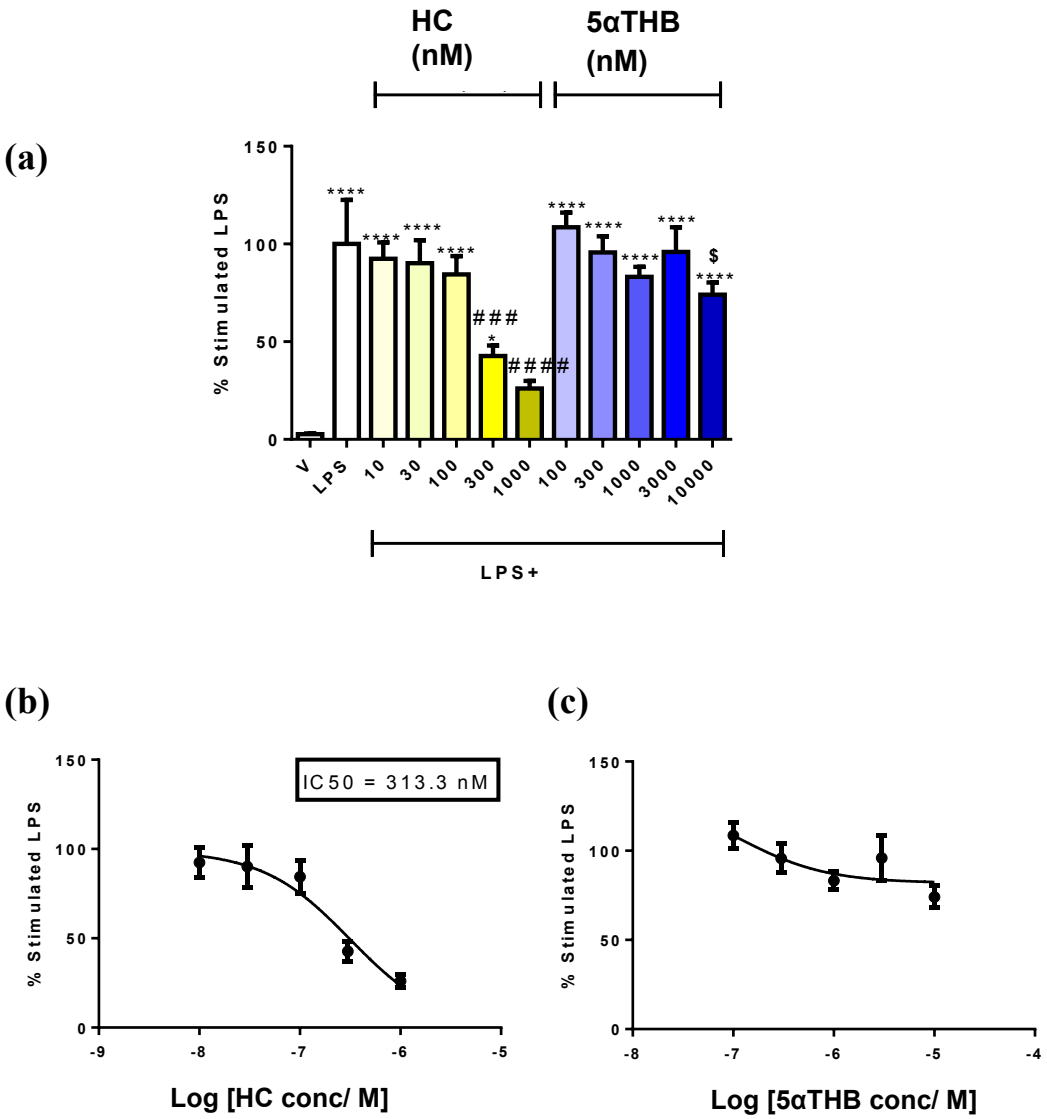

Figure 4.17: In mouse bone marrow-derived macrophages (BMDM) stimulated with 3 ng/mL LPS, hydrocortisone (HC) induced a concentration -dependent suppression of TNFα release, whereas 5αTHB had no effect. BMDM were treated with lipopolysaccharide (LPS; 3 ng/mL) to stimulate an inflammatory response, or with vehicle (V) as a negative control. One hour prior to this the cells had been primed with either vehicle (ethanol) (LPS), a HC concentration between 10 nM and 1000 nM, or a 5αTHB concentration between 100 nM and 10000 nM. The cells were incubated for 24 hours, and then their media removed for TNFα concentration measurement by ELISA. The concentration of TNFα released from BMDM after each treatment was plotted as a bar chart (a). LPS increased the concentration of TNFα released from BMDM. Hydrocortisone induced a concentration--dependent suppression of this TNFα release, achieving significance at 1000 nM in comparison to stimulated cells which were left untreated. 5αTHB did not have a significant effect on TNFα release. Concentration-response curves were plotted to show the effects of HC (b) or 5αTHB (c) on TNFα release. The IC50 for HC-induced suppression of TNFα release was determined as 313 nM. Data are mean±SEM of n=10. Data were analysed by one-way ANOVA and comparisons made using Dunnett's multiple comparisons test; ****=P<0.0001, *=P<0.05 vs V. ####=P<0.0001, ###=P<0.001 vs LPS, $=P<0.05 vs 100 nM 5αTHB.

4.6. Discussion

Recent work has suggested that the anti-inflammatory effects of 5αTHB may not be mediated by GR (Gastaldello, Livingstone et al. 2017). This is supported by work described in the previous chapter in which 5αTHB appeared to also target different mechanisms in the vasculature. Therefore, work described in this chapter addressed the role of GR in mediating responses induced by 5αTHB.

During investigation of steroid binding to GR, dexamethasone and hydrocortisone both displaced a GR-selective ligand in a commercial human GR competition assay whereas 5αTHB only displaced the ligand at high concentrations. This suggested that 5αTHB binds only very minimally to human GR, which is in contrast to previous work demonstrating that corticosterone, 5αTHB and 5αDHB had similar affinities in displacing tritiated dexamethasone from binding sites in rat hepatocytes (McInnes, Kenyon et al. 2004). The difference between this current assay and the previous work is that in the latter, whole rat hepatocytes were used, whereas our current model system contained human GR and only the LBD. Firstly, the LBD may be in a slightly different conformation when in its isolated form, with consequences on ligand binding. Secondly, dexamethasone may bind to sites other than just cytosolic GR in the hepatocytes, and 5αTHB may instead have been displacing dexamethasone from these alternative sites. One alternative proposed was the 'low affinity glucocorticoid binding sites' (LAGs) which are known to be present in the cell microsomal fraction and nuclear envelope (Ambellan, Swanson et al. 1981, Roszak, Lefebvre et al. 1990). Consistent with this, although 5αTHB displaced dexamethasone from whole hepatocytes and also from the microsomal fraction, the binding affinity of 5αTHB was much lower in the cytosolic fraction (McInnes 2003).

Alternatively, another possible receptor which dexamethasone may bind to (and may have been displaced from) in the microsomal fraction is the membrane GR. Although membrane GR originates from the same gene as cytoplasmic GR, it is suggested to vary through differential splicing, promoter switching or post translational editing (Stahn, Lowenberg et al. 2007). Furthermore it is reported to differ from cytoplasmic GR in its ligand binding specificities (Mitre-Aguilar, Cabrera-Quintero et al. 2015). It is, therefore, quite plausible that 5αTHB may bind to membrane GR but not the cytoplasmic GR. Another difference between this binding assay (using isolated human GR LBD) and the previous work (using whole rat hepatocytes) is the species difference. This is despite the fact that there is strong evolutionary pressure on conservation of the GR gene, and that GR structure and function are well conserved among all vertebrate species studied so far (Stolte, van Kemenade et al. 2006). Of these species, the amino acid sequences the of the mouse and rat GR most closely resemble that of human GR (Stolte, van Kemenade et al. 2006). This is reflected in the common use of murine models to study the effects of glucocorticoid, such as in the previous work investigating the effects of 5αTHB (Yang, Nixon et al. 2011, Gastaldello, Livingstone et al. 2017). However, although it is unlikely, it should be kept in mind that a small amino acid variation in the GR LBD due to species differences, may cause differences in ligand binding.

In order to investigate whether 5αTHB can induce GR to translocate into the nucleus, two alternative methods of 'immunofluorescence' and 'nuclear/ cytoplasmic (N/C) separation' were evaluated. Using the original immunofluorescence method there was a very narrow dynamic range between vehicle- and dexamethasone- treated cells. This resulted from high background immunofluorescence signal in the nucleus,

caused by a combination of non-specific secondary antibody binding and auto-fluorescence of cells in the green emission spectrum. It was determined that the fixing procedure (using paraformaldehyde) was causing cells to auto-fluoresce, consistent with the literature which reports non-specific binding of the secondary antibody to charged groups from unbound aldehydes used in fixation (Burry 2011). Furthermore it is reported that aldehyde-based chemicals can react with amines and proteins causing fluorescence with a green/yellow wavelength (Collins, 2006). The autofluorescence could be avoided by using alternative fixation methods or by aldehyde blocking (Thermofisher 2015, Collins 2006) but in this case a secondary antibody with a fluorophore which emits in the red (as opposed to green) emission spectrum was successful in eliminating the auto-fluorescence. However, due to non-specific secondary antibody binding, and also due to the nature of the scoring system used as the quantification method, the dynamic range between vehicle- and positive control (dexamethasone)-treated cells remained narrow. This meant that any attempts to identify intermediary effects were challenging. Improvements were attempted by using the alternative quantification method of continuous analysis by ImageJ. This was also performed blinded to treatment to eliminate bias. However, since cytoplasmic membranes could not be seen in images (only the nuclear outline as determined using DAPI staining) a caveat of this method was that cytoplasmic signal could not be determined, so the result is based only on nuclear signal. It may have been beneficial to include a membrane marker such as sodium-potassium-ATPase or cadherins (Abcam, 2016). However, since non-specific antibody binding was still present and could also limit reliability, it was decided instead to proceed by assessing steroid effects on GR nuclear translocation using the N/C separation method. The N/C

separation method had previously been used, albeit in a different cell type (myofibroblasts), by another group demonstrating that dexamethasone caused GR to be transported into the nucleus (Drebert, Bracke et al. 2015). In this current work, the model was successfully adopted to the nuclear and cytoplasmic separation of A549 cells, with a marked improvement in the dynamic range over the immunofluorescence method. The method was used to demonstrate that 5αTHB did not stimulate human GR to translocate into the nucleus in A549 cells, unlike dexamethasone. This is consistent with previous work in the same cell type by Gastaldello, in which 5αTHB did not induce phosphorylation of the Serine 211 residue in GR (known to correlate with GR nuclear translocation) whereas corticosterone did (Gastaldello, 2014). However, it should be noted that the A549 cells used in these studies are an artificial model (a secondary cell line). The recruitment of cofactors to GR is known to be cell-type specific (Chinenov, Gupte et al. 2013), and cofactors are known to be important for nuclear translocation as described in section 1.2.2. Therefore, it would also be beneficial to evaluate GR translocation in a primary cell line, where the conditions more closely resemble normal physiology. Indeed the results in A549 cells contrast with work by Yang (2009) in another secondary cell line (HEK293 cells). In her work she used fluorescence microscopy to monitor the movement of green fluorescent protein (GFP)-tagged GR (GFP-GR). Whereas dexamethasone (1 μM) or corticosterone (1 μM) induced nuclear translocation occurring within 15 and 30 minutes, respectively, the translocation observed after addition of 5αTHB (1 μM) was much slower (2 hours) and remained largely incomplete. Aside from the possibility that different co-regulators may be present, another explanation for the discrepancies between this past work and ours may be the fact that GFP-GR is a modified protein

and may not be representative of endogenous GR. GFP binding to GR may, therefore, modify its physiological processes (McMaster and Ray 2007).

As described in section 1.2.2, GR binding and nuclear translocation are strongly linked since the conformational change which takes place due to GR binding enables exposure of NLS and the formation of interactions required for nuclear translocation. The fact that 5αTHB only bound GR at very high concentrations, and also did not cause its nuclear translocation in this current work is therefore consistent. However, this does not exclude the possibility that the effects of 5αTHB are GR mediated. Indeed the displacement assay involved only the LBD of GR. It may be that 5αTHB binds at an allosteric GR site, resulting in non-genomic signalling, or alternatively it may act non-genomically through membrane GR. Indeed membrane GR is reported to have a different ligand binding specificity from cytosolic GR; for example, hydrocortisone had no binding affinity at membrane GR (Powell, Watson et al. 1999). As described in section 1.2.3.3, either binding to mGR or to an allosteric site could trigger signalling cascades which may result in the indirect modification of gene expression. This indirect regulation of gene expression would be consistent with the fact that 5αTHB suppressed topical inflammation only after 24 hours, whereas corticosterone-induced inhibition was evident after just 6 hours (Gastaldello, Livingstone et al. 2017). Alternatively, 5αTHB may bind to a different nuclear receptor, such as MR. Indeed endogenous GCs have a similar affinity for MR as aldosterone making MR a potential target (Nixon, Upreti et al. 2012). Whichever signalling mechanisms are used by 5αTHB, the results presented in this chapter suggest that 5αTHB does not cause GR to move into the nucleus. However, the question remains whether even a small amount of 5αTHB-bound GR, if able to enter

the nucleus, would be sufficient to alter GR-mediated gene regulation. To answer this, the effects of 5αTHB on co-regulator recruitment to GR were investigated.

GR binding to DNA is assisted and regulated by the recruitment of many co-regulator peptides, and ligand binding to GR allows it to adopt the conformation required to interact with these co-regulators. Pamgene's MARCoNI assay was utilised for this study because it enables the profiling of the effect of steroids on GR interaction with a range of co-regulator peptides. Dexamethasone induced clear increases and decreases in the interaction between GR and many of the co-regulator peptides investigated whereas 5αTHB had no effect. This suggests that 5αTHB does not stimulate the recruitment of co-regulator proteins to the GR, and is consistent with the demonstration in this chapter that 5αTHB did not bind GR LBD nor induce GR nuclear translocation. One critique of this assay is that equal concentrations (1 μM) of 5αTHB and dexamethasone were used, although 5αTHB is known to be less potent. Indeed 10 μM was required for 5αTHB binding to GR, whereas dexamethasone bound to a similar extent at 10 nM. Therefore, it is possible that a higher concentration of 5αTHB would influence interactions between co-regulator peptides and GR. Another critique is that since only the (human) GR LBD was used in this assay, it may be possible that 5αTHB binds to an allosteric site on GR and affects recruitment of co-regulator peptides from there. Alternatively, co-regulator peptides could be recruited to sites other than the LBD. However, consistent with the assay, initial ChIPseq experiments (collaboration with Alasdair Jubb, unpublished work) show that dexamethasone, but not 5αTHB, caused GR to bind GRE on typical response genes in human peripheral blood mononuclear cells (PBMCs). Since direct GRE binding is only one GR-

mediated mechanism which occurs in the nucleus, it would be interesting to also study the effect of 5αTHB on GR tethering to transcription factors such as AF1 and NFκB.

The hypotheses addressed in this chapter was that the previously-demonstrated anti-inflammatory effects of 5αTHB were mediated via GR. In the work of both Gastaldello (2014) and Yang (Yang, Nixon et al. 2011), 5αTHB suppressed IL6 and TNFα release from murine BMDM. Suppression of IL6 and TNFα by glucocorticoids is reported to largely occur through GR tethering to transcription factors (such as NFκβ and AP1), as described in section 1.3. Gastaldello employed the GR antagonist RU486 in this model in order to investigate the involvement of GR in these anti-inflammatory properties of 5αTHB. However, the experiments were inconclusive since RU486 actually suppressed IL6 release on its own. In this current work it was therefore decided to perform GR knockdown in these cells. The experiments of Gastaldello and Yang, showing suppression of cytokines by 5αTHB in mouse BMDM, were first re-performed in the absence of GR knockdown for control purposes. However unexpectedly, 5αTHB did not suppress IL6 release from LPS-stimulated BMDM whereas hydrocortisone did in a clear concentration-dependent manner. The lack of effect by 5αTHB could not be resolved by stimulating cells with a lower dose of LPS, nor by increasing the sample size to n=8 for increased power. This was not consistent with the work of Gastaldello and Yang. Furthermore in this current work 5αTHB also did not suppress release of the alternative cytokine TNFα from the same stimulated BMDM cells, also inconsistent with the work of Yang and Gastaldello. Since the effect of 5αTHB to suppress cytokines could not be recapitulated, the GR knockdown was not performed. It is unclear why the results in this chapter are inconsistent with previous findings. There are no major differences in how the experiments were

performed. The time course for treatment was the same, with cells being treated for 24 hours with steroid, and LPS given 1 hour after the steroid. Since hydrocortisone did induce a concentration-dependent suppression of cytokine release in this work, the absence of effect by 5αTHB cannot be due to problems with the ELISA kits used to quantify cytokines. Fresh steroid solutions were prepared in ethanol between each concentration-response experiment. A small optimisation had been made to the BMDM plating technique from the previous experiments performed by Gastaldello. Whereas she re-suspended her cells to give a constant volume each time and then plated a specific volume of the suspension per well, in this current study the cells were counted and a constant number of cells plated per well. Since this ensured that the same number of cells was present in each well, it controlled for intra- and inter-variability. However, if anything, this modification could be expected to increase the reproducibility of the data and is unlikely to explain the absence of effect in the current data. Furthermore, in the work performed by Yang a specific number of cells per well was also plated. Another small modification made during this study was that the data from each individual experiment were normalised to the cytokine concentration present in the media of LPS-only treated cells. The normalised data were then combined. This was in order to further reduce inter-assay variability; however, in the work by Yang and Gastaldello the raw cytokine concentrations (pg/ mL) were instead compared. Again, normalising the data would be expected to increase the reproducibility. Although the effect of 5αTHB was not significant compared to vehicle, a small concentration-dependent effect can be seen in the TNFα concentration-response, where TNFα release was significantly decreased after treatment with the highest (1000 nM) dose of 5αTHB, in comparison to treatment with

the lowest (100 nM) 5αTHB dose. The result in this chapter is, therefore, not entirely inconsistent with the previous work. Indeed, also in the previous work, 5αTHB consistently required a higher concentration than corticosterone to suppress IL6 and TNFα release in this model, with a threefold difference in potency indicated by Yang.

Anti-inflammatory effects of 5αTHB aside from those solely involving cytokine release, have also been demonstrated in past work. For example, 5αTHB suppressed inflammatory cell infiltration in a mouse model of thioglycolate-induced peritonitis, where IL6 suppression by 5αTHB occurred but was lost at higher concentrations (Yang, Nixon et al. 2011). Furthermore, more recently 5αTHB suppressed swelling and cell infiltration in a croton oil-induced mouse ear model of dermatitis, whereas real-time PCR analysis of gene transcripts revealed that, in this model, there was an also an absence of effects on IL6 and TNFα transcript expression. Therefore, despite my negative findings, 5αTHB may be suppressing inflammation by signalling through other mechanisms which have not been tested. In Gastaldello's mouse model of dermatitis, 5αTHB-induced suppression of inflammatory swelling was evident only after 24 hours, suggestive of mediation through alternative signalling pathways. Furthermore, in the thioglycolate-induced peritonitis model, whereas 5αTHB and corticosterone suppressed infiltration of neutrophils to the same extent, 5αTHB had less of an effect to suppress macrophage recruitment. There is, therefore, substantial evidence that 5αTHB acts through different mechanisms to suppress inflammation in comparison to other GCs.

In summary, the results of this chapter are consistent, indicating that 5αTHB does not work through the classical GR mechanism of action, namely by binding to GR LBD, stimulating GR nuclear translocation, and interacting with coregulatory

peptides. Therefore, this chapter suggests that 5αTHB does not have direct genomic effects through GR. Instead, 5αTHB may act through GR to initiate non-genomic mechanisms, either by binding the LBD at high concentrations, or by binding at an allosteric site. 5αTHB may also act through another receptor known to bind glucocorticoids, such as membrane GR or LAGs, which are also both associated with non-genomic effects of steroid (Falkenstein, Tillmann et al. 2000, Strehl and Buttgereit 2013). Alternatively, 5αTHB may have direct genomic effects through another receptor such as MR or an unidentified receptor. A microarray has recently been performed in which 5αTHB was shown to regulate gene expression in human peripheral blood derived macrophages. The next chapter of this thesis will, therefore, involve a gene expression analysis of this microarray data, in hope of further understanding the mechanisms of action of 5αTHB.

Chapter 5:
What is the mechanism of action of 5αTHB?

5. What is the mechanism of action of 5αTHB?

5.1. Introduction

There is compelling evidence *in vivo* of the anti-inflammatory properties of 5αTHB (Yang, Nixon et al. 2011, Gastaldello, Livingstone et al. 2017). Whilst its mechanisms remain unknown, evidence suggests that they are different from those of a typical glucocorticoid, and may underpin a safer therapeutic profile (Gastaldello, Livingstone et al. 2017). The requirement of GR for the effects of 5αTHB had not been substantiated by the work in this thesis or that of others (Gastaldello, Livingstone et al. 2017). Indeed the work presented in chapters 3 and 4 suggested that 5αTHB does not act through GR, at least not through genomic mechanisms. Therefore the receptor for 5αTHB, as well as its mechanisms of action, including whether they were largely genomic or non-genomic, remain unknown.

In previous work 5αTHB suppressed cytokine release from murine bone marrow derived macrophages (BMDM)(Gastaldello, 2014; Yang, 2009). Macrophages have high expression levels of transcriptionally-active GR, and GR binding sites have been identified in macrophage DNA, where they are enriched near to glucocorticoid-inducible genes (Jubb, Young et al. 2016, Jubb, Boyle et al. 2017). In past work, the GR antagonist RU486 attenuated the ability of both corticosterone and dexamethasone to suppress cytokine release from BMDM. However, it potentiated the suppression of cytokine release by 5αTHB (Gastaldello, 2014; Yang, 2009). In this current work, a significant suppression of cytokine release from these cells by 5αTHB could not be recapitulated. For this reason the targeted approach of GR knockdown to further investigate GR mediation of 5αTHB's effects in these cells could not be followed through. An exploratory approach was, therefore, pursued in

order to gain additional insight into the mechanisms of action of 5αTHB. The transcriptional response of human monocyte derived macrophages to dexamethasone exposure had recently been assessed by local collaborators (Jubb, Young et al. 2016). This was therefore an ideal model to also compare the effects of 5αTHB, for analysis in this thesis.

5.2. Hypothesis

The hypothesis addressed in this chapter is that 5αTHB regulates a different set of gene transcripts to conventional glucocorticoids.

5.3. Aims

The aim is to use the results of a microarray to assess gene regulation by 5αTHB in human monocyte derived macrophages, in order to generate hypotheses for a possible mechanism of action of 5αTHB. The individual aims are:

1. To identify actions of 5αTHB that may be mediated through classical GR genomic actions, by assessing genes commonly regulated by both 5αTHB and dexamethasone.
2. To identify independent mechanisms of 5αTHB, by assessing genes only regulated by 5αTHB but not by dexamethasone.

5.4. Methods

A microarray was performed in collaboration with Dr Alasdair Jubb in order to compare the effects of 5αTHB and dexamethasone to modulate gene expression in human monocyte derived macrophages (hMDMs). Dexamethasone was chosen as positive control as it has high affinity for GR and relatively low affinity for MR (Lan, Graham et al. 1982). All sample collection, preparation, analysis and data analysis to generate the gene lists described in table 5.2, was performed by Dr Alasdair Jubb. Whereas the genes regulated by dexamethasone have already been published (Jubb, Young et al. 2016), the 5αTHB-regulated gene lists were reserved for analysis in this thesis.

5.4.1. Sample collection and RNA analysis by microarray.

Human blood was collected from healthy volunteer donors aged 18-65 years: four donors had been used for the initial dexamethasone experiment and three were used for the follow up exploratory 5αTHB analysis. Ethical approval was provided by the South East Scotland Research Ethics Committee and full written consent obtained. From the blood samples, peripheral blood monocytes were then isolated by gradient separation of buffy coats followed by MACs CD14 +ve bead separation (Miltenyi Biotech, Surrey, UK) to isolate the monocyte fraction from the PBMCs. The full protocol is available at www.macrophages.com. Purified cells were cultured (RPMI supplemented with Penicillin/Streptomycin, Glutamax (Invitrogen) and 10% FCS) in the presence of recombinant human colony stimulating factor (CSF-1), also known as macrophage colony-stimulating factor (M-CSF)(10^4 U/mL) for 1 week, as per Hume lab standard operating procedure (Jubb, Young et al. 2016), to produce a stable population of monocyte-derived macrophages. Differentiated cells were re-plated at

$1x10^6$ cells/ mL and treated with either vehicle, dexamethasone (100nM, for 1h, 2h, 4h, 10h, and 24h) or 5αTHB (1μM, for 2h, 8h, and 24h). In previous work, 5αTHB suppressed inflammation after 24 hours but not after 6 hours (Gastaldello, Livingstone et al. 2017). Therefore it was anticipated in this work that the majority of 5αTHB-regulated genes would be evident after 24 hours, and that the functional analysis of dexamethasone- and 5αTHB- regulated genes could be compared at this time point. It was for this reason that the 24 hour time point was chosen to assess the effect of 5αTHB on gene expression, along with one early (2 hour) and one intermediate (8 hour) time point. After treating the cells, RNA was then extracted using RNeasy column-based extraction with on-column DNase treatment (Qiagen), and RNA quality was checked using a 2100 Bioanalyzer (Agilent Technologies, Stockport, UK). RNA was prepared for microarrays using standard Affymetrix protocols by Edinburgh Genomics and gene expression was measured using an Affymetrix HT HG- U133 plus PM (human) expression array.

5.4.2. Data analysis

Quality and outliers were assessed using the R package 'arrayQualityMetrics' (Gautier, Cope et al. 2004). Background correction and generation of raw expression values was performed using the 'affy' package in R (Kauffmann, Gentleman et al. 2009). To identify differentially expressed genes two complementary approaches had been taken for the response to dexamethasone (Jubb, Boyle et al. 2017)(Jubb, A, 2015). The first was using Biolayout Express 3D (Theocharidis, van Dongen et al. 2009) to assess for groups of genes with a correlated expression profile over the time course. This produced lists of genes that changes up or down at each phase of the response which were then filtered by requiring an absolute 2-fold change (log2 fold change of

1, adjusted p-value <0.05 (Benjamini-Hochberg)) to be retained in the analysis. In order to ensure genes with extreme profiles were not excluded by this approach the 'limma' package in R was used to identify differentially expressed genes with a minimum log2 fold change of 1.5 adjusted p value of <0.05 (Benjamini-Hochberg)(Smyth.G.K *et al*, 2005). The same approach was therefore taken to produce the gene lists for the response to 5αTHB (as described in table 5.1). The output for the purposes of the initial analysis in this thesis are lists of genes that responded to dexamethasone and/or 5αTHB at any time during the 24 hour time course.

Comparison Undertaken	Explanation
Dexamethasone	Dexamethasone-treated vs vehicle treated human PBMCs.
5αTHB	5αTHB-treated vs vehicle treated human PBMCs.

Table 5.1: A description of the comparisons undertaken vs (relative to) vehicle treated cells.

5.4.3. Functional analysis

A functional analysis is a high throughput tool which uses the biological knowledge accumulated in public databases in order to functionally analyse a large gene list (Huang da, Sherman et al. 2009). It, therefore, allows us to identify the most enriched and relevant biology within a gene list (Huang da, Sherman et al. 2009, Hong, Zhang et al. 2014). Metascape (www.metascape.org)(Developed by Sanford Burnham, UCSD, GNF) enrichment analysis tool was employed for the work described in this thesis based on the method it uses for the enrichment and output of enriched terms, as well as for the background databases with which it is linked. The KEGG pathway (www.genome.jp/kegg) and GO Biological Process (www.geneontology.org) background databases are available for annotation and were used here. Metascape uses the Singular Enrichment Analysis (SEA) method which, due to its efficiency in extracting the biological meaning behind large gene lists, is the most traditional and popular strategy (Huang da, Sherman et al. 2009, Hong, Zhang et al. 2014). Gene identifiers (from the input gene list) are first converted into Entrez gene IDs, and then the Entrez gene IDs are used to extract biological information about each gene from various background databases. Using these databases each gene is annotated according to which biological process or pathway terms ('annotation terms') they are associated with. A statistical test is then applied to identify the annotation terms which are 'enriched' for the genes in the list (so have a larger amount than expected) in comparison to control or reference background. The enriched annotation terms associated with the gene list therefore provide important insight into its biological themes. Metascape uses the hypergeometric statistical test to identify enriched annotation terms, and this is suitable for both small and large gene lists, so is flexible

depending on the length of the gene list (Hong, Zhang et al. 2014). For each gene list in table 2 enriched terms from publicly available databases (e.g. KEGG pathways, Gene Ontology (GO) terms) were sought using an enrichment p value cut off of $p<0.05$. A common limitation to this SEA strategy is that the large outputs of enriched annotation terms are often heavily overlapped and redundant, which can cause information to be overlooked (Huang da, Sherman et al. 2009). However, Metascape clusters redundant annotation terms, grouping them based on their similarities, and presenting the top 20 clusters in a heat map, focusing on the larger biological picture. For every 'cluster' representing a common pathway or process, the most enriched term is chosen as the representative term of the group. One limitation of clustering the annotation terms in this way is that the most enriched term within each cluster is chosen to represent it (forming the cluster name) on each diagram. Therefore, the cluster names may not necessarily represent all ontology terms included in it perfectly, and information could be missed. For this reason an appendix is also provided at the back of this thesis, which gives information on the individual terms within each cluster, as well as the genes responsible for the enrichment of each term or cluster, and their fold changes.

5.5. Results

5.5.1. Time point assessment

Of the genes which were differentially expressed between vehicle and 5αTHB treatments, 41 were regulated at the 2 hour time point, and 124 genes were regulated at the 8 hour time point. There were no differentially expressed genes after 24 hours following 5αTHB treatment of hMDMs. This was unexpected, and meant that the functional analysis of dexamethasone- and 5αTHB- regulated genes could not be compared at the 24 hour time point. Although the majority of 5αTHB- regulated genes were regulated at the intermediate 8 hour time point, gene expression in response to dexamethasone was not assessed after 8 hours, so a direct comparison of steroid effects at this time point also could not be made. Because of this limitation, all genes which were differentially expressed over the 24 hour period following steroid treatment were grouped together to perform the functional analyses described in section 5.5.3.

Since the time points were different between steroids, genes were grouped according to whether they first became differentially expressed at an early time point (between 0-2 hours), at an intermediate time point (between 2-8 hours by 5αTHB, or between 2-10 hours by dexamethasone), or at a late time point (between 8-24 hours by 5αTHB, or between 10-24 hours by dexamethasone). Figures 5.1 and 5.2 demonstrate the proportion of genes regulated at an early, intermediate, and late time point after dexamethasone and 5αTHB treatment respectively.

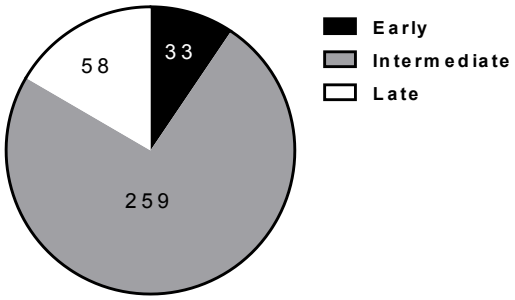

Figure 5.1: The proportion of genes which became differentially expressed at an early, intermediate, or late time point after dexamethasone treatment of human peripheral blood-derived macrophages. The early time point corresponds to genes which were regulated 0-2 hours post treatment (33 genes), intermediate corresponds to 2-10 hours post treatment (259 genes), and late corresponds to 10-24 hours post treatment (58 genes).

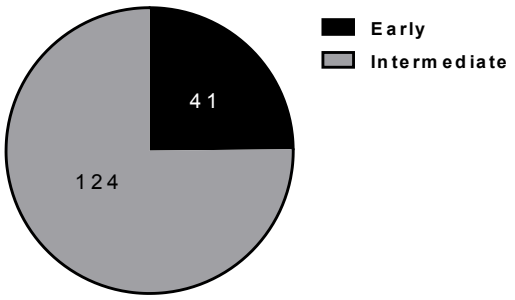

Figure 5.2: The proportion of genes which became differentially expressed at an early, intermediate, or late time point after 5αTHB treatment of human peripheral blood-derived macrophages. The early time point corresponds to genes which were regulated 0-2 hours post treatment (41 genes), intermediate corresponds to 2-8 hours post treatment (124 genes), and late corresponds to 8-24 hours post treatment. None of the genes regulated by 5αTHB required more than 8 hours to become differentially expressed.

5.5.2. Analysis of gene lists.

A total of 350 genes were identified as being differentially expressed between vehicle and dexamethasone treatments (table 5.2; list 1) over the 24 hour time course after treatment. 165 genes were differentially expressed between vehicle and 5αTHB treatments (table 5.2; list 2). Only 38 genes were commonly differentially expressed in response to both dexamethasone *and* 5αTHB (table 5.2; list 3). This means that a remaining 312 genes were *only* regulated by dexamethasone and not by 5αTHB (table 5.2; list 4). In addition, 127 genes were only regulated by 5αTHB and not by dexamethasone (table 5.2; list 5). The number of genes in each list is given in table 5.2, and the data is demonstrated in figure 5.3.

The 350 genes differentially expressed in response to dexamethasone have been published by Dr Alasdair Jubb (Jubb, Young et al. 2016). All other gene lists from table 5.2 are provided in the appendices of this thesis.

Gene list	Description	Total genes	Genes up-regulated	Genes down-regulated
1	All genes differentially expressed between dexamethasone and vehicle treatments.	350	225	125
2	All genes differentially expressed between 5αTHB and vehicle treatments.	165	133	32
3	Common genes which were differentially expressed between dexamethasone and vehicle treatments *and* between 5αTHB and vehicle treatments.	38	32	6
4	Genes *only* differentially expressed between dexamethasone and vehicle treatments (not between 5αTHB and vehicle treatments).	312	194	118
5	Genes *only* differentially expressed between 5αTHB and vehicle treatments (not between dexamethasone and vehicle treatments).	127	101	26

Table 5.2: A summary of the gene lists generated from a microarray comparing dexamethasone and 5αTHB effects on gene expression in human peripheral blood derived macrophages. The number of significant differentially regulated genes with fold change > 1.5 and adjusted p value < 0.05 are also given for each gene list.

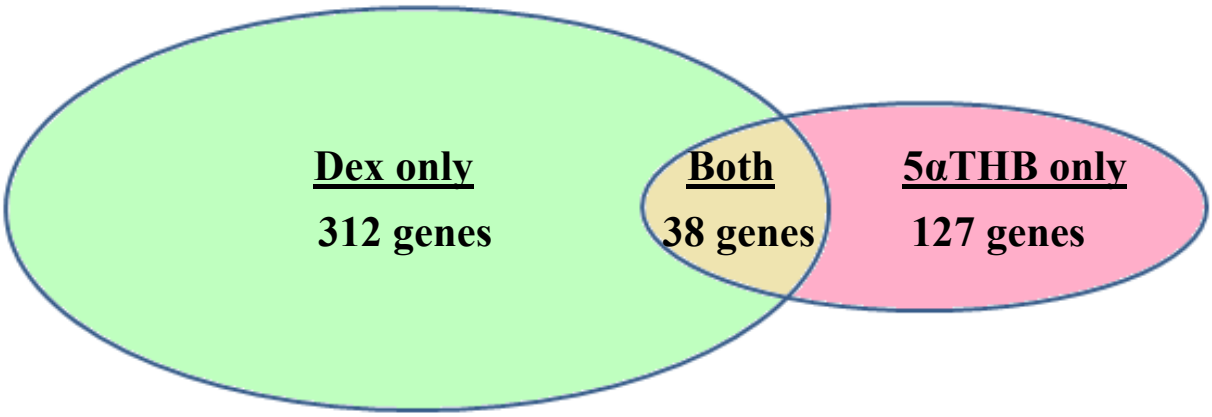

Figure 5.3: A Venn diagram demonstrating the number of differentially expressed genes in human peripheral blood mononuclear cells after dexamethasone and 5αTHB treatments respectively.

5.5.3. Enrichment analysis

Enrichment analyses of GO biological processes and KEGG pathways were first performed using all genes regulated by either dexamethasone (list 1, table 5.2) or 5αTHB (list 2, table 5.2) (section 2.2.1). Further enrichment analyses were then performed using the genes *only* regulated by *either* dexamethasone (list 4, table 5.2) or 5αTHB (list 5, table 5.2)(Section 2.2.2). Finally, enrichment analyses of the genes commonly regulated by both 5αTHB and dexamethasone (list 3, table 5.2) are described in section 2.2.3.

5.5.3.1. Enrichment analyses of all genes regulated by dexamethasone and 5αTHB

5.5.3.1.1. Enrichment of GO biological processes

5.5.3.1.1.1. Enrichment of GO biological processes by all genes regulated by dexamethasone

The top 20 GO biological process clusters identified as being significantly enriched, following analysis of the 350 genes regulated by dexamethasone, are given in figure 5.4a. Many of the most significantly-enriched clusters are related to inflammatory and immune responses. Examples are the GO biological processes of 'inflammatory response', 'response to cytokine' and 'regulation of cytokine production'. Other enriched processes include 'regulation of cell migration', 'negative regulation of cell proliferation' and 'single organism cell adhesion'.

Enrichment was subsequently assessed for up- and down-regulated genes separately, as different components of a given pathway or molecular function could be up- or down-regulated within a single comparison. The GO biological process terms which were significantly enriched for genes up-regulated and down-regulated by dexamethasone are given in figure 5.4b and c respectively.

Figure 5.4: Gene Ontology Biological process clusters enriched for genes which were (a) differentially expressed (both up-regulated and down-regulated genes), (b) up-regulated, or (c) down-regulated in human peripheral blood-derived macrophages between 0-24 hours after dexamethasone (100 nM) treatment.

5.5.3.1.1.2. Enrichment of GO biological processes by all genes regulated by 5αTHB

The top 20 significantly enriched ($p<0.05$) GO biological process clusters in the list of 165 differentially regulated genes after 5αTHB treatment (gene list 2, table 5.2) are given in figure 5.5a. The most significantly enriched GO biological process cluster was 'cellular response to lipid'; however, GO biological process clusters relating to inflammation were also enriched (such as 'Inflammatory response', 'cytokine production' and 'cytokine production involved in immune response'). These were less significantly enriched (higher p value) than by dexamethasone. Other enriched processes in the list of genes regulated by 5αTHB included 'blood vessel development', 'hematopoietic or lymphoid organ development' and 'fat cell differentiation'.

Up-regulated and down-regulated genes were also assessed separately as for dexamethasone. The top 20 significantly-enriched GO biological process clusters are given for the up-regulated genes in figure 5.5b, whereas only 4 GO biological process clusters were significantly enriched (at $p<0.05$) in the down-regulated genes, given in figure 5.5c.

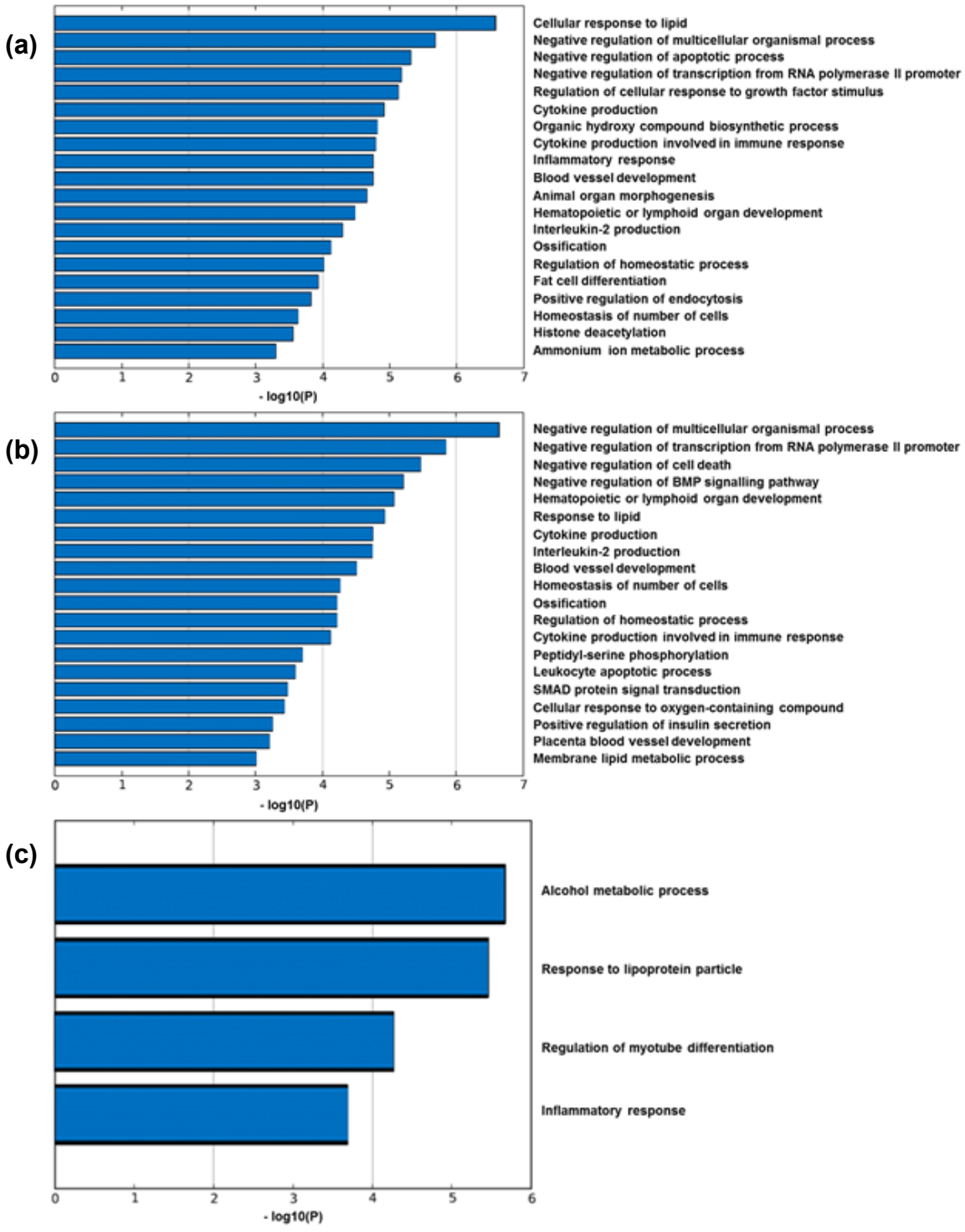

Figure 5.5: Gene Ontology Biological process clusters which were significantly enriched ($p<0.05$) in genes which were (a) differentially expressed (either up- and down-regulated), (b) up-regulated or (c) down-regulated (both adjusted $p<0.05$) in human peripheral blood-derived macrophages between 0-24 hours after treatment with 5αTHB (1 μM).

5.3.3.1.2. Enrichment of KEGG pathways.

5.3.3.1.2.1. Enrichment of KEGG pathways by all genes regulated by dexamethasone

All 350 genes differentially regulated in human PBMCs after dexamethasone treatment (list 1, table 5.2) were then used for an enrichment analysis of KEGG pathways. The top 20 significantly-enriched KEGG pathways are given in figure 5.6a. Many of these are involved with inflammatory and immune responses; such as 'NFκB signalling pathway' which was the most significantly enriched of the pathways. Others included 'cytokine-cytokine receptor interaction', 'TNF signalling pathway' and 'MAPK signalling pathway'. KEGG pathways relating to cancer were also commonly enriched, such as 'proteoglycans in cancer', 'transcriptional misregulation in cancer', 'bladder cancer' and 'endometrial cancer'.

Separate lists of up-regulated and down-regulated genes were then analysed, and the significantly enriched KEGG pathways within these separate lists are given in figures 5.6b and c respectively. There were 15 significantly enriched KEGG pathways for the up-regulated genes. The most significant was the 'FoxO signalling pathway', followed by 'transcriptional misregulation in cancer', 'mineral absorption', 'proteoglycans in cancer', 'AMPK signalling pathway' and 'MAPK signalling pathway'. For down-regulated genes, 10 KEGG pathways were significantly enriched. The top 3 were the 'NFκB signalling pathway', 'TNF signalling pathway' and 'cytokine-cytokine receptor interaction'.

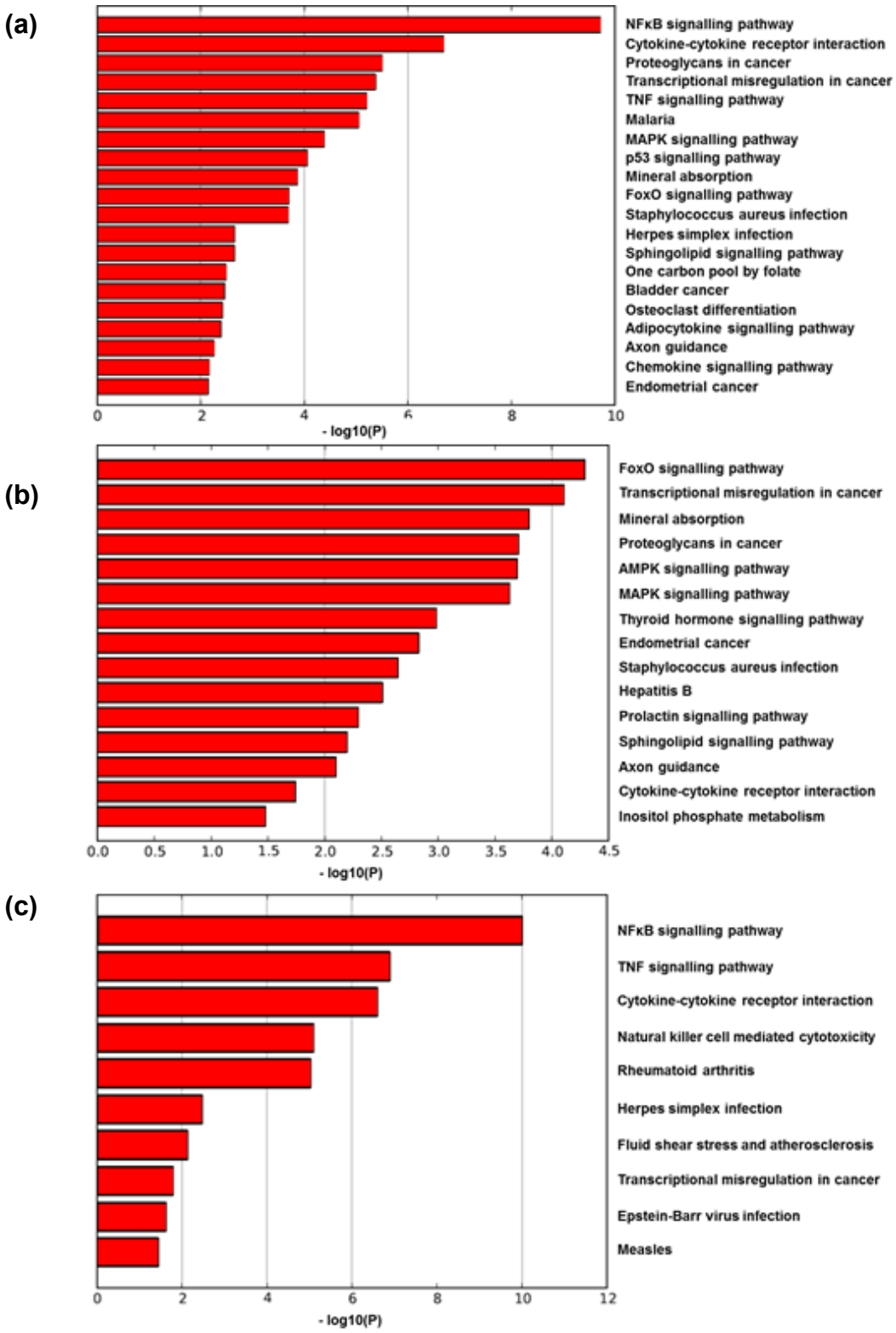

Figure 5.6: KEGG pathways (at p value<0.05) which were significantly enriched for (a) all differentially-expressed genes, (b) up-regulated genes, and (c) down-regulated genes in human peripheral blood derived macrophages between 0-24 hours after treatment with dexamethasone (100 nM).

5.5.3.1.2.2. Enrichment of KEGG pathways by all genes regulated by 5αTHB

An enrichment analysis of KEGG pathways for the list of 165 genes which were differentially expressed after 5αTHB treatment (list 2, table 5.2) was then performed. 13 KEGG pathways were significantly enriched, demonstrated in figure 5.7a. The most significantly enriched KEGG pathway cluster was 'Fc gamma R-mediated phagocytosis' which is related to an inflammatory response. Other enriched KEGG pathway clusters relating to inflammation were the 'TNF signalling pathway' (which did appear in the enrichment analysis of dexamethasone-regulated genes) and 'Th1 and Th2 cell differentiation' (which did not). Another of the enriched KEGG pathways was 'Aldosterone synthesis and secretion'

The genes up-regulated and down-regulated by 5αTHB were then analysed separately. There were 8 KEGG pathways specifically up- regulated by 5αTHB (figure 5.7b) but there were no down-regulated KEGG pathways. Fc gamma R-mediated phagocytosis was the most significantly enriched pathway in the list of up-regulated genes. This was followed by the 'TGF-beta signalling pathway', 'Th1 and Th2 cell differentiation' and 'Type II diabetes mellitus'.

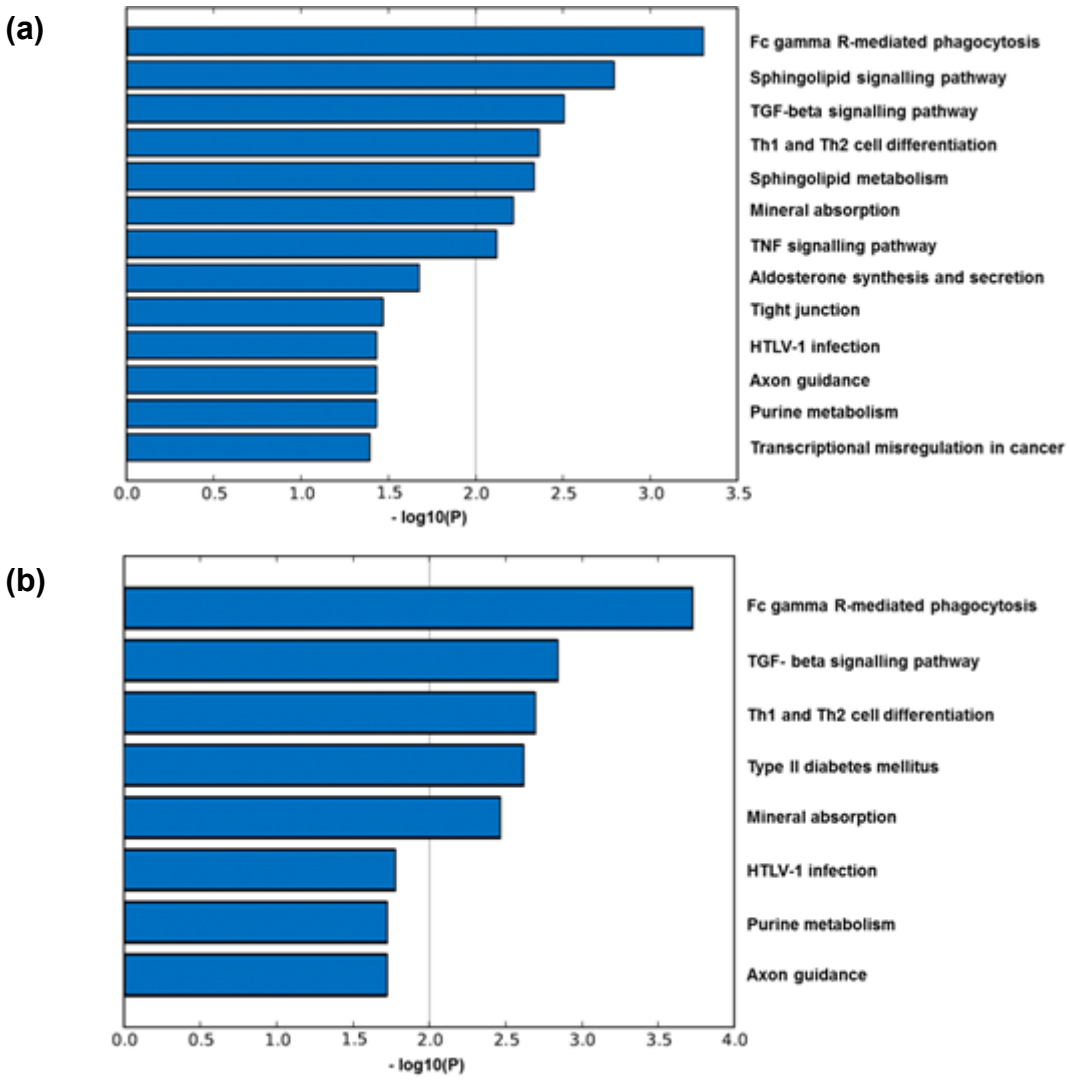

Figure 5.7: KEGG pathways (at p value<0.05) which were significantly enriched for (a) all differentially expressed genes and (b) up-regulated genes in human blood derived macrophages between 0-24 hours after treatment with 5αTHB (1 μM).

5.5.3.2. Enrichment analysis of genes only regulated by either dexamethasone or 5αTHB.

In order to compare pathways and processes commonly regulated by both drugs, or specifically targeted by one or the other, an enrichment analysis was performed on the genes which were *only* regulated by either dexamethasone or 5αTHB (lists 4 and 5 respectively, able 5.2) and those which were commonly regulated by both drugs (list 3, table 5.2).

5.5.3.2.1. Enrichment analysis of GO biological processes

5.5.3.2.1.1. Enrichment of GO biological processes by genes regulated *only* by dexamethasone

Many of the top GO Biological process clusters which were enriched in the genes only regulated by dexamethasone (and not 5αTHB)(list 4, table 5.2) were related to inflammatory and immune responses. Again, other enriched processes within these genes included cell migration and cell proliferation. The top 20 enriched GO biological process clusters are given in figure 5.8a.

The genes were then separated according to whether they were up-regulated or down-regulated in response to dexamethasone, and then enrichment analysis performed separately for each of these groups.

For the 194 total up-regulated genes, the enriched GO biological process clusters are given in figure 5.8b, and for the 118 down-regulated genes, the enriched GO biological process clusters are given in figure 5.8c.

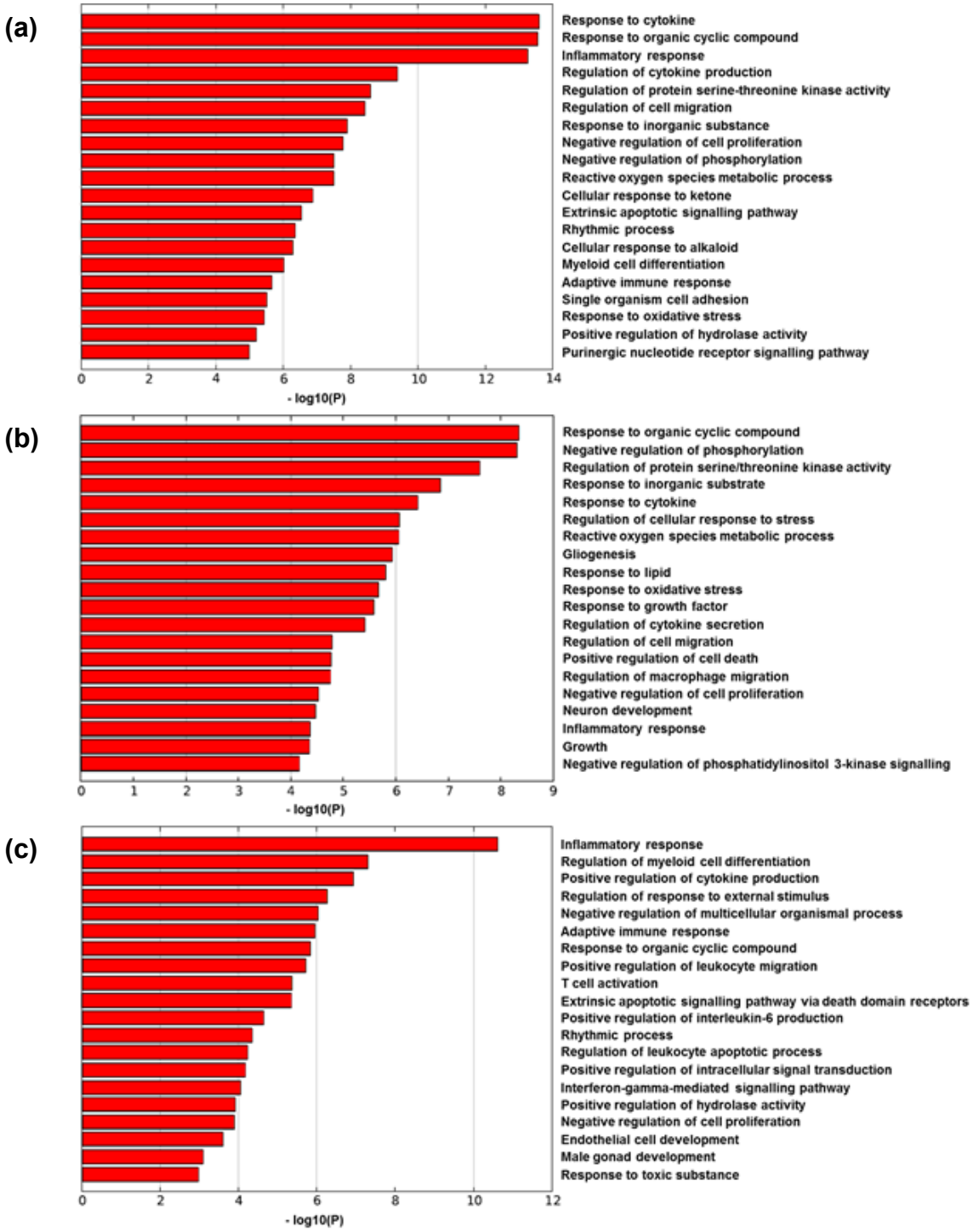

Figure 5.8: A list of the top 20 GO Biological process clusters which were enriched in genes found to be (a) differentially expressed (in either direction), (b) up-regulated or (c) down-regulated between 0-24 hours after dexamethasone (100 nM) treatment, but not by 5αTHB treatment, in human peripheral blood macrophage cells.

5.5.3.2.1.2. Enrichment of GO biological processes by genes *only* regulated by 5αTHB.

With regard to the genes which were *only* regulated by 5αTHB (and not by dexamethasone) (list 5, table 5.2) the GO biological processes which were significantly enriched ($p<0.05$) are given in figure 5.9a. 'Blood vessel development' was the second most significantly enriched cluster, after 'organic hydroxyl compound biosynthetic process' and followed by 'negative regulation of pathway-restricted SMAD protein phosphorylation'. Other enriched processes included 'leukocyte chemotaxis', 'fat cell differentiation', 'regulation of cellular localisation' and 'regulation of fibroblast proliferation'.

The up-regulated and down-regulated genes were then analysed separately. Figure 5.9b demonstrates that 'blood vessel development' is enriched by the genes which were up regulated by 5αTHB. Other processes enriched by the up-regulated genes were 'fat cell differentiation', 'regulation of fibroblast proliferation', 'regulation of microtubule-based process', 'SMAD protein signal transduction' and 'negative regulation of neurogenesis'.

Only 4 GO biological process clusters were significantly down-regulated at an enrichment p value of 0.05 (figure 5.9c). These were 'steroid metabolic process', 'response to lipoprotein particle', 'cellular response to interferon gamma', and 'microtubule-based process'.

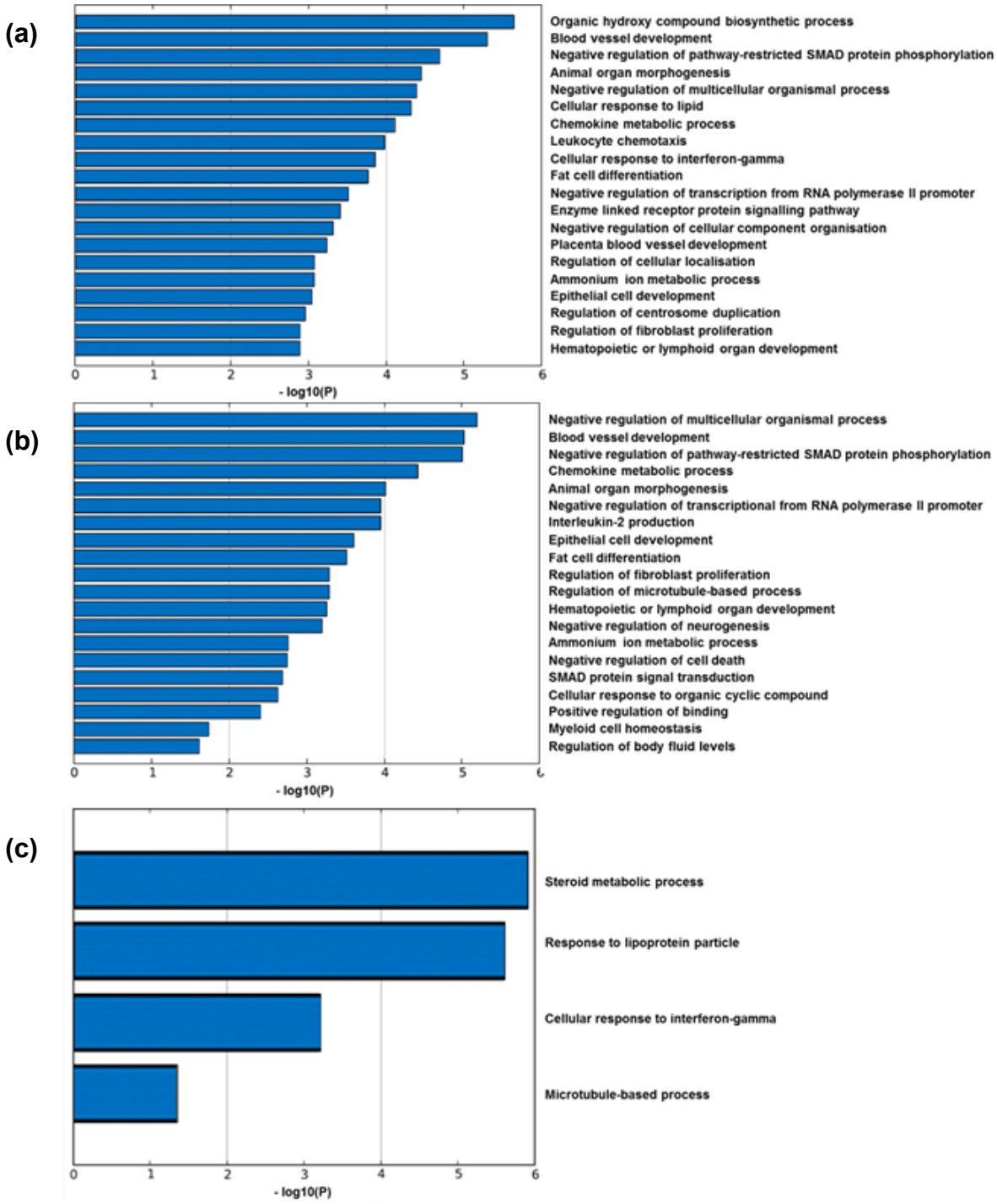

Figure 5.9: GO Biological process clusters which were enriched in the list of genes found to be (a) differentially expressed (in either direction), (b) up-regulated and (c) down-regulated between 0-24 hours after treatment with 5αTHB, but not by treatment with dexamethasone, in human peripheral blood macrophage cells.

5.5.3.2.2. Enrichment analysis of KEGG pathways

5.5.3.2.2.1. Enrichment analysis of KEGG pathways by genes regulated *only* by dexamethasone

The top 20 significantly enriched KEGG pathways in the genes regulated only by dexamethasone (but not 5αTHB)(list 4, table 5.2) are given in figure 5.10a. The results are similar to when the commonly regulated genes (by both dexamethasone and 5αTHB) were included; except now the 'TNF signalling pathway' has been removed. In addition, the following new pathways appear on this heat map: 'rheumatoid arthritis', 'amoebiasis', 'hepatitis B', 'apoptosis', 'AMPK signalling pathway', 'Epstein-Barr virus infection' and 'circadian entrainment'.

Genes up-regulated or down-regulated by dexamethasone (but not 5αTHB) were analysed separately. 19 KEGG pathways were significantly enriched by up regulated genes ($p<0.05$)(figure 5.10b).

10 KEGG pathways were significantly enriched by down-regulated genes, given in figure 5.10c.

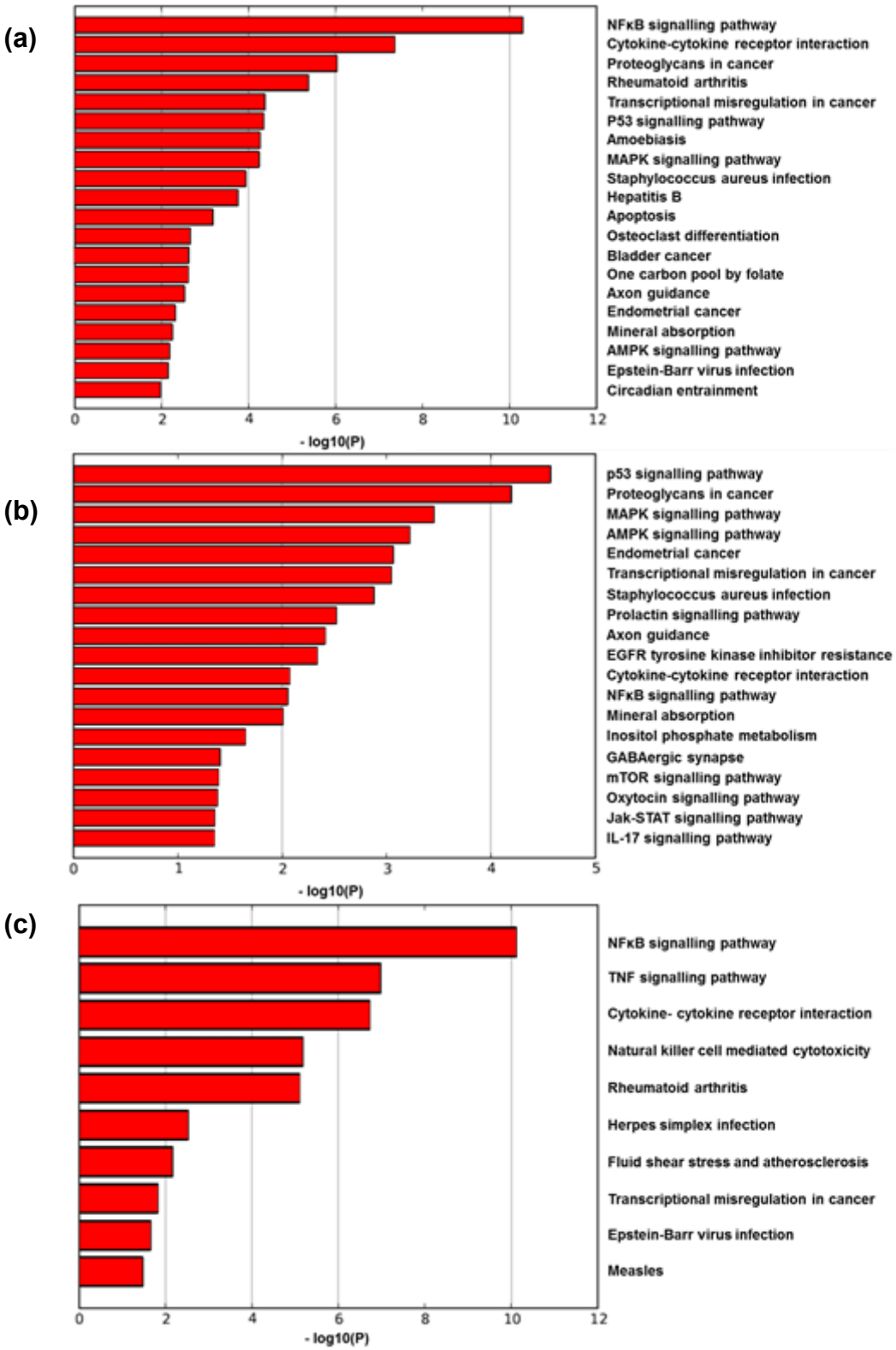

Figure 5.10: KEGG pathways which were enriched in the genes regulated only by dexamethasone (100 nM) (and not by 5αTHB) between 0-24 hours after treatment in human peripheral blood macrophages. Heat map (a) uses both up-regulated and down-regulated genes to determine enriched processes, whereas heat maps (b) and (c) use only genes which were up-regulated or down-regulated, respectively.

5.5.3.2.2.2. Enrichment of KEGG pathways by genes regulated only by 5αTHB

An enrichment analysis of KEGG pathways was then performed on genes which were *only* regulated by 5αTHB (and not dexamethasone). There were only 8 KEGG pathways significantly enriched ($p<0.05$) in this list of genes (list 5, table 5.2) which are given in figure 5.11a. The most significantly enriched pathway was the TGF-beta signalling pathway. This was followed by 'Fc-gamma R- mediated phagocytosis' and 'Th1 and Th2 cell differentiation' which are both pathways related to inflammation and immunity. In comparison to the heat map of pathways enriched by all genes (regulated by both dexamethasone and 5αTHB) many pathways have now disappeared from the list, so may be commonly targeted by both 5αTHB and dexamethasone. These include 'TNF signalling pathway', 'Aldosterone synthesis and secretion', 'sphingolipid signalling pathway', 'sphingolipid metabolism', 'mineral absorption', 'tight junction' and 'transcriptional misregulation in cancer'.

When up-regulated and down-regulated genes were analysed separately, 7 KEGG pathways were enriched for up-regulated genes (figure 5.11b) and these were very similar to the enriched pathways using *all* the 5αTHB up-regulated genes (figure 5.11b). The only differences are that the KEGG pathway clusters of 'Type II diabetes mellitus' and 'Mineral absorption' have now disappeared; hence, genes commonly regulated by both drugs are required for these processes to be enriched.

There were no KEGG pathways enriched in the list of 5αTHB down-regulated genes.

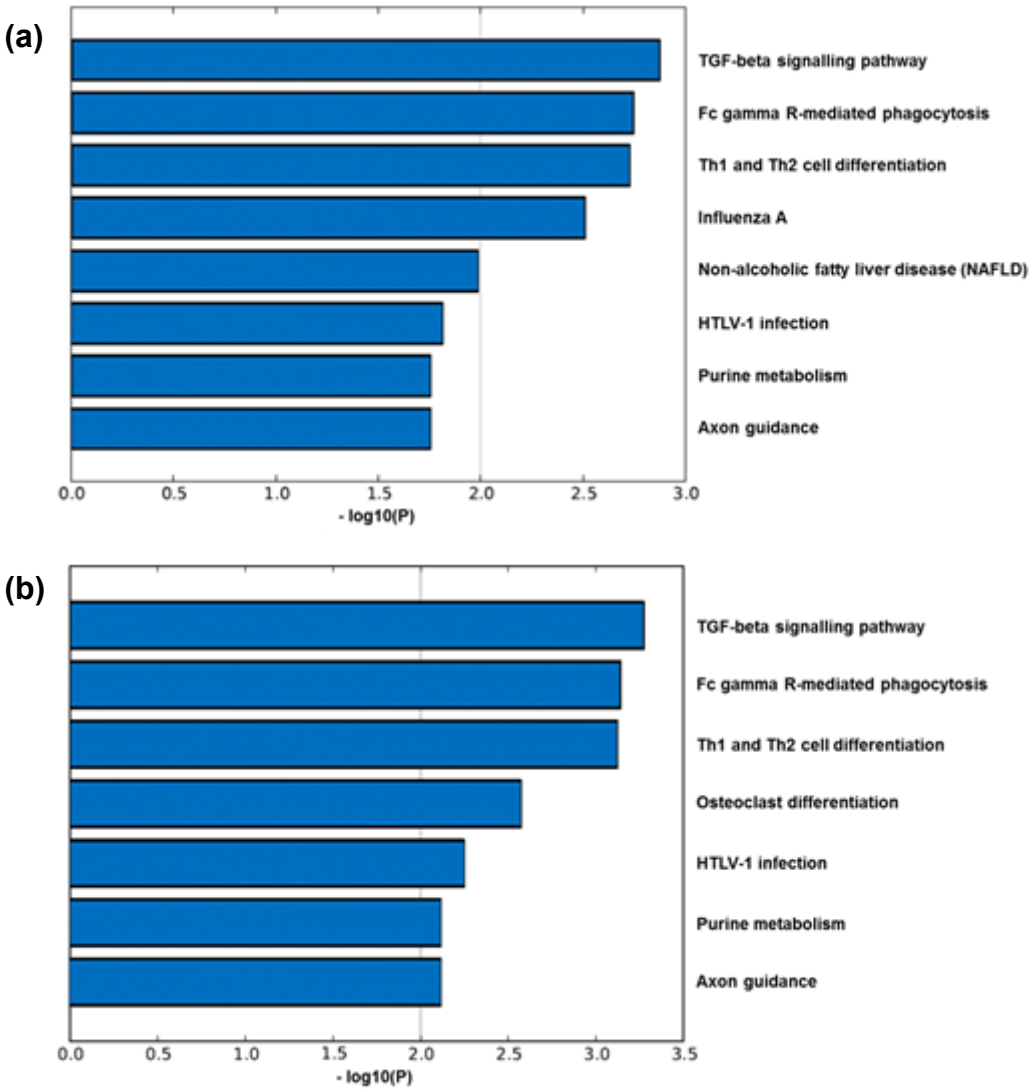

Figure 5.11: KEGG pathways which were enriched in the genes regulated only by 5αTHB (1 μM) between 0-24 hours after treatment in human peripheral blood macrophages. Heat map (a) gives the KEGG pathways which were enriched in the list of all genes differentially regulated by 5αTHB, and heat map (b) are gives the KEGG pathways which were enriched in only the up-regulated genes. There were no enriched KEGG pathways in the down-regulated genes.

5.5.3.3. Enrichment analysis of genes commonly regulated by both 5αTHB and dexamethasone

5.5.3.3.1. Enrichment of GO biological processes by genes commonly regulated by both 5αTHB and dexamethasone

Finally, an enrichment analysis was performed on the genes which were commonly regulated both by 5αTHB and by dexamethasone (list 3, table 5.2). 15 GO biological process clusters were enriched for these genes, which are given in figure 5.12a.

The up-regulated and down-regulated genes were then separated. 12 GO biological processes were significantly enriched for up-regulated genes (figure 5.12b). Many of these enriched processes were related to inflammation and immunity such as the negative regulation of leukocyte apoptotic process, inflammatory response and lymphocyte activation. Processes related to the negative regulation of apoptosis were among the most significantly enriched processes ('negative regulation of leukocyte apoptotic process' and 'negative regulation of apoptotic process') although 'regulation of cellular carbohydrate metabolic process' was the most significantly enriched. Other enriched processes were 'locomotory behaviour', 'response to lipid', 'membrane lipid metabolic process' and 'regulation of vesicle-mediated transport'.

There were no GO biological processes significantly enriched for down-regulated genes.

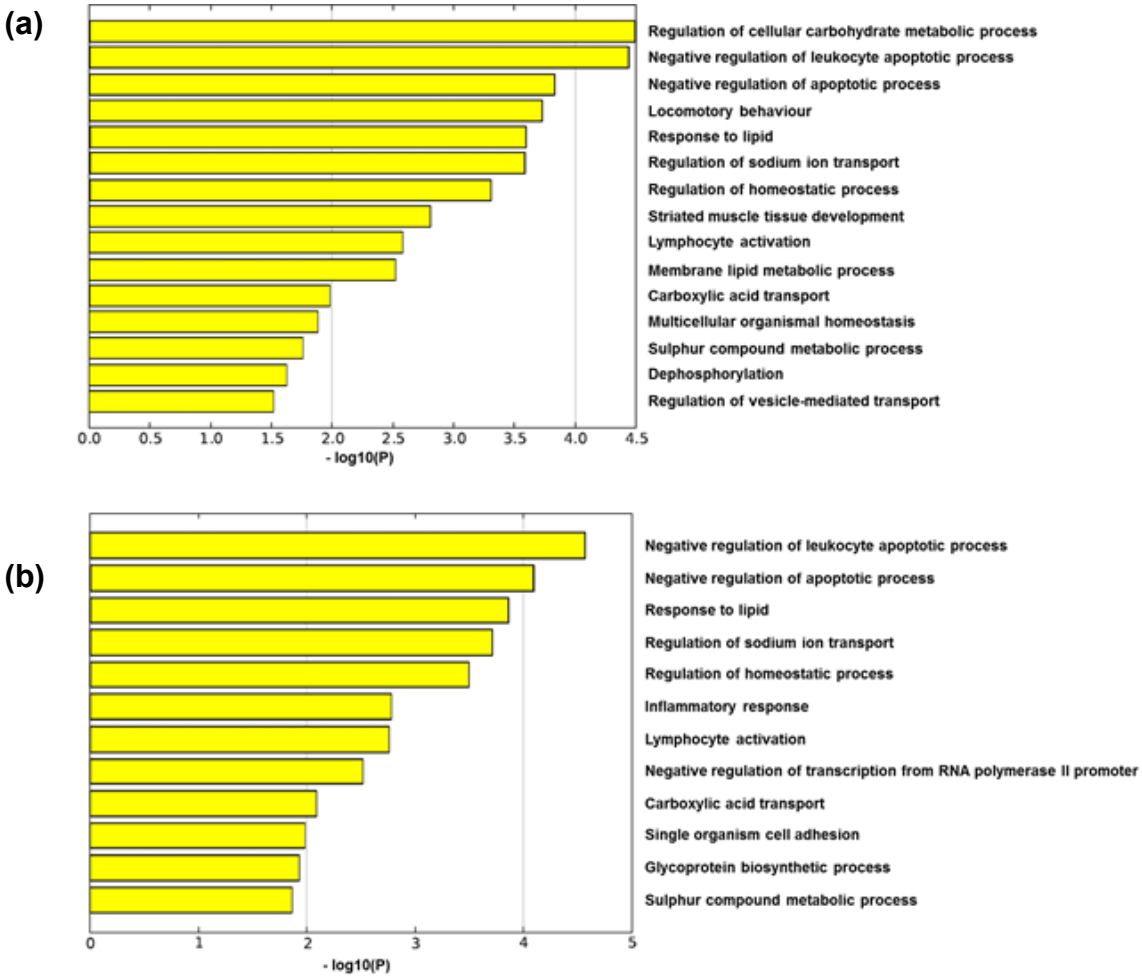

Figure 5.12: GO Biological process clusters which were enriched in the list of genes which were commonly differentially expressed between 0-24 hours after both 5αTHB (1 μM) and dexamethasone (100 nM) treatment. (a) are the GO Biological processes which were enriched by this total gene list, and (b) are the biological processes which were enriched only for the up-regulated genes. There were no enriched GO biological processes by the down-regulated genes.

5.5.3.3.2. Enrichment of KEGG pathways by genes commonly regulated by both 5αTHB and dexamethasone

In the genes which were commonly regulated by both dexamethasone and 5αTHB, there were 2 significantly enriched ($p<0.05$) KEGG pathways, which were 'sphingolipid signalling pathway' and 'cGMP-PKG' signalling pathway'. 2 genes (ADORA3 and PRKCE) were present in both enriched KEGG pathway clusters. Again, up-regulated and down-regulated genes were analysed separately. One KEGG pathway (cGMP-PKG) was enriched in the list of up-regulated genes whereas there were no enriched signalling pathways in the commonly down-regulated genes.

5.6. Discussion

Previous work suggested that 5αTHB retains some glucocorticoid activities but acts through a different mechanism from typical glucocorticoids (Gastaldello, Livingstone et al. 2017). The findings so far presented in this thesis (chapters 3 and 4) are consistent with this previous work. The mechanisms of action of 5αTHB remain unknown, and to gain some insight an exploratory approach was taken in this chapter whereby the transcriptional response of human monocyte derived macrophages (hMDMs) were compared between 5αTHB and the selective GR agonist dexamethasone. A microarray of the steroid-treated hMDMs showed that 165 genes were regulated by 5αTHB, and 350 by dexamethasone, whereas only 38 of these genes were commonly regulated by both steroids. It was unexpected that differential expression of all 5αTHB- regulated genes occurred in under 8 hours, whereas some dexamethasone-regulated genes required 24 hours to become differentially expressed. This contrasts with the *in vivo* work of Gastaldello *et al*, in which 5αTHB required 24 hours to suppress swelling and cell infiltration whereas corticosterone required only 6 hours (Gastaldello, Livingstone et al. 2017). However since Gastaldello assessed inflammation at only two time points (6 and 24 hours), it is possible that 5αTHB had an effect just after the 6 hour time point which was only detected at the later 24 hour time point, which would be consistent with the work presented here. It should be noted that the model used by Gastaldello *et al* used mice whilst the current work was performed in human cells. Furthermore, the croton oil model used by Gastaldello *et al* (Gastaldello, Livingstone et al. 2017) is an *in vivo* model and, therefore, is influenced by the full immune response and requires time for protein translation and the effect to become evident, whereas the microarray used in the current work was performed on

RNA taken from individual macrophages. However, since 5αTHB did not cause differential expression of any genes after 24 hours in this current work, a functional analysis of gene expression at this time point could not be performed. Instead, the functional analyses of dexamethasone- and 5αTHB- regulated genes were compared by using all genes regulated by each steroid over the course of the 24 hours after treatment, keeping the limitation in mind that gene regulation by 5αTHB was assessed at fewer time points than dexamethasone.

The 38 genes commonly regulated by both dexamethasone and 5αTHB included typical glucocorticoid responsive genes (such as *Per1, Fkbp51,* and *Gilz*) which contain GRE in their promoters for transactivation by GR. Whilst this may suggest mediation of effects through GR, it is not conclusive proof since all members of the NR3C nuclear receptor subfamily (mineralocorticoid, glucocorticoid, androgen, and progesterone receptors) have overlapping DNA binding preferences (Hudson, Youn et al. 2014). Furthermore MR also has overlapping preferences with GR for ligand binding, and MR has been shown to regulate all three of these genes (Fernandes-Rosa, Hubert et al. 2011, Hudson, Youn et al. 2014, Petrovich, Asher et al. 2014, Fletcher, Morgan et al. 2017). Interestingly, evidence has suggested that at least *Per1* and *Fkbp51* can be regulated by GR-MR heterodimers (Petrovich, Asher et al. 2014, Mifsud and Reul 2016). Therefore, in future work the involvement of MR, and perhaps of GR-MR heterodimers, for 5αTHB's effects should be investigated. Although there were some genes commonly regulated by both dexamethasone and 5αTHB, the fact that there were only 38 provides strong evidence that the two steroids largely act through different mechanisms in macrophages. One point to keep in mind is that a reason for the lack of commonly regulated genes may be that the selection criteria used

to select genes were too stringent, with the consequence that many more commonly regulated genes could have been missed. It was also considered that these 38 commonly regulated genes may be the genes which are key to achieving the anti-inflammatory effects of both compounds. In a functional analysis performed on these commonly-regulated genes to assess this, whereas three GO biological processes related to inflammation were enriched ('Negative regulation of leukocyte apoptotic process', 'Lymphocyte activation', and 'Inflammatory response'), there was enrichment of only two KEGG pathway terms, with just 3 genes responsible for enrichment of each term. This could indicate that, whilst dexamethasone and 5αTHB may target some of the same inflammatory processes, they may achieve this by acting through different molecular pathways.

Whereas dexamethasone caused differential expression of 350 genes in this study, a previous study had identified only 133 genes regulated by dexamethasone; however, this data is not directly comparable since in the previous study the cells were undifferentiated monocytes (Ehrchen, Steinmuller et al. 2007). In addition to the typical glucocorticoid responsive genes reported above, other transcription factors (*Nfil3, Jdp2, Irf1, Bcl)* and anti-inflammatory genes (*Sesn1, Fcar, Cd163*) were also identified among dexamethasone- regulated genes, which have been reported in previous studies to be glucocorticoid regulated (Ehrchen, Steinmuller et al. 2007, Chinenov, Coppo et al. 2014). This suggested that the microarray results are reliable. Many of the GO biological processes which were enriched for dexamethasone-regulated genes relate to inflammation. Furthermore the KEGG pathways enriched by dexamethasone-regulated genes in this study are consistent with the mechanisms known to be used by glucocorticoids to suppress inflammation. For example the most

enriched KEGG pathways among down-regulated genes include the NFκB and TNF signalling pathways, and among up-regulated genes include the MAPK signalling pathway which, as discussed in section 1.3, are all known to be involved in the suppression of inflammation by glucocorticoids. Among the genes *only* regulated by dexamethasone (i.e. when the 38 genes commonly regulated by dexamethasone and 5αTHB are taken away) the situation is very similar, with many enriched GO biological processes and KEGG signalling pathways relating to inflammation, perhaps suggesting that the overlapping genes are not crucial for the anti-inflammatory effect of dexamethasone.

The fact that 5αTHB caused differential expression of 165 genes demonstrates that it has effects on gene transcription in human peripheral blood macrophages, as opposed to acting solely via membrane receptors and second messenger signalling, for example. Among 5αTHB- regulated genes, the most enriched GO biological process is 'cellular response to lipid'. On inspection of the enrichment table for figure 3 in the appendices, the redundant processes within this cluster reflect a cellular response to steroid hormone, suggesting that 5αTHB does in some way engage in mechanisms associated with a classical steroid. The 'inflammatory response' GO biological process is also enriched among 5αTHB regulated genes, as are 'cytokine production' and 'cytokine production involved in the immune response', although not as significantly as their enrichment by dexamethasone-regulated genes. Another enriched cluster was 'blood vessel development' and, on inspection of the enrichment table for figure 3 in the appendices, the redundant terms within this cluster relate to angiogenesis, vascular development, and endothelial cell migration. Therefore, perhaps 5αTHB affects the release of growth factors from immune cells, which then act on the vasculature.

Whereas chapter 3 suggests that 5αTHB acts directly on the vasculature (for example to alter expression of adhesion molecules) the result here may, therefore, suggest that 5αTHB also acts *indirectly* on the vasculature through effects on immune cells (Gastaldello, Livingstone et al. 2017). The work here is in an inflammatory cell, and 5αTHB has been suggested to suppress inflammation mainly by reducing vascular permeability and subsequent inflammatory cell recruitment (Gastaldello, Livingstone et al. 2017). Genes involved in a reduction of vascular permeability may therefore have caused enrichment of the 'blood vessel development' term. Another explanation could be that 5αTHB induces a specific phenotype in the macrophages, which promotes angiogenesis. The M2 phenotype is known to promote angiogenesis and tissue healing (Shapouri-Moghaddam, Mohammadian et al. 2018). These functions are important after the initial proinflammatory response of the classical M1 macrophages, in order to restore tissue homeostasis (Shapouri-Moghaddam, Mohammadian et al. 2018). Further evidence for the presence of the M2 macrophage is presented by the demonstration that 'SMAD protein signal transduction' is another enriched process among up-regulated genes. SMAD signalling is activated by TGFβ, and a specific type of M2 macrophage (known as M2c) is known to release TGFβ (Gratchev 2017, Shapouri-Moghaddam, Mohammadian et al. 2018). Furthermore, the KEGG pathways enriched by 5αTHB-regulated genes include 'Fc gamma R-mediated phagocytosis', 'TGF-beta signalling pathway', and 'Th1 and Th2 cell differentiation'. Enrichment of these terms is consistent with the possibility that the macrophages treated with 5αTHB have developed the M2c phenotype. This relates to the concept that macrophages are not a homogenous cell population but may adopt distinct phenotypes and functions, depending on the presence of various stimuli (such as cytokines, growth factors, and

hormones) present in their microenvironment (Ehrchen, Steinmuller et al. 2007, Schmieder, Michel et al. 2012, Chazaud 2014, Gratchev 2017, Shapouri-Moghaddam, Mohammadian et al. 2018). The polarised phenotypes that macrophages acquire have been broadly classified into two major groups: Pro-inflammatory, classically-activated macrophages (M1) and anti-inflammatory, alternatively-activated macrophages (M2), which promote Th1 and Th2 responses, respectively (Rickard and Young 2009, Mills 2012, Schmieder, Michel et al. 2012, Shapouri-Moghaddam, Mohammadian et al. 2018). A change in phenotype from M1 to M2 can, therefore, explain enrichment of the term 'Th1 and Th2 cell differentiation'. M1 macrophages are polarised by a microbial trigger, such as LPS, or by Th1 cytokines, such as IFN-γ or TNFα (Rickard and Young 2009, Schmieder, Michel et al. 2012). They have robust antimicrobial activity, secreting various pro-inflammatory cytokines (such as IL6 and TNFα), chemokines, as well as reactive oxygen and nitrogen intermediates. Although this is effective in killing pathogens it also results in tissue destruction (Schmieder, Michel et al. 2012, Shapouri-Moghaddam, Mohammadian et al. 2018). In contrast, M2 macrophages actually suppress inflammation and function to promote tissue repair and remodelling, re-establishing homeostasis. They do this in part through an increase in angiogenesis, which is, therefore, consistent with enrichment of terms relating to the vasculature (Rickard and Young 2009, Schmieder, Michel et al. 2012, Chazaud 2014, Shapouri-Moghaddam, Mohammadian et al. 2018). There are a variety of M2 cells depending on the stimulus used for polarisation. For this reason M2 macrophages have been further classified into M2a, M2b, and M2c subfamilies (Schmieder, Michel et al. 2012, Chazaud 2014). The M2c subset can be induced by glucocorticoids, IL10, or TGFβ, and also release TGFβ as a mediator (Zizzo, Hilliard et al. 2012). The presence

of this M2c macrophage phenotype would, therefore, be consistent with enrichment of the 'TGF beta signalling pathway' KEGG term as well as with the GO biological process terms relating to SMAD signalling (Ehrchen, Steinmuller et al. 2007). Furthermore, M2c cells have a pro-healing function and increased phagocytic activity, consistent with enrichment of the term relating to phagocytosis (Zizzo, Hilliard et al. 2012). The increased phagocytic activity of M2c cells is associated with an up regulation of *Mertk*, and, interestingly, this gene was increased in the microarray in response to dexamethasone and 5αTHB, suggesting that this phenotype was also present in dexamethasone-treated cells to some extent (Shapouri-Moghaddam, Mohammadian et al. 2018).

Limitations of the enrichment analysis should not be ignored. First of all the macrophages were unstimulated, so they may not optimally model an inflammatory response. This is important since the macrophage phenotype is described to change upon stimulation, with microbial triggers such as LPS being reported to cause classical activation of macrophages into a pro inflammatory M1 phenotype (Rickard and Young 2009, Mills 2012, Schmieder, Michel et al. 2012, Shapouri-Moghaddam, Mohammadian et al. 2018). It must be noted that these macrophages had not been stimulated, and LPS stimulation is known to alter macrophage phenotype. Future work will compare the effect of dexamethasone and 5αTHB on gene expression in LPS-stimulated cells. Another limitation is that Metascape is limited by current knowledge of genes and of processes to which they relate. Therefore, it may be that many of the 5αTHB-regulated genes have a role in a large suppression of inflammation through mechanisms which are entirely undiscovered. However, since this information is not known the genes will not cause an enrichment of inflammatory terms in the database,

and, consequently, this will not be reflected in the Metascape diagrams. Metascape can be used only to provide hints of what may be happening, to direct future investigation.

In summary, the work described in this chapter suggest that 5αTHB acts largely through different mechanisms from dexamethasone in immune cells. The enrichment analysis of 5αTHB- regulated genes tentatively suggests the presence of a particular macrophage phenotype known as M2c. 5αTHB may, therefore, either selectively target these cells, or may induce a phenotypic change in macrophage cells into the reparative M2c subtype. This is, therefore, consistent with 5αTHB acting to suppress inflammation without detrimental effects to wound repair processes. The hypothesis that 5αTHB induces a phenotypic change in macrophages into the M2c phenotype will be investigated in future work. This could be achieved by testing surface marker expression typical of M2c cells in human peripheral blood macrophages after 5αTHB treatment, to confirm the change in phenotype. Although the work described in this chapter suggests that GR is probably not involved in mediating the effects of 5αTHB (since 5αTHB and dexamethasone largely regulated different genes) this is not conclusive and in the future the same microarray may be performed after GR knockdown, in order to provide conclusive evidence. Mediation of the effects of 5αTHB through MR will be tested in the future. Indeed 'Aldosterone synthesis and secretion' was an enriched KEGG pathway in the list of all of the 5αTHB-regulated genes, although this was not present on the heat map of enriched KEGG pathways in genes which were *only* regulated by 5αTHB. This chapter provides further evidence that 5αTHB acts through different mechanisms to glucocorticoids and suggests alternative mechanisms by which 5αTHB may suppress inflammation. The hypotheses

generated in this chapter will be investigated in future work, perhaps leading to the development of a safer class of anti-inflammatory therapy.

Chapter 6:
Summary and Future Work

6. Summary and Future Work

There has been a huge drive to find a selective modulator of GR activity over the past few years. This is in an attempt to better treat inflammatory diseases, since the current glucocorticoid treatments have side effects which restrict their use. The work described in this thesis was based on a glucocorticoid metabolite, 5αTHB, which is under investigation as a selective modulator of GR activity for topical anti-inflammatory treatment. The anti-inflammatory effects of 5αTHB had been robustly demonstrated *in vivo,* on the skin and in a model of peritonitis (Yang, Nixon et al. 2011, Gastaldello, Livingstone et al. 2017). However, the role of GR in mediating the effects of 5αTHB had not been established (Gastaldello, Livingstone et al. 2017). The work described in this thesis, therefore, investigated the mechanisms of action of 5αTHB, as well as further exploring the potential of 5αTHB as a topical steroid by studying its effects to delay wound repair, a side effect which is a particular problem of topical glucocorticoid treatments.

6.1. Is 5αTHB less detrimental to wound repair processes than current glucocorticoids?

The wound healing process involves many stages and cell types, and communication between the cells through release of growth factors and other mediators is crucial for coordinating the healing response (Eming, Brachvogel et al. 2007, Barrientos, Stojadinovic et al. 2008). In this thesis an attempt to compare steroid effects on different aspects of the wound repair process was performed, by using a scratch wound assay to measure the migration of endothelial, dermal fibroblast, and keratinocyte cells. However neither 5αTHB nor dexamethasone effected migration of

any cell type. In the literature it has since been demonstrated that paracrine signalling plays an important role in coordinating the behaviour of these cells. In future work the indirect effects of 5αTHB on cell behaviour should therefore be considered.

Angiogenesis is crucial for wound repair. Work described in this thesis using an aortic ring assay model provided further evidence that 5αTHB is a less potent inhibitor of angiogenesis than other topical glucocorticoids. It is therefore likely to be suitable for use as a safer topical anti-inflammatory treatment. This thesis expands on past work by showing that 5αTHB suppresses angiogenesis, at least in part, through direct effects on the vasculature. Furthermore, evidence was presented to suggest that 5αTHB may act *indirectly* through macrophages to promote, rather than inhibit, angiogenesis and tissue repair. The mechanisms of how angiogenesis is suppressed by 5αTHB were investigated by comparing steroid effects on gene expression in the mouse aorta. Glucocorticoids are reported to suppress angiogenesis mainly through effects on inflammatory signalling and on the ECM in the vessel basement membrane (Morgan, Keen et al. 2018). However unlike dexamethasone and hydrocortisone, 5αTHB had no effect on gene transcript abundance relating to components of the basement membrane, and also had no effect on transcript abundance of the inflammatory signalling gene *Cxcl5*, which was one of the most strongly down-regulated genes in a previous microarray investigating the effects of hydrocortisone in the aortic ring assay (Morgan, Keen et al. 2018).. Instead, 5αTHB tended to increase transcript levels of the monocyte chemoattractant gene *Mcp1,* and decreased transcript levels of the endothelial adhesion protein *Pecam1*. The gene expression analysis presented in this thesis, therefore, strongly suggested that 5αTHB was using different

mechanisms than dexamethasone and hydrocortisone to suppress angiogenesis in the mouse aorta.

Pecam1, which was selectively downregulated by 5αTHB in this work, encodes a protein which is expressed on the surface of all vascular cells, including platelets, endothelial cells, monocytes, neutrophils, and some T cells (Ilan and Madri 2003, Solowiej, Biswas et al. 2003, Woodfin, Voisin et al. 2007, Lertkiatmongkol, Liao et al. 2016). Pecam1 protein is highly enriched and one of the most abundant components at endothelial cell-cell junctions (Lertkiatmongkol, Liao et al. 2016), where it participates in cell-cell adhesion and the maintenance of junction integrity and permeability (Ilan and Madri 2003, Solowiej, Biswas et al. 2003). It is not clear from this current work which cell type was mainly responsible for the downregulation of *Pecam1,* and future work may investigate whether 5αTHB is able to decrease *Pecam1* expression specifically in endothelial cells. If so, then 5αTHB may be acting to suppress angiogenesis by interfering with the formation of new cell-cell contacts between endothelial cells. Another explanation could be that 5αTHB is inducing endothelial cells to undergo endothelial-to-mesenchymal transition (EndMT) since this is associated with a loss of Pecam1 as well as decreased angiogenesis (Miscianinov, Martello et al. 2018). EndMT causes endothelial cells to acquire a mesenchymal-like phenotype and undergo cytoskeletal rearrangement to develop a more stretched, fibroblast-like morphology (Miscianinov, Martello et al. 2018). Future work could address whether 5αTHB is able to induce EndMT in endothelial cells, both through direct and indirect effects. This could be achieved by observing the endothelial cells to assess whether they are developing a fibroblast-like morphology, after treatment with 5αTHB, as well as after culture with media taken from 5αTHB- treated

inflammatory cells. Endothelial cell gene expression could also be assessed: endothelial cells undergoing EndMT could be expected to have decreased expression of vascular endothelial cadherin (*VE-Cadherin*) and *Pecam1*, and increased expression of α-smooth muscle actin (*αSMA*), vimentin (*Vim*), *N-cadherin*, and ECM proteins such as collagen type 1 and 3 (Miscianinov, Martello et al. 2018).

Angiogenesis is just one stage during wound repair. In future work the ultimate effect of 5αTHB on wound repair should be compared *in vivo* with the effects of hydrocortisone (topical glucocorticoid) and dexamethasone (GR agonist). A mouse model of skin wound healing is available in which wound vascularisation and rate of closure can be reproducibly measured (Miscianinov, Martello et al. 2018). This model is also reported to be excellent for studying the impact of EndMT on vessel growth during wound healing, so would also help to gain insight into whether 5αTHB is inducing this process (Miscianinov, Martello et al. 2018). If 5αTHB is found to be less detrimental than glucocorticoids to the wound repair process, then the mechanisms underpinning why can then be investigated further.

6.2. Does 5αTHB work through GR?

Whereas 5αTHB was originally assumed to be an inert metabolite of corticosterone, it was later discovered to possess biological effects (McInnes, Kenyon et al. 2004). Various early model systems suggested, as would naturally be assumed, that its effects were mediated through GR (McInnes, Kenyon et al. 2004). However more recent experimental results have been contradictory. In the most recent work *in vivo*, RU486 attenuated the corticosterone-mediated suppression of inflammatory swelling in a mouse ear model of dermatitis, but did not block the effect of 5αTHB

(Gastaldello, Livingstone et al. 2017). This thesis presents new evidence to support the more recent work that suggests 5αTHB does not act through GR. In this work 5αTHB only minimally bound the isolated human GR, did not stimulate GR translocation into the nucleus, and did not cause changes in GR interaction with co-regulator peptides.

From the work described in chapter 5, 5αTHB predominantly regulated a different set of genes than dexamethasone in human macrophages. This provided evidence that 5αTHB has a distinct profile of biological action compared with conventional glucocorticoids, supporting the concept that it may not work through GR. There is also evidence from the aortic ring assay model of angiogenesis to suggest that GR was not involved for the effects of 5αTHB. The decrease in transcript abundance of *Pecam1* by 5αTHB in aortic rings was not antagonised by RU486, and although 5αTHB increased expression of *Per1* this was to a lesser extent than dexamethasone and hydrocortisone and was not prevented by RU486. Studies of suppression of vessel growth suggested that RU486 also did not antagonise the dose-dependent effect of 5αTHB whereas it suppressed the effect of dexamethasone, although caution should be taken when interpreting this data due to a lack of power in the experiments and the fact that RU486 alone suppressed vessel growth. Further work is needed to gain a definitive conclusion of whether GR is required for the effects of 5αTHB in the aortic ring assay model, and this should be addressed in future work. This could not be achieved using GR knockout mice since they die after birth due to respiratory failure (Cole, Blendy et al. 1995) however mice heterozygous for GR could be used in which GR is expressed to a lesser extent than wild type animals. A conditional knockout mouse model could also be generated in which GR is specifically disrupted in endothelial cells. In previous work by Logie *et al.,* dexamethasone inhibited tube-like

structure formation by cultured endothelial cells and this was blocked by RU486, demonstrating that glucocorticoid-induced suppression of angiogenesis is at least in part mediated through effects on GR in endothelial cells (Logie, Ali et al. 2010). Another approach could be to knockdown GR in the aortic ring assay, which can be achieved by transfecting the rings with siRNA (Baker, Robinson et al. 2012).

6.3. How does 5αTHB work?

A microarray of steroid effects in human peripheral blood-derived macrophages in chapter 5 suggested that 5αTHB mainly acts through different mechanisms from the selective GR ligand dexamethasone, but did cause differential expression of *Per1, Fkbp51, and Gilz,* which are regulated through GRE. Similarly, in chapter 3, 5αTHB increased transcripts of *Per1* in the mouse aorta, which was not antagonised by RU486. Since MR is also able to bind GRE, and since endogenous glucocorticoids are also able to bind MR, this seems the next most logical receptor to investigate for mediation of 5αTHB effects. This could be achieved in future work by assessing antagonism with the MR antagonist spironolactone. Alternatively, model systems could be used to investigate the effects of 5αTHB on MR translocation, such as the nuclear/cytoplasmic separation model. Initial results of experiments addressing the influence of 5αTHB on recruitment of co-regulator peptides at MR, are promising. However, MR is known to promote inflammation in macrophages (Bene, Alcaide et al. 2014). Therefore if 5αTHB is discovered to work through MR, further investigations of the downstream mechanisms will be required. Interestingly, differential regulation of *Per1* and *Fkbp51* has also been linked to MR-GR heterodimers, so mediation of the effect of 5αTHB through these heterodimers may

also be an avenue to explore in the future (Petrovich, Asher et al. 2014, Mifsud and Reul 2016).

A functional analysis of the genes which were differentially expressed by 5αTHB in the microarray, found enrichment of terms associated with a specific macrophage phenotype known as M2c. Two alternative hypotheses that may arise from this work are that 5αTHB may (a) specifically target this M2c subtype, or (b) induce a phenotypic change in macrophages into this M2c subtype. Future work should address these hypotheses and this could be achieved by staining 5αTHB-treated macrophages for Arg-1 in mouse, or MMR/CD206, TLR-1, or TLR-8 in human. Alternatively gene expression of IL10, TGFβ, CCL16, CCL18, and CXC13 could be tested which can be expected to increase in macrophages of the M2c phenotype (Shapouri-Moghaddam, Mohammadian et al. 2018). It must be noted that the macrophages in chapter 5 had not been stimulated, and the microarray should be performed in LPS-stimulated cells in future work for comparison. Furthermore, the macrophage subtypes (M1, M2, M2c) have been defined *in vitro* using well-defined stimuli. Realistically this is an oversimplified concept of the *in vivo* situation where macrophages are likely to be exposed to a combination of stimuli (Shapouri-Moghaddam, Mohammadian et al. 2018) and hence switch between one phenotype and another, as well as possessing intermediate phenotypes (Chazaud 2014, Shapouri-Moghaddam, Mohammadian et al. 2018). The effect of steroids on M2c polarisation could therefore also be tested by immunostaining for M2c macrophages on tissue taken from *in vivo* models.

One of the enriched pathways related to the M2c macrophage phenotype in 5αTHB regulated genes was the TGFβ pathway. Endothelial to mesenchymal

transition (EndMT) of endothelial cells is known to be dependent on the TGFβ pathway (Miscianinov, Martello et al. 2018). Since chapter 3 suggested that 5αTHB may be causing EndMT of endothelial cells in aortic rings, it may be possible that 5αTHB causes M2c polarisation of inflammatory cells, which then indirectly cause EndMT of endothelial cells through release of TGFβ. 5αTHB effects on gene expression relating to TGFβ signalling in endothelial cells and inflammatory cells could therefore be investigated in future work. TGFβ signals by binding to a heteromeric receptor complex formed by the TGFβ type I receptor (Tgfbr1) and the TGFβ type 2 receptor (Tgfbr2). This leads to activation of Smad2 and Smad3 proteins, which translocate to the nucleus and mediate TGFβ signalling by regulating transcription of target genes (Gratchev 2017, Miscianinov, Martello et al. 2018). In the microarray performed in hMDMs (described in chapter 5) 5αTHB caused upregulation of *Smad7* and *Tgif1* genes which are both inhibitors of TGFβ signalling (Gratchev 2017)(https://www.ncbi.nlm.nih.gov/gene/7050). Therefore, genes relating to TGFβ signalling which could be measured include *Tgif1, Tgfbr1, Tgfbr2, Smad2, Smad3,* and *Smad 7.*

6.4. Summary

In summary this thesis has shown that 5αTHB is less angiostatic than the topical glucocorticoid hydrocortisone and therefore is a promising candidate for a safer topical anti-inflammatory therapy. The thesis gives further evidence that 5αTHB acts through distinct mechanisms to glucocorticoids, likely independent of GR, and provides hypotheses for further exploration. Identification of the mechanisms used by 5αTHB

in future work may lead to the development of a whole new prototype of anti-inflammatory drug which could also be used systemically. This would allow safer treatment of patients requiring long term anti-inflammatory therapy, preventing much suffering and cost associated with current side effects.

References

Adams, M., O. C. Meijer, J. Wang, A. Bhargava and D. Pearce (2003). "Homodimerization of the glucocorticoid receptor is not essential for response element binding: activation of the phenylethanolamine N-methyltransferase gene by dimerization-defective mutants." Mol Endocrinol **17**(12): 2583-2592.
Alby, L. and R. Auerbach (1984). "Differential adhesion of tumor cells to capillary endothelial cells in vitro." Proc Natl Acad Sci U S A **81**(18): 5739-5743.
Amaya-Amaya, J., L. Montoya-Sanchez and A. Rojas-Villarraga (2014). "Cardiovascular involvement in autoimmune diseases." Biomed Res Int **2014**: 367359.
Ambellan, E., M. Swanson and A. Davidson (1981). "Glucocorticoid binding to rat liver microsomal fractions in vitro." J Steroid Biochem **14**(5): 421-428.
Baker, M., S. D. Robinson, T. Lechertier, P. R. Barber, B. Tavora, G. D'Amico, D. T. Jones, B. Vojnovic and K. Hodivala-Dilke (2012). "Use of the mouse aortic ring assay to study angiogenesis." Nat Protoc **7**(1): 89-104.
Barrientos, S., O. Stojadinovic, M. S. Golinko, H. Brem and M. Tomic-Canic (2008). "Growth factors and cytokines in wound healing." Wound Repair Regen **16**(5): 585-601.
Bayo, P., A. Sanchis, A. Bravo, J. L. Cascallana, K. Buder, J. Tuckermann, G. Schutz and P. Perez (2008). "Glucocorticoid receptor is required for skin barrier competence." Endocrinology **149**(3): 1377-1388.
Bekhbat, M., S. A. Rowson and G. N. Neigh (2017). "Checks and balances: The glucocorticoid receptor and NFkB in good times and bad." Front Neuroendocrinol **46**: 15-31.
Bene, N. C., P. Alcaide, H. H. Wortis and I. Z. Jaffe (2014). "Mineralocorticoid receptors in immune cells: emerging role in cardiovascular disease." Steroids **91**: 38-45.
Best, R., S. M. Nelson and B. R. Walker (1997). "Dexamethasone and 11-dehydrodexamethasone as tools to investigate the isozymes of 11 beta-hydroxysteroid dehydrogenase in vitro and in vivo." J Endocrinol **153**(1): 41-48.
Bledsoe, R. K., V. G. Montana, T. B. Stanley, C. J. Delves, C. J. Apolito, D. D. McKee, T. G. Consler, D. J. Parks, E. L. Stewart, T. M. Willson, M. H. Lambert, J. T. Moore, K. H. Pearce and H. E. Xu (2002). "Crystal structure of the glucocorticoid receptor ligand binding domain reveals a novel mode of receptor dimerization and coactivator recognition." Cell **110**(1): 93-105.
Boukamp, P., R. T. Petrussevska, D. Breitkreutz, J. Hornung, A. Markham and N. E. Fusenig (1988). "Normal keratinization in a spontaneously immortalized aneuploid human keratinocyte cell line." J Cell Biol **106**(3): 761-771.
Brandt, K., J. Grunler, K. Brismar and J. Wang (2015). "Effects of IGFBP-1 and IGFBP-2 and their fragments on migration and IGF-induced proliferation of human dermal fibroblasts." Growth Horm IGF Res **25**(1): 34-40.
Briquez, P. S., J. A. Hubbell and M. M. Martino (2015). "Extracellular Matrix-Inspired Growth Factor Delivery Systems for Skin Wound Healing." Adv Wound Care (New Rochelle) **4**(8): 479-489.
Burry, R. W. (2011). "Controls for immunocytochemistry: an update." J Histochem Cytochem **59**(1): 6-12.
Buttgereit, F. and A. Scheffold (2002). "Rapid glucocorticoid effects on immune cells." Steroids **67**(6): 529-534.
Buttgereit, F., R. H. Straub, M. Wehling and G. R. Burmester (2004). "Glucocorticoids in the treatment of rheumatic diseases: an update on the mechanisms of action." Arthritis Rheum **50**(11): 3408-3417.
Cain, D. W. and J. A. Cidlowski (2015). "Specificity and sensitivity of glucocorticoid signaling in health and disease." Best Pract Res Clin Endocrinol Metab **29**(4): 545-556.
Cain, D. W. and J. A. Cidlowski (2017). "Immune regulation by glucocorticoids." Nat Rev Immunol **17**(4): 233-247.

Castinetti, F., T. Brue and B. Conte-Devolx (2012). "The use of the glucocorticoid receptor antagonist mifepristone in Cushing's syndrome." Curr Opin Endocrinol Diabetes Obes **19**(4): 295-299.
Chapman, K., M. Holmes and J. Seckl (2013). "11beta-hydroxysteroid dehydrogenases: intracellular gate-keepers of tissue glucocorticoid action." Physiol Rev **93**(3): 1139-1206.
Charvat, S., M. C. Chignol, C. Souchier, C. Le Griel, D. Schmitt and M. Serres (1998). "Cell migration and MMP-9 secretion are increased by epidermal growth factor in HaCaT-ras transfected cells." Exp Dermatol **7**(4): 184-190.
Chazaud, B. (2014). "Macrophages: supportive cells for tissue repair and regeneration." Immunobiology **219**(3): 172-178.
Chen, Q., M. Jin, F. Yang, J. Zhu, Q. Xiao and L. Zhang (2013). "Matrix metalloproteinases: inflammatory regulators of cell behaviors in vascular formation and remodeling." Mediators Inflamm **2013**: 928315.
Chinenov, Y., M. Coppo, R. Gupte, M. A. Sacta and I. Rogatsky (2014). "Glucocorticoid receptor coordinates transcription factor-dominated regulatory network in macrophages." BMC Genomics **15**: 656.
Chinenov, Y., R. Gupte and I. Rogatsky (2013). "Nuclear receptors in inflammation control: repression by GR and beyond." Mol Cell Endocrinol **380**(1-2): 55-64.
Clayton, S. A., S. W. Jones, M. Kurowska-Stolarska and A. R. Clark (2018). "The role of microRNAs in glucocorticoid action." J Biol Chem **293**(6): 1865-1874.
Cohen, D. M. and D. J. Steger (2017). "Nuclear Receptor Function through Genomics: Lessons from the Glucocorticoid Receptor." Trends Endocrinol Metab **28**(7): 531-540.
Cole, T. J., J. A. Blendy, A. P. Monaghan, K. Krieglstein, W. Schmid, A. Aguzzi, G. Fantuzzi, E. Hummler, K. Unsicker and G. Schutz (1995). "Targeted disruption of the glucocorticoid receptor gene blocks adrenergic chromaffin cell development and severely retards lung maturation." Genes Dev **9**(13): 1608-1621.
De Bosscher, K. (2010). "Selective Glucocorticoid Receptor modulators." J Steroid Biochem Mol Biol **120**(2-3): 96-104.
De Bosscher, K., I. M. Beck and G. Haegeman (2010). "Classic glucocorticoids versus non-steroidal glucocorticoid receptor modulators: survival of the fittest regulator of the immune system?" Brain Behav Immun **24**(7): 1035-1042.
De Bosscher, K., I. M. Beck, D. Ratman, W. V. Berghe and C. Libert (2016). "Activation of the Glucocorticoid Receptor in Acute Inflammation: the SEDIGRAM Concept." Trends Pharmacol Sci **37**(1): 4-16.
De Bosscher, K., W. Vanden Berghe, I. M. Beck, W. Van Molle, N. Hennuyer, J. Hapgood, C. Libert, B. Staels, A. Louw and G. Haegeman (2005). "A fully dissociated compound of plant origin for inflammatory gene repression." Proc Natl Acad Sci U S A **102**(44): 15827-15832.
Desmet, S. J. and K. De Bosscher (2017). "Glucocorticoid receptors: finding the middle ground." J Clin Invest **127**(4): 1136-1145.
Ding, J. and E. E. Tredget (2015). "The Role of Chemokines in Fibrotic Wound Healing." Adv Wound Care (New Rochelle) **4**(11): 673-686.
Draper, N. and P. M. Stewart (2005). "11beta-hydroxysteroid dehydrogenase and the pre-receptor regulation of corticosteroid hormone action." J Endocrinol **186**(2): 251-271.
Drebert, Z., M. Bracke and I. M. Beck (2015). "Glucocorticoids and the non-steroidal selective glucocorticoid receptor modulator, compound A, differentially affect colon cancer-derived myofibroblasts." J Steroid Biochem Mol Biol **149**: 92-105.
Drebert, Z., M. MacAskill, D. Doughty-Shenton, K. De Bosscher, M. Bracke, P. W. F. Hadoke and I. M. Beck (2017). "Colon cancer-derived myofibroblasts increase endothelial cell migration by glucocorticoid-sensitive secretion of a pro-migratory factor." Vascul Pharmacol **89**: 19-30.

Duan, W. R., S. Patyna, M. A. Kuhlmann, S. Li and E. A. Blomme (2006). "A multitargeted receptor tyrosine kinase inhibitor, SU6668, does not affect the healing of cutaneous full-thickness incisional wounds in SKH-1 mice." J Invest Surg **19**(4): 245-254.
Ehrchen, J., L. Steinmuller, K. Barczyk, K. Tenbrock, W. Nacken, M. Eisenacher, U. Nordhues, C. Sorg, C. Sunderkotter and J. Roth (2007). "Glucocorticoids induce differentiation of a specifically activated, anti-inflammatory subtype of human monocytes." Blood **109**(3): 1265-1274.
Eming, S. A., B. Brachvogel, T. Odorisio and M. Koch (2007). "Regulation of angiogenesis: wound healing as a model." Prog Histochem Cytochem **42**(3): 115-170.
Falkenstein, E., H. C. Tillmann, M. Christ, M. Feuring and M. Wehling (2000). "Multiple actions of steroid hormones--a focus on rapid, nongenomic effects." Pharmacol Rev **52**(4): 513-556.
Fernandes-Rosa, F. L., E. L. Hubert, J. Fagart, N. Tchitchek, D. Gomes, E. Jouanno, A. Benecke, M. E. Rafestin-Oblin, X. Jeunemaitre, S. R. Antonini and M. C. Zennaro (2011). "Mineralocorticoid receptor mutations differentially affect individual gene expression profiles in pseudohypoaldosteronism type 1." J Clin Endocrinol Metab **96**(3): E519-527.
Fleseriu, M., B. M. Biller, J. W. Findling, M. E. Molitch, D. E. Schteingart and C. Gross (2012). "Mifepristone, a glucocorticoid receptor antagonist, produces clinical and metabolic benefits in patients with Cushing's syndrome." J Clin Endocrinol Metab **97**(6): 2039-2049.
Fletcher, E. K., J. Morgan, D. R. Kennaway, L. A. Bienvenu, A. J. Rickard, L. M. D. Delbridge, P. J. Fuller, C. D. Clyne and M. J. Young (2017). "Deoxycorticosterone/Salt-Mediated Cardiac Inflammation and Fibrosis Are Dependent on Functional CLOCK Signaling in Male Mice." Endocrinology **158**(9): 2906-2917.
Folkman, J. and D. E. Ingber (1987). "Angiostatic steroids. Method of discovery and mechanism of action." Ann Surg **206**(3): 374-383.
Folkman, J., R. Langer, R. J. Linhardt, C. Haudenschild and S. Taylor (1983). "Angiogenesis inhibition and tumor regression caused by heparin or a heparin fragment in the presence of cortisone." Science **221**(4612): 719-725.
Fyfe, A. I., A. Rosenthal and A. I. Gotlieb (1995). "Immunosuppressive agents and endothelial repair. Prednisolone delays migration and cytoskeletal rearrangement in wounded porcine aortic monolayers." Arterioscler Thromb Vasc Biol **15**(8): 1166-1171.
Gastaldello, A., D. E. Livingstone, A. J. Abernethie, N. Tsang, B. R. Walker, P. W. Hadoke and R. Andrew (2017). "Safer topical treatment for inflammation using 5alpha-tetrahydrocorticosterone in mouse models." Biochem Pharmacol **129**: 73-84.
Gautier, L., L. Cope, B. M. Bolstad and R. A. Irizarry (2004). "affy--analysis of Affymetrix GeneChip data at the probe level." Bioinformatics **20**(3): 307-315.
Generali, E., M. Folci, C. Selmi and P. Riboldi (2017). "Immune-Mediated Heart Disease." Adv Exp Med Biol **1003**: 145-171.
Giusti, I., A. Rughetti, S. D'Ascenzo, G. Di Stefano, M. R. Nanni, D. Millimaggi, L. Dell'orso and V. Dolo (2013). "The effects of platelet gel-released supernatant on human fibroblasts." Wound Repair Regen **21**(2): 300-308.
Gratchev, A. (2017). "TGF-beta signalling in tumour associated macrophages." Immunobiology **222**(1): 75-81.
Grose, R., S. Werner, D. Kessler, J. Tuckermann, K. Huggel, S. Durka, H. M. Reichardt and S. Werner (2002). "A role for endogenous glucocorticoids in wound repair." EMBO Rep **3**(6): 575-582.
Guo, S. and L. A. Dipietro (2010). "Factors affecting wound healing." J Dent Res **89**(3): 219-229.
Gurtner, G. C., S. Werner, Y. Barrandon and M. T. Longaker (2008). "Wound repair and regeneration." Nature **453**(7193): 314-321.

Haller, J., E. Mikics and G. B. Makara (2008). "The effects of non-genomic glucocorticoid mechanisms on bodily functions and the central neural system. A critical evaluation of findings." Front Neuroendocrinol **29**(2): 273-291.
Hench, P. (1950). "Effects of cortisone in the rheumatic diseases." Lancet **2**(6634): 483-484.
Holmes, C. J., J. K. Plichta, R. L. Gamelli and K. A. Radek (2015). "Dynamic Role of Host Stress Responses in Modulating the Cutaneous Microbiome: Implications for Wound Healing and Infection." Adv Wound Care (New Rochelle) **4**(1): 24-37.
Hong, G., W. Zhang, H. Li, X. Shen and Z. Guo (2014). "Separate enrichment analysis of pathways for up- and downregulated genes." J R Soc Interface **11**(92): 20130950.
Hopkinson, S. B., K. J. Hamill, Y. Wu, J. L. Eisenberg, S. Hiroyasu and J. C. Jones (2014). "Focal Contact and Hemidesmosomal Proteins in Keratinocyte Migration and Wound Repair." Adv Wound Care (New Rochelle) **3**(3): 247-263.
Hori, Y., D. E. Hu, K. Yasui, R. L. Smither, G. A. Gresham and T. P. Fan (1996). "Differential effects of angiostatic steroids and dexamethasone on angiogenesis and cytokine levels in rat sponge implants." Br J Pharmacol **118**(7): 1584-1591.
Huang da, W., B. T. Sherman and R. A. Lempicki (2009). "Bioinformatics enrichment tools: paths toward the comprehensive functional analysis of large gene lists." Nucleic Acids Res **37**(1): 1-13.
Huang, H., Z. Liu and H. Liu (2001). "[Effect of mycophenolic acid and dexamethasone on the angiogenic activity of human umbilical vein endothelial cells]." Zhonghua Yi Xue Za Zhi **81**(13): 801-804.
Hudson, W. H., C. Youn and E. A. Ortlund (2014). "Crystal structure of the mineralocorticoid receptor DNA binding domain in complex with DNA." PLoS One **9**(9): e107000.
Hwang, C. and E. I. Heath (2010). "Angiogenesis inhibitors in the treatment of prostate cancer." J Hematol Oncol **3**: 26.
Ilan, N. and J. A. Madri (2003). "PECAM-1: old friend, new partners." Curr Opin Cell Biol **15**(5): 515-524.
Jaffe, E. A., R. L. Nachman, C. G. Becker and C. R. Minick (1973). "Culture of human endothelial cells derived from umbilical veins. Identification by morphologic and immunologic criteria." J Clin Invest **52**(11): 2745-2756.
Jiang, X. P., D. X. Zhang, M. Teng, Q. Zhang, J. P. Zhang and Y. S. Huang (2013). "Downregulation of CD9 in keratinocyte contributes to cell migration via upregulation of matrix metalloproteinase-9." PLoS One **8**(10): e77806.
Johnson, K. E. and T. A. Wilgus (2014). "Vascular Endothelial Growth Factor and Angiogenesis in the Regulation of Cutaneous Wound Repair." Adv Wound Care (New Rochelle) **3**(10): 647-661.
Jozic, I., S. Vukelic, O. Stojadinovic, L. Liang, H. A. Ramirez, I. Pastar and M. Tomic Canic (2017). "Stress Signals, Mediated by Membranous Glucocorticoid Receptor, Activate PLC/PKC/GSK-3beta/beta-catenin Pathway to Inhibit Wound Closure." J Invest Dermatol **137**(5): 1144-1154.
Jubb, A. W., S. Boyle, D. A. Hume and W. A. Bickmore (2017). "Glucocorticoid Receptor Binding Induces Rapid and Prolonged Large-Scale Chromatin Decompaction at Multiple Target Loci." Cell Rep **21**(11): 3022-3031.
Jubb, A. W., R. S. Young, D. A. Hume and W. A. Bickmore (2016). "Enhancer Turnover Is Associated with a Divergent Transcriptional Response to Glucocorticoid in Mouse and Human Macrophages." J Immunol **196**(2): 813-822.
Kadmiel, M. and J. A. Cidlowski (2013). "Glucocorticoid receptor signaling in health and disease." Trends Pharmacol Sci **34**(9): 518-530.
Kauffmann, A., R. Gentleman and W. Huber (2009). "arrayQualityMetrics--a bioconductor package for quality assessment of microarray data." Bioinformatics **25**(3): 415-416.

Keenan, C. R., M. J. Lew and A. G. Stewart (2016). "Biased signalling from the glucocorticoid receptor: Renewed opportunity for tailoring glucocorticoid activity." Biochem Pharmacol **112**: 6-12.
Kino, T. (2000). Glucocorticoid Receptor. Endotext. L. J. De Groot, G. Chrousos, K. Dungan et al. South Dartmouth MA, MDText.com, Inc.
Korn, C. and H. G. Augustin (2015). "Mechanisms of Vessel Pruning and Regression." Dev Cell **34**(1): 5-17.
Lan, N. C., B. Graham, F. C. Bartter and J. D. Baxter (1982). "Binding of steroids to mineralocorticoid receptors: implications for in vivo occupancy by glucocorticoids." J Clin Endocrinol Metab **54**(2): 332-342.
Lee, B., C. Vouthounis, O. Stojadinovic, H. Brem, M. Im and M. Tomic-Canic (2005). "From an enhanceosome to a repressosome: molecular antagonism between glucocorticoids and EGF leads to inhibition of wound healing." J Mol Biol **345**(5): 1083-1097.
Lee, T. S., J. J. Lin, Y. N. Huo and W. S. Lee (2015). "Progesterone Inhibits Endothelial Cell Migration Through Suppression of the Rho Activity Mediated by cSrc Activation." J Cell Biochem **116**(7): 1411-1418.
Lertkiatmongkol, P., D. Liao, H. Mei, Y. Hu and P. J. Newman (2016). "Endothelial functions of platelet/endothelial cell adhesion molecule-1 (CD31)." Curr Opin Hematol **23**(3): 253-259.
Lewis-Tuffin, L. J., C. M. Jewell, R. J. Bienstock, J. B. Collins and J. A. Cidlowski (2007). "Human glucocorticoid receptor beta binds RU-486 and is transcriptionally active." Mol Cell Biol **27**(6): 2266-2282.
Lieber, M., B. Smith, A. Szakal, W. Nelson-Rees and G. Todaro (1976). "A continuous tumor-cell line from a human lung carcinoma with properties of type II alveolar epithelial cells." Int J Cancer **17**(1): 62-70.
Ligr, M., Y. Li, S. K. Logan, S. Taneja, J. Melamed, H. Lepor, M. J. Garabedian and P. Lee (2012). "Mifepristone inhibits GRbeta coupled prostate cancer cell proliferation." J Urol **188**(3): 981-988.
Liu, W., J. Wang, N. K. Sauter and D. Pearce (1995). "Steroid receptor heterodimerization demonstrated in vitro and in vivo." Proc Natl Acad Sci U S A **92**(26): 12480-12484.
Livingstone, D. E., P. Barat, E. M. Di Rollo, G. A. Rees, B. A. Weldin, E. A. Rog-Zielinska, D. P. MacFarlane, B. R. Walker and R. Andrew (2015). "5alpha-Reductase type 1 deficiency or inhibition predisposes to insulin resistance, hepatic steatosis, and liver fibrosis in rodents." Diabetes **64**(2): 447-458.
Livingstone, D. E., E. M. Di Rollo, T. C. Mak, K. Sooy, B. R. Walker and R. Andrew (2017). "Metabolic dysfunction in female mice with disruption of 5alpha-reductase 1." J Endocrinol **232**(1): 29-36.
Livingstone, D. E., E. M. Di Rollo, C. Yang, L. E. Codrington, J. A. Mathews, M. Kara, K. A. Hughes, C. J. Kenyon, B. R. Walker and R. Andrew (2014). "Relative adrenal insufficiency in mice deficient in 5alpha-reductase 1." J Endocrinol **222**(2): 257-266.
Logie, J. J., S. Ali, K. M. Marshall, M. M. Heck, B. R. Walker and P. W. Hadoke (2010). "Glucocorticoid-mediated inhibition of angiogenic changes in human endothelial cells is not caused by reductions in cell proliferation or migration." PLoS One **5**(12): e14476.
Losel, R. and M. Wehling (2003). "Nongenomic actions of steroid hormones." Nat Rev Mol Cell Biol **4**(1): 46-56.
Madrigal, J. L., B. Garcia-Bueno, A. E. Hinojosa, P. Polak, D. L. Feinstein and J. C. Leza (2010). "Regulation of MCP-1 production in brain by stress and noradrenaline-modulating drugs." J Neurochem **113**(2): 543-551.
Mahmoudi, M., S. Aslani, R. Fadaei and A. R. Jamshidi (2017). "New insights to the mechanisms underlying atherosclerosis in rheumatoid arthritis." Int J Rheum Dis **20**(3): 287-297.

Markiewicz, M., K. Panneerselvam and N. Marks (2016). "Role of Klotho in migration and proliferation of human dermal microvascular endothelial cells." Microvasc Res **107**: 76-82.
Martin, P. and R. Nunan (2015). "Cellular and molecular mechanisms of repair in acute and chronic wound healing." Br J Dermatol **173**(2): 370-378.
Martinez-Mora, C., A. Mrowiec, E. M. Garcia-Vizcaino, A. Alcaraz, J. L. Cenis and F. J. Nicolas (2012). "Fibroin and sericin from Bombyx mori silk stimulate cell migration through upregulation and phosphorylation of c-Jun." PLoS One **7**(7): e42271.
Martinez, C. E., P. C. Smith and V. A. Palma Alvarado (2015). "The influence of platelet-derived products on angiogenesis and tissue repair: a concise update." Front Physiol **6**: 290.
McInnes, K. J., C. J. Kenyon, K. E. Chapman, D. E. Livingstone, L. J. Macdonald, B. R. Walker and R. Andrew (2004). "5alpha-reduced glucocorticoids, novel endogenous activators of the glucocorticoid receptor." J Biol Chem **279**(22): 22908-22912.
McMaster, A. and D. W. Ray (2007). "Modelling the glucocorticoid receptor and producing therapeutic agents with anti-inflammatory effects but reduced side-effects." Exp Physiol **92**(2): 299-309.
McSweeney, S. J., P. W. Hadoke, A. M. Kozak, G. R. Small, H. Khaled, B. R. Walker and G. A. Gray (2010). "Improved heart function follows enhanced inflammatory cell recruitment and angiogenesis in 11betaHSD1-deficient mice post-MI." Cardiovasc Res **88**(1): 159-167.
Mifsud, K. R. and J. M. Reul (2016). "Acute stress enhances heterodimerization and binding of corticosteroid receptors at glucocorticoid target genes in the hippocampus." Proc Natl Acad Sci U S A **113**(40): 11336-11341.
Mills, C. D. (2012). "M1 and M2 Macrophages: Oracles of Health and Disease." Crit Rev Immunol **32**(6): 463-488.
Min, J., L. Perera, J. M. Krahn, C. M. Jewell, A. F. Moon, J. A. Cidlowski and L. C. Pedersen (2018). "Probing Dominant Negative Behavior of Glucocorticoid Receptor beta through a Hybrid Structural and Biochemical Approach." Mol Cell Biol.
Miscianinov, V., A. Martello, L. Rose, E. Parish, B. Cathcart, T. Mitic, G. A. Gray, M. Meloni, A. Al Haj Zen and A. Caporali (2018). "MicroRNA-148b Targets the TGF-beta Pathway to Regulate Angiogenesis and Endothelial-to-Mesenchymal Transition during Skin Wound Healing." Mol Ther **26**(8): 1996-2007.
Mitre-Aguilar, I. B., A. J. Cabrera-Quintero and A. Zentella-Dehesa (2015). "Genomic and non-genomic effects of glucocorticoids: implications for breast cancer." Int J Clin Exp Pathol **8**(1): 1-10.
Morgan, R., J. Keen, D. Halligan, A. O'Callaghan, R. Andrew, D. Livingstone, A. Abernethie, G. Maltese, B. Walker and P. Hadoke (2018). "Species-specific regulation of angiogenesis by glucocorticoids reveals contrasting effects on inflammatory and angiogenic pathways." PLoS One **13**(2): e0192746.
Newton, R. (2013). "Anti-inflammatory glucocorticoids: Changing concepts." Eur J Pharmacol.
Nguyen, D. and S. Mizne (2017). "Effects of Ketoconazole on the Pharmacokinetics of Mifepristone, a Competitive Glucocorticoid Receptor Antagonist, in Healthy Men." Adv Ther **34**(10): 2371-2385.
Nixon, M., R. Andrew and K. E. Chapman (2013). "It takes two to tango: dimerisation of glucocorticoid receptor and its anti-inflammatory functions." Steroids **78**(1): 59-68.
Nixon, M., S. D. Mackenzie, A. I. Taylor, N. Z. Homer, D. E. Livingstone, R. Mouras, R. A. Morgan, D. J. Mole, R. H. Stimson, R. M. Reynolds, A. P. Elfick, R. Andrew and B. R. Walker (2016). "ABCC1 confers tissue-specific sensitivity to cortisol versus corticosterone: A rationale for safer glucocorticoid replacement therapy." Sci Transl Med **8**(352): 352ra109.
Nixon, M., R. Upreti and R. Andrew (2012). "5alpha-Reduced glucocorticoids: a story of natural selection." J Endocrinol **212**(2): 111-127.

Nolan, D. J., M. Ginsberg, E. Israely, B. Palikuqi, M. G. Poulos, D. James, B. S. Ding, W. Schachterle, Y. Liu, Z. Rosenwaks, J. M. Butler, J. Xiang, A. Rafii, K. Shido, S. Y. Rabbany, O. Elemento and S. Rafii (2013). "Molecular signatures of tissue-specific microvascular endothelial cell heterogeneity in organ maintenance and regeneration." Dev Cell **26**(2): 204-219.
Oberleithner, H., S. W. Schneider, L. Albermann, U. Hillebrand, T. Ludwig, C. Riethmuller, V. Shahin, C. Schafer and H. Schillers (2003). "Endothelial cell swelling by aldosterone." J Membr Biol **196**(3): 163-172.
Park, S., C. M. Sorenson and N. Sheibani (2015). "PECAM-1 isoforms, eNOS and endoglin axis in regulation of angiogenesis." Clin Sci (Lond) **129**(3): 217-234.
Peeters, B. W., G. S. Ruigt, M. Craighead and P. Kitchener (2008). "Differential effects of the new glucocorticoid receptor antagonist ORG 34517 and RU486 (mifepristone) on glucocorticoid receptor nuclear translocation in the AtT20 cell line." Ann N Y Acad Sci **1148**: 536-541.
Petrovich, E., C. Asher and H. Garty (2014). "Induction of FKBP51 by aldosterone in intestinal epithelium." J Steroid Biochem Mol Biol **139**: 78-87.
Portou, M. J., D. Baker, D. Abraham and J. Tsui (2015). "The innate immune system, toll-like receptors and dermal wound healing: A review." Vascul Pharmacol **71**: 31-36.
Powell, C. E., C. S. Watson and B. Gametchu (1999). "Immunoaffinity isolation of native membrane glucocorticoid receptor from S-49++ lymphoma cells: biochemical characterization and interaction with Hsp 70 and Hsp 90." Endocrine **10**(3): 271-280.
Pross, C., M. M. Farooq, J. S. Lane, N. Angle, C. K. Tomono, A. E. Xavier, J. A. Freischlag, A. E. Collins, R. E. Law and H. A. Gelabert (2002). "Rat and human aortic smooth muscle cells display differing migration and matrix metalloproteinase activities in response to dexamethasone." J Vasc Surg **35**(6): 1253-1259.
Reeves, E. K., S. Rayavarapu, J. M. Damsker and K. Nagaraju (2012). "Glucocorticoid analogues: potential therapeutic alternatives for treating inflammatory muscle diseases." Endocr Metab Immune Disord Drug Targets **12**(1): 95-103.
Reichardt, H. M., K. H. Kaestner, J. Tuckermann, O. Kretz, O. Wessely, R. Bock, P. Gass, W. Schmid, P. Herrlich, P. Angel and G. Schutz (1998). "DNA binding of the glucocorticoid receptor is not essential for survival." Cell **93**(4): 531-541.
Reuter, K. C., C. R. Grunwitz, B. M. Kaminski, D. Steinhilber, H. H. Radeke and J. Stein (2012). "Selective glucocorticoid receptor agonists for the treatment of inflammatory bowel disease: studies in mice with acute trinitrobenzene sulfonic acid colitis." J Pharmacol Exp Ther **341**(1): 68-80.
Reuter, K. C., S. M. Loitsch, A. U. Dignass, D. Steinhilber and J. Stein (2012). "Selective non-steroidal glucocorticoid receptor agonists attenuate inflammation but do not impair intestinal epithelial cell restitution in vitro." PLoS One **7**(1): e29756.
Rickard, A. J. and M. J. Young (2009). "Corticosteroid receptors, macrophages and cardiovascular disease." J Mol Endocrinol **42**(6): 449-459.
Rose, J. D. and F. L. Moore (1999). "A neurobehavioral model for rapid actions of corticosterone on sensorimotor integration." Steroids **64**(1-2): 92-99.
Rosen, J. and J. N. Miner (2005). "The search for safer glucocorticoid receptor ligands." Endocr Rev **26**(3): 452-464.
Rosique, R. G., M. J. Rosique and J. A. Farina Junior (2015). "Curbing Inflammation in Skin Wound Healing: A Review." Int J Inflam **2015**: 316235.
Roszak, A. W., Y. A. Lefebvre, G. M. Howell and P. W. Codding (1990). "Structural requirements for the binding of dexamethasone to nuclear envelopes and plasma membranes." J Steroid Biochem Mol Biol **37**(2): 201-214.

Russell, D. W. and J. D. Wilson (1994). "Steroid 5 alpha-reductase: two genes/two enzymes." Annu Rev Biochem **63**: 25-61.
Savory, J. G., G. G. Prefontaine, C. Lamprecht, M. Liao, R. F. Walther, Y. A. Lefebvre and R. J. Hache (2001). "Glucocorticoid receptor homodimers and glucocorticoid-mineralocorticoid receptor heterodimers form in the cytoplasm through alternative dimerization interfaces." Mol Cell Biol **21**(3): 781-793.
Schacke, H., W. D. Docke and K. Asadullah (2002). "Mechanisms involved in the side effects of glucocorticoids." Pharmacol Ther **96**(1): 23-43.
Schacke, H., H. Rehwinkel, K. Asadullah and A. C. Cato (2006). "Insight into the molecular mechanisms of glucocorticoid receptor action promotes identification of novel ligands with an improved therapeutic index." Exp Dermatol **15**(8): 565-573.
Schacke, H., A. Schottelius, W. D. Docke, P. Strehlke, S. Jaroch, N. Schmees, H. Rehwinkel, H. Hennekes and K. Asadullah (2004). "Dissociation of transactivation from transrepression by a selective glucocorticoid receptor agonist leads to separation of therapeutic effects from side effects." Proc Natl Acad Sci U S A **101**(1): 227-232.
Schacke, H., T. M. Zollner, W. D. Docke, H. Rehwinkel, S. Jaroch, W. Skuballa, R. Neuhaus, E. May, U. Zugel and K. Asadullah (2009). "Characterization of ZK 245186, a novel, selective glucocorticoid receptor agonist for the topical treatment of inflammatory skin diseases." Br J Pharmacol **158**(4): 1088-1103.
Scheschowitsch, K., J. A. Leite and J. Assreuy (2017). "New Insights in Glucocorticoid Receptor Signaling-More Than Just a Ligand-Binding Receptor." Front Endocrinol (Lausanne) **8**: 16.
Schmieder, A., J. Michel, K. Schonhaar, S. Goerdt and K. Schledzewski (2012). "Differentiation and gene expression profile of tumor-associated macrophages." Semin Cancer Biol **22**(4): 289-297.
Schoepe, S., H. Schacke, A. Bernd, N. Zoller and K. Asadullah (2010). "Identification of novel in vitro test systems for the determination of glucocorticoid receptor ligand-induced skin atrophy." Skin Pharmacol Physiol **23**(3): 139-151.
Schoepe, S., H. Schacke, E. May and K. Asadullah (2006). "Glucocorticoid therapy-induced skin atrophy." Exp Dermatol **15**(6): 406-420.
Sevilla, L. M. and P. Perez (2018). "Roles of the Glucocorticoid and Mineralocorticoid Receptors in Skin Pathophysiology." Int J Mol Sci **19**(7).
Shapouri-Moghaddam, A., S. Mohammadian, H. Vazini, M. Taghadosi, S. A. Esmaeili, F. Mardani, B. Seifi, A. Mohammadi, J. T. Afshari and A. Sahebkar (2018). "Macrophage plasticity, polarization, and function in health and disease." J Cell Physiol **233**(9): 6425-6440.
Shikatani, E. A., A. Trifonova, E. R. Mandel, S. T. Liu, E. Roudier, A. Krylova, A. Szigiato, J. Beaudry, M. C. Riddell and T. L. Haas (2012). "Inhibition of proliferation, migration and proteolysis contribute to corticosterone-mediated inhibition of angiogenesis." PLoS One **7**(10): e46625.
Sinno, H. and S. Prakash (2013). "Complements and the wound healing cascade: an updated review." Plast Surg Int **2013**: 146764.
Small, G. R., P. W. Hadoke, I. Sharif, A. R. Dover, D. Armour, C. J. Kenyon, G. A. Gray and B. R. Walker (2005). "Preventing local regeneration of glucocorticoids by 11beta-hydroxysteroid dehydrogenase type 1 enhances angiogenesis." Proc Natl Acad Sci U S A **102**(34): 12165-12170.
Solowiej, A., P. Biswas, D. Graesser and J. A. Madri (2003). "Lack of platelet endothelial cell adhesion molecule-1 attenuates foreign body inflammation because of decreased angiogenesis." Am J Pathol **162**(3): 953-962.
Song, I. H. and F. Buttgereit (2006). "Non-genomic glucocorticoid effects to provide the basis for new drug developments." Mol Cell Endocrinol **246**(1-2): 142-146.

Souverein, P. C., A. Berard, T. P. Van Staa, C. Cooper, A. C. Egberts, H. G. Leufkens and B. R. Walker (2004). "Use of oral glucocorticoids and risk of cardiovascular and cerebrovascular disease in a population based case-control study." Heart **90**(8): 859-865.
Stahn, C., M. Lowenberg, D. W. Hommes and F. Buttgereit (2007). "Molecular mechanisms of glucocorticoid action and selective glucocorticoid receptor agonists." Mol Cell Endocrinol **275**(1-2): 71-78.
Stolte, E. H., B. M. van Kemenade, H. F. Savelkoul and G. Flik (2006). "Evolution of glucocorticoid receptors with different glucocorticoid sensitivity." J Endocrinol **190**(1): 17-28.
Straub, R. H. and C. Schradin (2016). "Chronic inflammatory systemic diseases: An evolutionary trade-off between acutely beneficial but chronically harmful programs." Evol Med Public Health **2016**(1): 37-51.
Strehl, C. and F. Buttgereit (2013). "Optimized glucocorticoid therapy: teaching old drugs new tricks." Mol Cell Endocrinol **380**(1-2): 32-40.
Sun, Y., M. Fang, H. Davies and Z. Hu (2014). "Mifepristone: a potential clinical agent based on its anti-progesterone and anti-glucocorticoid properties." Gynecol Endocrinol **30**(3): 169-173.
Suthar, S. K. and M. Sharma (2014). "Recent Developments in Chimeric NSAIDs as Safer Anti-Inflammatory Agents." Med Res Rev.
Syed, F., S. Singh and A. Bayat (2013). "Superior effect of combination vs. single steroid therapy in keloid disease: a comparative in vitro analysis of glucocorticoids." Wound Repair Regen **21**(1): 88-102.
Tasker, J. G., S. Di and R. Malcher-Lopes (2006). "Minireview: rapid glucocorticoid signaling via membrane-associated receptors." Endocrinology **147**(12): 5549-5556.
Terao, M. and I. Katayama (2016). "Local cortisol/corticosterone activation in skin physiology and pathology." J Dermatol Sci **84**(1): 11-16.
Terao, M., M. Tani, S. Itoi, T. Yoshimura, T. Hamasaki, H. Murota and I. Katayama (2014). "11beta-hydroxysteroid dehydrogenase 1 specific inhibitor increased dermal collagen content and promotes fibroblast proliferation." PLoS One **9**(3): e93051.
Theocharidis, A., S. van Dongen, A. J. Enright and T. C. Freeman (2009). "Network visualization and analysis of gene expression data using BioLayout Express(3D)." Nat Protoc **4**(10): 1535-1550.
Tiganescu, A., M. Hupe, Y. Uchida, T. Mauro, P. M. Elias and W. M. Holleran (2014). "Increased glucocorticoid activation during mouse skin wound healing." J Endocrinol **221**(1): 51-61.
Tiganescu, A., M. Hupe, Y. Uchida, T. Mauro, P. M. Elias and W. M. Holleran (2018). "Topical 11beta-Hydroxysteroid Dehydrogenase Type 1 Inhibition Corrects Cutaneous Features of Systemic Glucocorticoid Excess in Female Mice." Endocrinology **159**(1): 547-556.
Tiganescu, A., A. A. Tahrani, S. A. Morgan, M. Otranto, A. Desmouliere, L. Abrahams, Z. Hassan-Smith, E. A. Walker, E. H. Rabbitt, M. S. Cooper, K. Amrein, G. G. Lavery and P. M. Stewart (2013). "11beta-Hydroxysteroid dehydrogenase blockade prevents age-induced skin structure and function defects." J Clin Invest **123**(7): 3051-3060.
Tiganescu, A., E. A. Walker, R. S. Hardy, A. E. Mayes and P. M. Stewart (2011). "Localization, age- and site-dependent expression, and regulation of 11beta-hydroxysteroid dehydrogenase type 1 in skin." J Invest Dermatol **131**(1): 30-36.
Tochio, T., H. Tanaka, S. Nakata and H. Hosoya (2010). "Fructose-1,6-bisphosphate aldolase A is involved in HaCaT cell migration by inducing lamellipodia formation." J Dermatol Sci **58**(2): 123-129.
Trapp, T., R. Rupprecht, M. Castren, J. M. Reul and F. Holsboer (1994). "Heterodimerization between mineralocorticoid and glucocorticoid receptor: a new principle of glucocorticoid action in the CNS." Neuron **13**(6): 1457-1462.

Upreti, R., K. A. Hughes, D. E. Livingstone, C. D. Gray, F. C. Minns, D. P. Macfarlane, I. Marshall, L. H. Stewart, B. R. Walker and R. Andrew (2014). "5alpha-reductase type 1 modulates insulin sensitivity in men." J Clin Endocrinol Metab **99**(8): E1397-1406.
Vahedi, K. and S. Alamowitch (2011). "Clinical spectrum of type IV collagen (COL4A1) mutations: a novel genetic multisystem disease." Curr Opin Neurol **24**(1): 63-68.
Vandevyver, S., L. Dejager, J. Tuckermann and C. Libert (2013). "New insights into the anti-inflammatory mechanisms of glucocorticoids: an emerging role for glucocorticoid-receptor-mediated transactivation." Endocrinology **154**(3): 993-1007.
Vandewalle, J., A. Luypaert, K. De Bosscher and C. Libert (2018). "Therapeutic Mechanisms of Glucocorticoids." Trends Endocrinol Metab **29**(1): 42-54.
Vos, T., A. D. Flaxman, M. Naghavi, R. Lozano, C. Michaud, M. Ezzati, K. Shibuya, J. A. Salomon, S. Abdalla, V. Aboyans, J. Abraham, I. Ackerman, R. Aggarwal, S. Y. Ahn, M. K. Ali, M. Alvarado, H. R. Anderson, L. M. Anderson, K. G. Andrews, C. Atkinson, L. M. Baddour, A. N. Bahalim, S. Barker-Collo, L. H. Barrero, D. H. Bartels, M. G. Basanez, A. Baxter, M. L. Bell, E. J. Benjamin, D. Bennett, E. Bernabe, K. Bhalla, B. Bhandari, B. Bikbov, A. Bin Abdulhak, G. Birbeck, J. A. Black, H. Blencowe, J. D. Blore, F. Blyth, I. Bolliger, A. Bonaventure, S. Boufous, R. Bourne, M. Boussinesq, T. Braithwaite, C. Brayne, L. Bridgett, S. Brooker, P. Brooks, T. S. Brugha, C. Bryan-Hancock, C. Bucello, R. Buchbinder, G. Buckle, C. M. Budke, M. Burch, P. Burney, R. Burstein, B. Calabria, B. Campbell, C. E. Canter, H. Carabin, J. Carapetis, L. Carmona, C. Cella, F. Charlson, H. Chen, A. T. Cheng, D. Chou, S. S. Chugh, L. E. Coffeng, S. D. Colan, S. Colquhoun, K. E. Colson, J. Condon, M. D. Connor, L. T. Cooper, M. Corriere, M. Cortinovis, K. C. de Vaccaro, W. Couser, B. C. Cowie, M. H. Criqui, M. Cross, K. C. Dabhadkar, M. Dahiya, N. Dahodwala, J. Damsere-Derry, G. Danaei, A. Davis, D. De Leo, L. Degenhardt, R. Dellavalle, A. Delossantos, J. Denenberg, S. Derrett, D. C. Des Jarlais, S. D. Dharmaratne, M. Dherani, C. Diaz-Torne, H. Dolk, E. R. Dorsey, T. Driscoll, H. Duber, B. Ebel, K. Edmond, A. Elbaz, S. E. Ali, H. Erskine, P. J. Erwin, P. Espindola, S. E. Ewoigbokhan, F. Farzadfar, V. Feigin, D. T. Felson, A. Ferrari, C. P. Ferri, E. M. Fevre, M. M. Finucane, S. Flaxman, L. Flood, K. Foreman, M. H. Forouzanfar, F. G. Fowkes, R. Franklin, M. Fransen, M. K. Freeman, B. J. Gabbe, S. E. Gabriel, E. Gakidou, H. A. Ganatra, B. Garcia, F. Gaspari, R. F. Gillum, G. Gmel, R. Gosselin, R. Grainger, J. Groeger, F. Guillemin, D. Gunnell, R. Gupta, J. Haagsma, H. Hagan, Y. A. Halasa, W. Hall, D. Haring, J. M. Haro, J. E. Harrison, R. Havmoeller, R. J. Hay, H. Higashi, C. Hill, B. Hoen, H. Hoffman, P. J. Hotez, D. Hoy, J. J. Huang, S. E. Ibeanusi, K. H. Jacobsen, S. L. James, D. Jarvis, R. Jasrasaria, S. Jayaraman, N. Johns, J. B. Jonas, G. Karthikeyan, N. Kassebaum, N. Kawakami, A. Keren, J. P. Khoo, C. H. King, L. M. Knowlton, O. Kobusingye, A. Koranteng, R. Krishnamurthi, R. Lalloo, L. L. Laslett, T. Lathlean, J. L. Leasher, Y. Y. Lee, J. Leigh, S. S. Lim, E. Limb, J. K. Lin, M. Lipnick, S. E. Lipshultz, W. Liu, M. Loane, S. L. Ohno, R. Lyons, J. Ma, J. Mabweijano, M. F. MacIntyre, R. Malekzadeh, L. Mallinger, S. Manivannan, W. Marcenes, L. March, D. J. Margolis, G. B. Marks, R. Marks, A. Matsumori, R. Matzopoulos, B. M. Mayosi, J. H. McAnulty, M. M. McDermott, N. McGill, J. McGrath, M. E. Medina-Mora, M. Meltzer, G. A. Mensah, T. R. Merriman, A. C. Meyer, V. Miglioli, M. Miller, T. R. Miller, P. B. Mitchell, A. O. Mocumbi, T. E. Moffitt, A. A. Mokdad, L. Monasta, M. Montico, M. Moradi-Lakeh, A. Moran, L. Morawska, R. Mori, M. E. Murdoch, M. K. Mwaniki, K. Naidoo, M. N. Nair, L. Naldi, K. M. Narayan, P. K. Nelson, R. G. Nelson, M. C. Nevitt, C. R. Newton, S. Nolte, P. Norman, R. Norman, M. O'Donnell, S. O'Hanlon, C. Olives, S. B. Omer, K. Ortblad, R. Osborne, D. Ozgediz, A. Page, B. Pahari, J. D. Pandian, A. P. Rivero, S. B. Patten, N. Pearce, R. P. Padilla, F. Perez-Ruiz, N. Perico, K. Pesudovs, D. Phillips, M. R. Phillips, K. Pierce, S. Pion, G. V. Polanczyk, S. Polinder, C. A. Pope, 3rd, S. Popova, E. Porrini, F. Pourmalek, M. Prince, R. L. Pullan, K. D. Ramaiah, D. Ranganathan, H. Razavi, M. Regan, J. T. Rehm, D. B. Rein, G. Remuzzi, K. Richardson, F. P. Rivara, T. Roberts, C. Robinson, F. R. De Leon, L. Ronfani, R. Room, L. C. Rosenfeld, L. Rushton, R. L. Sacco, S. Saha, U. Sampson, L. Sanchez-Riera, E. Sanman, D. C.

Schwebel, J. G. Scott, M. Segui-Gomez, S. Shahraz, D. S. Shepard, H. Shin, R. Shivakoti, D. Singh, G. M. Singh, J. A. Singh, J. Singleton, D. A. Sleet, K. Sliwa, E. Smith, J. L. Smith, N. J. Stapelberg, A. Steer, T. Steiner, W. A. Stolk, L. J. Stovner, C. Sudfeld, S. Syed, G. Tamburlini, M. Tavakkoli, H. R. Taylor, J. A. Taylor, W. J. Taylor, B. Thomas, W. M. Thomson, G. D. Thurston, I. M. Tleyjeh, M. Tonelli, J. A. Towbin, T. Truelsen, M. K. Tsilimbaris, C. Ubeda, E. A. Undurraga, M. J. van der Werf, J. van Os, M. S. Vavilala, N. Venketasubramanian, M. Wang, W. Wang, K. Watt, D. J. Weatherall, M. A. Weinstock, R. Weintraub, M. G. Weisskopf, M. M. Weissman, R. A. White, H. Whiteford, S. T. Wiersma, J. D. Wilkinson, H. C. Williams, S. R. Williams, E. Witt, F. Wolfe, A. D. Woolf, S. Wulf, P. H. Yeh, A. K. Zaidi, Z. J. Zheng, D. Zonies, A. D. Lopez, C. J. Murray, M. A. AlMazroa and Z. A. Memish (2012). "Years lived with disability (YLDs) for 1160 sequelae of 289 diseases and injuries 1990-2010: a systematic analysis for the Global Burden of Disease Study 2010." Lancet **380**(9859): 2163-2196.

Vukelic, S., O. Stojadinovic, I. Pastar, C. Vouthounis, A. Krzyzanowska, S. Das, H. H. Samuels and M. Tomic-Canic (2010). "Farnesyl pyrophosphate inhibits epithelialization and wound healing through the glucocorticoid receptor." J Biol Chem **285**(3): 1980-1988.

Walker, B. R. (2007). "Glucocorticoids and cardiovascular disease." Eur J Endocrinol **157**(5): 545-559.

Wamil, M., R. Andrew, K. E. Chapman, J. Street, N. M. Morton and J. R. Seckl (2008). "7-oxysterols modulate glucocorticoid activity in adipocytes through competition for 11beta-hydroxysteroid dehydrogenase type." Endocrinology **149**(12): 5909-5918.

Wehling, M. (1997). "Specific, nongenomic actions of steroid hormones." Annu Rev Physiol **59**: 365-393.

Wei, L., T. M. MacDonald and B. R. Walker (2004). "Taking glucocorticoids by prescription is associated with subsequent cardiovascular disease." Ann Intern Med **141**(10): 764-770.

Whirledge, S. and D. B. DeFranco (2018). "Glucocorticoid Signaling in Health and Disease: Insights From Tissue-Specific GR Knockout Mice." Endocrinology **159**(1): 46-64.

Woodfin, A., M. B. Voisin and S. Nourshargh (2007). "PECAM-1: a multi-functional molecule in inflammation and vascular biology." Arterioscler Thromb Vasc Biol **27**(12): 2514-2523.

Xie, Y., K. Gao, L. Hakkinen and H. S. Larjava (2009). "Mice lacking beta6 integrin in skin show accelerated wound repair in dexamethasone impaired wound healing model." Wound Repair Regen **17**(3): 326-339.

Yang, C., M. Nixon, C. J. Kenyon, D. E. Livingstone, R. Duffin, A. G. Rossi, B. R. Walker and R. Andrew (2011). "5alpha-reduced glucocorticoids exhibit dissociated anti-inflammatory and metabolic effects." Br J Pharmacol **164**(6): 1661-1671.

Yang, N., D. W. Ray and L. C. Matthews (2012). "Current concepts in glucocorticoid resistance." Steroids **77**(11): 1041-1049.

Yang, S. and L. Zhang (2004). "Glucocorticoids and vascular reactivity." Curr Vasc Pharmacol **2**(1): 1-12.

Zhu, T., Q. Yao, X. Hu, C. Chen, H. Yao and J. Chao (2015). "The Role of MCPIP1 in Ischemia/Reperfusion Injury-Induced HUVEC Migration and Apoptosis." Cell Physiol Biochem **37**(2): 577-591.

Zizzo, G., B. A. Hilliard, M. Monestier and P. L. Cohen (2012). "Efficient clearance of early apoptotic cells by human macrophages requires M2c polarization and MerTK induction." J Immunol **189**(7): 3508-3520.